

AFML-TR-76-246

TECHNICAL
LIBRARY

METHODS FOR THE DETERMINATION OF THE SENSITIVITY OF NDE TECHNIQUES

*GENERAL DYNAMICS/FORT WORTH DIVISION
FORT WORTH, TEXAS*

*VANDERBILT UNIVERSITY
NASHVILLE, TENNESSEE*

DECEMBER 1976

TECHNICAL REPORT AFML-TR-76-246
Final Report for Period November 1975 – October 1976

Approved for public release; distribution unlimited.

AIR FORCE MATERIALS LABORATORY
AIR FORCE WRIGHT AERONAUTICAL LABORATORIES
AIR FORCE SYSTEMS COMMAND
WRIGHT-PATTERSON AIR FORCE BASE, OHIO 45433


DTIC QUALITY INSPECTED 1

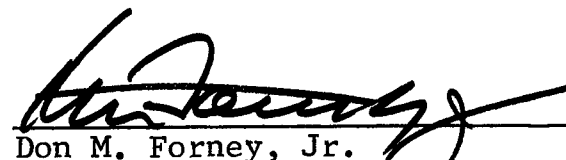
19970908 153

NOTICE

When Government drawings, specifications, or other data are used for any purpose other than in connection with a definitely related Government procurement operation, the United States Government thereby incurs no responsibility nor any obligation whatsoever; and the fact that the government may have formulated, furnished, or in any way supplied the said drawings, specifications, or other data, is not to be regarded by implication or otherwise as in any manner licensing the holder or any other person or corporation, or conveying any rights or permission to manufacture, use, or sell any patented invention that may in any way be related thereto.

This report was submitted by the authors in February 1977. The technical report has been reviewed and is approved for publication.


Freddy D. Mullins
Project Engineer
Nondestructive Evaluation Branch
Metals and Ceramics Division
Air Force Materials Laboratory


Don M. Forney, Jr.
Chief, Nondestructive Evaluation
Branch
Metals and Ceramics Division
Air Force Materials Laboratory

Copies of this report should not be returned unless return is required by security considerations, contractual obligations, or notice on a specific document.

UNCLASSIFIED

SECURITY CLASSIFICATION OF THIS PAGE (When Data Entered)

REPORT DOCUMENTATION PAGE		READ INSTRUCTIONS BEFORE COMPLETING FORM
1. REPORT NUMBER	2. GOVT ACCESSION NO.	3. RECIPIENT'S CATALOG NUMBER
4. TITLE (and Subtitle) METHODS FOR THE DETERMINATION OF THE SENSITIVITY OF NDE TECHNIQUES		5. TYPE OF REPORT & PERIOD COVERED 11-19-75/11-19-76 Final Technical Report
		6. PERFORMING ORG. REPORT NUMBER FZM-6644
7. AUTHOR(s) Francis H. Chang, Jerry R. Bell, Thomas C. Walker, James M. Norton, Paul F. Packman, Lewey O. Gilstrap, Jr.		8. CONTRACT OR GRANT NUMBER(s) F33615-76-C-5066
9. PERFORMING ORGANIZATION NAME AND ADDRESS GENERAL DYNAMICS/FORT WORTH DIVISION FORT WORTH, TEXAS 76101 VANDERBILT UNIVERSITY, NASHVILLE, TN 37235		10. PROGRAM ELEMENT, PROJECT, TASK AREA & WORK UNIT NUMBERS 73510947
11. CONTROLLING OFFICE NAME AND ADDRESS Air Force Materials Laboratory Air Force Systems Command Wright-Patterson Air Force Base, Ohio		12. REPORT DATE February 1977
14. MONITORING AGENCY NAME & ADDRESS (if different from Controlling Office)		13. NUMBER OF PAGES
		15. SECURITY CLASS. (of this report) Unclassified
		15a. DECLASSIFICATION/DOWNGRADING SCHEDULE
16. DISTRIBUTION STATEMENT (of this Report) Approved for public release; distribution unlimited		
17. DISTRIBUTION STATEMENT (of the abstract entered in Block 20, if different from Report)		
18. SUPPLEMENTARY NOTES		
19. KEY WORDS (Continue on reverse side if necessary and identify by block number) Nondestructive evaluation, nondestructive testing, reliability, probability of detection, translation model, inspection sensitivity, linear regression analysis, adaptive learning network		
20. ABSTRACT (Continue on reverse side if necessary and identify by block number) This report describes the work accomplished under a 12-month program conducted for the purpose of developing a model to trans- late the nondestructive evaluation (NDE) capabilities assessed from aluminum and steel specimens with simple geometries to equivalent detection sensitivity for specimens with complex		

UNCLASSIFIED

SECURITY CLASSIFICATION OF THIS PAGE (When Data Entered)

UNCLASSIFIED

SECURITY CLASSIFICATION OF THIS PAGE(When Data Entered)

20. Abstract (Continued)

geometries. The NDE methods include ultrasonic, eddy current, magnetic particle, penetrant and radiography. NDE reliability data base compiled under a previous NASA program was enlarged. An adaptive learning technique and a linear regression analysis were developed to establish the parametric relationships between inspection sensitivity and NDE parameters. Translation models were developed on the basis of the parametric study to translate inspection results obtained on flat plate specimens to equivalent results on specimens with more complex geometries. Results obtained in this program were limited to aluminum and the NDE techniques of ultrasonic, penetrant and eddy currents due to the inadequacy of the existing data. Data deficiencies were identified during the model development process. Based on the parametric study results and the translation models developed in the program, an optimum demonstration program was designed to evaluate the NDE capability of industrial facilities.

UNCLASSIFIED

SECURITY CLASSIFICATION OF THIS PAGE(When Data Entered)

SUMMARY

First generation demonstration programs such as A-10 and B-1 provided useful information and experience in the determination of the NDE capability of a facility. A large amount of reliability data has been generated since these demonstration programs which should aid in the development of a more valid second generation demonstration program. The purpose of the present program is to develop a model to translate the non-destructive evaluation (NDE) capabilities assessed from aluminum and steel specimens with simple geometries to equivalent detection sensitivity for specimens with complex geometries. Five NDE methods are included in this study: ultrasonics, eddy current, magnetic particle, penetrant and radiography.

The NDE reliability data base compiled under a previous NASA program was enlarged, updated and edited. Adaptive learning techniques and a linear regression analysis method were used to establish parametric relationships between inspection sensitivity and NDE parameters. Based on results from the parametric study, translation models were developed to translate inspection results obtained from flat plate specimens to equivalent results on fillet areas, weldments, and tandem T specimens. The parametric relationships and translation models developed in this program were limited to the material of aluminum and the NDE techniques of ultrasonics, eddy currents and penetrant. The limitations were due to the scope of the existing data. Overall, the translation model from aluminum flat plate to fillet specimens was most successful. Data deficiencies were identified during the model development. An optimum demonstration program was designed to be used as a guideline for future validation and NDE facility qualification programs.

FOREWORD

This is a final technical report and covers work performed under AFML contract F33615-76-C-5066 for the period 19 November 1975 through 19 November 1976. This contract was accomplished under the technical direction of Mr. F. D. Mullins, Nondestructive Evaluation Branch (AFML/LLP), Metals and Ceramics Division, Air Force Materials Laboratory, Wright-Patterson AFB, Ohio.

The contract work was performed by the Materials Research Laboratory of General Dynamics Corporation/Fort Worth Division under the leadership of the Head of the Laboratory, Dr. B. G. W. Yee, and Vanderbilt University, Nashville, Tennessee. The program manager and project leader was Dr. F. H. Chang and the associate project leader was Dr. P. F. Packman. Mr. L. O. Gilstrap, Jr. was responsible for the adaptive learning technique logic development. General Dynamics personnel involved in the program were Dr. F. H. Chang, J. R. Bell, T. C. Walker, Dr. J. C. Couchman in the Materials Research Laboratory, and Dr. J. M. Norton in the Reliability and Parts Control Standardization Group.

The authors wish to express appreciation for the generous contributions and help extended by personnel from other aerospace companies and government agencies, especially Mr. W. D. Rummel from Martin Marietta Aerospace Corp./Denver Division. The data presented in this report were analyzed for the parametric relationship study and translation model development. These data do not necessarily reflect the NDE capability of any company.

Table of Contents

<u>Section</u>	<u>Page</u>
LIST OF TABLES	vii
LIST OF ILLUSTRATIONS	viii
I INTRODUCTION	1
II PROGRAM OBJECTIVES AND APPROACH	4
III DATA BASE	6
IV METHODOLOGY	17
4.1 Linear Regression Analysis	17
4.1.1 Introduction to Multiple Linear Regression	17
4.1.2 Formal Development	18
4.1.3 Preliminaries to Model Specification	21
4.1.4 Building the Appropriate Linear Model	24
4.1.5 Error Determination	26
4.2 Adaptive Learning Technique	27
4.2.1 Introduction to Adaptive Learning Techniques	27
4.2.2 Adaptive Learning Logic	27
V MODEL DEVELOPMENT	32
5.1 Linear Regression Technique in Model Development	32
5.1.1 Translation Model Development	32
5.1.2 Analysis Capabilities	34
5.1.3 Data Problems	41
5.1.4 General Comparative Comments	42
VI RESULTS	43
6.1 NDE Parameter Study	43
6.1.1 Parameter Identification	43
6.1.2 Parametric Relationship	43
6.1.2.1 Comparison of Statistical Evaluation Schemes	44
6.1.2.2 Point Estimate of Probability of Detection (POD)	44
6.1.2.3 Statistical Fitting Schemes	52
6.1.2.4 Summary of Parametric Relationship Study	60

Table of Contents (Cont'd)

<u>Section</u>	<u>Page</u>
6.2 Translation Model	70
6.2.1 Ultrasonic Inspection	70
6.2.2 Penetrant Inspection	73
6.2.3 Eddy Current Inspection	74
6.2.4 Transfer Function	92
6.2.5 Summary of Translation Model Development	103
6.3 Data Deficiencies	105
VII OPTIMUM DEMONSTRATION PROGRAM DESIGN	108
7.1 Introduction	108
7.2 Specimen Configuration	110
7.3 Management and Documentation	115
7.4 Inspection and Analysis	116
7.5 Validation of Translation Model	119
VIII CONCLUSIONS	120
APPENDIX A - Samples of Cover Sheets for Eddy Current, Radiography, Magnetic Particle, and Penetrant Techniques	121
APPENDIX B - Overall Logic and Codes of Computer Programs for the Adaptive Learning Analysis	126
APPENDIX C - Comparison of Statistical Schemes for POD Calculation	158
APPENDIX D - Examples of Computer Generated Histograms Obtained by the Point Estimate Method	166
APPENDIX E - Linear Regression Translation Model	185
REFERENCES	191

List of Tables

<u>Table No.</u>		<u>Page</u>
1	Data Set Listing	7
2	Relevant NDE Parameters for Ultrasonic Method	15
3	Summary of Contributions in Linear Regression Analysis	22
4	A List of NDE Parameters Included in Parametric Study	47
5	Conclusion of Parametric Relationship, Ultrasonic	66
6	Conclusion of Parametric Relationship, Penetrant	67
7	Conclusion of Parametric Relationship, Eddy Current	68
8	Summary - Translation Model	104
9	Estimate of Fatigue Fracture and Durability Critical Parts for F-16 and B-1	106
A-1	Relevant NDE Parameters for Eddy Current Method	122
A-2	Relevant NDE Parameters for Radiography Method	123
A-3	Relevant NDE Parameters for Magnetic Particle Method	124
A-4	Relevant NDE Parameters for Penetrant Method	125
E-1	Linear Regression Model - Ultrasonic	187
E-2	Linear Regression Model - Penetrant	188
E-3	Linear Regression Model - Eddy Current	189
E-4	Linear Regression Model - X-Ray	190

List of Illustrations

<u>Figure No.</u>		<u>Page</u>
1	POD Difference for Etched and Unetched Surfaces (Eddy Current, Integrally Stiffened Panel Specimens)	45
2	Specimen Geometries	49
3	Example of Computer Printouts of Point Estimate Comparisons in Parametric Relationship Study on Flat Plate Specimens	50
4	Effects of Surface Finish on POD by Adaptive Learning Technique (Ultrasonic)	54
5	Effects of Specimen History on POD by Linear Regression Technique (Ultrasonic)	55
6	Effects of Specimen History and Surface Finish on POD by Adaptive Learning Technique (Ultrasonic)	56
7	Effects of Specimen History, Surface Finish, and Thickness on POD by Adaptive Learning Technique (Ultrasonic)	57
8	Effects of $a/2c$ on POD by Adaptive Learning Technique (Ultrasonic, Flat Plate Specimens)	58
9	Effects of $a/2c$ on POD by Adaptive Learning Technique (Ultrasonic, Integrally Stiffened Panel Specimens)	59
10	Effects of Specimen History and Surface Finish on POD by Linear Regression Technique (Penetrant)	61
11	Effects of Specimen History on POD by Linear Regression Technique (Penetrant)	62
12	Effects of Specimen History on POD by Linear Regression Technique (Eddy Current)	63
13	Comparison of NDE Methods Sensitivity by Linear Regression Technique (Unetched Surface)	64

List of Illustrations (Cont'd)

<u>Figure No.</u>		<u>Page</u>
14	Comparison of NDE Methods Sensitivity by Linear Regression Technique (Etched Surface)	65
15	Translation Model by Adaptive Learning Technique - Flat Plate/Integrally Stiffened Panel (Ultrasonic)	71
16	Translation Model by Linear Regression Technique - Flat Plate/Integrally Stiffened Panel (Ultrasonic)	72
17	Translation Model by Adaptive Learning Technique - Flat Plate/Long. Flush Weld (Ultrasonic)	74
18	Translation Model by Linear Regression Technique - Flat Plate/Long. Flush Weld (Ultrasonic)	75
19	Translation Model by Adaptive Learning Technique - Flat Plate/Transverse Weld w/Crown (Ultrasonic)	76
20	Translation Model by Linear Regression Technique - Flat Plate/Transverse Weld w/Crown (Ultrasonic)	77
21	Translation Model by Adaptive Learning Technique - Flat Plate/Tandem T (Ultrasonic)	78
22	Translation Model by Adaptive Learning Technique - Flat Plate/Integrally Stiffened Panel (Penetrant)	79
23	Translation Model by Linear Regression Technique - Flat Plate/Integrally Stiffened Panel (Penetrant)	80
24	Translation Model by Adaptive Learning Technique - Flat Plate/Long. Flush Weld (Penetrant)	81

List of Illustrations (Cont'd)

<u>Figure No.</u>		<u>Page</u>
25	Translation Model by Linear Regression Technique - Flat Plate/Long. Flush Weld (Penetrant)	82
26	Translation Model by Adaptive Learning Technique - Flat Plate/Transverse Weld w/Crown (Penetrant)	83
27	Translation Model by Linear Regression Technique - Flat Plate/Transverse Weld w/Crown (Penetrant)	84
28	Translation Model by Adaptive Learning Technique - Flat Plate/Integrally Stiffened Panel (Eddy Current)	85
29	Translation Model by Linear Regression Technique - Flat Plate/Integrally Stiffened Panel (Eddy Current)	86
30	Translation Model by Adaptive Learning Technique - Flat Plate/Long. Flush Weld (Eddy Current)	87
31	Translation Model by Linear Regression Technique - Flat Plate/Long. Flush Weld (Eddy Current)	88
32	Translation Model by Adaptive Learning Technique - Flat Plate/Transverse Weld w/Crown (Eddy Current)	89
33	Translation Model by Linear Regression Technique - Flat Plate/Transverse Weld w/Crown (Eddy Current)	90
34	Translation Model by Adaptive Learning Technique - Flat Plate/Bolt Hole (Eddy Current)	91
35	NDE Methods Sensitivity for Flat Plates by Point Estimate Method	93
36	NDE Methods Sensitivity for Integrally Stiffened Panels by Point Estimate Method	94

List of Illustrations (Cont'd)

<u>Figure No.</u>		<u>Page</u>
37	NDE Methods Sensitivity for Longitudinal Flush Weld by Point Estimate Method	95
38	NDE Methods Sensitivity for Transverse Weld w/Crown by Point Estimate Method	96
39	NDE Methods Sensitivity for Longitudinal Weld with Crown by Point Estimate Method	97
40	NDE Methods Sensitivity for Riveted Plate to Integrally Stiffened Panel by Point Estimate Method	98
41	NDE Methods Sensitivity for Weld Panels with LOP by Point Estimate Method	99
42	NDE Methods Sensitivity for Bolt Holes by Point Estimate Method	100
43	NDE Methods Sensitivity for Tandem T by Point Estimate Method	101
44	Transfer Function for Flat Plate/ Integrally Stiffened Panel	102
B-1	Hypersurface Fitting Program Initialize and Load BTDE and SBTDE	132
B-2	Adaptive Learning Technique Main Program Listing	142
B-3	Teletype Output from Overlay 1	143
B-4	Teletype Output from Overlays 2, 3, and 4	144
B-5	Teletype Output from Overlay 5	145
B-6	Teletype Output from Overlay 6	146
B-7	Teletype Output from Overlays 7 and 8	147
B-8	Fitting Program Logic	153

List of Illustrations (Cont'd)

<u>Figure No.</u>		<u>Page</u>
B-9	Final Training Set Results	154
B-10	Final Testing Set Results	155
D-1	Comparison of POD of Flat Plate Specimen Thickness (Eddy Current, 1st and 2nd Columns Represent Specimens with Thicknesses of 0.214 and 0.060 In. Respectively. DSN = 15-18, 31)	168
D-2	Comparison of POD of Flat Plate Specimen Thickness (Ultrasonic, 1st and 2nd Columns Represent Specimens with Thicknesses of 0.214 and 0.060 In. Respectively. DSN = 12, 13, 14, 29, 30)	169
D-3	Comparison of POD of Flat Plate Specimen Thickness (Penetrant, 1st and 2nd Columns Represent Specimens with Thicknesses of 0.214 and 0.060 In. Respectively. DSN = 24-28, 60, 61)	170
D-4	Comparison of POD of Flat Plate Specimen Thickness (X-ray, 1st and 2nd Columns Represent Specimens with Thicknesses of 0.214 and 0.060 In. Respectively. DSN = 10, 11, 20-23, 59)	171
D-5	Comparison of POD of Specimen History (Eddy Current, 1st and 2nd Columns Represent Specimens with Etched and Unetched Surface Treatment Respectively)	172
D-6	Comparison of POD of Specimen History (Ultrasonic, 1st and 2nd Columns Represent Specimens with Etched and Unetched Surface Treatment Respectively)	173
D-7	Comparison of POD of Specimen History (Penetrant, 1st and 2nd Columns Represent Specimens with Etched and Unetched Surface Treatment Respectively)	174

List of Illustrations (Cont'd)

<u>Figure No.</u>		<u>Page</u>
D-8	Comparison of POD of Flat Plate Specimen History (X-ray, 1st and 2nd Columns Represent Specimens with Etched and Unetched Surface Treatment Respectively)	175
D-9	Comparison of POD of Different Inspectors Using Penetrant, Eddy Current, and X-Ray Techniques on Flat Plate Specimens (1st, 2nd and 3rd Columns Represent Different Inspectors within One Company)	176
D-10	Comparison of POD for Different Companies Using the Same Flat Plate Specimens (1st, 2nd and 3rd Columns Represent Companies A, B, and C Respectively)	178
D-11	Comparison of POD for Two Different Part Geometries Obtained by the Same Company (1st and 2nd Columns Represent Flat Plate and Integrally Stiffened Panel Specimen Geometries Respectively)	179
D-12	Comparison of POD for Three Different Part Geometries Obtained by Three Companies (1st, 2nd, and 3rd Columns Represent Specimen Geometries of Flat Plate, Integrally Stiffened Panel (ISP) and ISP with Riveted Plate Respectively)	180
D-13	Comparison of POD of Different Part Geometries Using Ultrasonic, Eddy Current and Magnetic Particle Inspections (1st and 2nd Columns Represent Specimen Geometries as Indicated Above the Histogram Bars)	181
D-14	Comparison of POD for Different Specimen Histories (1st and 2nd Columns Represent As Welded and Scarfed Weld Crown Respectively)	182
D-15	Comparison of POD for Weld Specimens with Lack of Penetration Defects Before (1st Column) and After (2nd Column)	184

S E C T I O N I

I N T R O D U C T I O N

The design damage tolerance requirements (MIL-A-83444) specify the maximum allowable initial flaw sizes in aircraft structure. The damage tolerance design approach is based on a sound fracture mechanics principles. It assumes that an aircraft hardware item contains an initial defect or flaw of some minimum size which can be reliably detected with a demonstrated NDE capability. The Aircraft Structural Integrity Program (MIL-STD-1530) specifies that a NDE demonstration program shall be performed to verify that all flaws equal to or greater than the design flaw size will be detected to the required reliability and confidence level. The demonstration program is required if, and only if, the designer elects not to accept the design flaw size specified in MIL-A-83444.

Demonstration programs conducted in the past produced useful information as required by their respective specific objective. These first generation programs may not have been totally adequate from the standpoints of flaw size distribution, NDE parameters identification, and sensitivity interpretation. The A-10 and B-1 demonstration programs were among these first generation programs that provided useful knowledge and experiences in the attempt to determine the NDE capability of a facility. A large amount of data in the area of NDE reliability has been generated after these demonstration programs were completed. The knowledge gained from these studies allow us to develop a more valid second generation demonstration program.

The need for the design of a more valid demonstration program is illustrated by an example of the B-1 demonstration program. In that program flat plate specimens were used which contained fatigue cracks grown under cyclic fatigue loads. Specimens with this simple geometry have the advantages of low cost as well as ease in crack growth and flaw size control. However, in actual B-1 structures there are fracture critical areas in fillets and curved surfaces for which no reliability data was available at that time. The NDE capability demonstrated by a facility on flat plate specimens should be translated to the equivalent capability on specimens with complex geometries.

Such a translation was made possible by two programs sponsored by NASA Johnson Space Center^(1,2). In these programs, reliability data were generated by the same facility on specimens with flat plate and complex geometries to allow a valid comparison of the inspection sensitivity.

The data base for the NDE parametric study and translation model development consists of twenty sets of relevant NDE reliability data compiled from previous research programs conducted in different aerospace companies. A computerized reliability data bank was compiled by General Dynamics and Vanderbilt University under a program sponsored by the NASA Lewis Research Center⁽³⁾. In this program twenty sets of relevant NDE reliability data were identified, collected, compiled, and categorized. Three on-going programs generating relevant data were also identified. The criteria for data selection for statistical analysis consideration were formulated on the basis of the completeness of pertinent NDE parameter records, requirement for instrument calibration, verification of flaw dimensions, and other relevant factors. A comprehensive computer program was prepared to calculate the probability of flaw detection (POD) at 50 and 95 percent confidence levels by using the binomial statistical method.

Three data cumulation procedures were used in plotting the POD as a function of flaw size: (1) range interval (RI), (2) overlapping 60 points (OSP), and (3) optimized probability method (OPM). In the RI method the data were separated into groups of equal flaw size increments. The probability of detection at the onesided lower confidence limit was computed for each group separately and plotted as a histogram bar. The OSP method combined detection results for the largest 60 cracks and plotted the POD for this interval at the largest flaw size. The next data increment was obtained by starting at the median flaw size of the first interval and combining the data for the next smaller 60 cracks. The POD of the second set was plotted at its largest flaw size and the process was repeated until all data were combined. In the OPM method the ordered NDI data were grouped into a given number of intervals of successively increasing size range. POD for the largest size range and its successive combinations with the smaller sizes were calculated. The largest value of the POD was plotted at the largest flaw size contained in the corresponding composite grouping. The largest flaw size interval was then removed from consideration and the procedure was repeated starting from the next to largest flaw size grouping. The latter was repeated until the given number of intervals of POD was plotted.

Seven sets of reliability data collected in the NASA program were statistically analyzed by using the cumulative schemes described in the above paragraph. These seven sets of data met the selection criteria established in that program. Among these seven sets were data collected on flat plate specimens containing fatigue cracks in the NDI studies initiated by NASA Johnson Space Center.

With the availability of more and more NDE reliability data, it has become necessary to start examining the parameters that can potentially influence the inspection results. These parameters need to be identified and their relative influence on the inspection results determined by systematic parametric studies. Specimen geometry, defect type and orientation, surface condition, inspection environment, human factors and the statistical methods chosen for the capability determination are but a few of the NDE parameters that may influence the inspection results. A model to translate results obtained from practical test specimens to complex aircraft hardware needs to be developed. Such a model will be in the form of a family of probability of detection (POD) curves plotted as a function of flaw size with the specimen geometry as the independent parameter. This family of curves will provide a comparison of POD for any two specimen geometries at a specific flaw size. Equivalently, translation tables may be constructed in which the differences in POD for any two specimen geometries are provided.

S E C T I O N I I
P R O G R A M O B J E C T I V E
A N D A P P R O A C H

The overall objective of this program was to develop a model to translate the NDE capabilities assessed from aluminum and steel specimens with simple geometries to equivalent detection sensitivity for specimens with complex geometries. The specific objectives were:

- o Enlarge the NDE reliability data base compiled under a previous NASA program
- o Develop analytic techniques to analyze the reliability data
- o Establish the parametric relationships between inspection sensitivity and NDE parameters
- o Identify data deficiencies in the reliability data base and outline experiments to overcome the deficiencies
- o Develop translation models for NDE techniques of ultrasonic, penetrant, eddy current, magnetic particle and X-ray
- o Design an optimum demonstration program to evaluate the NDE capability of industrial facilities.

The basic approach to achieve the objectives of this program was to use existing reliability data, identify those data containing inspection reliability results on specimens with simple and complex shapes obtained under similar conditions, and to build translation models based on the available data. However, the existing reliability data did not have a systematic variation in NDE parameters to allow the variables to be readily separated in parametric studies. Therefore, statistical methods must be developed or adapted to analyze the data for the parametric study and translation model

development. A standard linear regression method and an adaptive learning technique were used in this program in the statistical analyses. The analyses were conducted by computer codes applicable to an IBM 370 and a PDP 11/45 digital computer. The NDE parameters in a given data set or subset were treated as independent variables while the probabilities of detection associated with the crack size ranges in that data set or subset were considered the dependent outputs in the parametric study. When the specimen geometry was considered as the independent variable while other NDE parameters were held constant, the variation in the POD for the specimen geometries formed the basis of a translation model. Knowing how the NDE parameters affected the inspection sensitivity and how much difference in inspection sensitivity existed between specimens with simple geometries and specimens with complex configurations, an optimum demonstration program could be designed. This optimum demonstration program defined the important NDE parameters to be maintained in the execution of the program, and interpreted results obtained in the program for simple test specimens in terms of equivalent NDE capability as applied to more complex components.

The results obtained in this program were limited mostly to aluminum and the NDE techniques of ultrasonic, penetrant and eddy current. The limitation was due to the inadequacy of the existing data for steel and for the two NDE techniques of X-ray and magnetic particle. Titanium was not selected as one of the materials to be analyzed in this program on account of data deficiency for this material.

S E C T I O N I I I

D A T A B A S E

The NDT reliability data base developed by General Dynamics under a NASA contract⁽¹⁾ has been enlarged, updated and modified to serve as a basis for the parametric study and translation model development in this program. Seventy additional data sets were entered into the computer data bank, bringing the total number of data sets to 222. The additional data were generated by Martin Marietta Corporation/Aerospace Division⁽²⁾. These data consisted of NDT inspection results on aluminum specimens in the configuration of integrally stiffened panels and welded panels. Fatigue cracks in the fillet area of the integrally stiffened panels and weld joints as well as lack of penetration (LOP) in the welded panels constituted the flaw types in the specimens. Specimen history included as machined and chemically etched surface, scarfed and unscarfed crowns, and proof loaded to 90 percent of the yield strength. NDT methods used in the inspection were liquid penetrant, ultrasonic, eddy current and X-radiography techniques. A complete listing of all the data sets in the data bank is tabulated in Table 1.

The additional data sets entered into the computer data bank supplemented the basic reliability data needed for the NDT parameter relationship and translation model development. Similar data were generated by the same company under an earlier NASA sponsored research program using flat plates as specimens⁽³⁾. The facilities and procedures of the inspections were essentially the same for the two programs. Two other companies, Rockwell International/Space Division and General Dynamics/Convair Division, also participated in the earlier program. The 34 data sets compiled by the three participating companies in the earlier program plus the 70 data sets compiled by Martin Marietta in the latter program are well documented and well balanced statistically. The categories and individual parameters for each data set are shown in the data set listing in Table 1.

Several data sets analyzed in the NASA program⁽¹⁾ were not used in the translation model development. Some of the data collected in the NASA program lacked information on NDE parameters. Some data were well documented but the POD for the flawed specimens were so high that a curve cannot be plotted in the process of building a translation model.

TABLE 1 DATA SET LISTING

TABULATION SHEET

DEPARTMENT 08
FMP 2640-0-04

Data Set No.	No. of Data Points	Company	Data Source	NDE Method	Material	Part Geometry	Flaw Type	Specimen History	Inspection Environment
01	983	Martin Mar.	NASA CR2369	Penet.	Al	Flat Plate	Fatigue Crack	As Machined	Lab
02				Penet.				Etched	
03				E/C				As Machined	
04				X-ray				"	
05				X-ray				Etched	
06				Ultra.				As Machined	
07				Ultra.				"	
08				Ultra.				Etched	
09	983	Martin Mar.	NASA CR2369	Ultra.					
10	419	Rockwell ISD	Space Shuttle	X-ray					
11				X-ray					
12				Ultra.					
13				Ultra.					
14				Ultra.					
15				E/C					
16				E/C					
17				E/C					
18		Rockwell ISD	Space Shuttle	E/C					
19		Martin Mar.	NASA CR2369	E/C					
20		Rockwell ISD	Space Shuttle	X-ray					
21				X-ray					
22				X-ray					
23				X-ray					
24				Penet.					
25				Penet.					
26				Penet.					
27				Penet.					
28				Penet.					
29				Ultra.					
30				Ultra.					
31		Rockwell ISD	Space Shuttle	E/C					
32	100	Lockheed GA	NFMI-68-32	Penet.	Steel	Cylinder			
33	100			Penet.	Steel			As Machined	
34	110			Ultra.	Al		Fatigue Crack		
35	110	Lockheed GA	NFMI-68-32	X-ray	Al				

TABLE 1 DATA SET LISTING
(Continued)

Data Set No.	Data Points	Company	Data Source	NDE Method	Material	Part Geometry	Flaw Type	Specimen History	Inspection Environment
36	100	Lockheed GA	AFML-68-32	Ultrasonic	Steel	Cylinder	Fatigue Crack	As Machined	Lab
37	100			Penet.	Al				
38	110			Penet.	Al				
39	110	Lockheed GA	AFML-68-32	E/C	Al				
40	180	Rockwell B-1	B-1 SPQ Demo	Penet.	Ti	Flat Plate			Production
41	100				"				
42	100				Al				
43	100				"				
44	100				Ti				
45	100				Steel			Corrosive En. As Machined	
46	200				Al				
47	200			Penet.	Ti	Angle Chan.			
48	100			Mag. Part.	Steel	Flat Plate			
49	300			Ultra.	Ti	Welded Flat			
50	200			"	Steel				
51	200			Ultra.	Steel				
52	130			Penet.	Ti				
53	127			Penet.	Al				
54	126			Mag. Part.					
55	137			E/C					
56	48	Lockheed GA	AFML-TR-68-32	Mag. Part.	Steel	Cylinder	Fat. Crack	As Machined	Lab
57	50								
58	100			X-Ray	Steel	Cylinder			
59	419	Rockwell ISD	Space Shuttle	X-Ray	Al	Flat Plate		Etched	Lab
60	419			Penet.	Al	"			
61	419			Penet.	Al	"			
62	18	Boeing 707	Center Wing	Eddy Current	Al	"	Fatigue Crack	Fas. Hole	Field
63	20								
64	11								
65	11								
66	19								
67	127		Left Wing						
68	159								
69	152								
70	154	Boeing 707	Left Wing	Eddy Current					

GENERAL DYNAMICS

Fort Worth Division

TABLE 1 DATA SET LISTING
(Continued)

TABULATION SHEET

DEPARTMENT 08
FWP 2545-0-04

Data Set No.	No. of Data Points	Company	Data Source	NDE Method	Material	Part Geometry	Flaw Type	Specimen History	Inspection Environment
71	153	Boeing 707		Eddy Current		Left Wing (H)	Fat.	As Machined	Field
72	150					Lower Wing S			
73	88								
74	88								
75	150					Right Wing			
76	191								
77	244								
78	197								
79	190								
80	197								
81	45	Boeing Comm.	AFML-TR-74-241	Liquid Penet.	Steel	Flat Bar	Compr.		Prod.
82	114				Al	Tandem T			
83	69				Steel	Sol.Thd.Cyl.			
84	48					Hol.Fil.Cyl.			
85	95					Flat Bar	H2EMBR		
86	57					Str.Hol.Cyl.	Compr.		
87	175					Str.Sol.Cyl.			
88	31					Flat Bar	Grind		Lab.
89	187				Al	Tandem T	Compr.		
90	115				Steel	Sol.Thd.Cyl.			
91	95					Hol.Fil.Cyl.			
92	72					Flat Bar	H2EMBR		
93	32					Hol.Str.Cyl.	Compr.		
94	87					Sol.Fil.Cyl.			
95	92					Str.Hol.Cyl.			
96	47			Ultrasonics		Flat Bar	Grind		Prod.
97	170				Al	Tandem T	Compr.		
98	40				Steel	Sol.Thd.Cyl.			
99	47					Hol.Fil.Cyl.			
100	84					Flat Bar	H2EMBR		
101	65					Hol.Str.Cyl.	Compr.		
102	89					Sol.Fil.Cyl.			
103	122					Sol.Str.Cyl.			
104	144					Sol.Str.Cyl.			Lab
105	87	Boeing Comm.	AFML-TR-74-241	Ultrasonics	Steel	Sol.Fil.Cyl.	Compr.		Lab

TABLE 1 DATA SET LISTING
(Continued)

TABULATION SHEET

DEPARTMENT OF
FWP 2645-9-84

Data Set No.	No. of Points	Company	Data Source	NDE Method	Material	Part Geometry	Flaw Type	Specimen History	Inspection Environment
106	47	Boeing	AFML-TR-74-241	1 Ultrasonics	Steel	Hol.Str.Cyl.	Compr.	As Machined	Lab
107	108					Flat Bar	H ₂ EMBR		
108	48					Hol.Fil.Cyl.	Compr.		
109	196				Al	Tandem T	"		
110	29				Steel	Flat Bar	Grind		
111	51			X-ray		Sol.Str.Cyl.	Compr.		Prod.
112	19					Sol.Fil.Cyl.	"		
113	40					Str.Hol.Cyl.	"		
114	29					Hol.Fil.Cyl.	"		Prod.
115	67					Flat Bar St.	H ₂ EMBR		
116	11					Sol.Thd.Cyl.	Compr.		
117	123				Al	Tandem T	"		
118	35				Steel	Flat Bar	Grind		
119	18					Sol.Str.Cyl.	Compr.		Lab
120	16					Hol.Fil.Cyl.	"		
121	32					Flat Bar	Grind		
122	14					Sol.Fil.Cyl.	Compr.		
123	14					Str.Hol.Cyl.	"		
124	115			Mag. Part.	Steel	Sol.Str.Cyl.	"		Prod.
125	136			X-ray	Al	Tandem T	"		Lab
126	89			Mag. Part.	Steel	Sol.Fil.Cyl.	"		Prod.
127	59					Hol.Str.Cyl.	"		
128	119					Flat Bar St.	H ₂ EMBR		
129	54					Hol.Fil.Cyl.	Compr.		
130	58					Sol.Thd.Cyl.	"		
131	43					Flat Bar	Grind		
132	43					Flat Bar	"		Lab
133	142					Sol.Str.Cyl.	Compr.		
134	106					Hol.Fil.Cyl.	"		
135	134					Flat Bar St.	H ₂ EMBR		
136	28					Sol.Thd.Cyl.	Compr.		
137	57					Sol.Fil.Cyl.	"		
138	68			Mag. Part.		Hol.Str.Cyl.	"		
139	93			Eddy Current		Sol.Str.Cyl.	"		Prod.
140	65	Boeing	AFML-TR-74-241	"		Sol.Fil.Cyl.	"		Prod.

TABLE 1 DATA SET LISTING
(Continued)

GENERAL DYNAMICS
Fort Worth Division

NO. OF
TABULATION SHEET

DEPARTMENT 88
FMP 2045-0-04

Data Set No.	Data Points	Company	Data Source	NDE Method	Material	Part Geometry	Flaw Type	Specimen History	Inspection Environment
141	21	Boeing	Comm.AFML-TR-74-241	Eddy Current	Steel	Str.Hol.Cyl.	Compr.	As Machined	Prod.
142	72				Steel	Flat Bar St.	H ₂ EMBR		
143	29				Al	Hol.Fil.Cyl.	Compr.		
144	219				Al	Tandem T			
145	19				Steel	Flat Bar St.	Grind		Lab
146	29				"	"	"		
147	174				Al	Tandem T	Compr.		
148	141				Steel	Str.Sol.Cyl.	"		
149	93					Hol.Fil.Cyl.	"		
150	77					Flat Bar St.	H ₂ EMBR		
151	99					Sol.Fil.Cyl.	Compr.		
152	50	Boeing	Comm.AFML-TR-74-241	Eddy Current		Str.Hol.Cyl.			
153	416	Martin Mar.	MCR-75-212	Penetrant		Int.Stf.Pan.	Fatigue Crack	Unetched Etched	
154						"	"		
155						"	"	Riveted Pl.	
156				Ultrasonics		"	"	Unetched Etched	
157						"	"		
158						"	"	Riveted Pl.	
159				Eddy Current		"	"	Unetched Etched	
160				"		"	"		
161				"		"	"	Riveted Pl.	
162				"		Top in Butti welded Panel		As welded,etched	
163				"		"	"	Scarfed	
164				"		"	"	90% proofload	
165				X-ray		"	"	As welded,etched	
166				"		"	"	Scarfed	
167	416			"		"	"	90% Proofload	
168	191			Penetrant		"	"	As welded,etched	
169				"		"	"	Scarfed	
170				"		"	"	Scarfed,etched	
171	191			"		"	"	90% Proofload	
172	548			Ultrasonics		"	"	As welded	
173	416			"		"	"	Scarfed	
174	548			"		"	"	90% Proofload	
175	158	Martin-Mar.	MCR-75-212	Penetrant	Steel	Fat.Crack (Long)		As machined	Lab

TABLE 1 DATA SET LISTING
(Continued)

No. TABULATION SHEET

DEPARTMENT 88
FWP 2648-6-54

Data Set No.	Data Points	Company	Data Source	NDE Method	Material	Part Geometry	Flaw Type	Specimen History	Inspection Environment
176	159	Martin Marietta (Denver)	MCR-75-212	Penetrant	A1	Flat Plate (Weld w/crown)	Fatigue Crack (Long)	Etched Proof Load	Lab
177	"			Ultrasonic				As Machined Etched	
178	261			"				Proof Load	
179	159			"				As Machined Etched	
180	261			Eddy Current				Proof Load	
181	159			"				As Machined Etched	
182	"			"				Proof Load	
183	"			"				As Machined Etched	
184	"			X-ray				Proof Load	
185	"			"				As Machined Etched	
186	"			"				Proof Load	
187	161			Penetrant				As Machined Etched	
188	"			"				Proof Load	
189	"			"				As Machined Etched	
190	185			Ultrasonic				Proof Load	
191	161			"				As Machined Etched	
192	185			"				Proof Load	
193	161			Eddy Current				As Machined Etched	
194	"			"				Proof Load	
195	"			"				As Machined Etched	
196	"			"				Proof Load	
197	"			X-ray				As Machined Etched	
198	"			"				Proof Load	
199	287			Penetrant				As Machined Etched	
200	"			"				Proof Load	
201	"			"				As Machined Etched	
202	311			Ultrasonic				Proof Load	
203	287			"				As Machined Etched	
204	311			"				Proof Load	
205	287			Eddy Current				As Machined Etched	
206	"			"				Proof Load	
207	"			"				As Machined Etched	
208	"			X-ray				Proof Load	
209	"			"				As Machined Etched	
210	"			"				Proof Load	

TABLE 1 DATA SET LISTING
(Continued)

TABULATION SHEET
No. Of

DEPARTMENT 06
FMP 2845-6.0A

Data Set No.	Data Points	Company	Data Source	NDE Method	Material	Part Geometry	Flaw Type	Specimen History	Inspection Environment
211	53	Martin-Mar.	MCR-75-212	Penetrant	Al	Flush Weld	Crack (Tran)	Etched	Lab
212				"				90% Proofload	
213								As Machined	
214				Ultrasonic				Etched	
215				"				90% Proofload	
216								As Machined	
217				Eddy Current				Etched	
218				"				90% Proofload	
219				"				As Machined	
220				X-ray				Etched	
221				X-ray				90% Proofload	
222	53	Martin-Mar.	MCR-75-212	X-ray	Al	Flat Plate	Fatigue Crack (Tran)	90% Proofload	Lab

Considerable effort has been expended in the modification and updating of the data file format and contents for their utilization in this program. Continual corrections have been made from surveys and personal contacts to improve the accuracy of the data and associated NDT parameters. The cover sheet format identifying the pertinent information on each data set has been modified to expedite data pooling and information retrieval. Modifications to the entire data bank system were also made to provide flexibility for future additions. An example of the cover sheets for the ultrasonic method is given in Table 2. The data set number (DSN) and inspection date comprise the heading in each table. The last entry in the heading shows the date on which the cover sheets for the NDT techniques of eddy current, radiography, magnetic particle and penetrant methods are presented in Tables A-1 to A-4 respectively in Appendix A.

An industry NDE facility survey was conducted during the program period. The objectives of the survey were: (1) to acquire detailed information on the data contributed by each facility, (2) to obtain general information on NDT equipment, reference standards, and inspector levels in each facility, and (3) to solicit opinions from NDT personnel in each facility in the design of an optimum demonstration program. Martin Marietta Corporation/Aerospace Division, the B-1 and the Space Division of Rockwell International Corporation were objects of the survey. Useful information pertaining to the B-1 demonstration program such as the history, specimen type, flaw type and inspection procedures were furnished by NDE personnel at the B-1 Division of the Rockwell International Corporation. Details of the penetrant inspection in that demonstration program were discussed during the survey. One of the important conclusions from the discussion was that the inspection capability should not be treated as a monotonic function of the sensitivity of the penetrant. Whether the fatigue crack was the proper flaw type to be used in specimens for demonstration program designed to verify production inspection was also discussed. At the Space Division of the Rockwell International Corporation, the Space Shuttle NDE demonstration program was discussed in detail. Procedures for certifying penetrants for the Space Shuttle inspection were provided by the Space Division personnel. Details on the fabrication of the flat plate specimens and specimens with complex geometries were provided by personnel at the Aerospace Division of Martin Marietta Corporation.

TABLE 2 RELEVANT NDE PARAMETERS FOR ULTRASONIC METHOD

DSN :	6	INSP. DATE : 1974	:	ULTRASONIC	01-MAR-77
1>	5	NDE METHOD	:	MARTIN MARIETTA	
2>	4	COMPANY NAME	:	DETECTION OF FATIGUE CRACKS	
3>	2	PROGRAM ID	:	ALUMINUM 2219-T87	
4>	1	MATERIAL	:	FATIGUE CRK./NO CYCLE/REMOVE EDM	
5>	1	DEFECT TYPE	:	NA	
6>	0	OPERATOR ID	:	QUALIFIED ACCORDING TO MIL-STD-453	
7>	7	QUALIFICATION	:	PRODUCTION	
8>	1	INSP. ENVIRONMENT	:	STD. INSP. / MULTIPLE FLAW SPEC.	
9>	2	INSP. PROCEDURE	:	RECORD OF METER OR SCOPE DISPLAY	
10>	4	DATA RECORD TYPE	:	MECHANICAL SCAN AND INDEX	
11>	3	MODE OF SCAN	:	FLAT BOTTOM HOLE	
12>	3	REFERENCE STANDARD	:	AIR	
13>	1	DEFECT MATERIAL	:	FLAT PLATE	
14>	1	PART GEOMETRY	:	FLAT PLATE SURFACE FLAW	
15>	1	DEFECT LOCATION	:	SPECIMEN CUT OPEN	
16>	1	DEFECT VERIFICATION	:	AS MACHINED OR WELDED	
17>	1	SAMPLE HISTORY	:	SHEAR : PULSE ECHO	
26>	1	ULTRASONIC METHOD	:	10 MEG HZ.	
27>	4	FREQUENCY	:	FLAT FACE , .95 CM	
28>	1	XMITTER TYPE/SIZE	:	FLAT FACE , .95 CM	
29>	1	RECEIVER TYPE/SIZE	:	UM 715 , 10N PULSER/RECIEVER	
30>	1	EQUIPMENT TYPE	:	NA	
31>	0	GAIN SET % OF SS	:	NA	
32>	0	ALARM SET % OF SS	:	WATER IMERSION	
33>	1	TYPE OF COUPLING	:	27.25 DEG.	
34>	1	ANGLE OF INCIDENCE	:	318 CM (125 IN.)	
35>	1	INDEX INTERVAL	:	SF:NO TK:NO	
MCL:NO		CD: Y MCD: Y			

From the facilities included in the survey, first hand information was obtained on the NDE equipment, reference standards, and inspector levels. It was found that most of the aerospace companies were purchasing newer automated NDE equipment to replace the older manual models. The choice of reference standards was still a baffling problem to most of the NDE community. The results of the survey on inspector level strengthened the previous opinion that nondestructive testing inspectors at the same level of technical classification may differ significantly in the degree of skill. Before conducting a demonstration, the inspectors were usually screened or updated in training. The information acquired in the survey of the facilities, as well as similar information gathered in-house at the Fort Worth Division of General Dynamics Corporation, formed the background data for the translation model development and served to mold the design of the optimum demonstration program. Valuable opinions were obtained from personnel in these facilities in the areas of flaw type, flaw location, NDE methods applicable to critical flaws, and the specimen geometry for most commonly occurring flaws in certain types of aircraft (e.g. B-1). Corrections in the NDE reliability data were made in some instances which had the impact of increasing the accuracy of the NDE parametric relationships and translation model development in this program.

Several potential sources for the expansion of the reliability data bank have been identified during the course of the program. The NDE facilities participating in the NASA Space Shuttle NDE Program generated additional data on steel components. Much needed magnetic particle inspection data were included in this category of data. A program titled "Reliability of Non-destructive Inspection on Aircraft Structures" is currently being conducted at Lockheed-Georgia Company under the sponsorship of AFLC at Kelly Air Force Base. The field inspection results from the NDI reliability program will be available in 1978. These inspection results will supplement the data bank file in the field and depot inspection category. Results from an on-going AF program "Quantitative Evaluation of Penetrant Inspection Materials and Procedures" (Contract No. F33615-76-C-5166) will also be available in 1977. In addition to the above on-going programs, the analysis of results from an ASNT-sponsored round robin program on ultrasonic inspection of steel and aluminum parts will be completed in the fall of 1977. The reliability data from these four programs will substantially enlarge the existing data file.

S E C T I O N I V

M E T H O D O L O G Y

In addition to a straightforward method of point estimate plot of the probability of detection, two data fitting techniques were used in the analysis. These two techniques, linear regression analysis and adaptive learning, provided the mathematical tools in fitting the reliability data in well behaved probability of detection curves. The parametric study and translation model development were based on the successful applications of these techniques. In the following sections, a brief introduction of each of the two techniques will be given. Details of the methodologies and associated computer software programs are presented in Appendix B.

4.1 LINEAR REGRESSION ANALYSIS

The development of the multiple linear regression analysis technique and the development procedure of a linear translation model will be discussed in the following paragraphs.

4.1.1 Introduction to Multiple Linear Regression

The purpose of using multiple linear regression techniques is to assist in the development of an informative model for the POD as a function of several NDE variables. A good model must "fit" the data reasonably well. (However, undue concern about "fitness" should be avoided because it is easy to construct models which fit sets of data with no error and yet are almost totally uninformative). It should isolate the effects of the various NDE variables as much as possible and for this specific application its form must be suitable for transfer function development.

The general principle that motivates regression analysis is that the variability in the observations of the dependent variable (POD) can be narrowed (or accounted for when the variability is measured numerically) by knowledge of one or more of the independent variables (crack length, specimen geometry, specimen thickness, etc.) that were observed along with the POD. It should be kept in mind that the NDE personnel should be in control of building the model and his knowledge of NDE variables should be reflected in the final model because regression procedures do not automatically produce meaningful and valid results.

4.1.2 Formal Development

The general linear model can be presented most concisely in terms of matrix operations as follows:

$$Y = X\beta + e$$

where Y is a $N \times 1$ vector of observations of the dependent variable,

X is a $N \times P$ matrix which specifies the form in which P independent variables are related to Y ,

β is a $P \times 1$ vector of unknown coefficients which are to be estimated from the data, and

e is a $N \times 1$ vector of errors which can only be observed explicitly if β is known.

There are several assumptions underlying a regression analysis, as follow:

1. The components of X are constants which are measured without error.
2. $E(e) = 0$, that is, the average error is 0.
3. $COV(e) = \sigma^2 I_N$, where σ^2 is a constant and I_N is the $N \times N$ identity matrix (the covariance matrix has the variances of the errors on the main diagonal and the covairances of the errors in the off-diagonal positions, so the above form of the covariance matrix is a method of stating the error variances are homogeneous and the errors are uncorrelated).

The additional assumption of normally distributed errors permits one to test hypotheses about the coefficients (components of β) and to establish confidence limits or prediction intervals about the regression line or surface.

The criterion which is used to determine the coefficients is the least squares criterion. Some notation and basic facts are needed to outline the least squares criterion:

\hat{Y} = the value predicted by the model for Y .

$Y - \hat{Y}$ = the amount the model misses in predicting Y , called a residual, R ,

$$R = Y - \hat{Y},$$

$$\hat{\beta} = \text{the estimate of } \beta,$$

$$\hat{Y} = X\hat{\beta},$$

$R'R$ = the sum of the squares of the components of R where a primed superscript of a matrix indicates the transpose of the matrix.

The least squares criterion is to select the components of $\hat{\beta}$ so that $R'R$ is a minimum. After algebraic manipulation it can be shown that:

$$\hat{\beta} = (X'X)^{-1} X'Y \text{ whenever } X'X \text{ has an inverse}^{(4)}.$$

In some instances it is appropriate to use $\frac{R'R}{N-P}$ as an estimator of σ^2 (this will be discussed in more detail in a later section).

Since probabilities are being predicted a truncation rule must be used which truncates predicted probabilities larger than 1, to 1 exactly and which truncates negative probabilities to 0.

A simple example will illustrate some of these matrix operations. Suppose there are 5 observations of (X,Y) and the linear relationship between X and Y is to be determined. The model is

$$\begin{bmatrix} Y_1 \\ Y_2 \\ Y_3 \\ Y_4 \\ Y_5 \end{bmatrix} = \begin{bmatrix} 1 & X_1 \\ 1 & X_2 \\ 1 & X_3 \\ 1 & X_4 \\ 1 & X_5 \end{bmatrix} \begin{bmatrix} \beta_0 \\ \beta_1 \end{bmatrix} + \begin{bmatrix} e_1 \\ e_2 \\ e_3 \\ e_4 \\ e_5 \end{bmatrix}.$$

The transpose of the matrix X is: $X' = \begin{bmatrix} 1 & 1 & 1 & 1 & 1 \\ X_1 & X_2 & X_3 & X_4 & X_5 \end{bmatrix}$.

The product of the matrices X' and X is:

$$(X'X) = \begin{bmatrix} 5 & \sum X_i \\ \sum X_i & \sum X_i^2 \end{bmatrix}.$$

The inverse of the product is:

$$(X'X)^{-1} = \begin{bmatrix} \frac{\sum X_i^2}{Q} & , & \frac{-\sum X_i}{Q} \\ \frac{-\sum X_i}{Q} & , & \frac{5}{Q} \end{bmatrix}, \text{ where } Q = 5 \sum X_i^2 - (\sum X_i)^2 .$$

The product of the matrices X' and Y is:

$$X'Y = \begin{bmatrix} \sum Y_i \\ \sum X_i Y_i \end{bmatrix} .$$

Therefore, the estimate of the coefficient vector $\hat{\beta}$ is:

$$\hat{\beta} = \begin{bmatrix} \hat{\beta}_0 \\ \hat{\beta}_1 \end{bmatrix} = \begin{bmatrix} \frac{(\sum X_i^2) \sum Y_i - (\sum X_i Y_i)(\sum X_i)}{Q} \\ \frac{5 \sum X_i Y_i - (\sum X_i)(\sum Y_i)}{Q} \end{bmatrix} .$$

4.1.3 Preliminaries to Model Specification

Some terminology and basic concepts from experimental statistics, illustrated by an example from the current data base, are needed before the problem of model specification is attacked in the next section. Suppose that the only variables which have an effect on the POD are crack length (9 intervals) and specimen geometry (geometries 1, 2 and 3). There are 27 combinations of crack length and geometry which can be displayed in a two-way table (a specific combination in the table will be referred to as a cell). The POD observed in each cell is assumed to be the sum of several components. A constant which is the same in all cells is the first component. The next components are a contribution from the crack length interval the cell is in, a contribution from the geometry the cell is in, a contribution from the combination of geometry and crack length the cell is in and finally an error which cannot be observed. To illustrate this point analytically, let μ be the constant, α_i , $i = 1, 2, \dots, 9$ be the crack length contribution, β_j , $j = 1, 2, 3$ be the geometry contribution, $(\alpha\beta)_{ij}$ and e_{ij} , $i = 1, 2, \dots, 9$, $j = 1, 2, 3$ be the crack length geometry combination contribution and error contribution respectively. Table 3 summarizes the above formulation.

The α_i 's and β_j 's are referred to as main variable effects because they are used for comparing the PODs of one crack length with the PODs of another crack length, or for comparing PODs on specimens with different geometries. The $(\alpha\beta)_{ij}$'s are referred to as two-factor interactions. If all the variables are fixed, except one, and if comparisons are made among the levels of that variable then these comparisons can be called simple comparisons. For example, the difference in PODs for crack length 3 and crack length 4 at geometry 1 is a simple comparison. There are a very large number of simple comparisons that can be made. The only theoretical problem with simple comparisons is that the inferences from them are very restricted or narrow. Comparisons of levels of one variable "averaged" over all the levels of all the other variables, can be called main comparisons. In the above example if the POD for crack length 3 is compared with the POD for crack length 4, averaged over all three geometries then the comparison is a main comparison with much broader inference possible.

Main comparisons must be used with caution when interactions are present, for example, the MEAN of the PODs at crack length 3 (neglecting error terms) is $\mu + \alpha_3 + \frac{\beta_1 + \beta_2 + \beta_3}{3} +$

$\frac{(\alpha\beta)_{31} + (\alpha\beta)_{32} + (\alpha\beta)_{33}}{3}$, while the MEAN of the PODs at

TABLE 3
SUMMARY OF CONTRIBUTIONS IN LINEAR REGRESSION ANALYSIS

CRACK LENGTH (i)									
	1	2	3	4	5	6	7	8	9
1	$\mu + \alpha_1 + \beta_1$ $+(\alpha\beta)_{1,1}$ $+e_{1,1}$	$\mu + \alpha_2 + \beta_1$ $+(\alpha\beta)_{2,1}$ $+e_{2,1}$	$\mu + \alpha_3 + \beta_1$ $+(\alpha\beta)_{3,1}$ $+e_{3,1}$	$\mu + \alpha_4 + \beta_1$ $+(\alpha\beta)_{4,1}$ $+e_{4,1}$	$\mu + \alpha_5 + \beta_1$ $+(\alpha\beta)_{5,1}$ $+e_{5,1}$	$\mu + \alpha_6 + \beta_1$ $+(\alpha\beta)_{6,1}$ $+e_{6,1}$	$\mu + \alpha_7 + \beta_1$ $+(\alpha\beta)_{7,1}$ $+e_{7,1}$	$\mu + \alpha_8 + \beta_1$ $+(\alpha\beta)_{8,1}$ $+e_{8,1}$	$\mu + \alpha_9 + \beta_1$ $+(\alpha\beta)_{9,1}$ $+e_{9,1}$
2	$\mu + \alpha_1 + \beta_2$ $+(\alpha\beta)_{1,2}$ $+e_{1,2}$	$\mu + \alpha_2 + \beta_2$ $+(\alpha\beta)_{2,2}$ $+e_{2,2}$	$\mu + \alpha_3 + \beta_2$ $+(\alpha\beta)_{3,2}$ $+e_{3,2}$	$\mu + \alpha_4 + \beta_2$ $+(\alpha\beta)_{4,2}$ $+e_{4,2}$	$\mu + \alpha_5 + \beta_2$ $+(\alpha\beta)_{5,2}$ $+e_{5,2}$	$\mu + \alpha_6 + \beta_2$ $+(\alpha\beta)_{6,2}$ $+e_{6,2}$	$\mu + \alpha_7 + \beta_2$ $+(\alpha\beta)_{7,2}$ $+e_{7,2}$	$\mu + \alpha_8 + \beta_2$ $+(\alpha\beta)_{8,2}$ $+e_{8,2}$	$\mu + \alpha_9 + \beta_2$ $+(\alpha\beta)_{9,2}$ $+e_{9,2}$
3	$\mu + \alpha_1 + \beta_3$ $+(\alpha\beta)_{1,3}$ $+e_{1,3}$	$\mu + \alpha_2 + \beta_3$ $+(\alpha\beta)_{2,3}$ $+e_{2,3}$	$\mu + \alpha_3 + \beta_3$ $+(\alpha\beta)_{3,3}$ $+e_{3,3}$	$\mu + \alpha_4 + \beta_3$ $+(\alpha\beta)_{4,3}$ $+e_{4,3}$	$\mu + \alpha_5 + \beta_3$ $+(\alpha\beta)_{5,3}$ $+e_{5,3}$	$\mu + \alpha_6 + \beta_3$ $+(\alpha\beta)_{6,3}$ $+e_{6,3}$	$\mu + \alpha_7 + \beta_3$ $+(\alpha\beta)_{7,3}$ $+e_{7,3}$	$\mu + \alpha_8 + \beta_3$ $+(\alpha\beta)_{8,3}$ $+e_{8,3}$	$\mu + \alpha_9 + \beta_3$ $+(\alpha\beta)_{9,3}$ $+e_{9,3}$

crack length 4 (neglecting error terms) is $\mu + \alpha_4 + \frac{\beta_1 + \beta_2 + \beta_3}{3} + \frac{(\alpha\beta)_{41} + (\alpha\beta)_{42} + (\alpha\beta)_{43}}{3}$. The difference

between these two MEANS is $\alpha_3 - \alpha_4 + \frac{(\alpha\beta)_{31} + (\alpha\beta)_{32} + (\alpha\beta)_{33}}{3} - \frac{(\alpha\beta)_{41} + (\alpha\beta)_{42} + (\alpha\beta)_{43}}{3}$. If there is no interaction,

this comparison is exactly $\alpha_3 - \alpha_4$ as desired, but if interaction is present the comparison of MEANS is "contaminated" by the interaction terms.

When the data is examined, it is seen that some of the effects cannot be estimated because of lack of data in some cells. Consider the crack length and geometry data (from the ultrasonic data base):

Crack Length Interval

	1	2	3	4	5	6	7	8	9	Average		
ometry	1	.23	.36	.47	.79	.89	.88	.95	.96	.98	.774	(M = Missing)
	2	M	M	M	.29	.59	.77	.91	.96	.88	.745	
	3	M	M	M	.83	.38	.38	.77	.95	.93	.724	

(NOTE: The average for each geometry cannot be computed directly from the table, because there are unequal numbers of observations in each cell).

$(\alpha\beta)_{12}$ appears only in cell (1,2) which is missing, hence there is no logical way to estimate $(\alpha\beta)_{12}$. In cell (1,2) there is also μ , α_1 , β_2 but they appear in other cells which are not missing and thus can be estimated. A model which includes parameters that are not estimateable can only add confusion to the final results.

This data also illustrates that averaging over levels of variables without accounting for the pattern of missing observations can lead to erroneous conclusions. The MEAN POD for geometry 1 is .774, and for geometry 2 is .745, but the observations for a crack lengths 1, 2 and 3 (where the POD would be expected to be small) are missing for geometry 2. If there were observations available for these missing crack lengths, the

differences that were observed would have been much larger. The model of the form discussed in this section accounts for the missing observations as well as any other model. Keeping these concepts and problems in mind, some specific models are discussed in the next section.

4.1.4 Building the Appropriate Linear Model

Determining the form and complexity of the model are important first tasks in the model development. Consider the form of the model first. If there is some knowledge of the relationship between the POD and any of the NDE variables this should be utilized in the model. If it were known that POD increased exponentially with crack length, a coefficient could be included that estimates the rate of exponential increase. For this specific problem no information is assumed to be known about the form of the relationship between any NDE variable and the POD, hence two general types of linear models were considered. These two models are the polynomial regression model and the analysis of variance (AOV) model (discussed and illustrated in the previous section) implemented through regression techniques. An example will help illustrate the similarities and differences between the two models. Suppose a model for POD as a function of only specimen geometry is desired, and further suppose there are eight specimen geometries in the data base. The polynomial regression model written without the matrix form would be:

$$y = \beta_0 + \beta_1 X + \beta_2 X^2 + \dots + \beta_7 X^7 + e$$

where,

y = POD observed,

β_i , $i = 0, \dots, 7$ are unknown coefficients to be estimated,

$X = 1, 2, \dots, 8$ depending on the geometry (other codings of the X 's are also permissible),

e = unobserved random error.

The analysis of variance model would be:

$$y = \mu + a_1 I_{x_1} + a_2 I_{x_2} + \dots + a_8 I_{x_8} + e$$

where

y = POD observed,

μ , a_i , $i = 1, \dots, 8$ are unknown coefficients to be estimated,

I_{x_i} , $i = 1, \dots, 8$ are indicator variables equal to 1 when the geometry is X_i and equal to 0 otherwise,

e = unobserved random error.

(NOTE: For any specific geometry exactly one of the indicator variables is equal to 1.)

The indicator variables are usually dropped from the notation after they have been formally introduced, although they are understood to still be present. The AOV model discussed informally in the previous section does not display the indicator variables explicitly. The AOV model is most suitable for classification variables (variables where the numerical value assigned to the variable is arbitrary), because the coefficients can be used in a straightforward manner to compare levels of variables (i.e., comparing flat plate specimens with integrally stiffened panel specimens). It should be noted that these two models will provide exactly the same "fit" of the data, but the AOV model provides an easier and clearer method of developing a translation model.

The second task is selecting the complexity of the model (the AOV model was selected in the previous step). The general principle used is: the simplest model which fits the data reasonably well and which is most suitable for translation model development, is the best model. The best method of estimating the error variance cannot be used (discussed in the next section) so high order interactions must be used to estimate the noise level. There are several two-factor interactions that are expected to be large (those with crack length) and several which are important for translation model development (those variables interacting with specimen geometry) that would be included in the model if they were estimateable, but the pattern of missing observations in the data base is a limiting factor (this will be discussed in the data problems section). There is still some flexibility left so that after the initial model is fitted to the data, revisions can be made which drop variables or variable interactions having little impact on the POD.

4.1.5 Error Determination

If all the NDE variables are fixed at some level and the POD is observed repeatedly, then the scatter in the data must be due to error variability (recall the error variance is denoted by σ^2 in the model), which may be thought of as the "noise" level in the data. However, in the present data base this information is not available. If the higher order interactions do not exist, the amount of variability attributed to them (in an analysis of variance summary) is really error variability. In the present data all three-factor and higher order interactions were pooled together and used as an estimate of σ^2 .

The optimal method of estimating σ^2 cannot be used because there are no repeated observations of POD under identical test conditions. The best alternative is to pool higher-order interactions to estimate σ^2 . The decision to pool all three-factor or higher interactions is made from practical considerations. First, the pattern of observations is irregular with missing combinations of the factors, some three-factor interactions cannot be estimated at all. Secondly, there is a limit on the number of coefficients that the computer can estimate, the inclusion of three-factor or higher interactions increases dramatically the number of coefficients that must be estimated. The result is that main effects and two-factor interactions would have to be sacrificed in order to estimate the higher order interactions. Lastly, the inclusion of three-factor or higher order interactions would increase the complexity of the tables of coefficients and some loss of clarity would surely result.

When one examines the values predicted by a regression equation there is another type of error that must be considered, error in estimating the regression coefficients. Knowledge of the magnitude of this error allows the computation of confidence or prediction bounds to be placed on the estimated regression equation. In the regression model all the information about the variances and covariances of the estimated coefficients is contained in the covariance matrix of $\hat{\beta}$, which is $(X'X)^{-1} \sigma^2$. It is to be noted that the adaptive regression does not specify the model which is being fit to the data and hence is not able to estimate the variability due to error in estimation of its regression coefficients. This is a serious weakness because no legitimate confidence bounds can be placed on the regression equation.

4.2 ADAPTIVE LEARNING TECHNIQUES

The adaptive analysis of the NDE reliability data consists of three phases; a training and testing set formation, hyper-surface fitting and analysis. A simplified explanation of these three phases is given in the following paragraphs. Flow charts, mathematical equations and users' instructions for these computer programs are presented in Appendix B.

4.2.1 Introduction to Adaptive Learning Techniques

Adaptive learning is a mathematical technique for solving problems where the dependent variables depend in an unknown way upon many independent variables and the relationship can be expressed as a multinomial over some bounded regions of the independent variables.

The adaptive learning approach has successfully been implemented to predict the diameters of flat bottom holes⁽⁵⁾. The nonlinear adaptive learning network correctly classified 46 out of 48 flat bottom hole defects. The largest error in the classification was for flat bottom holes with diameters less than 1/64 inch. The accuracy of predicting true hole diameter was 97.2 percent.

The adaptive learning network has been used to detect and measure subsurface fatigue cracks⁽⁶⁾. The adaptive learning network detected and measured the subsurface fatigue crack in the size range of 0 to 279 mils to within 70 percent of their nominally characterized length.

4.2.2 Adaptive Learning Logic

The adaptive learning method deals with high degree polynomials in many variables and performs a stochastic search to evaluate the polynomial coefficients and then determine the output of a given net connectivity pattern.

The data base consisted of 46,369 data points with each point defined as an individual inspection performed by an operator with the associated NDT parameters such as environment, specimen finish, or crack length. It will be noted that crack length was treated as an independent parameter in the analysis. Depending upon the purpose of the analysis, the data points were divided into groups with common NDT parameters (or input variables). Each group of data points was defined as

a vector. Associated with each vector was a point estimate of the detectability which was obtained by dividing the number of detections by the total number of inspections. No confidence level was involved in the point estimate. If the crack length (CL), specimen history (SH), surface finish (SF) and specimen thickness (TK) were selected as the common input variables, then the point estimate (y_t) associated with the vector can be expressed as:

$$y_t = f(CL_i, SH_j, SF_k, TK_l)$$

where i, j, k, l were subscripts signifying the particular range of each NDT parameter. The data base was divided into a training set and a testing set each having an equal number of vectors. It would have been desirable to divide the data base into three sets, and use the third set for evaluation. However, in most cases, the data base was not large enough to be divided into three sets and still retain enough population.

Adaptive learning methodology establishes a polynomial with estimated coefficients which will fit the data. The form of the polynomial is established from the basic connectivity net pattern and the form of polynomial selected for the basic net input.

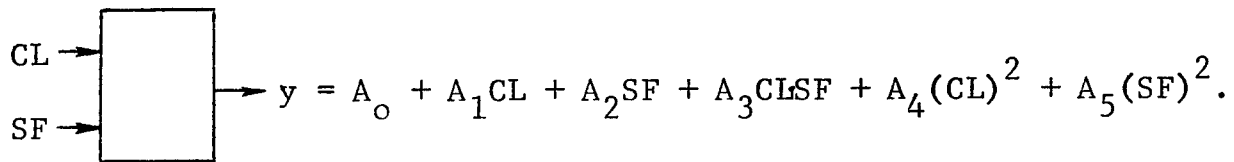
The NDT parameters were grouped into pairs and each pair was fed into a basic net in a predetermined order. The output from the basic nets was one of two types of polynomials as indicated below:

$$A) \quad y = A_0 + A_1X_1 + A_2X_2 + A_3X_1X_2 + A_4X_1^2 + A_5X_2^2$$

$$B) \quad y = A_0 + A_1X_1 + A_2X_2 + A_3X_1X_2$$

where y is the output of the basic net, X_1 and X_2 are input parameters and the A 's are coefficients. For most of the NDE data the complete multinomial of degree two was used. This polynomial when compared to the linear polynomial seemed to better fit the data. A simple example of a basic net using the NDE parameters of crack length (CL) and surface finish (SF) is

shown below:



It should be noted that the predicted point estimate is obtained from the output of the complete network. The basic connectivity net pattern used in this program was a rectangular network with exponential pitch. The number of rows is equal to the number of input parameter pairs. The number of columns were optional.

There are three major types of feed forward nets: rectangular, triangular, and exponential. The effectiveness of the three nets is about the same for a given class of problems, and the decision as to which net to use can usually be made on the grounds of programming ease or computer running time. Since the smallest possible net for a given number of inputs is an exponential net, this net is the most logical choice for a first analysis of a problem. Since the rectangular net can be made with an arbitrary number of columns and since the degree of the highest power terms in the multinomial is roughly proportional to the number of columns in a net, the rectangular net is also a useful net for many problems.

The basis of the fitting program was a stochastic search in which the polynomial coefficients were changed. The predictive point estimate was calculated for each set of coefficients and compared to the true average point estimate of the vectors. The comparison was quantified by a score which is defined as follows:

$$\text{SCORE} = \frac{\sum_{i=1}^N \left[(y_t)_i - (y_p)_i \right]^2}{N}$$

where N is the number of vectors, y_t and y_p are the true point estimate and the predictive point estimate of the detectability respectively.

Initially a score was obtained from the training set vectors by using a random set of coefficients (BTDTR), where N is the number of vectors. After obtaining initial scores the iterative process of determining coefficients for the best fit to the data is started. On the first trial the search resorts to an unguided search. Unguided refers to the selection of a set of bounded random coefficients (ACCUR). After going through the unguided phase a programmable integer (N) option is selected so that the search will not be permitted to go unguided until after N trials. This is referred to as embedding. Using ACCUR a score is computed for the training set, and a new set of coefficients is computed as follows:

$$ADELT = ACCUR - BTDTR.$$

The search will either branch to the training-testing paradigm or the reversal phase described below depending on whether the score has improved.

The reversal phase determines a new set of coefficients as follows:

$$ACCUR = BTDTR - ADELT.$$

ACCUR is checked to insure that the coefficients do not exceed the bounded region. The reversal phase uses ACCUR to calculate the training set score. Depending on the score the search will either branch to the training-testing paradigm or the guided phase of the search.

In the guided phase a new set of coefficients (DELT) is determined from scaled random numbers. These coefficients are used to determine an additional set as follows:

$$ACCUR = BTDTR + DELT.$$

The set of coefficients (ACCUR) is checked to insure that the coefficients do not exceed the bounded region. A score for the training set is computed using ACCUR. The search will either branch to the training-testing paradigm or reversal depending on whether the score has been improved. Any time the training

set score is improved, the search branches to the training-testing paradigm, and the training set coefficients are updated as follows:

$$\text{BTDTR} = \text{ACCUR}.$$

The set of coefficients (BTDTR) is used in conjunction with the test set vectors to determine the score of the testing set. If the test set score is improved, this set of coefficients is retained and the search branches to the acceleration phase.

In the acceleration phase a new set of coefficients is obtained as follows:

$$\text{ADELT} = 2 * \text{DELT}.$$

A set of coefficients is then determined by using ADELT in conjunction with BTDTR as follows:

$$\text{ACCUR} = \text{ADELT} + \text{BTDTR}.$$

The set of coefficients (ACCUR) is used to determine the score of the training set. If the score represents an improvement the search branches to the training-testing paradigm. If no improvement in score is obtained the search will branch to the guided phase. The search continues in this iterative manner described above until the test set score has been reduced to a minimum.

In the final phase of analysis, a parametric study is performed. Results from this study are in the form of graphical plots which show the predicted point estimate as a function of crack length. This calculation can only be made providing the remaining input parameters are fixed. If all the coefficients of a net are known and all the other variables are fixed except crack length, then it is possible to calculate the predicted point estimate as a function of crack length.

SECTION V

MODEL DEVELOPMENT

The linear regression techniques and the adaptive learning techniques described in the previous section were used to develop the translation model. A successful model takes into consideration all the pertinent parameters that influence the inspection results. The inspection results in a NDE facility are expressed in terms of probability of detection for some defect size in a material. The flaw detection capability was related to each of the pertinent NDE parameters by a parametric study. Effects on the inspection results from a combination of the parameters have been included in the model development.

The procedures for the translation model development using the two analytical techniques are presented in this section. The presentation will be conducted in the form of examples to illustrate the development process. Problems encountered during the development for each technique will be discussed and a comparison of the pros and cons of the two techniques will be made. The results of the parametric study and translation model development will be postponed until the next section.

5.1 LINEAR REGRESSION TECHNIQUE IN MODEL DEVELOPMENT

The model development procedures, analysis capabilities, data problems encountered in the analysis, and some general comments will be presented in the following paragraphs.

5.1.1 Translation Model Development

The purpose of the translation model is to compare the PODs for flat plate specimens with the PODs for specimens with more complex geometries. There are two basic methods that can be used to make this comparison, the ratio method and the difference method. For comparison purposes assume that the POD has been modeled as a function of geometry, crack length, surface finish and operator in the following way:

$$Y_{ijkl} = \mu + \alpha_i + \beta_j + \gamma_k + \delta_l + (\alpha\beta)_{ij} + (\beta\gamma)_{jk}$$

where Y_{ijkl} = POD observed with geometry i ,
 crack length j ,
 surface finish k , and
 operator l ,

μ = constant,

α_i = geometry effect ($i = 1$ is flat plate, $i = 2$
 is integrally stiffened panel (ISP)),

β_j = crack length effect,

γ_k = surface finish effect,

δ_l = operator effect,

$(\alpha \beta)_{ij}$ = geometry by crack length interaction,

$(\beta \gamma)_{jk}$ = crack length by surface finish interaction.

For purpose of simplicity in this illustrative example some interaction terms have been deleted. The ratio of POD on flat plate specimens to the POD on integrally stiffened panel specimens is then:

$$\frac{Y_{1 jkl}}{Y_{2 jkl}} = \frac{\mu + \alpha_1 + \beta_j + \gamma_k + \delta_l + (\alpha \beta)_{1j} + (\beta \gamma)_{jk}}{\mu + \alpha_2 + \beta_j + \gamma_k + \delta_l + (\alpha \beta)_{2j} + (\beta \gamma)_{jk}} .$$

(Notice that this ratio is a function of crack length, surface finish and operator.)

The difference between the POD on flat plate specimens and the POD on integrally stiffened panel specimens is:

$$Y_{1 jkl} - Y_{2 jkl} = \alpha_1 - \alpha_2 + (\alpha \beta)_{1j} - (\alpha \beta)_{2j} .$$

Notice the difference is a function of only crack length, which means the inference is much broader. Another important point, suppose there is a large difference between the PODs on flat plate and stiffened panel specimens, the numerator and denominator of the ratio contain several common terms which can obscure the difference. The difference does not have these common factors and is thus much more sensitive to differences in PODs. When a translation model is developed it is desirable to be able to estimate the extent of error in the model. The statistical distribution of the ratio type model is very difficult to obtain but the distribution of the difference type model is much easier.

Most of the information to compute confidence bounds or prediction bounds on the difference in PODs is available in the Statistical Analysis System program package currently in use at different statistical analysis centers.

The only terms in the difference type model that do not cancel during subtraction are the main effects due to geometry differences and interactions of variables with geometry. The implication is that special attention should be given to variable interactions with geometry. The actual model's fit with the corresponding translation model is detailed in the example given in the following section.

5.1.2 Analysis Capabilities

The total amount of variability in the observations of the POD can be measured quantitatively by the sum of squared deviations from the mean POD. Each variable or interaction of variables will explain part of the total variability, the larger the fraction of the variability explained (quantitatively expressed in terms of sums of squared deviations) the larger the impact on the POD. It is most desirable to partition the total variability into disjoint parts, with each part being unambiguously associated with an independent variable. However this is not possible in the present data set because of the pattern of missing data cells. The next best solution is to sequentially partition the total variability. This means that one variable is selected and the amount of the total variability (sum of squares) that it accounts for is computed. Another variable or interaction of variables is then selected and the amount of variability, which remained after the first variable accounted for its portion, is computed. The process continues with each successive variable being given a chance to account for variability left over from the previous variables. This process is obviously "order of variable selection" dependent, hence the most important variables (physically meaningful in the opinion of the NDE personnel) should be included first in this sequential partition. Fortunately the values of the coefficients estimated are independent of order.

In analyzing whether the model which was fitted is adequate, the original observed values of the POD along with the values predicted by the model are printed out. Patterns in the residuals can be used to revise the model if necessary.

If one is willing to assume normality of errors then tests of hypothesis about whether a particular variable is accounting for a significant amount of variability can be performed. Confidence or prediction intervals can be computed to quantify the

amount of error that should be associated with the regression equation (POD model). As mentioned in the error determination section, higher order interactions are pooled together to provide an estimate of error variability. The indications are good that proper selections were made of interactions that were pooled for "error", because the amount of variability accounted for per degree of freedom is 6.6 times higher for the terms in the model than for the "error" terms. In the sample that follows, the coefficients needed for a difference or ratio translation model are presented. In some cases the estimated coefficients are 0 due to lack of observations in critical data cells (this problem and related data problems are discussed in the next section). It is also to be noted that the notation is slightly different, i.e., $(CL)_i$ is used to represent crack length effect, etc.

The data to be discussed in this sample relate to flat plate and integrally stiffened panel specimens, both ultrasonically inspected. There are a total of 259 observed PODs, hence 258 degrees of freedom are associated with the observations. The total amount of variability in the POD (dependent variable) as measured by the sum of squared deviations from the mean is 17.94. In the example below, 65 coefficients were estimated. (See source of variation table below. There is one degree of freedom for every estimated coefficient). By estimating 65 regression coefficients, it is possible to account for 12.37 of the total 17.94 sum of squares, which is about 69 percent of the total variability. This information can be summarized in an "analysis of variance" table, as follows.

<u>Source of Variation</u>	<u>DF</u>	<u>SS</u>	<u>MS</u>
Total (corrected)	258	17.94	
Regression Coefficients	65	12.37	.190
"ERROR"	193	5.57	.029

where

DF = Degrees of Freedom
SS = Sum of Squares
MS = Mean Square = SS/DF.

Detailed Breakdown of Source
of Variation for Regression
Coefficients

	<u>DF</u>	<u>SS</u>
Crack Length	8	7.80
Operator	5	1.07
Geometry	1	.16
Crack Length by Geometry Interaction	5	.68

Detailed Breakdown of Source
of Variation for Regression
Coefficients (Cont'd)

<u>Source of Variation</u>	<u>DF</u>	<u>SS</u>
Crack Length by Thickness interaction	15	.47
Crack Length by Surface finish interaction	25	2.03
Surface Finish by Geometry interaction	1	.04
Specimen History by Geometry interaction	2	.04
Surface Finish by Thickness interaction	<u>3</u>	<u>.08</u>
Total	65	12.37

The linear model for this data can be written in an abbreviated form as:

$$\begin{aligned}
 \text{POD}_{ijklmn} = & \mu + (\text{CL})_i + (\text{OPID})_j + (\text{Geom})_k + (\text{CL} * \text{Geom})_{ik} \\
 & + (\text{CL} * \text{TK})_{il} + (\text{CL} * \text{SF})_{im} + (\text{SF} * \text{Geom})_{mk} + (\text{Hist} * \text{Geom})_{nk} \\
 & + (\text{SF} * \text{TK})_{ml} + \text{error}
 \end{aligned}$$

where

CL = Crack Length
 OPID = Operator ID
 Geom = Specimen Geometry
 TK = Thickness
 SF = Surface Finish
 Hist = Specimen History
 * = Symbol indicating variable interaction effect
 μ = constant

The coefficients for this model follow:

$$\mu = .826$$

CL	1	-.698
	2	-.733
	3	-.193
	4	-.801
	5	-.053
	6	.019
	7	-.095
	8	.081
	9	0

OPID	0	.064
	15	-.025
	16	.070
	17	-.064
	18	.028
	19	0

Geom	1	.106
	2	0

		Geom				TK			
		1	2			0	1	2	3
CL	1	0	0	CL	1	-.009	0	0	0
	2	0	0		2	-.048	0	0	0
	3	0	0		3	-.220	.057	0	0
	4	.656	0		4	-.037	.111	0	0
	5	.019	0		5	-.055	.020	0	0
	6	.019	0		6	-.074	-.037	0	0
	7	.008	0		7	.064	-.127	0	0
	8	-.071	0		8	.010	-.127	0	0
	9	0	0		9	0	0	.067	0

		SF					
		0	1	2	3	4	5
CL	1	0	0	0	0	0	0
	2	0	0	.319	0	.187	0
	3	0	0	-.040	-.771	0	0
	4	0	.430	.013	.033	-.230	0
	5	0	-.449	-.004	.063	-.148	0
	6	0	-.152	-.088	.002	-.137	0
	7	0	.110	.157	.076	0	0
	8	0	-.074	.090	.183	0	0
	9	0	-.038	-.041	0	-.062	0

		Geom				Geom	
		1	2			1	2
SF	0	0	0	Hist	1	-.077	-.036
	1	.063	0		2	0	0
	2	0	0				
	3	0	0				
	4	0	0				
	5	0	0				

		TK			
		0	1	2	3
SF	0	0	0	0	0
	1	0	.159	0	0
	2	0	.015	0	0
	3	0	0	0	0
	4	0	.113	0	0
	5	0	0	0	0

The information above can be summarized in the following tables of differences:

$$(\text{Geom})_1 - (\text{Geom})_2 = .106$$

$$(\text{CL} * \text{Geom})_{i1} - (\text{CL} * \text{Geom})_{i2},$$

i = 1	0
2	0
3	0
4	.656
5	.019
6	.019
7	.008
8	-.071
9	0

$$(\text{SF} * \text{Geom})_{m1} - (\text{SF} * \text{Geom})_{m2},$$

m = 0	0
1	.063
2	0
3	0
4	0
5	0

$$(\text{Hist} * \text{Geom})_{n1} - (\text{Hist} * \text{Geom})_{n2}$$

n = 1	-.041
2	0

It will be noted that the main effect of thickness had virtually no impact on the POD and was dropped from the model, hence no table was necessary. Furthermore, the interactions of thickness by geometry, specimen history and operator ID were also found to be insignificant and were dropped from the model. However, only the thickness by crack length interaction and thickness by surface finish contributions were more sizeable than the main effect of the specimen thickness. These two interaction terms were retained in the model.

An example is given for using the tables of coefficients to estimate the POD. Suppose it is desired to predict the POD on a specimen whose CL = 5, Geom = (flat plate). TK = 1, SF = 2, Hist = 1, and OPID = 15. Begin with the constant $\mu = .826$. Correct this value additively for each variable and variable interaction on the model given on page 36:

(CL) ₅	=	- .053
(OPID) ₁₅	=	- .025
(Geom) ₁	=	.106
(CL*Geom) _{5,1}	=	.019
(CL*TK) _{5,1}	=	.020
(CL*SF) _{5,2}	=	- .004
(SF*Geom) _{2,1}	=	0
(Hist*Geom) _{1,1}	=	- .077
(SF*TK) _{2,1}	=	.015

Totaling the corrections yields + .001, added to $\mu = .826$ gives us .827 as the estimated POD under the conditions stated above.

The POD under the same conditions except that the specimen geometry is integrally stiffened panel rather than flat plate is found in the same manner as for flat plate specimens:

Flat Plate (Geom = 1)

$\mu = .826$

(CL) ₅	=	- .053
(OPID) ₁₅	=	- .025
(Geom) ₁	=	.106
(CL*Geom) _{5,1}	=	.019
(CL*TK) _{5,1}	=	.020
(CL*SF) _{5,2}	=	- .004
(SF*Geom) _{2,1}	=	0
(Hist*Geom) _{1,1}	=	- .077
(SF*TK) _{2,1}	=	.015

.827

ISP (Geom = 2)

$\mu = .826$

(CL) ₅	=	- .053
(OPID) ₁₅	=	- .025
(Geom) ₂	=	0
(CL*Geom) _{5,2}	=	0
(CL*TK) _{5,1}	=	.020
(CL*SF) _{5,2}	=	- .004
(SF*Geom) _{2,2}	=	0
(Hist*Geom) _{1,2}	=	- .036
(SF*TK) _{2,1}	=	.015

.743

Looking down the two lists of corrections, it is seen that the only terms that change are terms involving geometry. Therefore to find the difference in POD on flat plate specimens compared to integrally stiffened panel specimens all the tables on page 37 are not needed. From the tables of differences on page 38 the differences are:

$$\begin{array}{rcl}
 (\text{Geom})_1 - (\text{Geom})_2 & = & .106 \\
 (\text{CL} * \text{Geom})_{5,1} - (\text{CL} * \text{Geom})_{5,2} & = & .019 \\
 (\text{SF} * \text{Geom})_{2,1} - (\text{SF} * \text{Geom})_{2,2} & = & 0 \\
 (\text{Hist} * \text{Geom})_{1,1} - (\text{Hist} * \text{Geom})_{1,2} & = & -.041 \\
 \hline
 \text{Total} & & .084
 \end{array}$$

The difference between the POD for flat plate (.827) and the POD for ISP (.743) is .084. A comment is appropriate here about additional testing which would improve the precision of the estimates derived from the data. Since variables interacting with geometry determine the difference in POD, maximum information on these interactions is desirable. The two-factor interactions can be estimated adequately if data for all combinations of geometries with the other variables are available for analysis.

5.1.3 Data Problems

The most difficult types of data to be analyzed statistically are large sets of data with many variables represented along with an irregular pattern of missing data cells. The first problem is with confounded variable effects. This problem occurs when the effects of variables are being isolated. For example, suppose there are 9 possible combinations of surface finish and thickness but only 3 observed PODs as follows:

		Surface Finish			
		1	2	3	
Thickness	1	Y_{11}	M	M	(M = missing)
	2	M	Y_{22}	M	
	3	M	M	Y_{33}	

When the difference between the Y's (PODs) is being explained, it is impossible to determine whether the differences are due to changes in surface finish or are due to changes in thickness. This is a rather obvious case of complete variable confounding. There are many more subtle cases of confounding in the data. These problems may be identified at least partially by the sequential partition of the total sum of squares. The amount of variability accounted for by thickness, after surface finish has accounted for its portion, is zero. Likewise the amount of variability accounted for by surface finish, after thickness has accounted for its portion, is also zero.

When the confounding is not complete as in the previous example there may be a partial overlapping of variable effects, the "partial sum of squares" is the amount of variability accounted for by a variable after all the other variables have had an opportunity to account for variability.

Another problem can be illustrated with the same example above, namely the problem of nonestimable variable effects caused by missing data cells. In the example above, it may be desirable to estimate thickness effects, surface finish effects and thickness by surface finish interaction effects. However, there is not enough data to estimate all these effects. It is

important to understand that a number could be associated with each of these effects but there would be absolutely no confidence in the result.

All of the analysis problems occur because of missing data cells which result in irregular data patterns. The present study has provided indications of which variables are most significant. If the list of variables could be narrowed to the point where it would be feasible to fill in all or most of the missing variable combinations, the quality of the resulting analysis would be improved immeasurably.

5.1.4 General Comparative Comments

The linear regression approach is to specify the model that is to be fitted to the data and then to estimate the unknown coefficients in the model (as outlined in a previous section). The coefficients are not constrained. If a model is specified with more than 200 coefficients, the present computing capability is exceeded. This is the only motivation for the adaptive approach to regression. The adaptive approach uses a random search method to establish coefficients for terms in a polynomial. The coefficients are functionally related, the exact form of the dependency is determined by the "net" used to generate the polynomial. If a net can be found which induces constraints which are compatible with the data, a reasonably good fit may result.

As was pointed out previously, the coefficients in a polynomial regression model are difficult to use directly to compare the effects of NDE variables. This problem is compounded by the artificial constraints placed on the coefficients by the adaptive procedure. Since no model is specified, and since there are constraints among the coefficients, it is impossible to determine how each estimated coefficient is derived from the data. Therefore it is impossible to estimate the error that is being made in estimating the coefficients. It also follows that confidence intervals or prediction intervals cannot legitimately be placed on the estimated model. The adaptive procedure uses the "training-testing paradigm" to avoid "overfitting" the data. The properties of this procedure have not been defined, especially for cases where many data cells are missing. Further development of the adaptive learning procedures is needed for future incorporation into the standard linear regression procedures.

S E C T I O N V I

R E S U L T S

The results of the parametric study and the translation model development are presented in this section. These results were obtained by using the statistical analysis schemes described in the two previous sections. The parametric relationship and the translation model established in this program were the keystones for the design of an optimum demonstration program. The translation model also makes the interpretation of the capabilities of a facility more realistic.

6.1 NDE PARAMETER STUDY

The successful development of a demonstration program to assess the flaw detection capability of a NDE facility is contingent on a sound knowledge of the parameters that may influence inspection results and their degree of influence. Based on the data compiled in the computer data bank, the identification of pertinent NDE parameters and a study of the parametric relationships were successfully completed.

6.1.1 Parameter Identification

A comprehensive list of pertinent parameters was compiled for each NDE technique considered in this program. The parameters are separated into two general categories: (1) those that are common to all techniques and (2) those that apply specifically to one technique. A cover sheet preceding each data set in the computer data bank contains information about the parameters pertinent to that data set. Each parameter is identified by a computer code with its associated description to facilitate sorting of parameters in parametric studies. A list of the relevant NDT parameters for each of the five techniques, ultrasonic, eddy current, X-ray, magnetic particle, and liquid penetrant, was presented in Table 2 earlier and in Tables A-1 to A-4 in Appendix A.

6.1.2 Parametric Relationships

The parametric relationship between the inspection results and the pertinent NDE parameters was studied by three different analytical methods: (1) optimum probability method (OPM),

(2) point estimate, and (3) statistical fitting schemes. A subjective comparison of different statistical schemes indicated that the OPM scheme appears to be the best procedure among the statistical procedures discussed in Reference 1. However, this scheme is not considered appropriate for the purpose of comparing the influence of different parameters on POD due to the inequality in sample size. Therefore, the point estimate and the statistical fitting schemes were selected for the parametric relationships study

6.1.2.1 Comparison of Statistical Evaluation Schemes

A detailed discussion of the pros and cons of the range, overlapping 60 points, and OPM schemes for calculating the PODs is presented in Appendix C. The results of this subjective evaluation indicated that the OPM scheme is the best procedure because it takes into consideration the problem of unequal sample size and makes full use of the available data. The disadvantage of this scheme is the liberal bias in crack size regions where the POD curve is either flat or increasing slowly.

Qualitative comparisons of the influences of NDE parameters on the inspection capabilities can be obtained by comparing the POD plots as a function of crack length. In these comparisons, the detection threshold (D.T.) is defined as a minimum detectable crack length with a POD above 0.90 at 95 percent confidence level. Figure 1 presents a comparison of the POD difference due to surface finish in integrally stiffened panel specimens for eddy current technique. This figure represents an example of the POD curves available through the computer retrieval and analysis system of the data bank of 222 data sets. These POD curves provide a valid comparison of the influences of NDE parameters from a NDE demonstration program standpoint since MIL-A-83444 requires that a minimum detectable crack size be determined in terms of 0.90 POD at 95 percent confidence level. Although these criteria may not be appropriate from the standpoint of parametric relationship study, they will certainly be instrumental in the application of the parametric relationship towards the translation model development.

6.1.2.2 Point Estimate of POD

In the point estimate comparison, the inspection results for each technique were grouped in 1/8 in. crack length intervals and plotted in the form of histograms for the POD. Analysis of

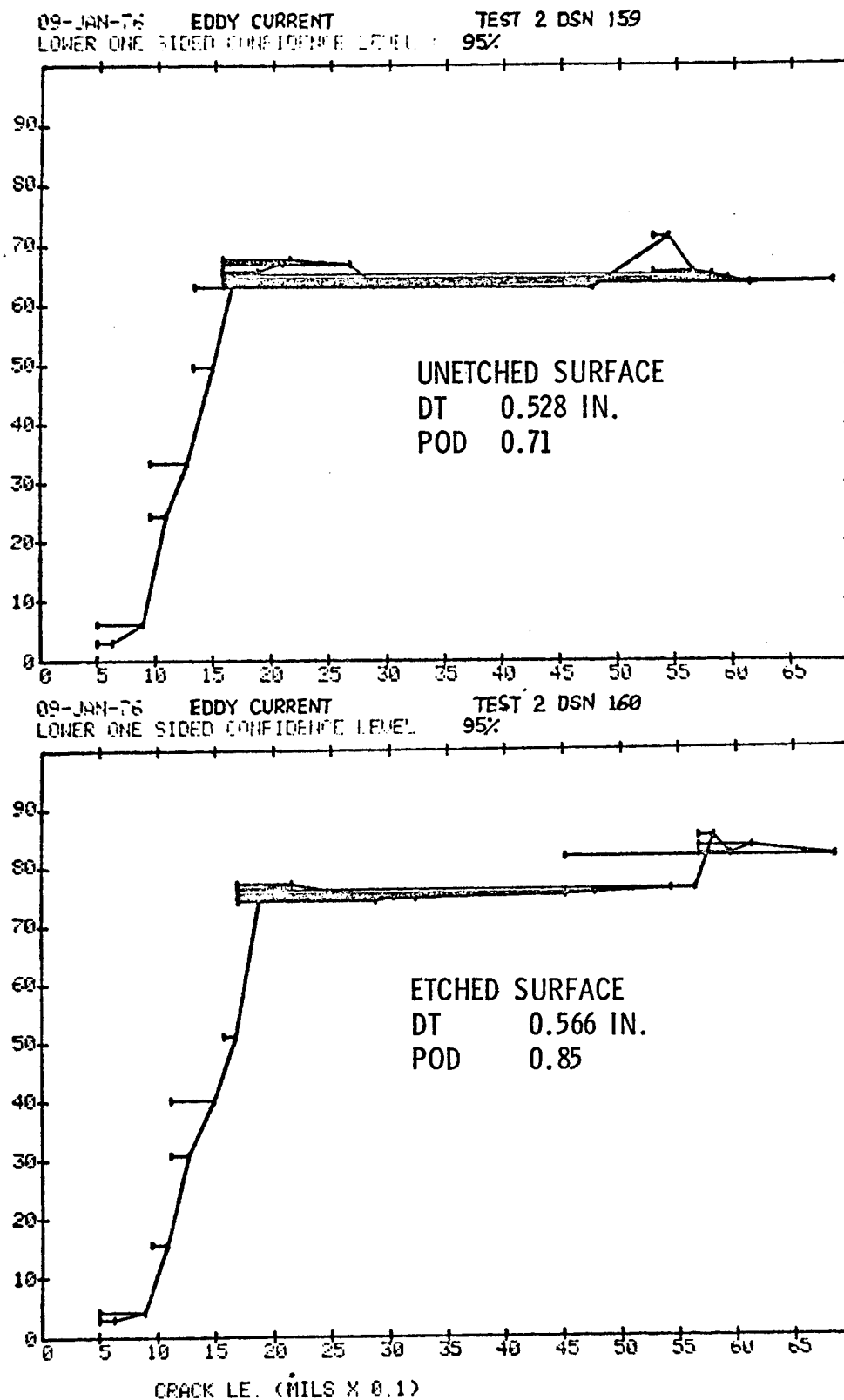


Figure 1. POD Difference for Etched and Unetched Surfaces
(Eddy Current, Integrally Stiffened Panel Specimens)

the histogram data provided a good indication of the order of importance of the influencing parameters on the POD and indicated data deficiencies in some areas. The NDE reliability data base is such that not all the NDE parameters can be analyzed by linear regression analysis or adaptive learning techniques due to insufficient number of inspections in most cases. Table 4 presents a list of the parameters that were included in the point estimate comparison and linear regression analysis. Figure 2 shows sketches of some specimen geometries listed in Table 4. Some of the specimens were inspected with as-machined surfaces and then re-inspected after etching to determine the effect of surface treatment on the POD. Cracks in the form of compressed notches were present on the flat portions of the tandem T specimens⁽⁷⁾. These compressed notch cracks were fabricated by grinding grooves of 0.020 in. radius in the specimen blanks and placing EDM notches of 0.005 to 0.008 in. in the grooves. The specimens were then subjected to axial compression loading of sufficient magnitude to close the notches by plastic deformation. Following compression, the grooves were machined to attain the final configuration. Typical crack opening of the compressed notch cracks in aluminum was approximately 0.0002 in. Compressed notch cracks on the inner and external surfaces of straight hollow or solid cylinders can be similarly fabricated. These specimen geometries were not illustrated in Figure 2. The weld specimens had crowns (weld beads) in the as-welded condition. They were inspected in that configuration and then re-inspected after the beads were machined off until the surface in the weld zone was flush with the surface of the parent material. The machining operation was termed scarfing in the specimen fabrication process⁽²⁾.

A computer program was coded to divide the specimen crack length into eight equal intervals of 0.125 in. in each data set. The number of detections in each crack length interval was divided by the number of inspections to obtain the point estimate. Any of the parameters listed in Table 4 could be compared to any other. The comparison is conducted by obtaining the ratio of the point estimates of the PODs corresponding to the two parameters. An example is given in Figure 3 to show one of the parametric relationships presented in a computer-printed histogram form. The NDE method for the histogram is printed as a heading followed by the data set numbers from which the data have been obtained. In some cases subsets from the data sets are identified by their parameter codes such as surface finish. The printouts starting from the middle of the second row identify the parameter whose relationship to POD is to be determined. The date and time of the estimates are placed at the extreme right hand end of the second row. Other illustrations of the computer generated histograms for comparing the effects on POD of other NDE parameters are shown in Appendix D. Only pertinent conclusions are summarized in the following paragraphs.

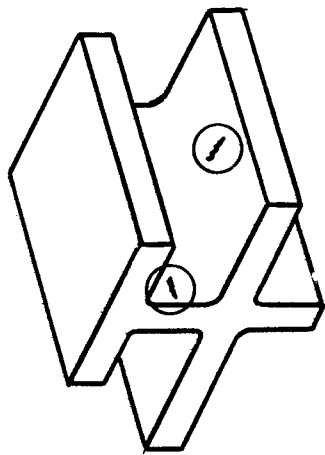
TABLE 4

A LIST OF NDE PARAMETERS INCLUDED
IN THE PARAMETRIC STUDY

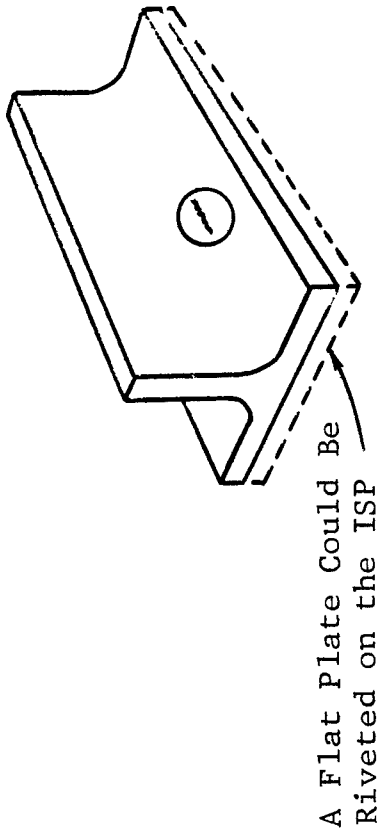
<u>Category</u>	<u>Code</u>	<u>Key</u>
NDT Method	1	Eddy Current (EC)
	2	Liquid Penetrant (Penetrant)
	3	Magnetic Particle
	4	X-Ray
	5	Ultrasonics
Sample History	1	As Machined Surface
	2	Etched Surface (Etched)
	3	Scarfed
	4	Proof Loaded (Proof)
Data Source	1	Martin Marietta/Denver Div. (NAS CR-2369)
	2	Rockwell International/Space Div. (NAS 9-14000)
	3	General Dynamics/Convair Div. (NAS 9-14000)
	4	Martin Marietta/Denver Div. (NAS 9-14000)
	5	Boeing Commercial Airplane Co. (AFML-TR-74-241)
	6	Martin Marietta/Denver Div. (NAS 9-13578)
Part Geometry	1	Flat Plate (FP)
	2	Integrally Stiffened Panel (ISP)
	3	Flat Plat Riveted to Integrally Stiffened Panel
	4	Lack of Penetration (LOP) for Welded Panel
	5	Longitudinal Welded Panel with Crowns
	6	Transverse " " " "
	7	Longitudinal " " without Crowns
	8	Tandem T
Operator ID	1	Operator A
	2	Operator B
	'	'
	'	'
	'	'
	'	'
	'	'
	24	Operator X

TABLE 4 (CONTINUED)
A LIST OF NDE PARAMETERS INCLUDED
IN THE PARAMETRIC STUDY

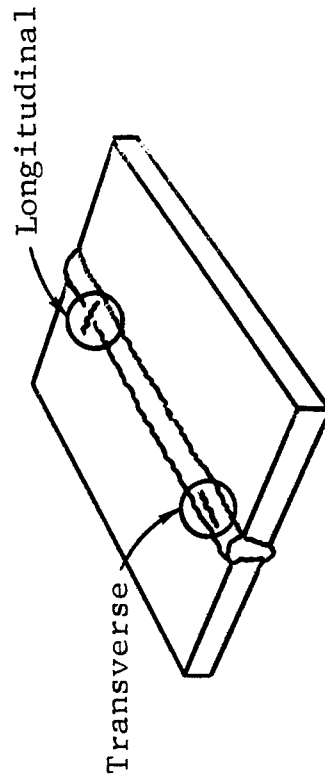
<u>Category</u>	<u>Code</u>	<u>Key</u>
Inspection Environment	1	Production
	2	Laboratory
Material	1	Aluminum
	2	Steel
Specimen Finish	1	1-32 RMS
	2	33-64 RMS
	3	65-128 RMS
	4	129-250 RMS
	5	Larger than 250 RMS
Specimen Thickness	1	1-200 Mils
	2	201-300 Mils
	3	301-500 Mils
a/2c	1	Below 0.17
	2	0.17 - 0.34
	3	Above 0.34



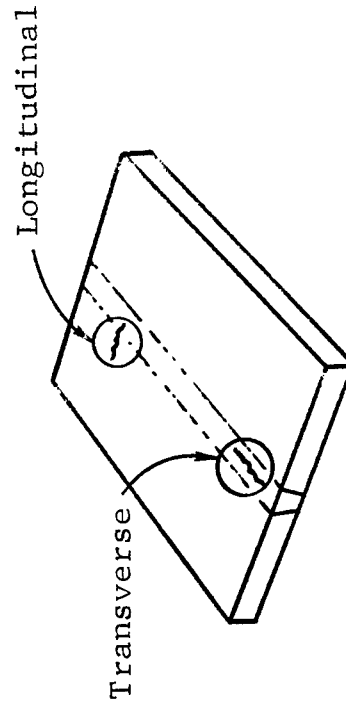
TANDEM T SPECIMENS



INTEGRALLY STIFFENED PANEL (ISP)



WELD SPECIMENS WITH CROWN



FLUSHED SPECIMEN (SCARFED)

Figure 2 Specimen Geometries

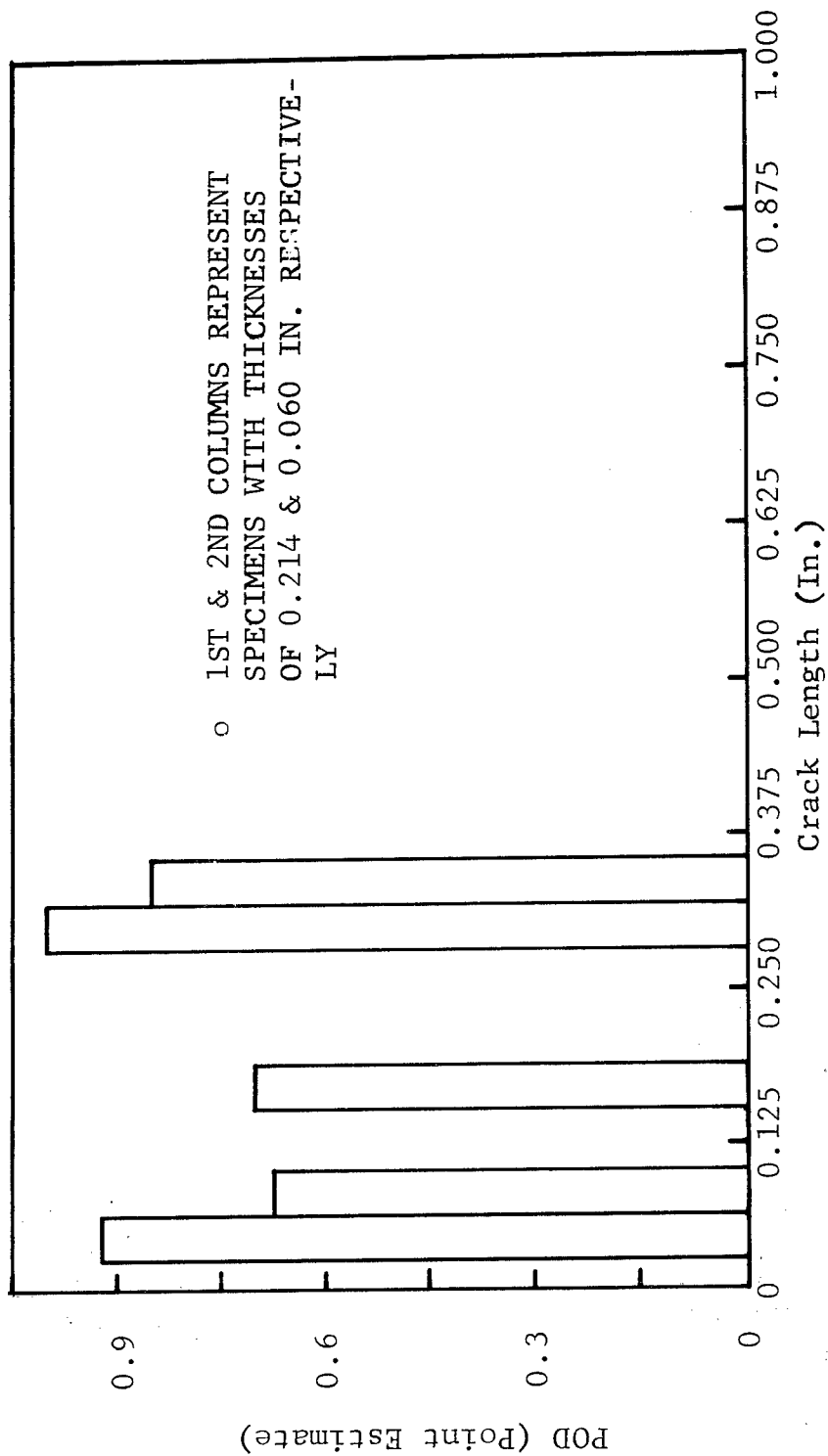


Figure 3 Example of Computer Printouts of Point Estimate Comparisons in Parametric Relationship Study on Flat Plate Specimens

Specimen surface finish was observed to have negligible effect on the POD for ultrasonic and X-ray methods. For eddy current and penetrant inspections the effect is noticeable only in the smallest crack length region of 0 - 0.125 in. Comparing specimen thicknesses, the only significant difference in POD for specimens with two different thicknesses was observed for the X-ray technique. Etching the specimen surface was found to increase the POD for eddy current, penetrant and X-ray technique. No noticeable effect could be discerned from the etching for the ultrasonic technique. A comparison of the POD for different inspectors within the same company revealed that the inspection efficiency for these inspectors appeared to be quite uniform. Similar comparison conducted on three companies using the same specimens with fatigue cracks showed very little variation in inspection efficiency. Comparing specimen geometry, the POD for the simpler geometry were higher than those for the more complex geometry for all three NDT techniques. However, the difference was significant only for the smallest crack length range in the case of ultrasonic inspection.

For NDT techniques of penetrant, eddy current, and ultrasonics, PODs obtained on flat plates were higher than corresponding values for the integrally stiffened panels (ISP) and ISP with a riveted plate. However, little difference could be discerned for the integrally stiffened panels with and without a riveted plate. A comparison of POD for weld specimens with as-welded and scarfed joints using penetrant, ultrasonic, and eddy current techniques showed that the PODs for the two types of specimen histories were essentially equivalent for the ultrasonic and eddy current techniques. For the penetrant technique, lower PODs were evident for specimens with scarfed joints. This appeared to be contradictory to the expected trend. The reason for the anomaly could be attributed to a smearing of the scarfed surfaces of the aluminum weld specimen. The flaw openings to the specimen surface were closed by the metal chips preventing the penetration of the penetrants. Except for the eddy current technique, the PODs obtained for weld specimens with lack of penetration defects after a proof loading of 90 percent of the yield stress were much higher compared to those obtained before proof loading. The point estimate comparison of the PODs provided a good indication of the order of importance of the influencing parameters on the NDE sensitivity.

6.1.2.3 Statistical Fitting Schemes

The parametric relationships between the POD and NDE parameters determined by the adaptive learning techniques and the linear regression analysis method are presented in the following paragraphs. Due to the non-uniform distribution of the reliability data caused by the grouping of data according to different NDE parameters, only selected comparisons could be made among the large number of combinations of NDE parameters. The relationship established by the adaptive learning techniques is in the form of POD (point estimate) plot as a function of crack length. The statistical nature of the fitting program was such that the POD was allowed to reach a maximum of 1.1 in order to arrive at the best fit for the data points at the small crack length ranges. The idea of a POD in excess of 1.0 appears to be absurd at first sight. It should be noted, however, that the majority of data points were in the lower crack length ranges. Consequently, it will be more appropriate to attempt a better fit at these ranges at the expense of entertaining a higher than 1.0 POD. The programs could be easily changed to suppress the POD to a value no larger than 1.0, but it would be accomplished at a price of artificially shifting down the POD at the lower crack length ranges.

The horizontal axis of the POD curves for results obtained by the adaptive learning techniques as well as the linear regression analysis is divided into ten equal increments of 0.064 in. It should be noted, however, that the data points in the calculation process were actually selected in logarithmically equal increments of crack length. The equal increments in logarithmic scale were used instead of equal increments in linear scale for the purpose of achieving a better sampling population at the lower crack length ranges where the POD curves generally had the fastest change in slope. In order to present the POD curves at a more conventional way, the data plots were changed back into a familiar linear crack length scale.

The computer programs developed for the adaptive learning techniques generated two POD curves for comparing a pair of values for each NDE parameter. In order to conserve space in the presentation of these comparisons, POD curves for several values of each NDE parameter were placed in the same figure by transposing the curves. The surface finish and specimen thickness for the curves are identified by their codes (see Table 4) as a pair of numbers in a parenthesis. For example, (1,2) signifies that the surface finish of the specimen was in the range of

1-32 rms and the thickness of the specimen was in the range of 201-300 mils. Parametric relationships obtained from adaptive learning technique and linear regression techniques were mostly for ultrasonic inspection due to the large population of inspection data for this NDE technique. Figure 4 shows a comparison of POD for flat plate specimens with three different surface finishes. The POD for smoother specimen surface finish was higher than that for a rougher surface. Figure 5 presents a comparison of etched and unetched specimen surfaces for flat plate and integrally stiffened panel specimens. Specimens with etched surface appear to have a higher POD compared to specimens with unetched surfaces. The trend applied to both specimen geometries. The specimen surface finish did not appear to affect the POD for longitudinal weld without crown for both etched and unetched surfaces, as shown in Figure 6. The specimens with etched surfaces had a higher POD compared to those with unetched surfaces, but the surface finish apparently had little effect on the POD. A similar indifference to specimen surface finish was evident for transverse weld specimens with crown in Figure 7. In this figure, the same conclusion could be reached for two different specimen thicknesses and for etched as well as unetched surfaces. However, etching the surface of this type of specimen tended to lower the POD when curves C and D are compared to curves E and F. By comparing curves A and B to curves C and D, the effect of specimen thickness on POD for the transverse weld specimens can be observed.

The thesis that the depth to length ratio ($a/2c$) of fatigue cracks is an important parameter for determining the POD for the ultrasonic shear wave inspection has been contended by many NDE personnel. However, no systematic and statistical evidence exists to date to support this contention. One of the important NDE parametric relationships established in this program was that $a/2c$ was indeed a factor in POD determination. Figure 8 shows that the POD curves of three $a/2c$ values for flat plate specimens were such that the largest depth to length ratio had the highest PODs. Similar trend could be observed in Figure 9 for integrally stiffened panel specimens. It will be noted that a comparison of POD for cracks with the same length can be obtained from Figures 8 and 9 by drawing a vertical line from the desired crack length on the horizontal axis. The vertical line intersects the three curves at three different points corresponding to three $a/2c$ values. Since the crack length $2c$ on the vertical line is the same, the three intersecting points will represent cracks with three different depths. The ordinates of these three points will represent the PODs for the cracks with three different depths.

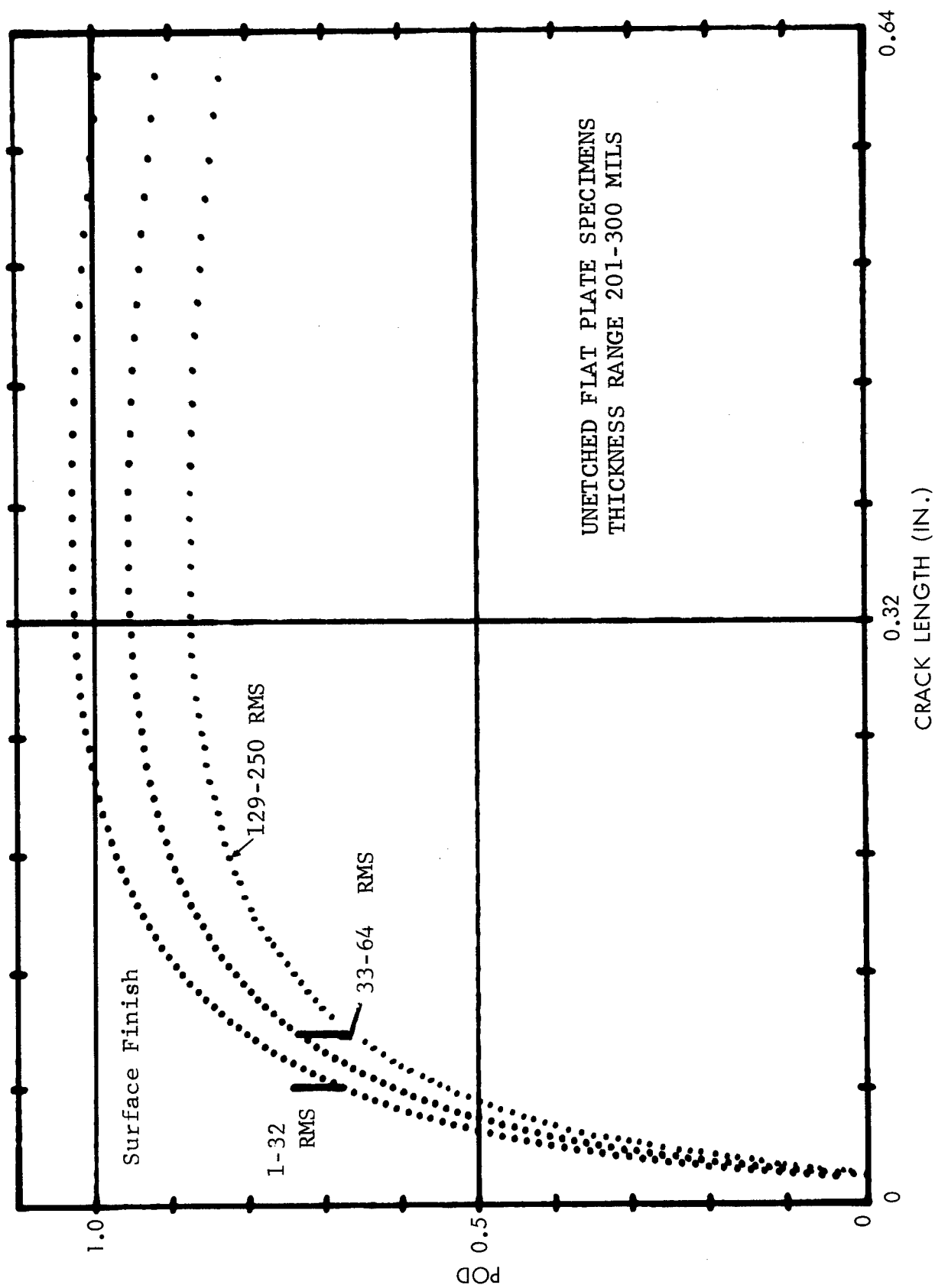


Figure 4 Effects of Surface Finish on POD by Adaptive Learning Technique (Ultrasonic)

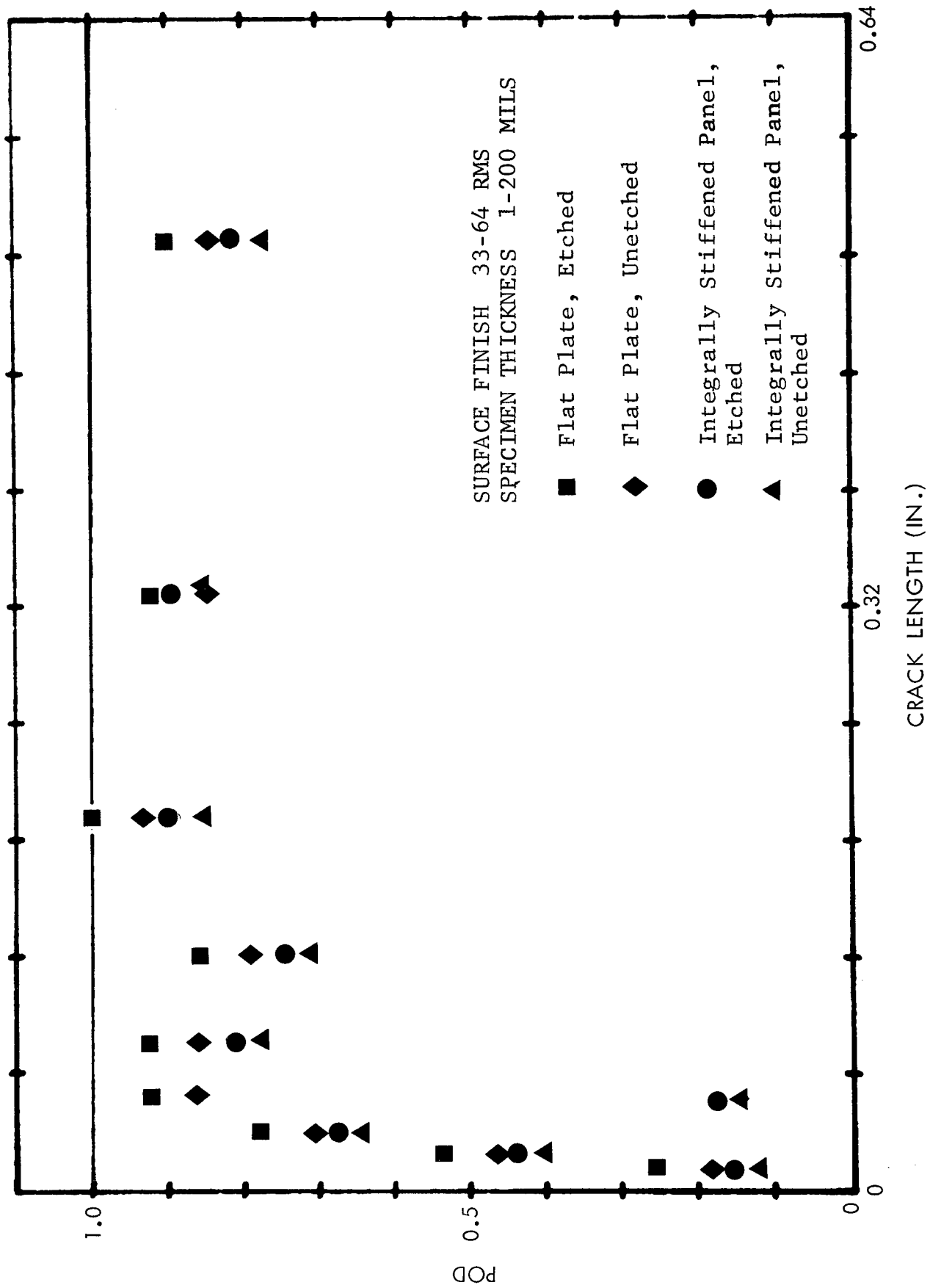


Figure 5 Effects of Specimen History on POD by Linear Regression Technique (Ultrasonics)

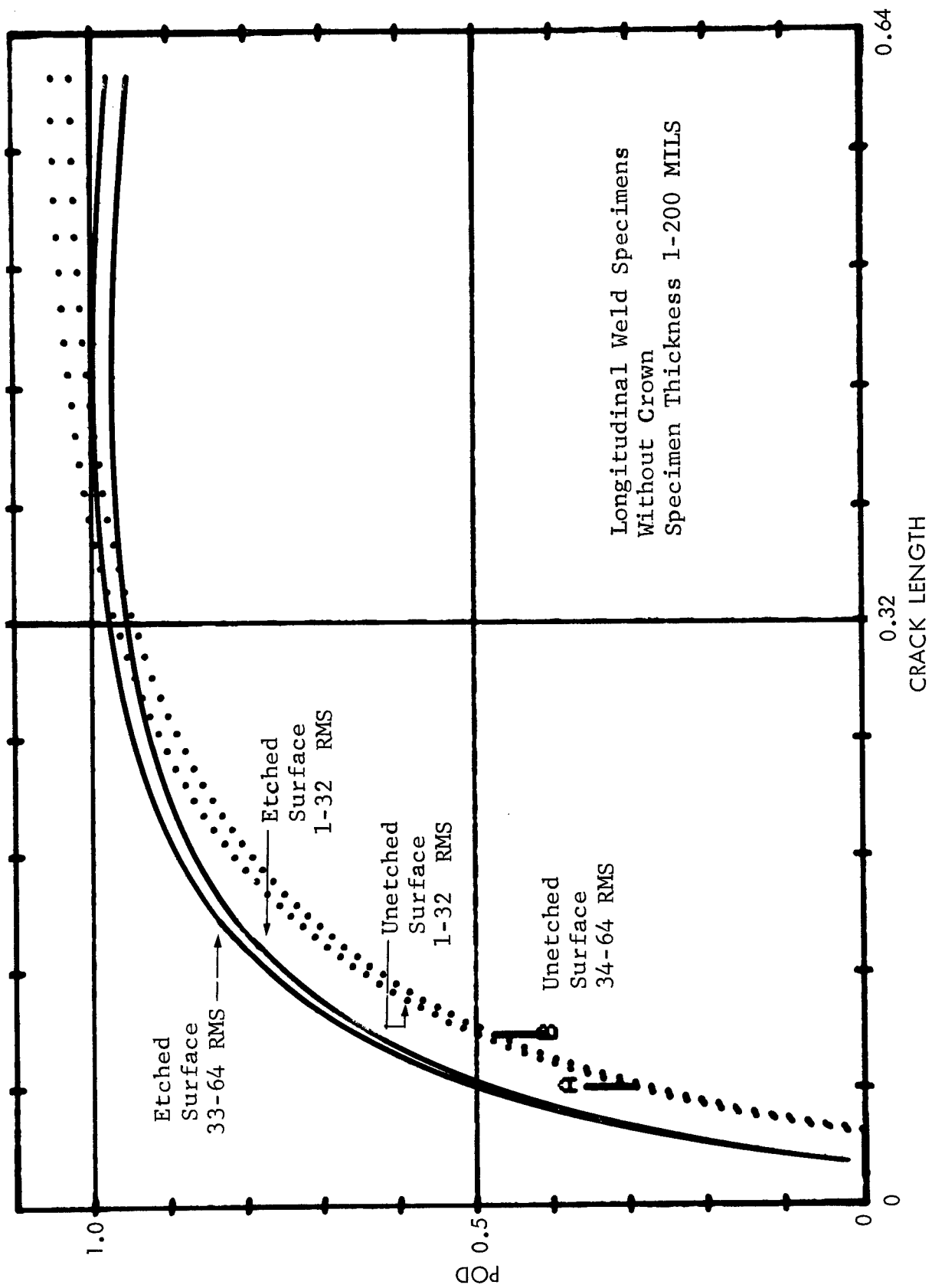


Figure 6 Effects of Specimen History & Surface Finish on POD by Adaptive Learning Technique (Ultrasonic)

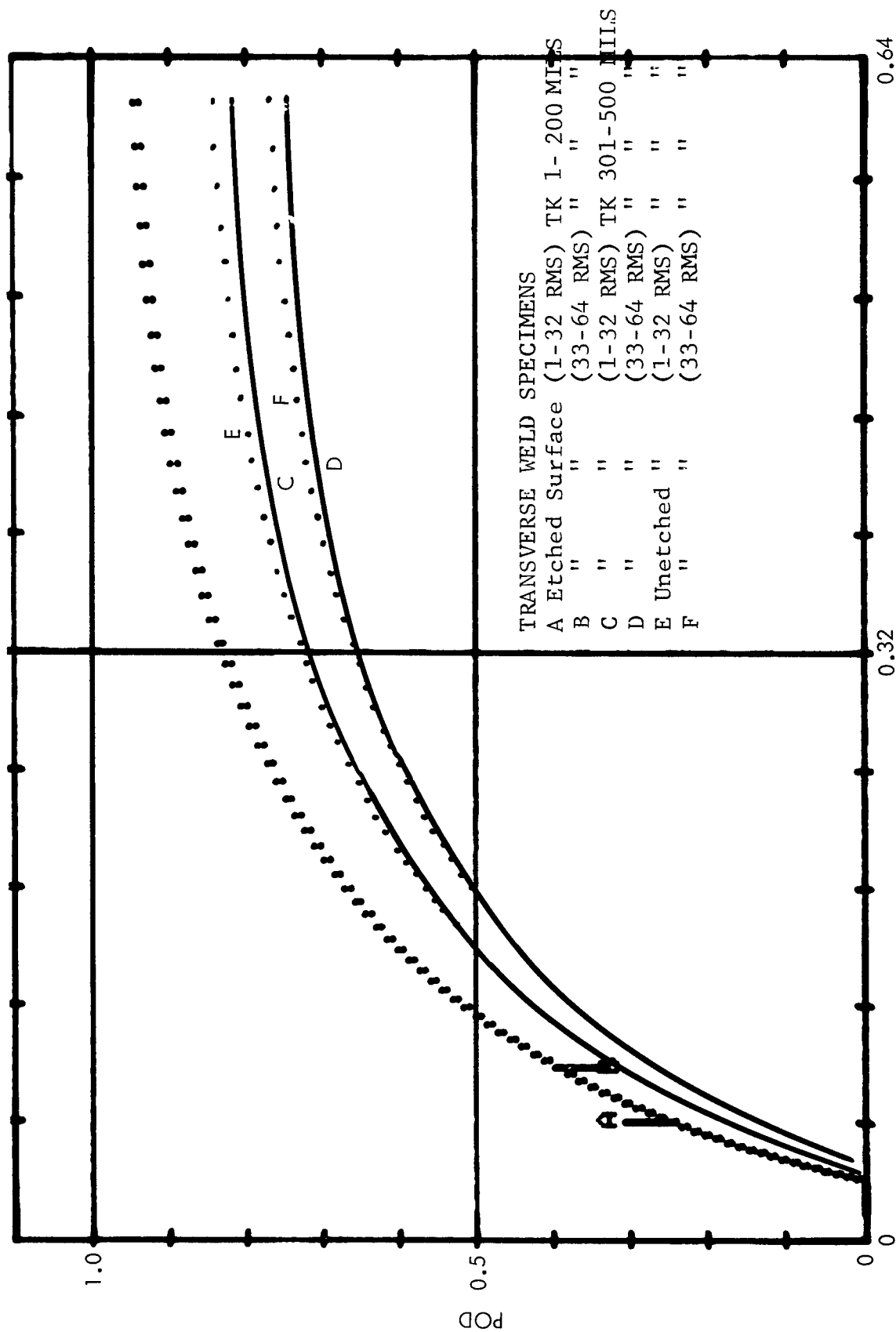


Figure 7 Effects of Specimen History, Surface Finish & Thickness on POD by Adaptive Learning Technique (Ultrasound)

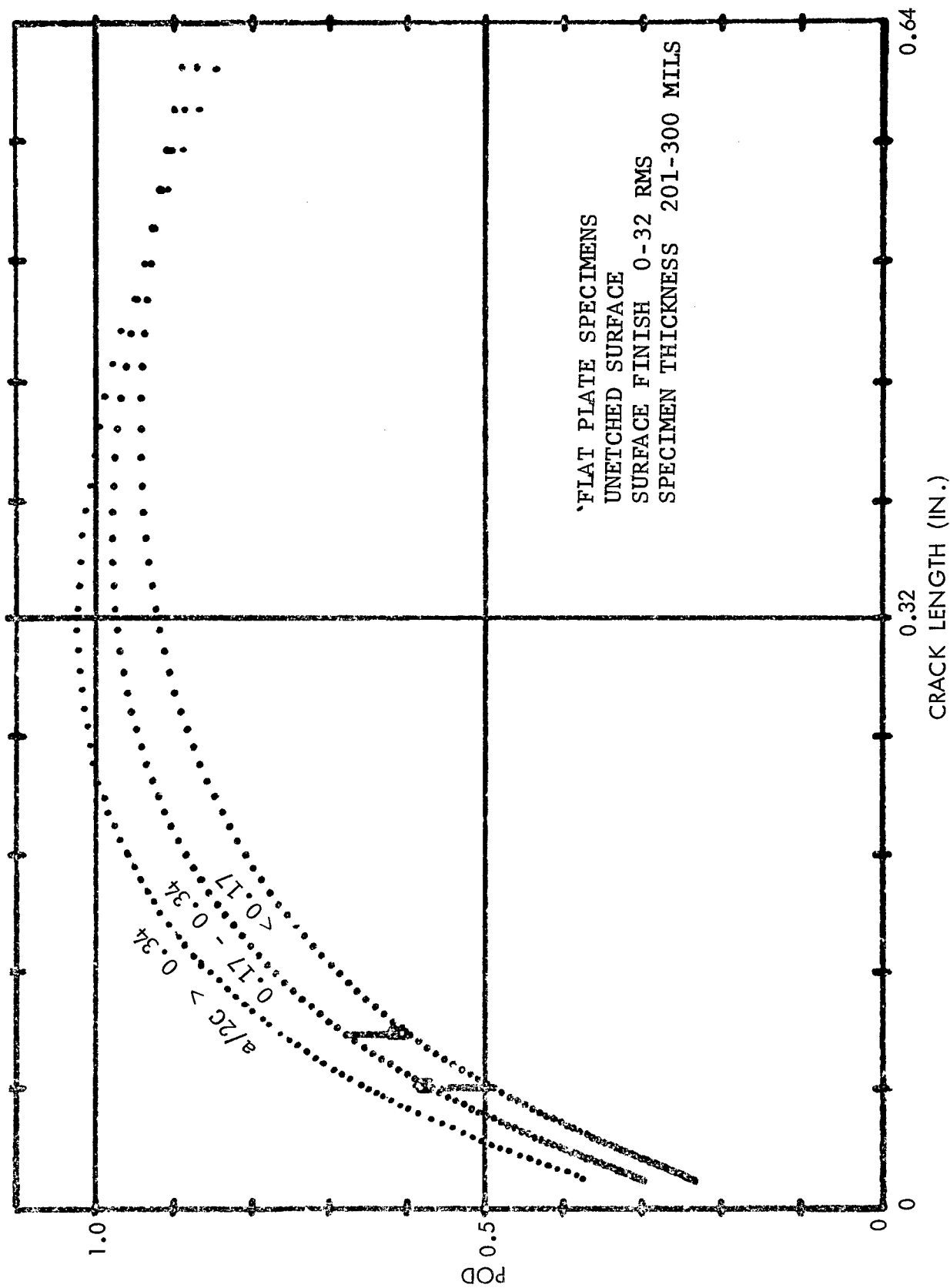


Figure 8 Effects of $a/2C$ on POD by Adaptive Learning Technique (ULTRASONIC, Flat Plate Specimens)

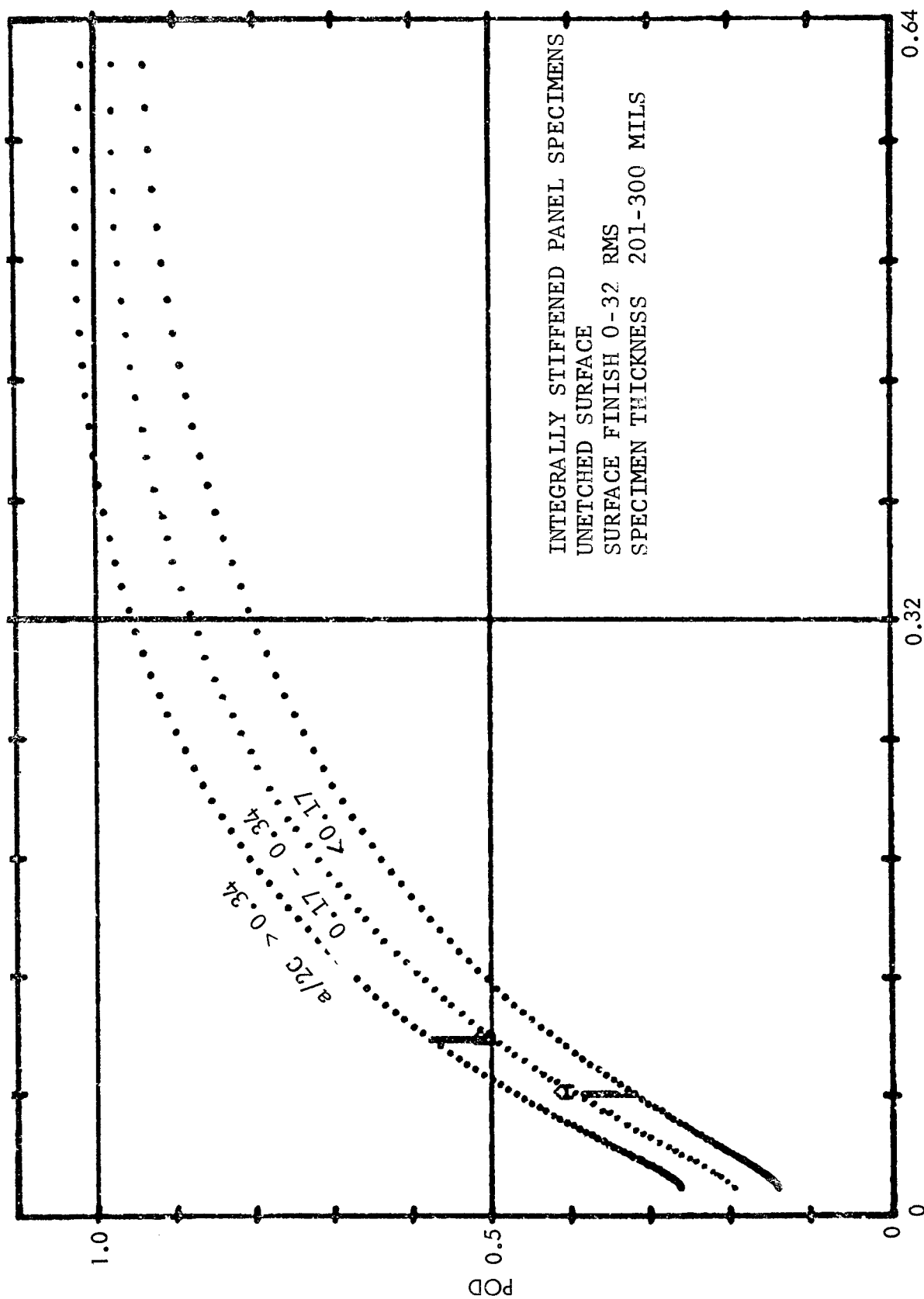


Figure 9 Effects of $a/2c$ on POD by Adaptive Learning Technique (ULtrasonic Integrally Stiffened Panel Specimens)

The effects of specimen history and surface finish on the POD of integrally stiffened panel and transverse weld specimens for the penetrant technique by using the linear regression analysis are presented in Figures 10 and 11. As expected, higher PODs were obtained on integrally stiffened panel specimens after the surfaces were etched. In general, a smoother surface finish produced a higher POD. The effect of etching the specimen surface was similar in transverse weld specimens. However, the effect of proof loading the specimens to 90 percent of yielding stress did not appear to increase the POD to a point higher than that for specimens with unetched surfaces. For the eddy current technique, similar effects of the specimen surface finish were observed for flat plate specimens from the linear regression analysis. Figure 12 shows the difference in POD at different crack length ranges for specimens with etched and unetched surfaces.

An interesting comparison of POD curves of flat plate specimens with unetched surfaces for the ultrasonic, penetrant, and eddy current techniques from the linear regression analysis is shown in Figure 13. An average difference in POD of 0.2 was seen to exist between the eddy current/ultrasonic and ultrasonic/penetrant techniques. The corresponding POD curves for flat plate specimens with etched surfaces are shown in Figure 14. The POD curve for the penetrant technique is seen to approach that for the ultrasonic technique after the specimen surfaces were etched as shown by the solid line. However, etching the surface appears to have a reversed effect for the eddy current technique. The PODs at the lower crack length were actually lower after etching. This result is in good agreement with that obtained by the point estimate scheme.

6.1.2.4 Summary of Parametric Relationship Study

Summaries of the parametric relationship for the ultrasonic, penetrant, and eddy current techniques are tabulated in Tables 5, 6 and 7, respectively. These summaries are comprised of matrices of four specimen geometries and nine NDE parameters. A dash mark in the matrix indicates insufficient or no data available. YES indicates a definite relationship exists while NO signifies negligible or no effect on POD. Although these parametric relationships were often established by one or more analytical or fitting techniques, the degrees of confidence based on the number of data points in most cases were such that a qualitative evaluation was judged to be more appropriate.

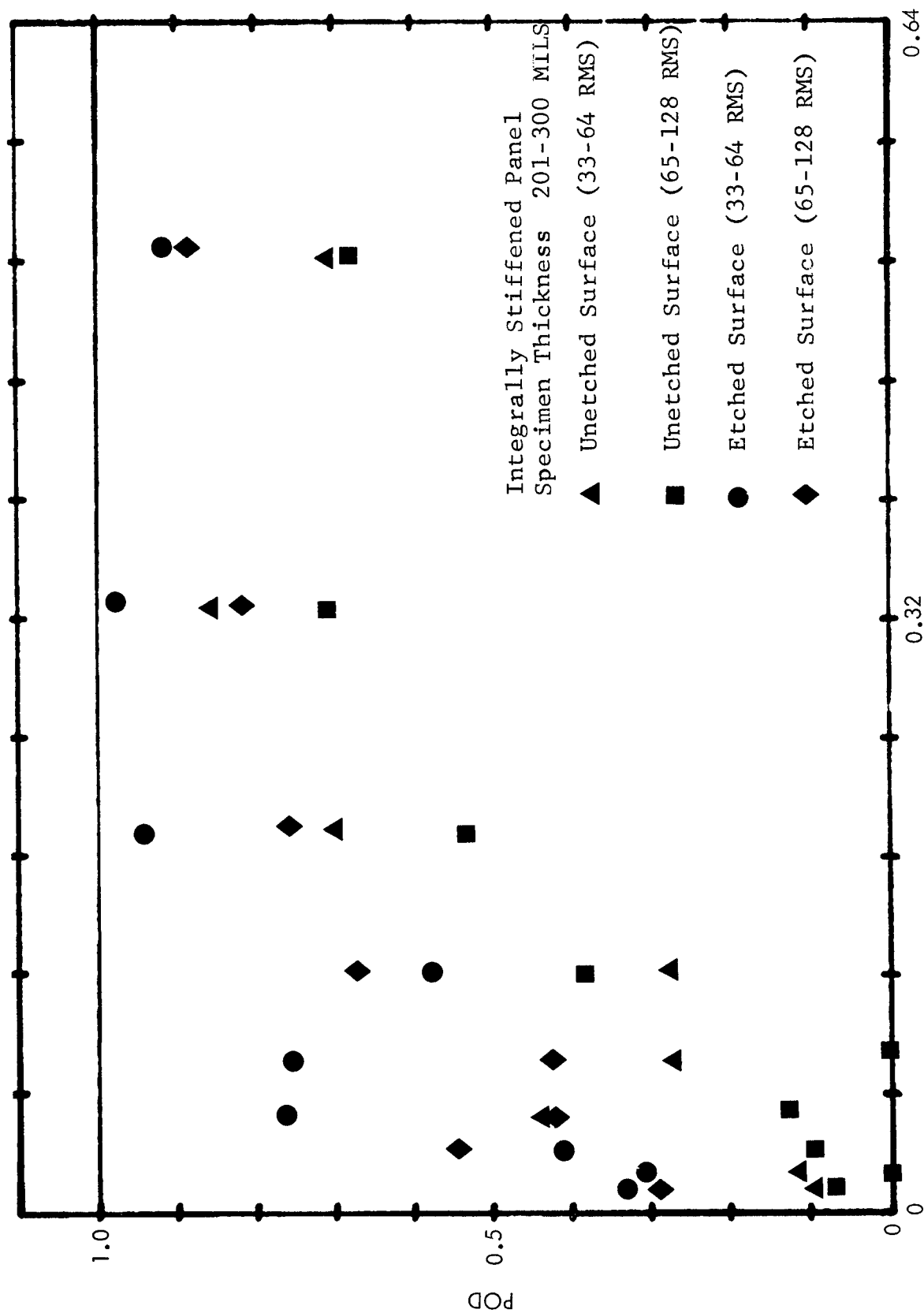


Figure 10 Effects of Specimen History and Surface Finish on POD by Linear Regression Technique (Penetrant)

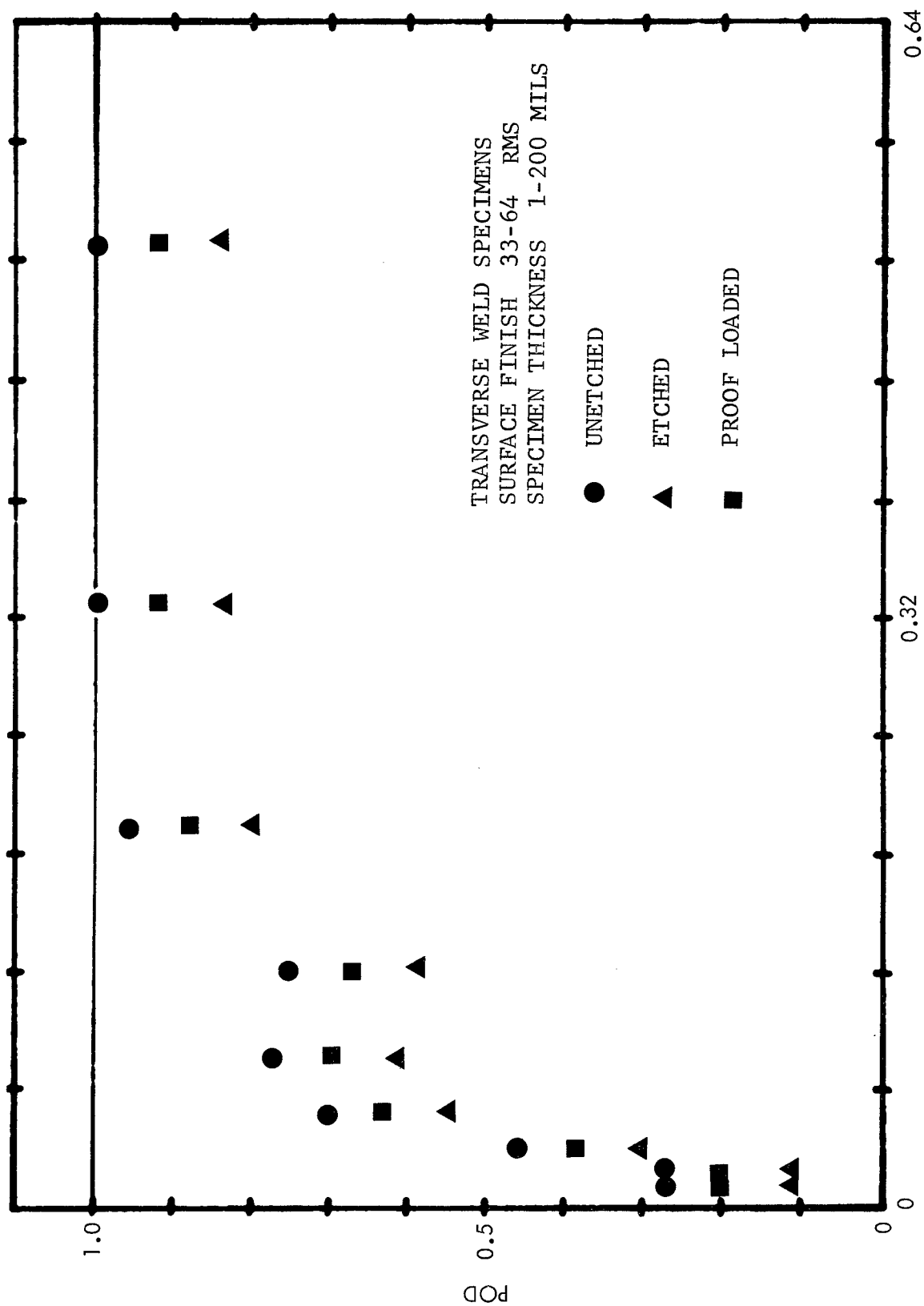


Figure 11 Effects of Specimen History on POD by Linear Regression Technique (Penetrant)

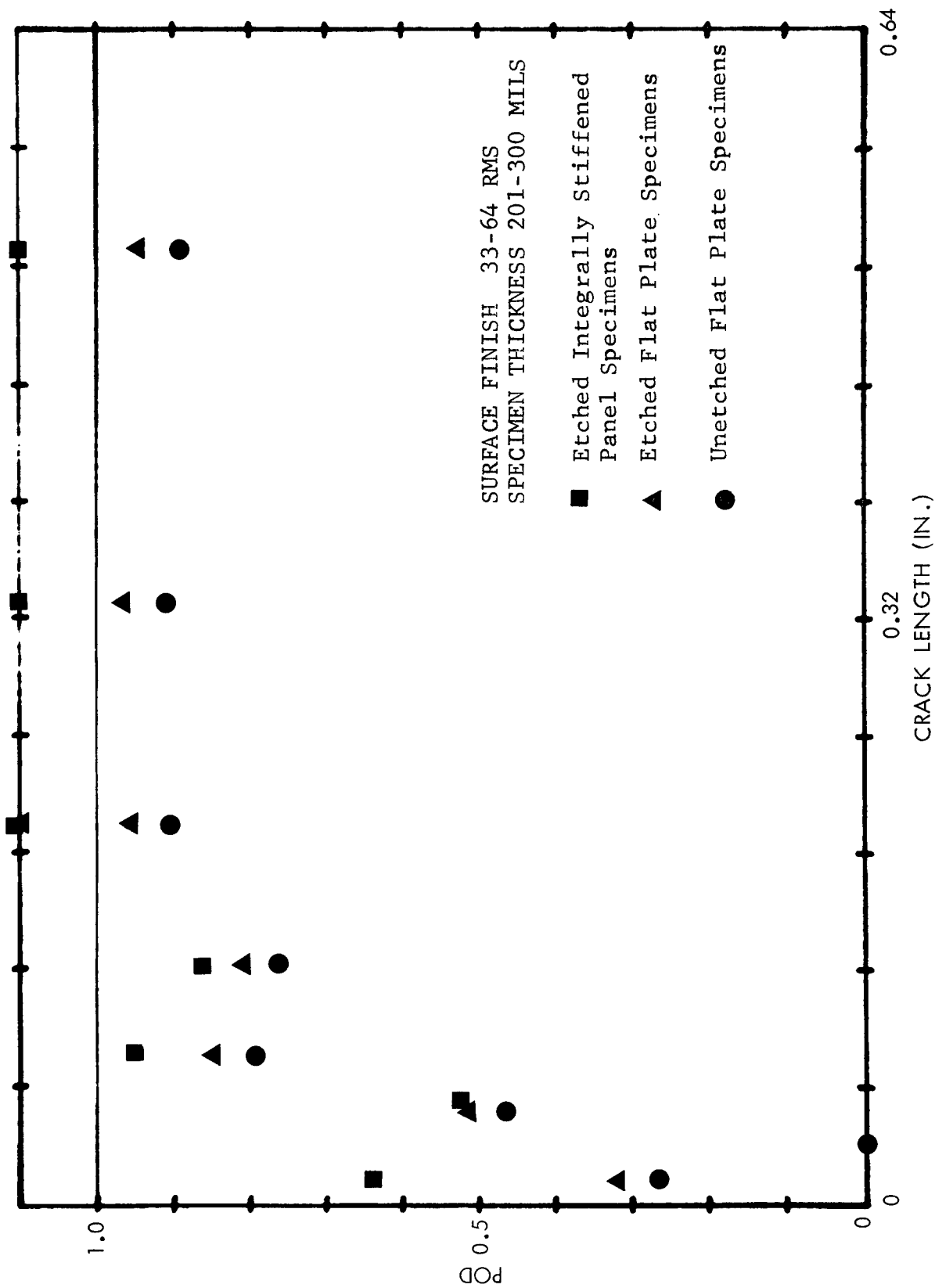


Figure 12 Effects of Specimen History on POD by Linear Regression Technique (Eddy Current)

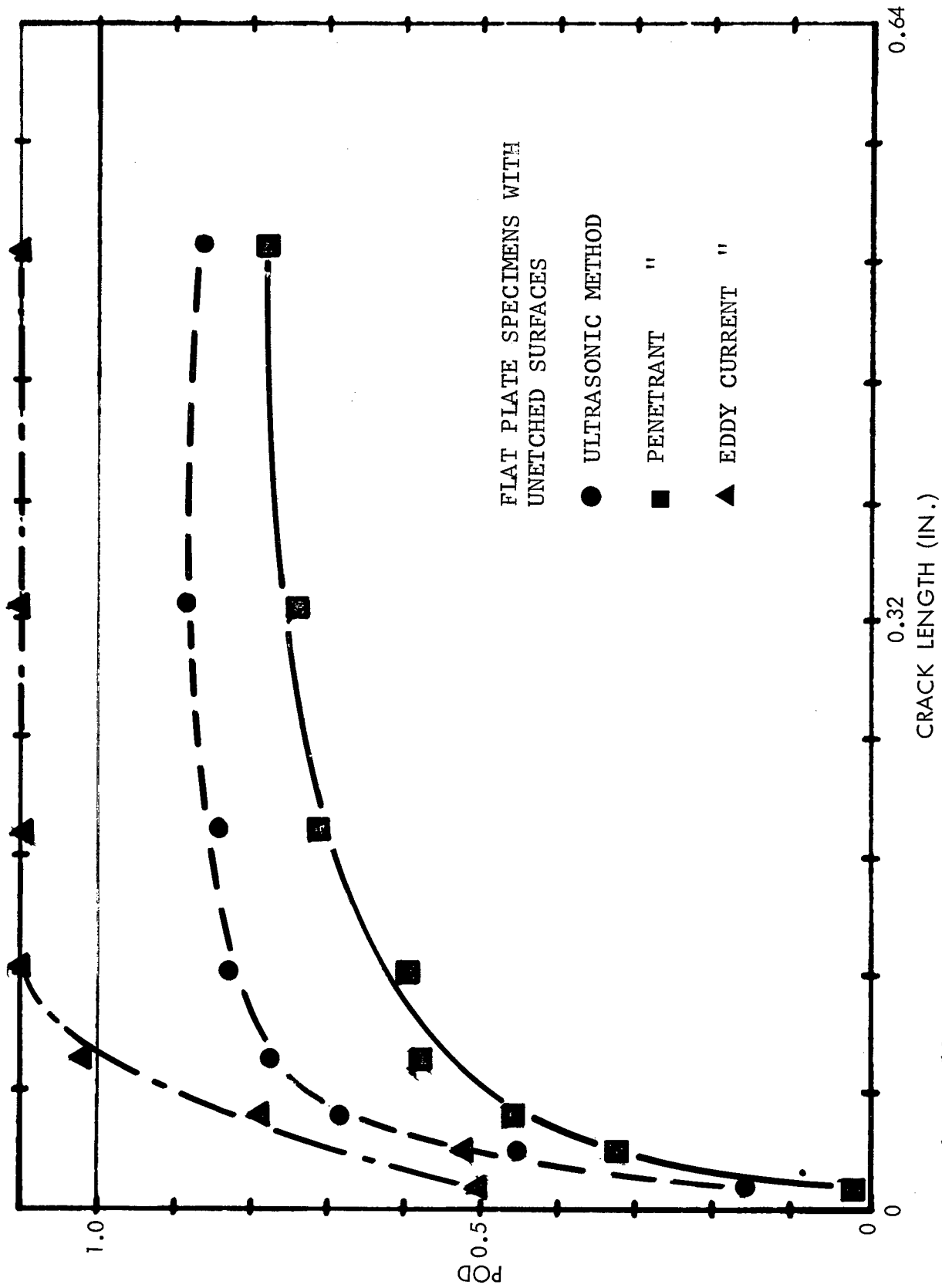


Figure 13 Comparison of NDE Methods Sensitivity by Linear Regression Technique (Unetched Surface)

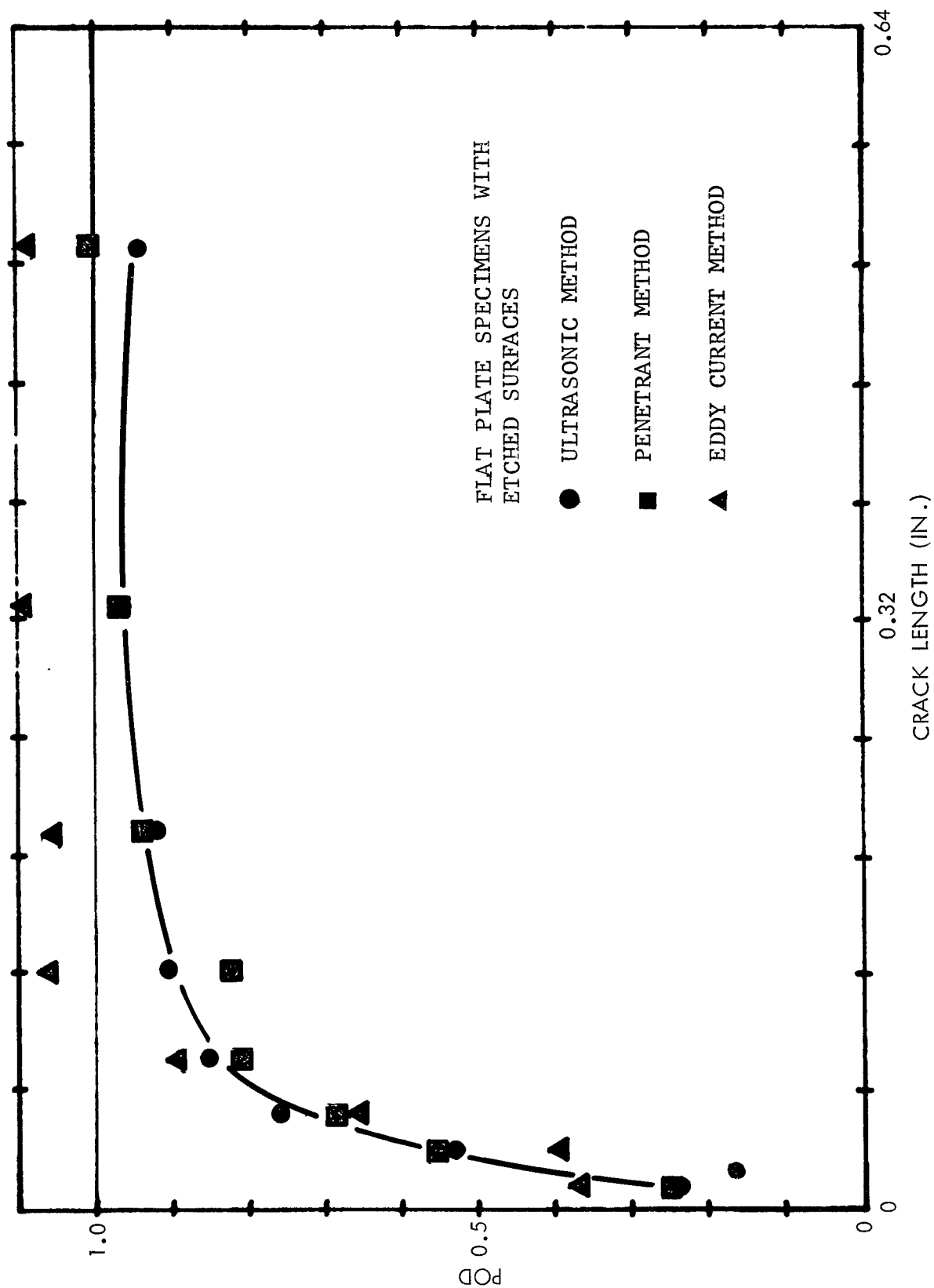


Figure 14 Comparison of NDE Methods Sensitivity by Linear Regression Technique (Etched Surface)

TABLE 5

CONCLUSION — PARAMETRIC RELATIONSHIP, ULTRASONIC

PART GEOMETRY	ETCHED SURFACE	PROOF LOAD	DATA SOURCE	OPERATOR ID	INSPECTION ENVIRONMENT	SPECIMEN FINISH	SPECIMEN THICKNESS	DEFECT TYPE	a/2c
FLAT PLATE	YES	—	NO	*	NO	YES	YES	NO	YES
INTEGRALLY STIFFENED PANEL	YES	—	NO	*	NO	YES	YES	—	YES
TRANSVERSE WELD W/CROWN	NO	YES	NO	*	NO	YES	YES	—	YES (Proof Load)
LONGITUDINAL FLUSH WELD	YES	YES	NO	*	NO	YES	YES	—	YES (Proof Load)

* Only Isolated Cases Were Affected

TABLE 6

CONCLUSION — PARAMETRIC RELATIONSHIP, PENETRANT

PART GEOMETRY	ETCHED SURFACE	PROOF LOAD	DATA SOURCE	OPERATOR ID	INSPECTION ENVIRONMENT	SPECIMEN FINISH	SPECIMEN THICKNESS	DEFECT TYPE
FLAT PLATE	YES	—	NO	*	NO	YES	NO	YES
INTEGRALLY STIFFENED PANEL	YES	—	NO	*	NO	YES	NO	—
TRANSVERSE WELD W/CROWN	YES	YES	NO	*	NO	YES	NO	—
LONGITUDINAL FLUSH WELD	—	—	NO	*	NO	YES	NO	—

* Only Isolated Cases Were Affected

TABLE 7

CONCLUSION – PARAMETRIC RELATIONSHIP, EDDY CURRENT

NOT METHOD	ETCHED SURFACE	PROOF LOAD	DATA SOURCE	OPERATOR ID	INSPECTION ENVIRONMENT	SPECIMEN FINISH	SPECIMEN THICKNESS	DEFECT TYPE
FLAT PLATE	YES	NO	NO	*	NO	YES	NO	YES
INTEGRALLY STIFFENED PANEL	YES	NO	NO	*	NO	YES	NO	-
TRANSVERSE WELD W/CROWN	NO	NO	NO	*	NO	YES	NO	-
LONGITUDINAL FLUSH WELD	YES	NO	NO	*	NO	YES	NO	-

* Only Isolated Cases Were Affected

The summaries of parametric relationships indicated that the inspection environment had no effect on the POD for all three inspection techniques. The inspection environments studied in the comparison were laboratory and production environments where the capabilities of operators did not differ significantly. Only in isolated cases the performance of an operator would fall below average for a certain reason. A final observation was that the defect types of fatigue crack and EDM compressed notches did not have significant effect on the POD in the case of ultrasonic inspection. For penetrant and eddy current techniques, the difference in defect type did produce a difference in POD as expected.

6.2 TRANSLATION MODEL

Based on the parametric relationships established between the NDE parameters and POD, translation models were developed for the ultrasonic, penetrant, and eddy current techniques. The models could be used to translate the POD obtained on flat plate specimens to specimens with other geometries such as integrally stiffened panel, longitudinal weld, transverse weld, and tandem T. The models developed by adaptive learning techniques are expressed in the form of POD curves for the flat plate geometry and the geometry to be translated. Models developed by the linear regression analysis are best expressed in the form of difference tables. These tables are presented in Appendix E for reference purposes. For convenience in comparison, the linear regression models are also presented in graphical form and discussed in conjunction with results obtained from adaptive learning techniques. These results will be presented according to NDE techniques. In addition to the statistical fitting schemes, a point estimate transfer function approach was also used to assess the difference in POD for different specimen geometries. Results of this comparison are rather interesting and will be presented in a separate paragraph.

6.2.1 Ultrasonic Inspection

The translation models developed by the adaptive learning and linear regression techniques for ultrasonic inspection from flat plate to integrally stiffened panel specimens are shown in Figures 15 and 16, respectively. Curves A and C in Figure 15 were POD curves for flat plate specimens while curves B and D were for integrally stiffened panel specimens. A significant difference is seen to exist between the two POD curves. Curves A and B were obtained by using a weighting factor to account for the decreasing significance in curve fitting for crack ranges where data points were scarce. Curves C and D were equivalent curves obtained by not using the weighting factor. It is seen that the difference with and without the factor was not significant. All the curves obtained by using the adaptive learning technique incorporated the weighting factors which were merely concerned with the curve fitting process and had no impact on the calculation of probability of detection. From the linear regression model shown in Figure 16, it can be seen that the basic model agreed well with that shown in Figure 15. The difference in POD for the two models disagreed somewhat.

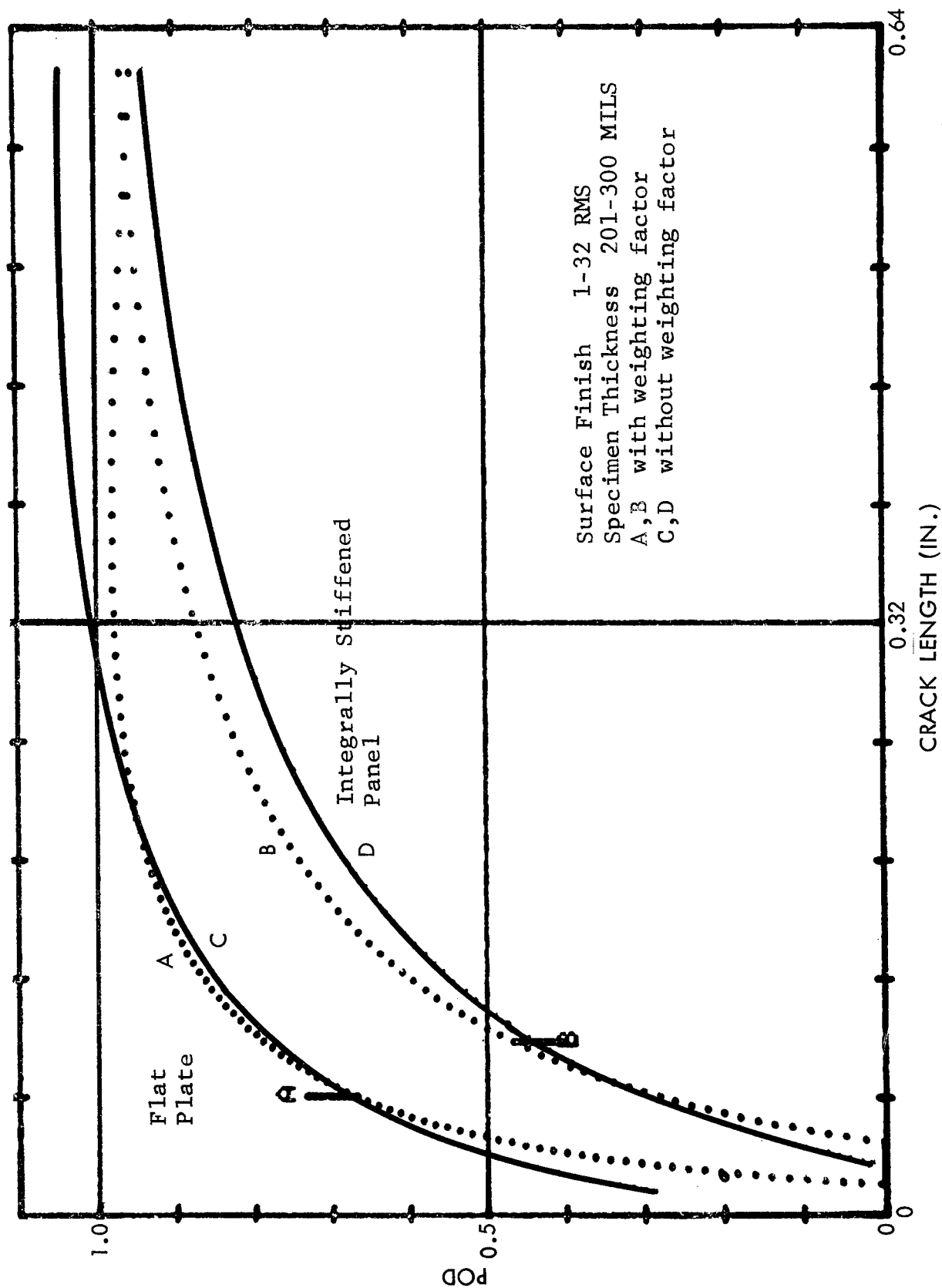


Figure 15 Translation Model by Adaptive Learning Technique - Flat Plate/
Integrally Stiffened Panel (Ultrasonic)

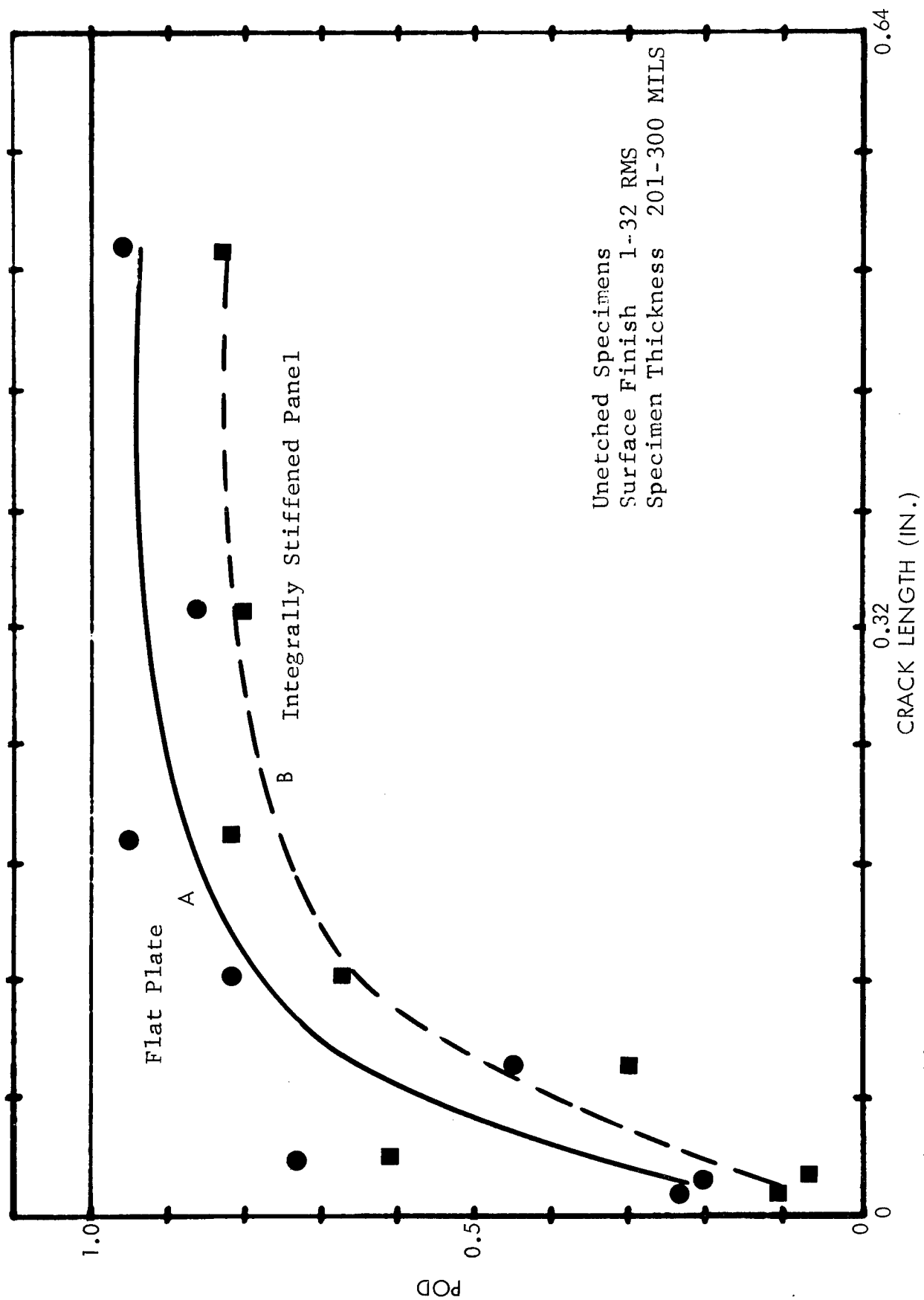


Figure 16 Translation Model by Linear Regression Technique - Flat Plate/
Integrally Stiffened Panel (Ultrasonic)

Figures 17 and 18 show the translation models developed from the adaptive learning and linear regression techniques, respectively, for the translation from flat plate to longitudinal weld specimens. Although a large difference in POD was observed in Figure 17, an inconsistent difference for various crack lengths existed in Figure 18. A similar situation was noted for the translation from flat plate to transverse weld specimens as shown in Figures 19 and 20 for adaptive learning and linear regression techniques, respectively. Figure 21 shows the adaptive learning translation model from flat plate to tandem T specimens. A small and almost negligible difference exists in the POD curves for these specimen geometries.

6.2.2 Penetrant Inspection

The adaptive learning and linear regression translation models for the penetrant technique translating flat plate to integrally stiffened panel specimens are presented in Figures 22 and 23, respectively. A sizeable difference in POD curves was observed in both figures for the two geometries. In Figures 24 and 25, essentially no systematic difference in POD curves was observed for the geometries of flat plate to longitudinal weld specimens. The same is true for the translation from flat plate to transverse weld specimens as shown in Figures 26 and 27 for the adaptive learning and linear regression models, respectively. Basically, the models for the penetrant technique followed closely the pattern set by the ultrasonic technique. The quantitative differential, however, was slightly decreased.

6.2.3 Eddy Current Inspection

The adaptive learning and linear regression translation models for the eddy current inspection translating flat plate to integrally stiffened and flat plate specimens to longitudinal weld followed the same trend for the ultrasonic and penetrant inspection. These models are shown in Figures 28 to 31. A large difference in POD curve was observed in the adaptive learning model translating flat plate to transverse weld specimens as shown in Figure 32. The corresponding linear regression model presented in Figure 33 showed inconsistent differences at different crack ranges. An interesting comparison of POD curves for flat plate and bolt hole geometries from adaptive learning technique is presented in Figure 34. The comparison is termed translation model only in the sense that both specimen geometries contained fatigue cracks. The inspection environment for the bolt hole

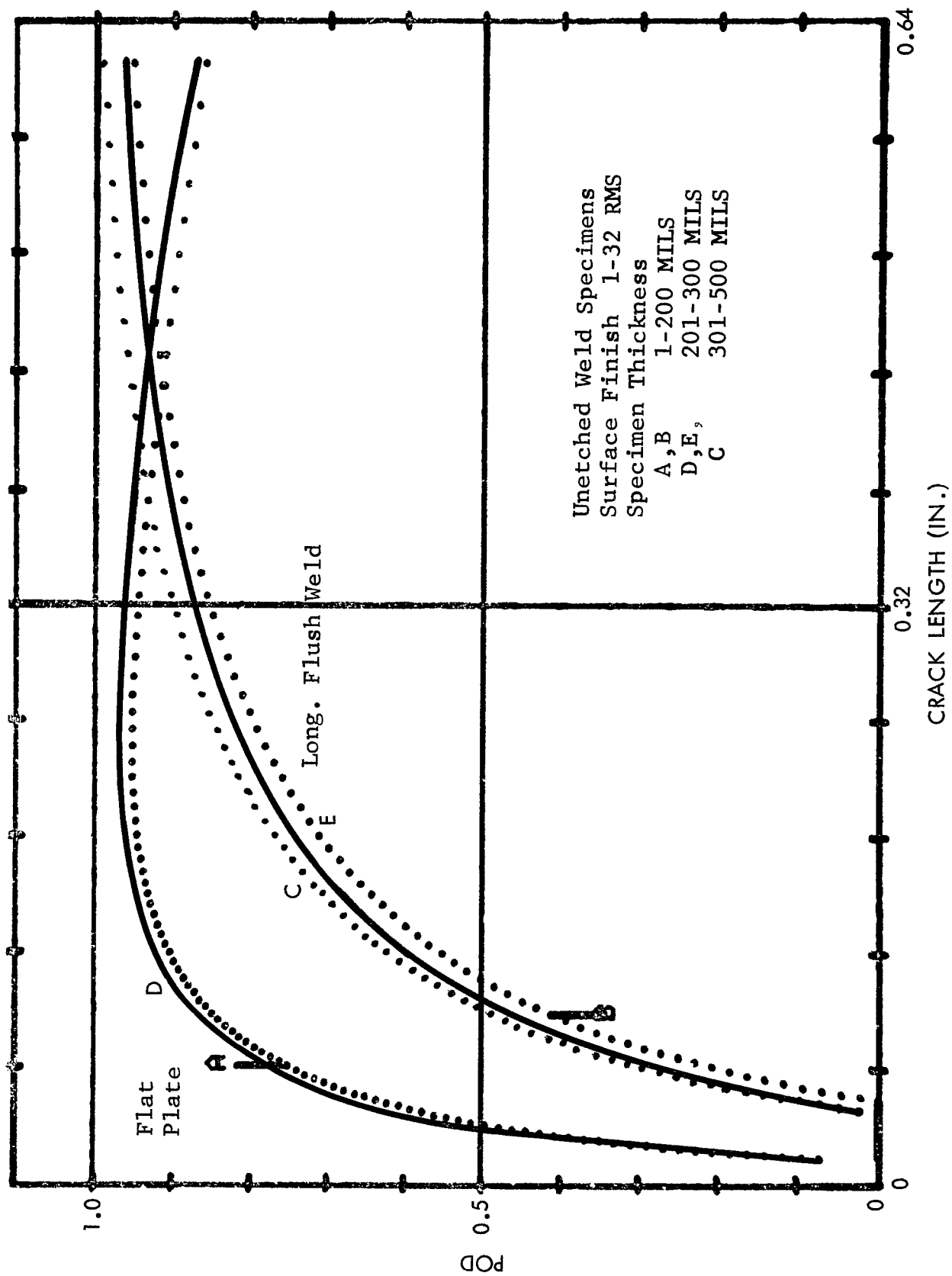


Figure 17 Translation Model by Adaptive Learning Technique - Flat Plate/
Long. Flush Weld (Ultrasonic)

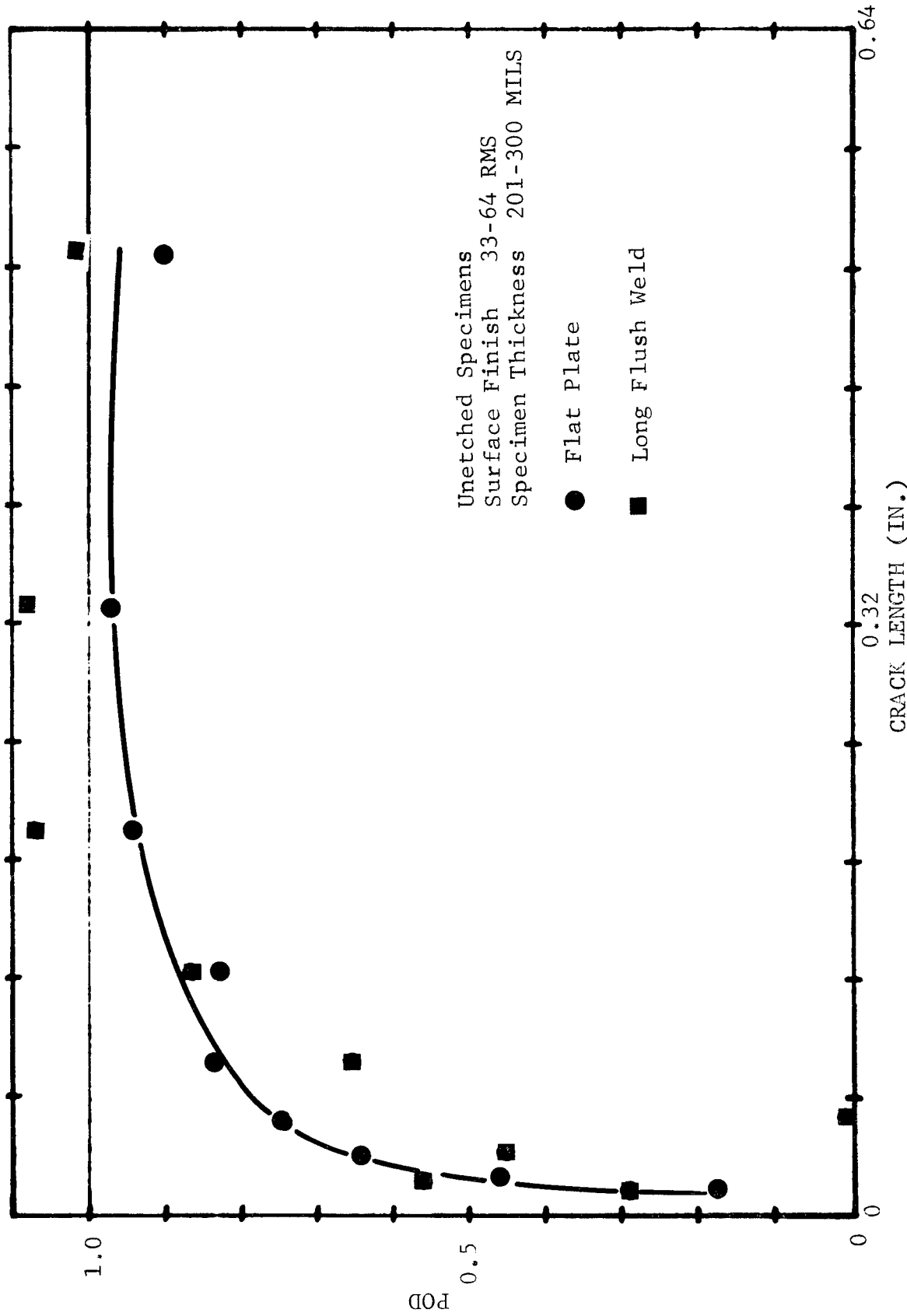


Figure 18 Translation Model by Linear Regression Technique - Flat Plate/Long. Flush Weld (Ultrasonic)

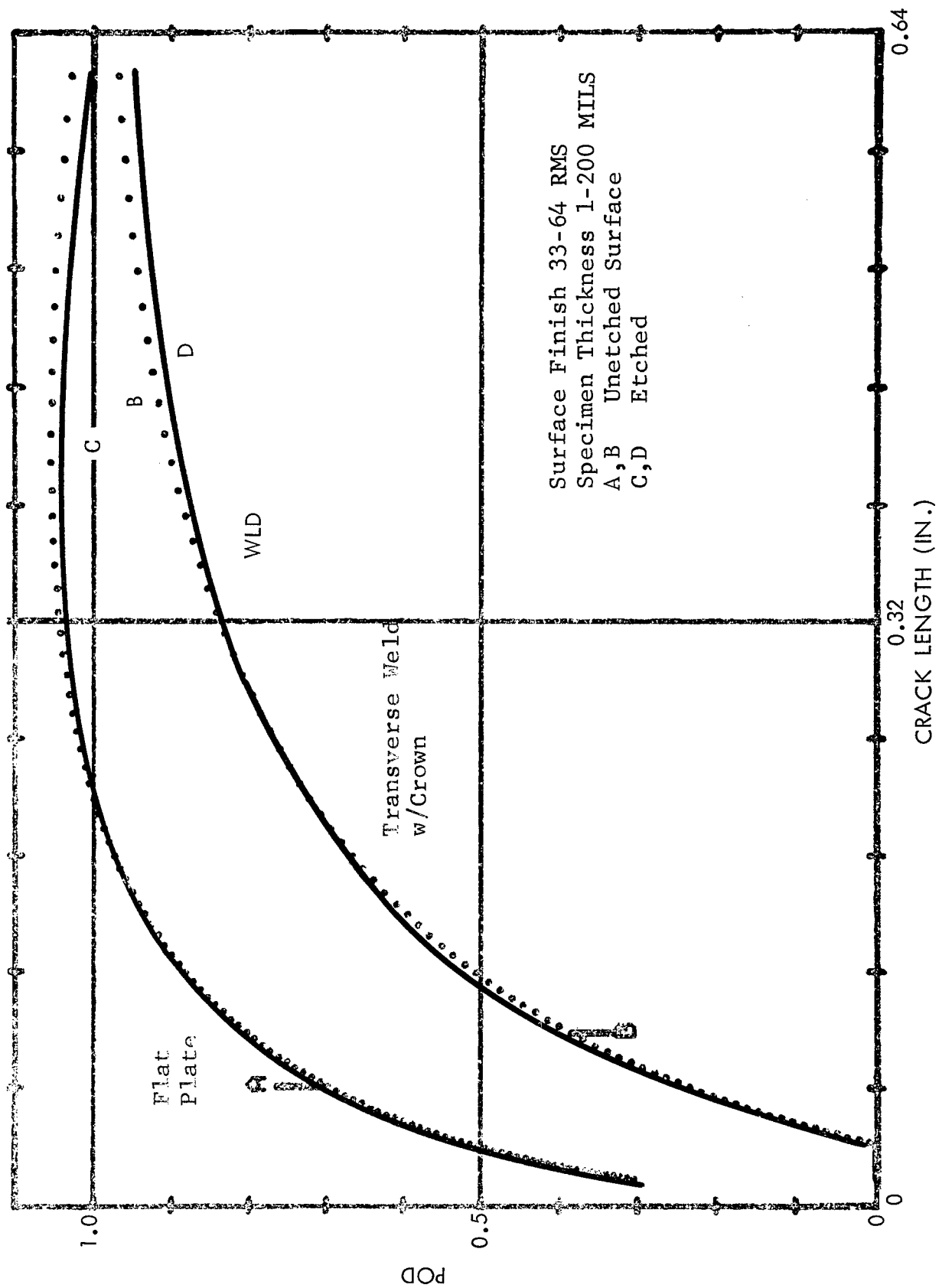


Figure 19 Translation Model by Adaptive Learning Technique - Flat Plate/Transverse Weld w/Crown (Ultrasonic)

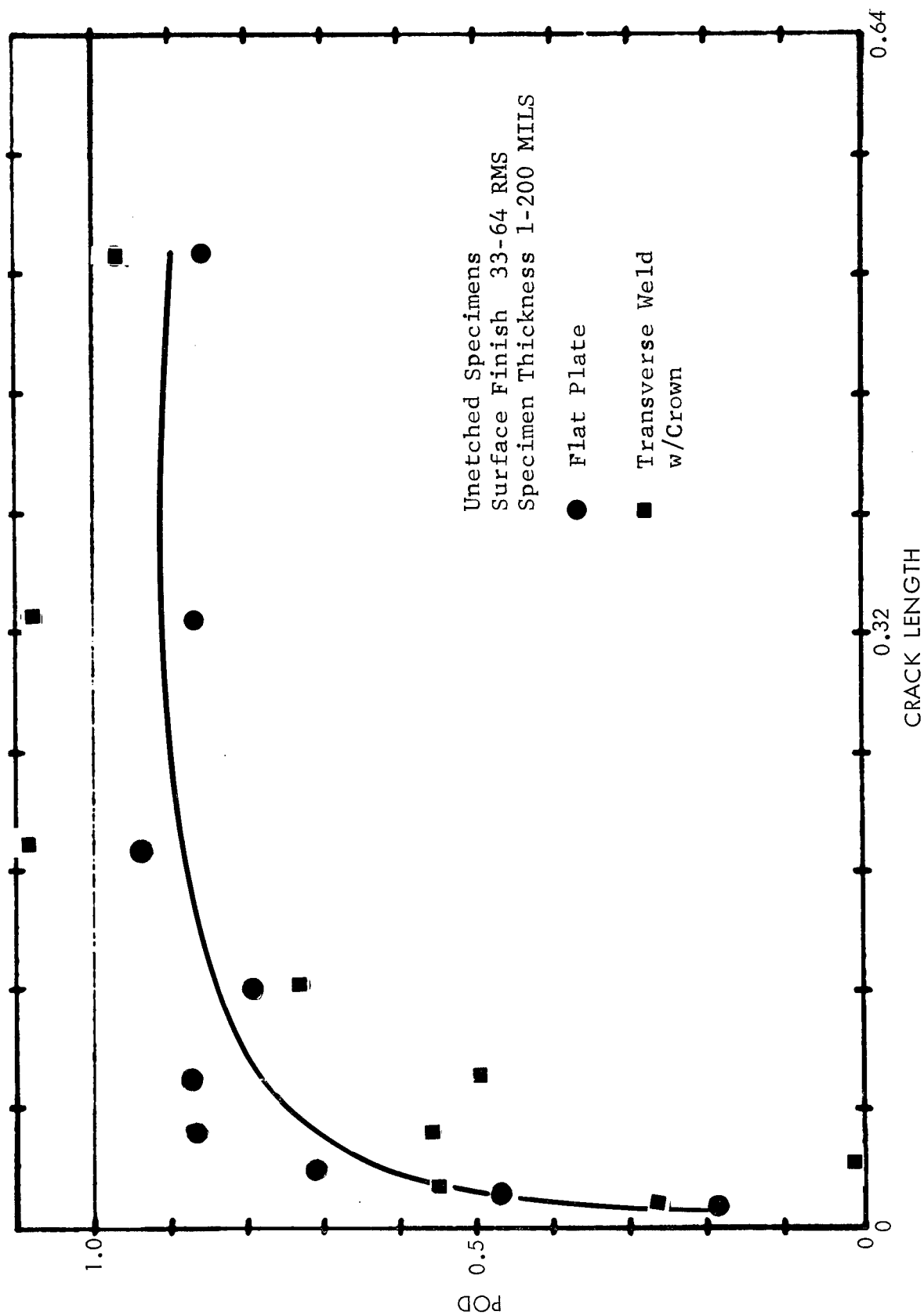


Figure 20 Translation Model by Linear Regression Technique - Flat Plate/Transverse Weld w/Crown (Ultrasonic)

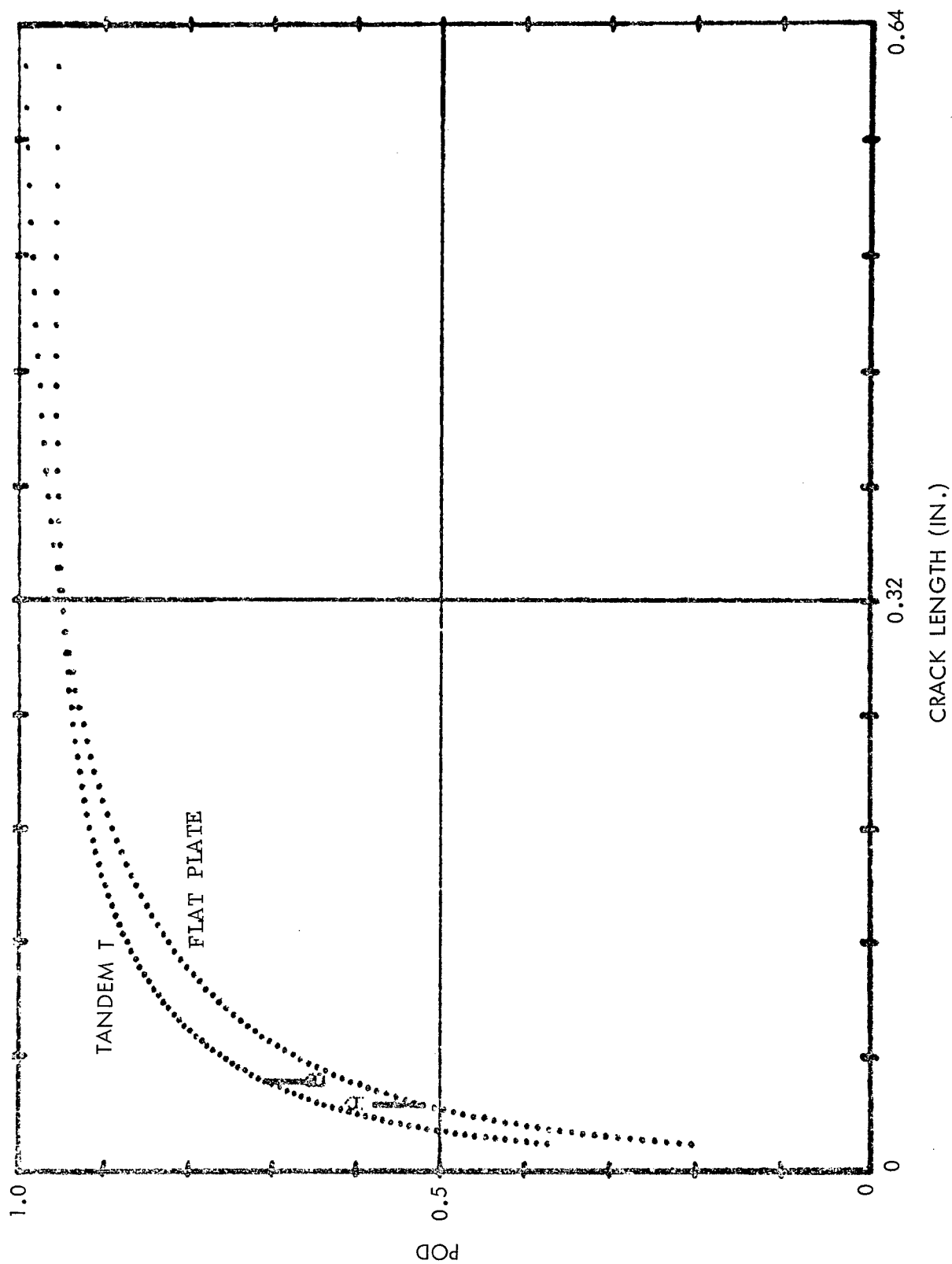


Figure 21 Translation Model by Adaptive Learning Technique - Flat Plate/Tandem T (Ultrasonic)

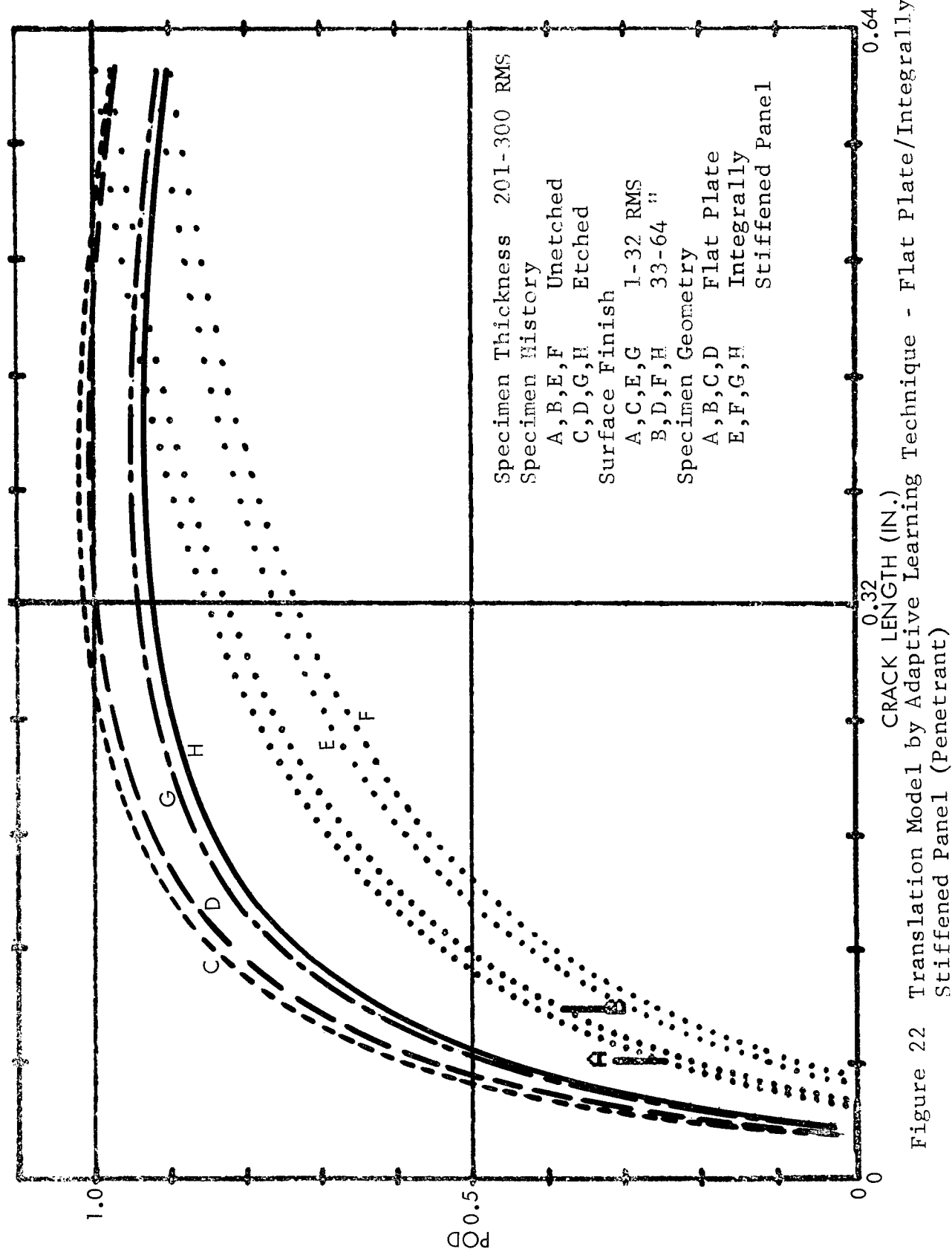


Figure 22 Translation Model by Adaptive Learning Technique - Flat Plate/Integrally Stiffened Panel (Penetrant)

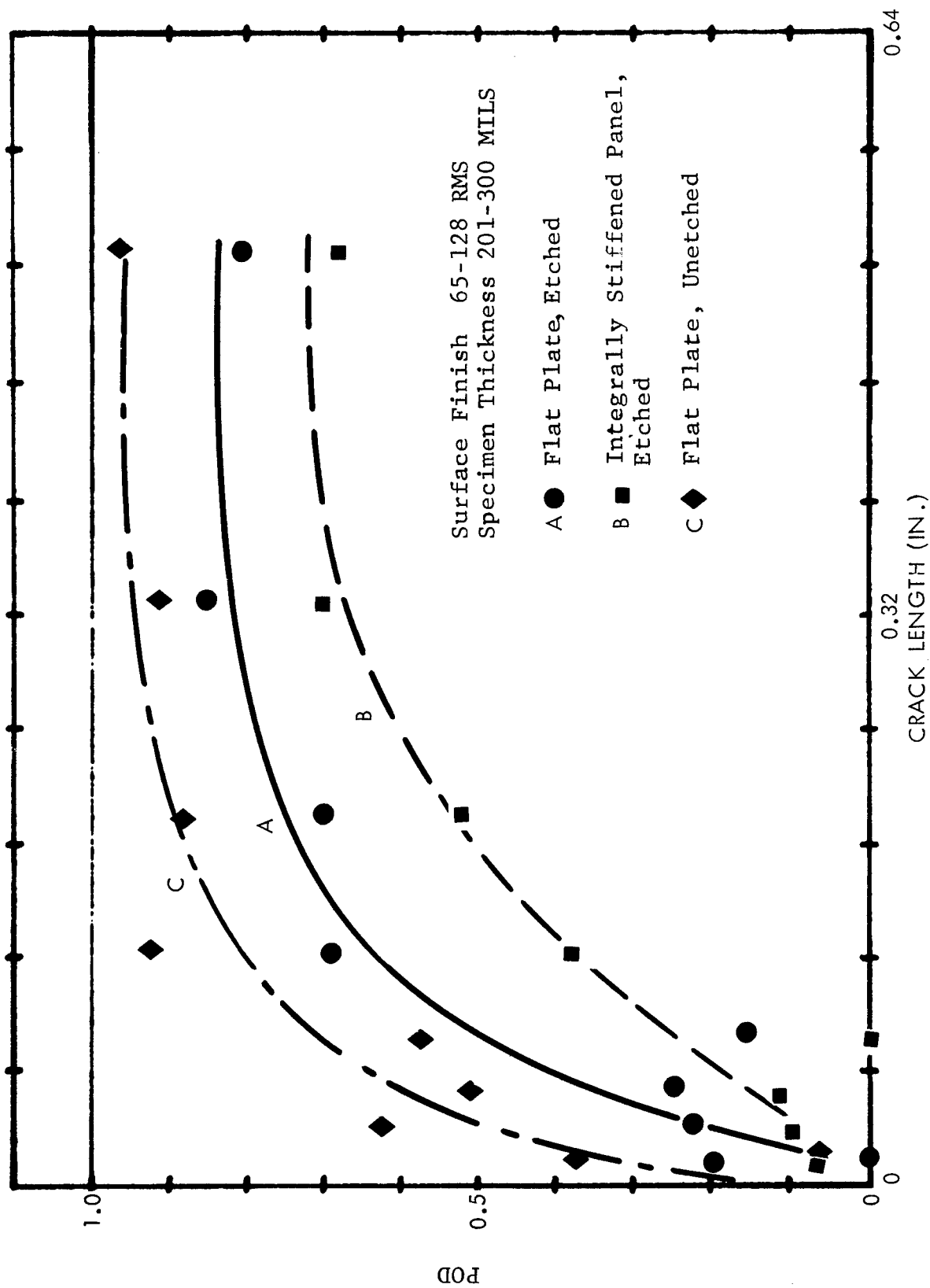


Figure 23 Translation Model by Linear Regression Technique - Flat Plate/Integrally Stiffened Panel (Penetrant)

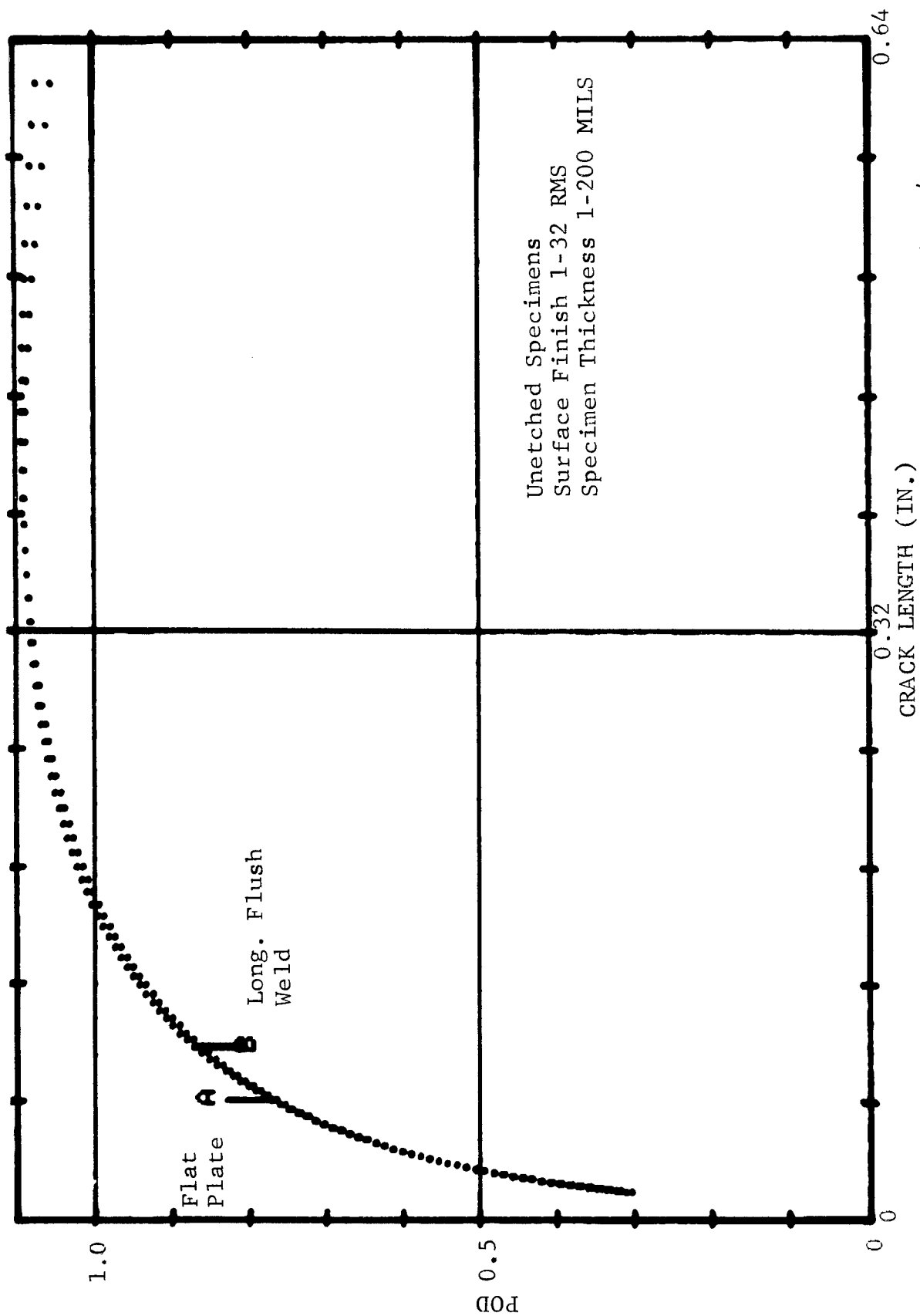


Figure 24 Translation Model by Adaptive Learning Technique - Flat Plate/Long. Flush Weld (Penetrant)

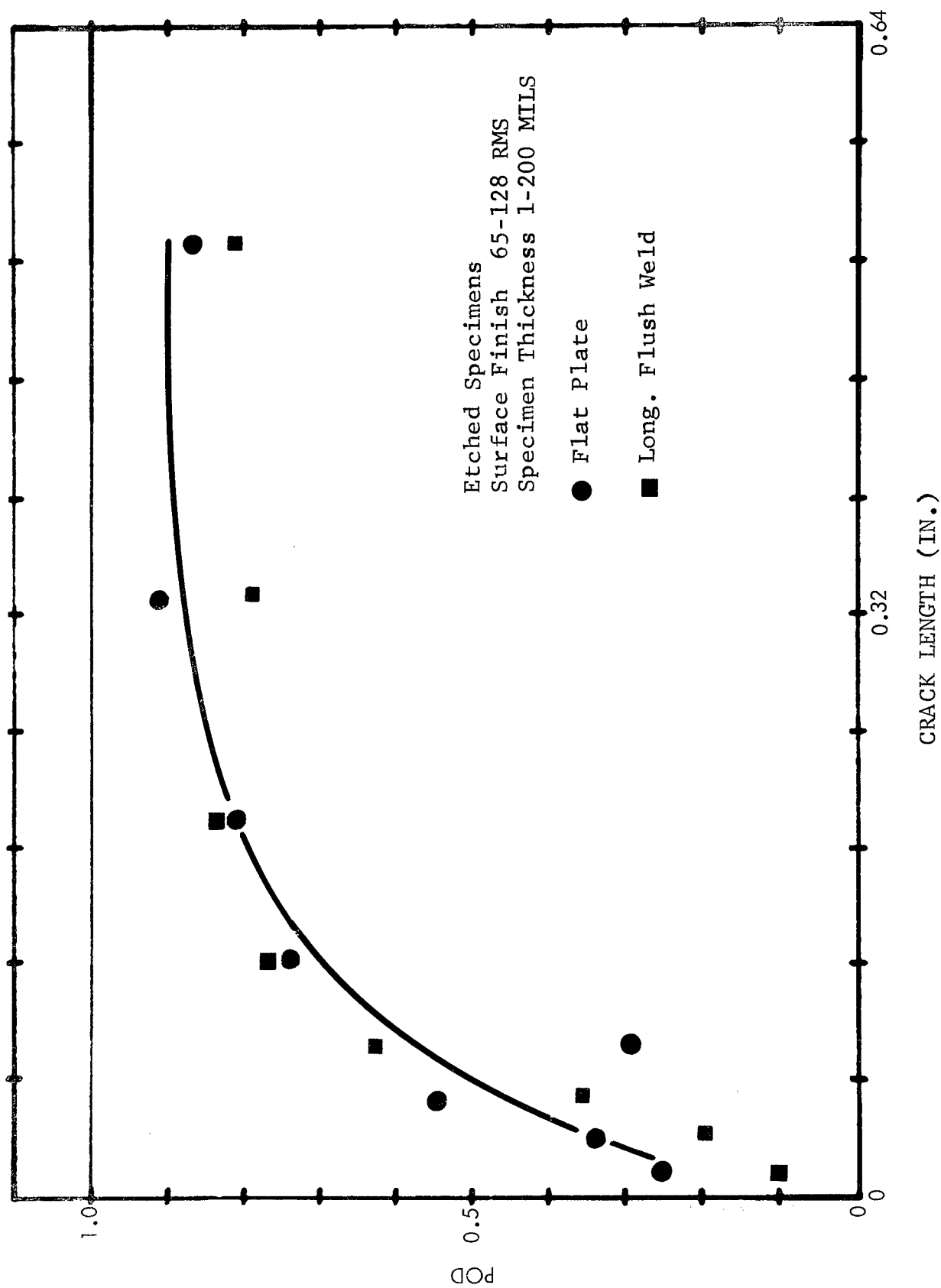


Figure 25 Translation Model by Linear Regression Technique -
Flat Plate/Long. Flush Weld (Penetrant)

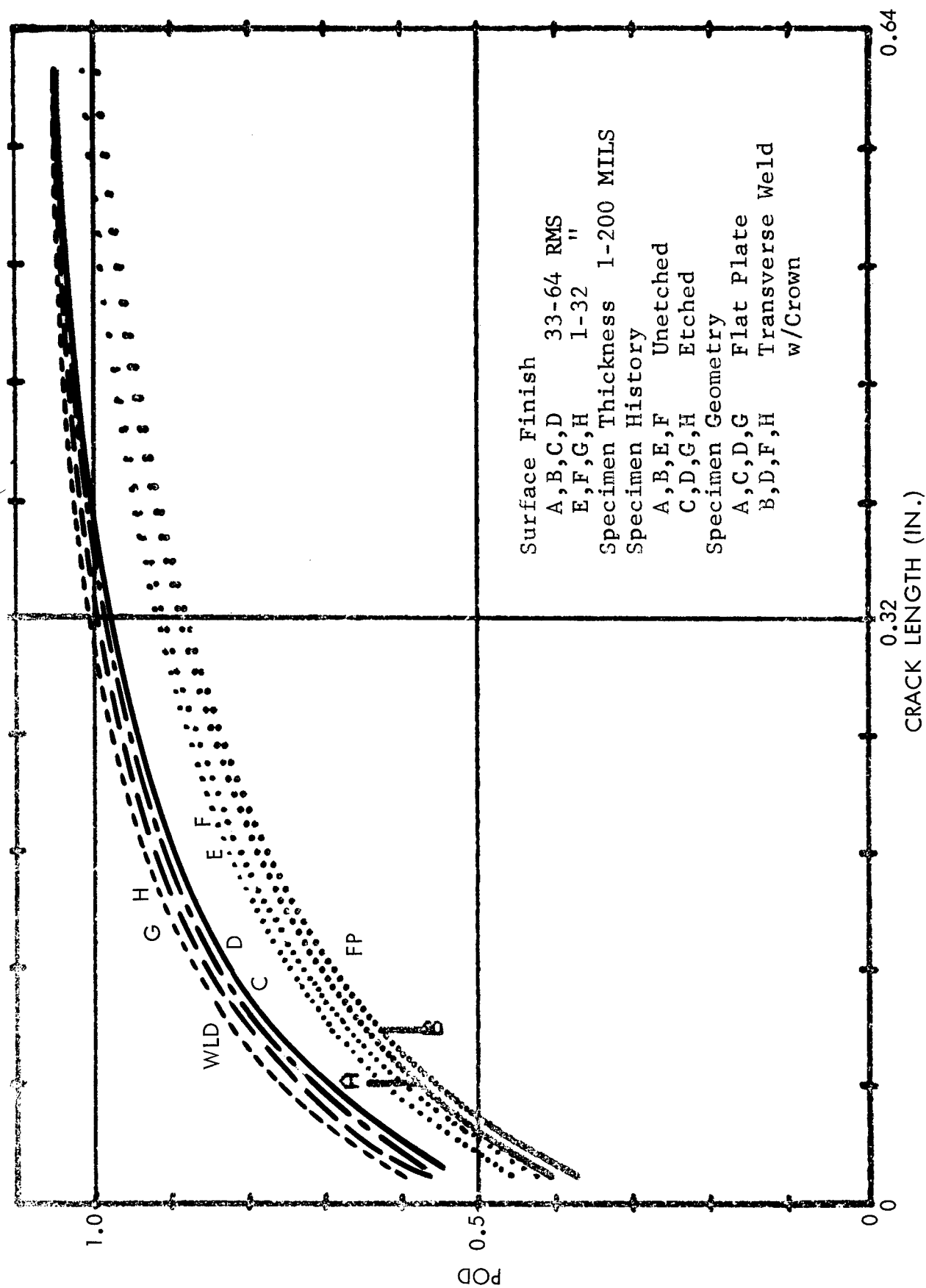


Figure 26 Translation Model Adaptive Learning Technique - Flat Plate/Transverse Weld w/Crown (Penetrant)

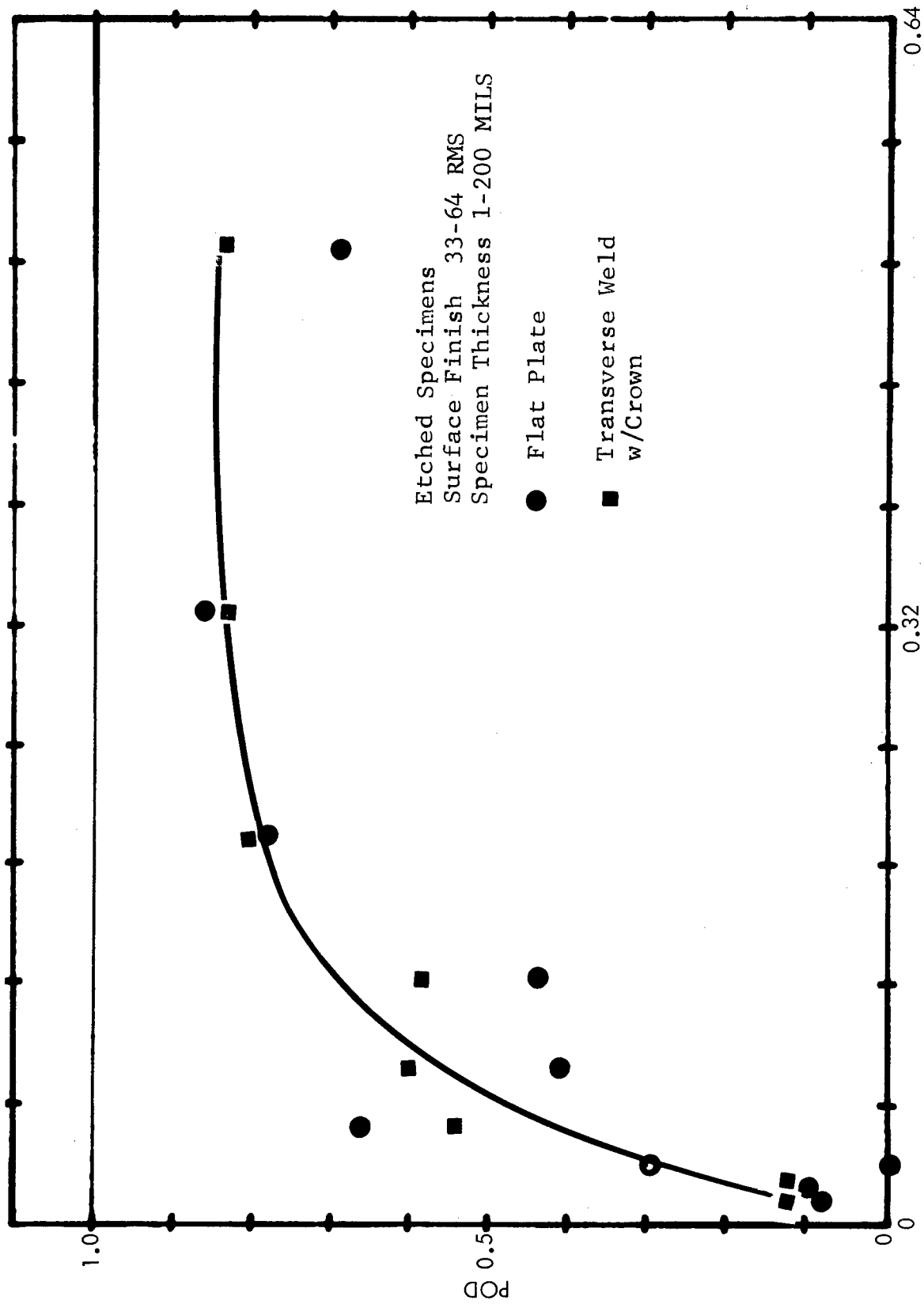


Figure 27 Translation Model by Linear Regression Technique - Flat Plate/
Transverse Weld w/Crown (Penetrant)

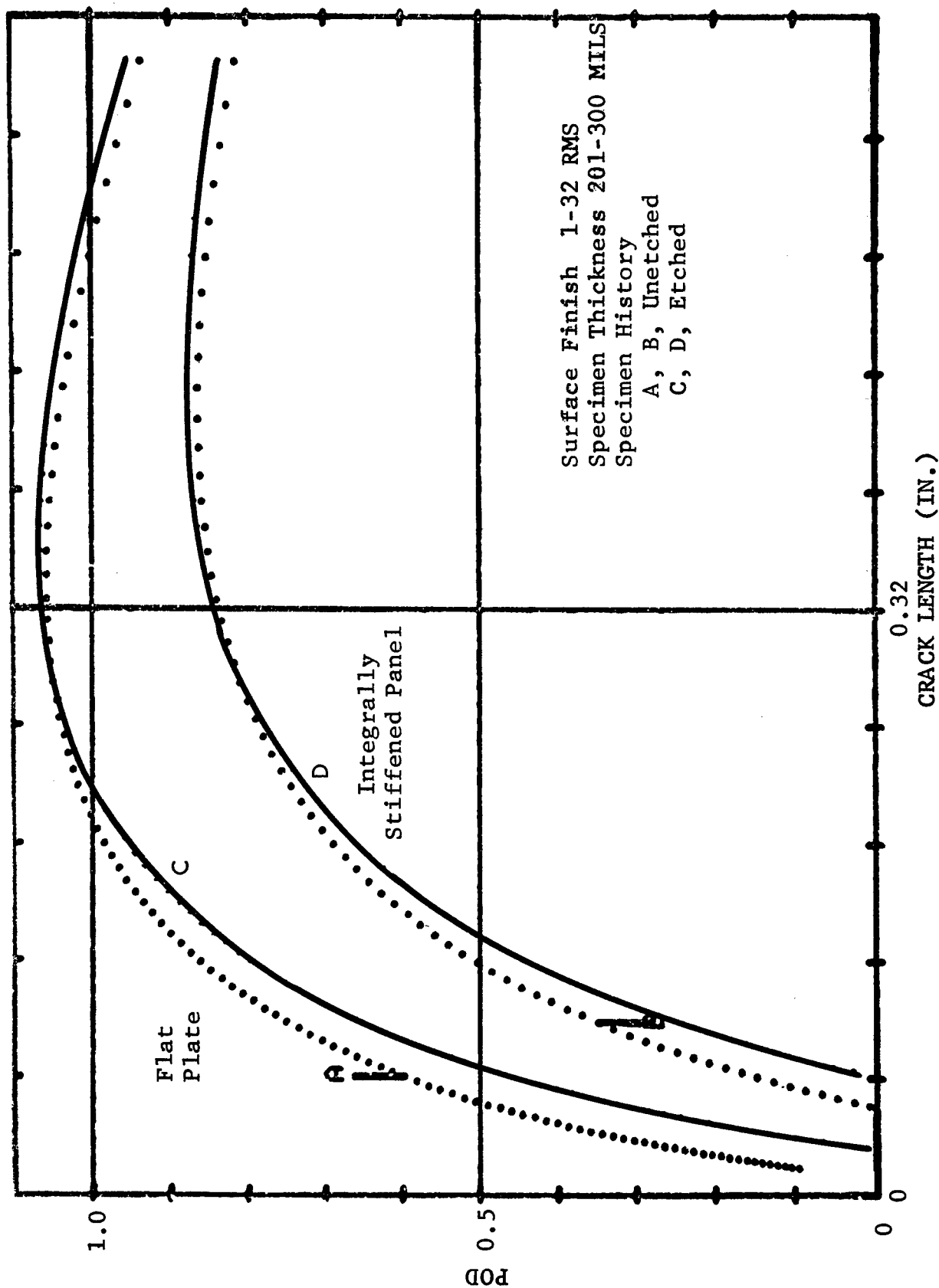


Figure 28 Translational Model by Adaptive Learning Technique - Flat Plate/
 Integrally Stiffened Panel (Eddy Current)

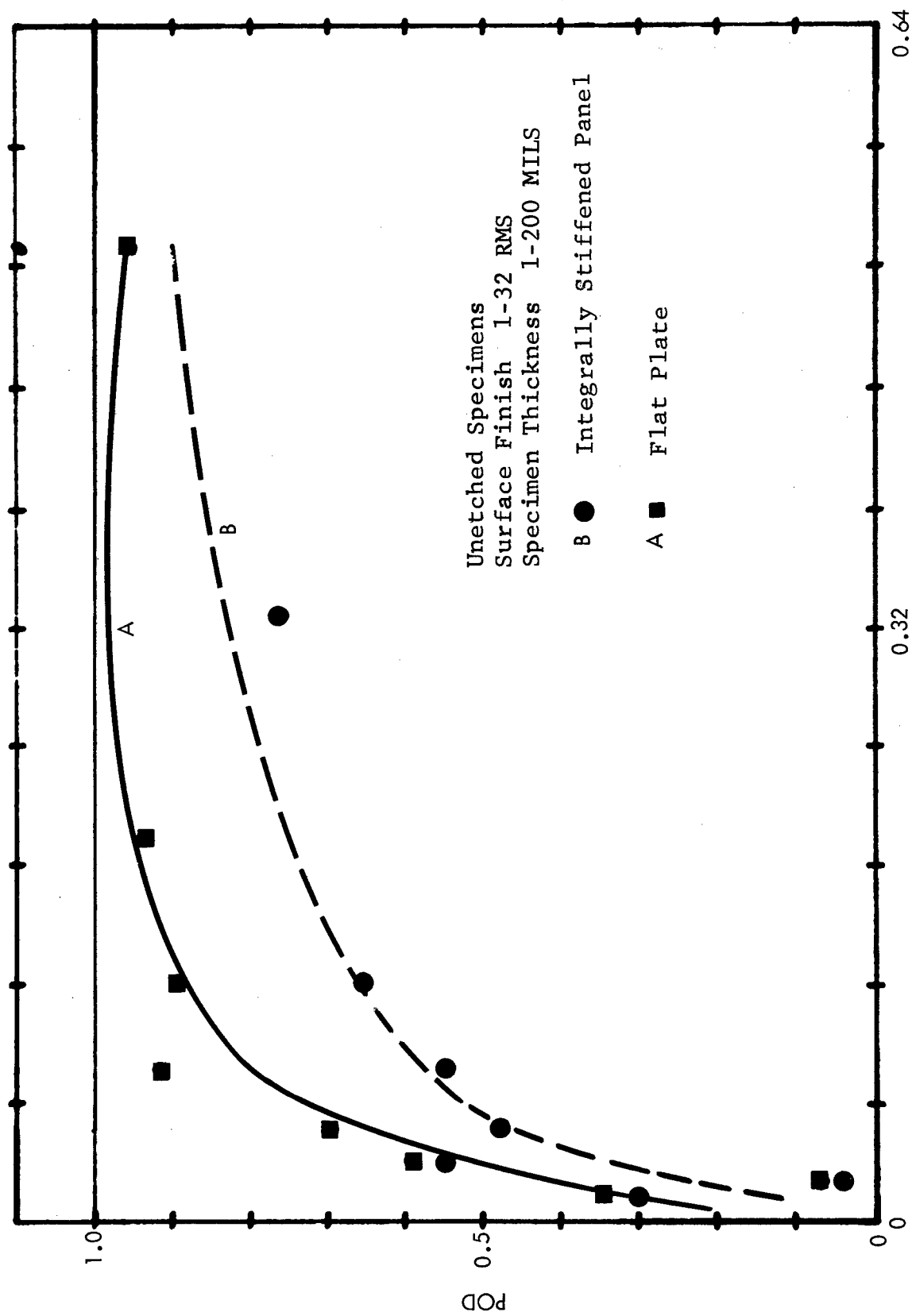


Figure 29 Translation Model by Linear Regression Technique - Flat Plate/Integrally Stiffened Panel (Eddy Current)

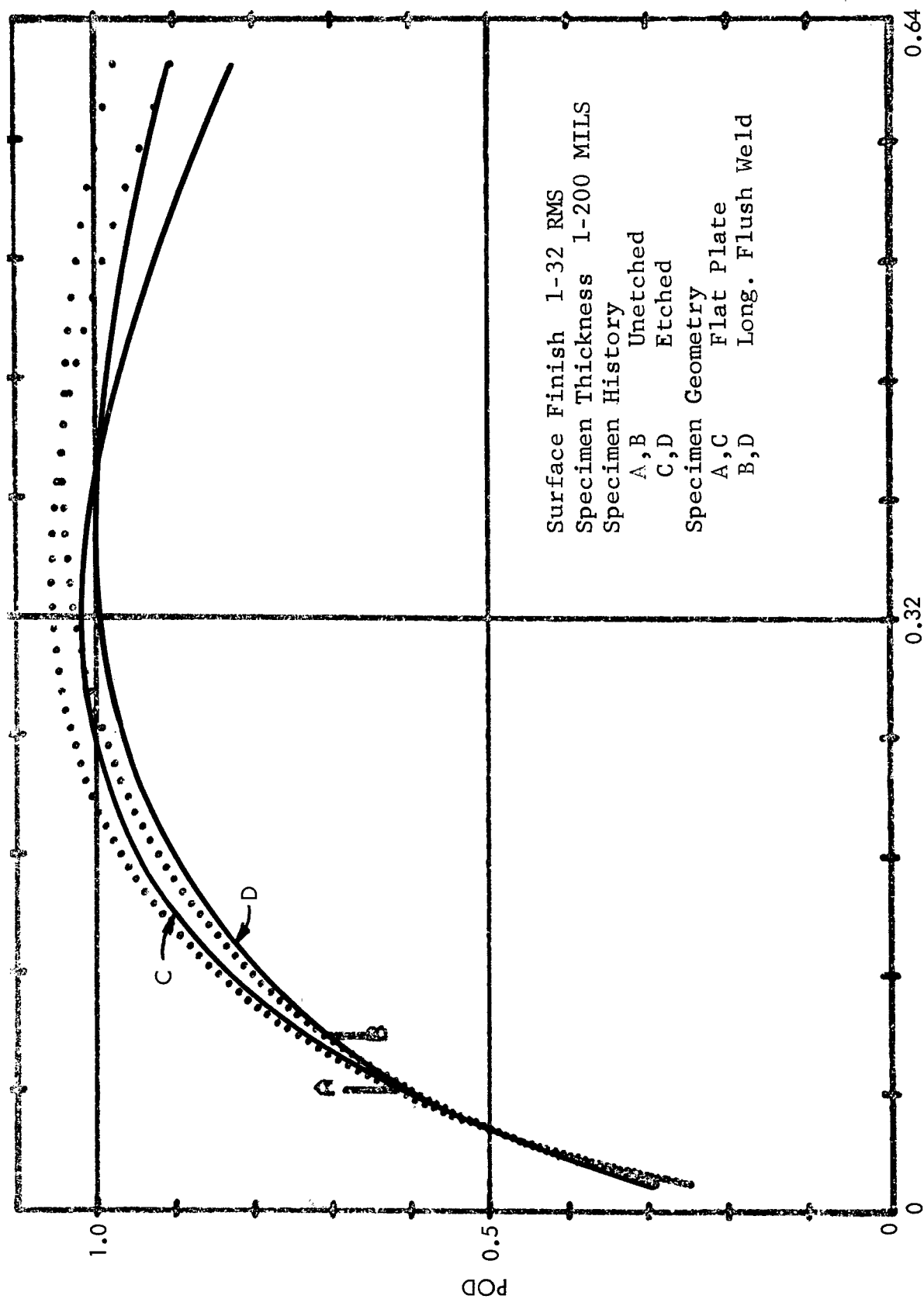


Figure 30 Translation Model by Adaptive Learning Technique - Flat Plate/Long. Flush Weld (Eddy Current)

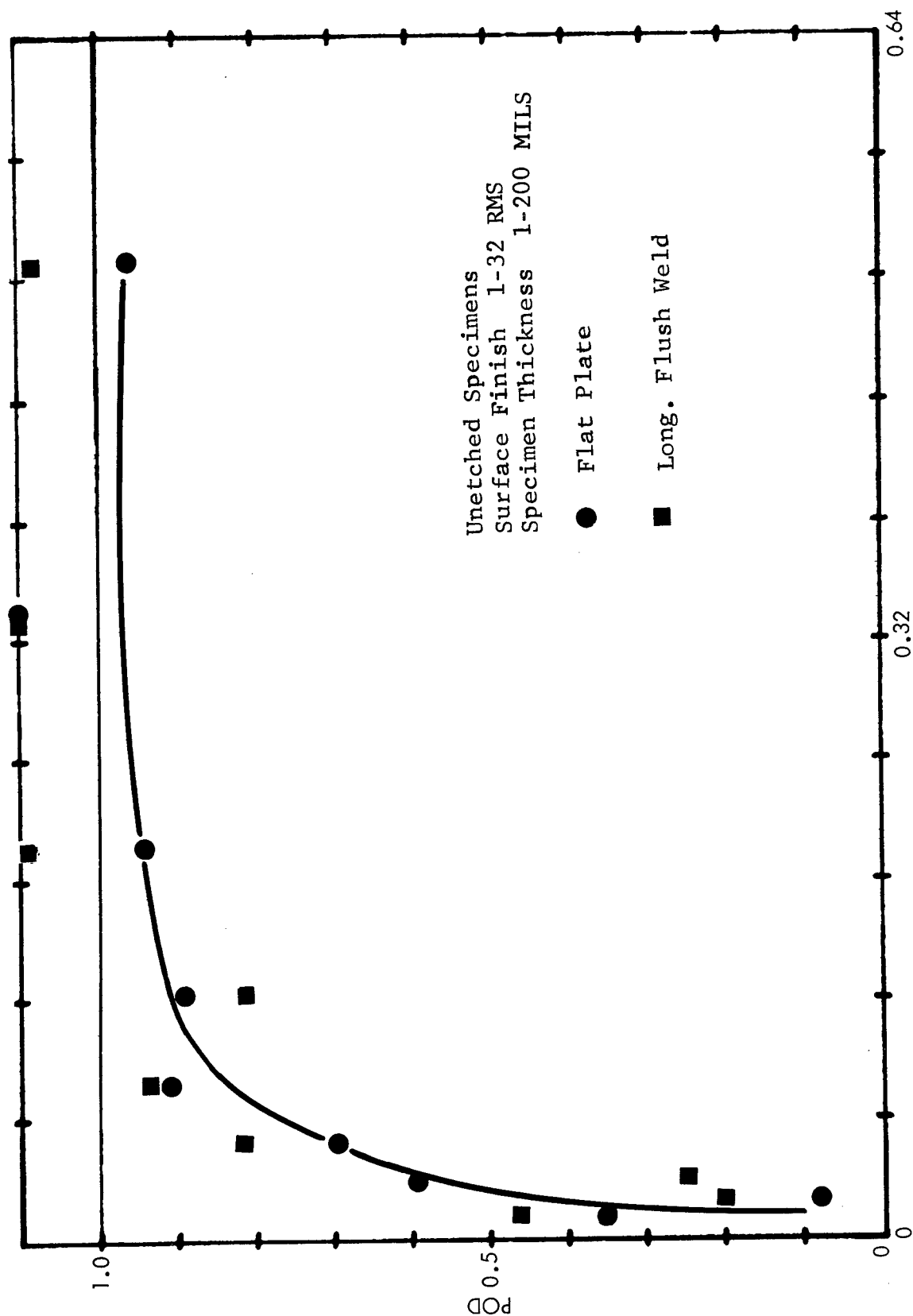


Figure 31 Translation Model by Linear Regression Technique - Flat Plate/Long. Flush Weld (Eddy Current)

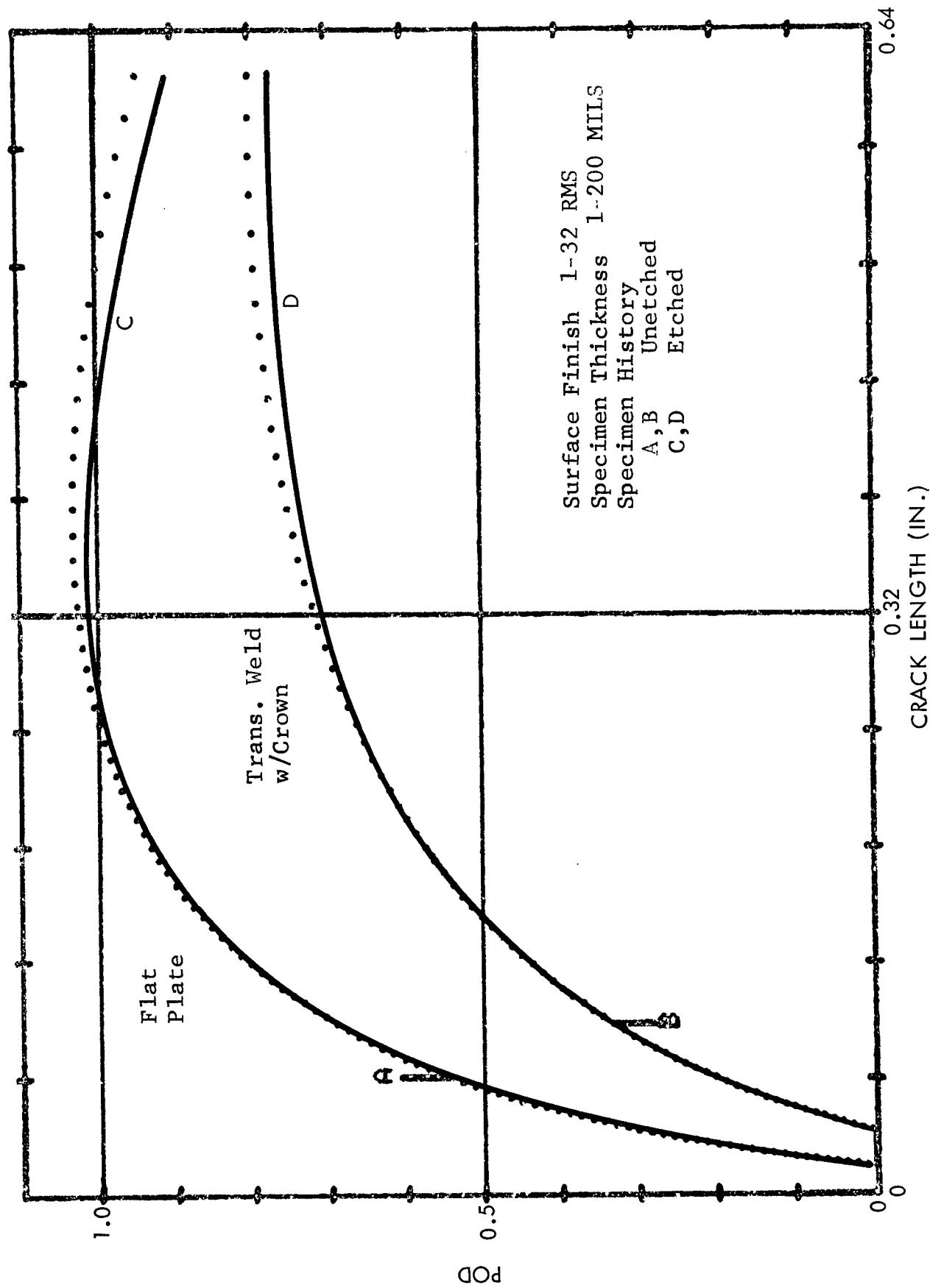


Figure 32 Translation Model by Adaptive Learning Technique - Flat Plate/Transverse Weld w/Crown (Eddy Current)

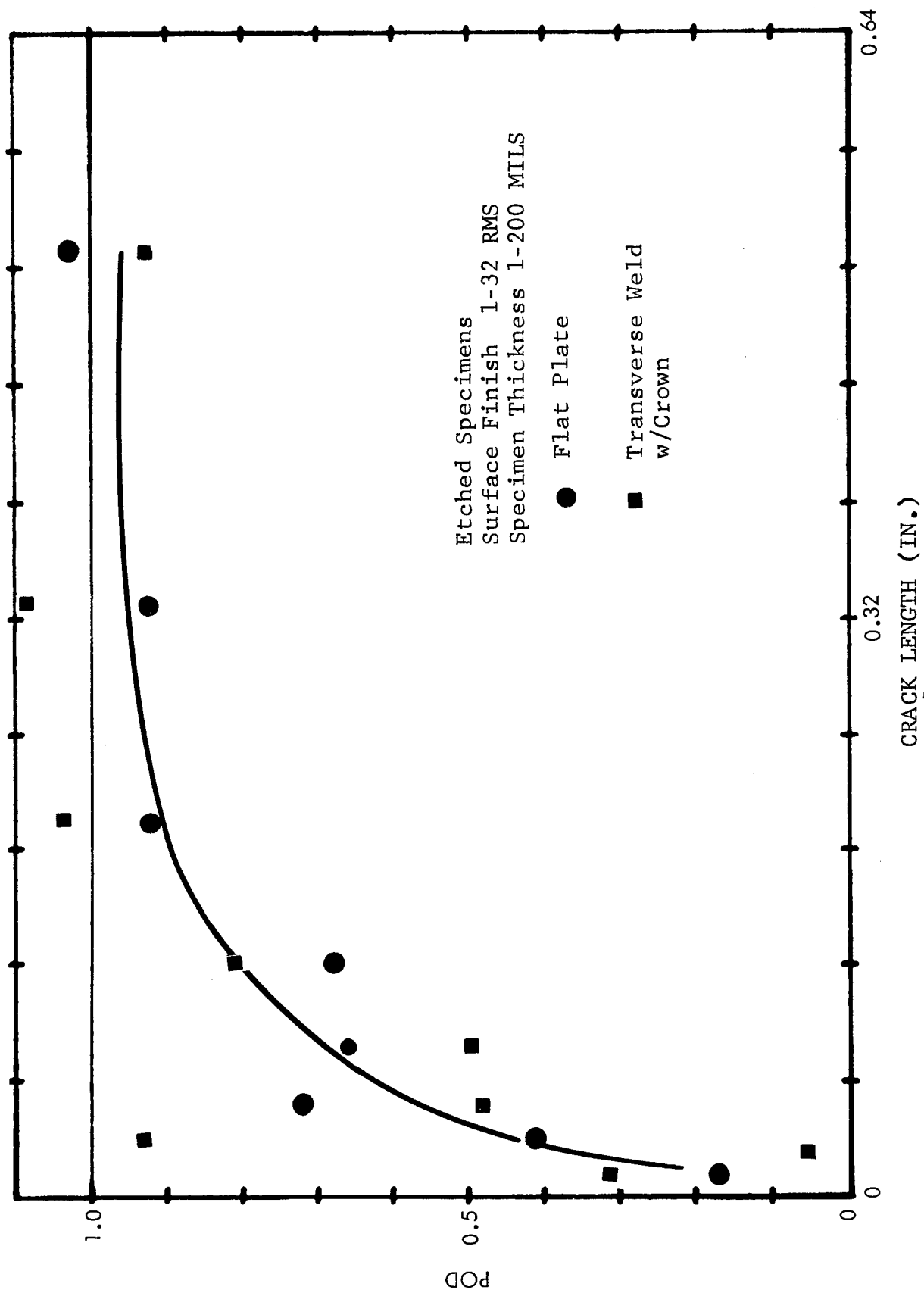


Figure 33 Translation Model by Linear Regression Technique - Flat Plate/
Transverse Weld w/Crown (Eddy Current)

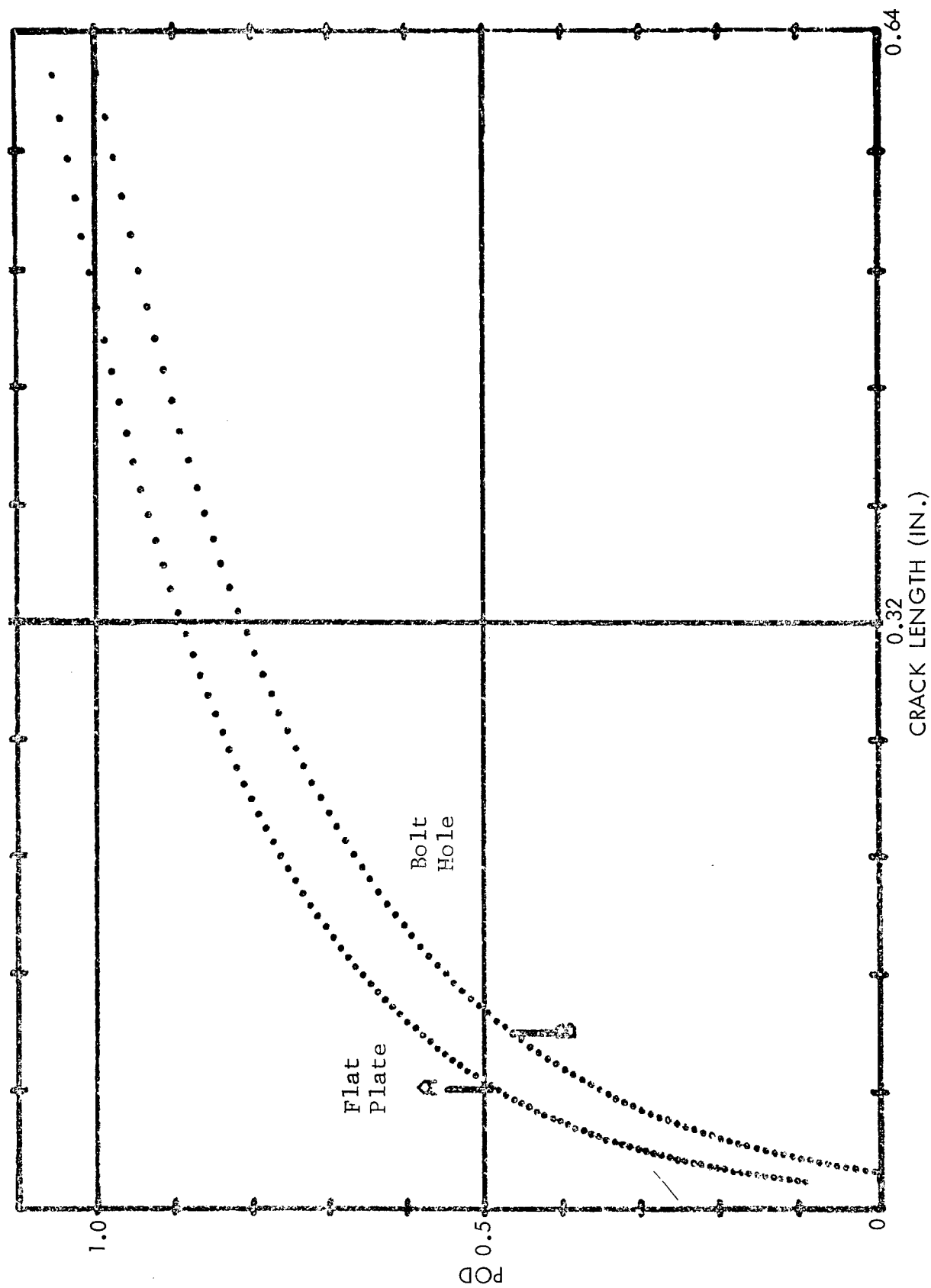


Figure 34 Translation Model by Adaptive Learning Technique - Flat Plate/Bolt Hole (Eddy Current)

specimens was a field and depot type inspection while the flat plate geometry inspection was conducted in a laboratory environment with an automatic scanning device. The bolt hole POD curve is the only one available for model development in the data bank.

6.2.4 Transfer Function

The NDE methods sensitivity for each specimen geometry was studied for the ultrasonic, penetrant, and eddy current inspections by pooling all the data pertaining to that particular geometry without separating the other NDE parameters. The PODs were calculated by using the point estimate method. Figures 35 through 43 show the POD curves for the geometries of flat plate, integrally stiffened panel, longitudinal flush weld, transverse weld with crown, longitudinal weld with crown, riveted plate to integrally stiffened panel, weld panels with LOP, bolt holes, and tandem T, respectively. Each of these figures contains data points for three inspection techniques. The total number of data points (N) for each inspection technique is indicated in parenthesis. For the sake of clarity, only a curve joining the ultrasonic data points was drawn in each figure.

The flat plate specimens contained the largest number of data points. They represent the reliability data generated by several companies using the same specimens. These data are considered to be the most complete and well-balanced data sets in the reliability data bank. The well-behaved POD curves for this specimen geometry reflect the large population of data point in Figure 35. The second most populous curve is the POD curve for bolt holes for the eddy current inspection (N=1896). The curve is also well-behaved although the POD levels for the curve were rather low.

A transfer function to relate the ultrasonic data from flat plates to specimens with each of the other geometries can be obtained from the data in Figures 35 to 43. It is defined by the following relationship:

$$\text{Transfer Function} = \frac{\text{POD (Other Geometries)}}{\text{POD (Flat Plate)}} .$$

The transfer function for translating POD curves from flat plate to integrally stiffened panel specimens was calculated and plotted in Figure 44. Similar curves could be generated for the other

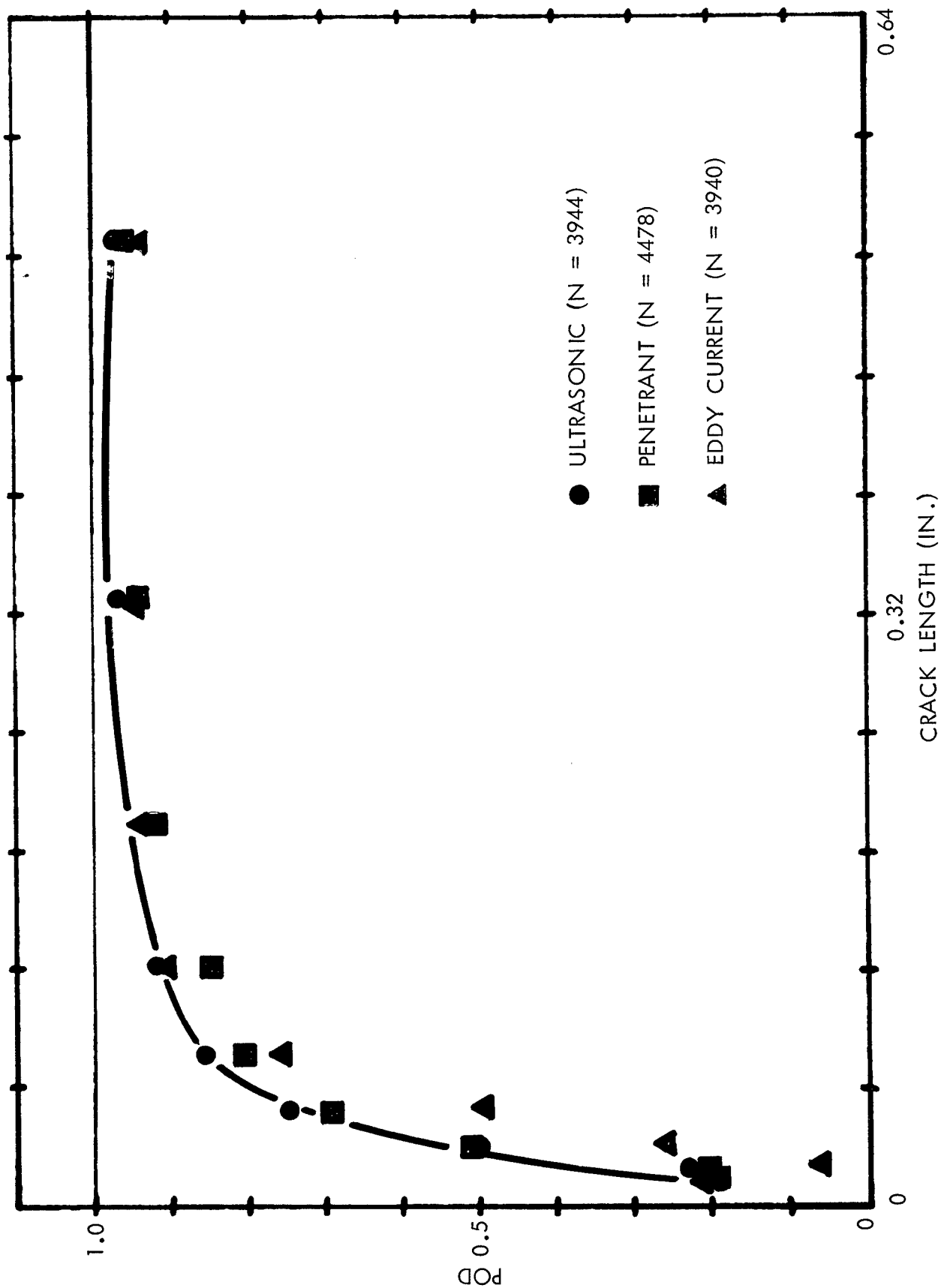


Figure 35 NDE Methods Sensitivity for Flat Plates by Point Estimate Method

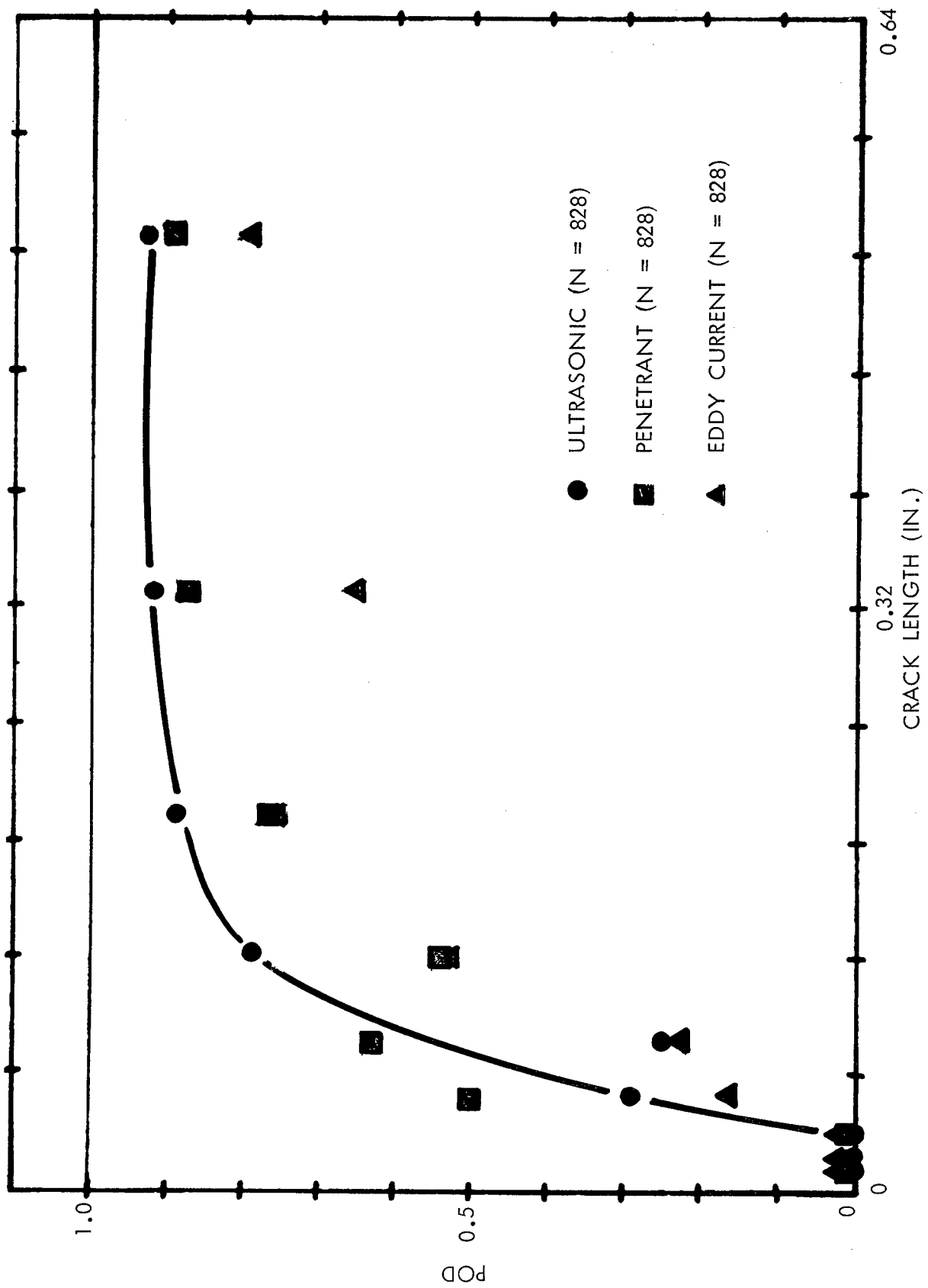


Figure 36 NDE Methods Sensitivity for Integrally Stiffened Panels
by Point Estimate Method

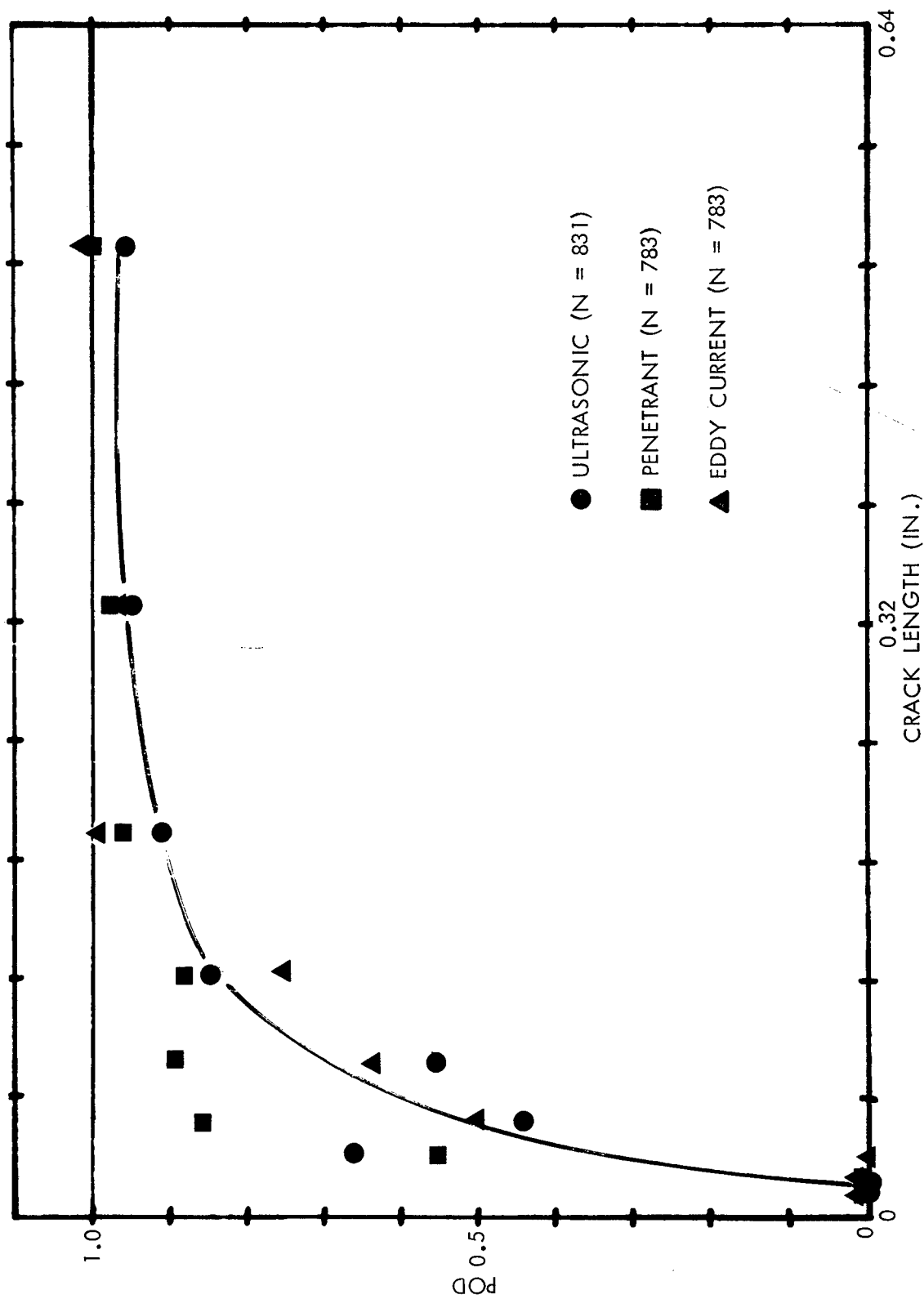


Figure 37 NDE Methods Sensitivity for Longitudinal Flush Weld by Point Estimate Method

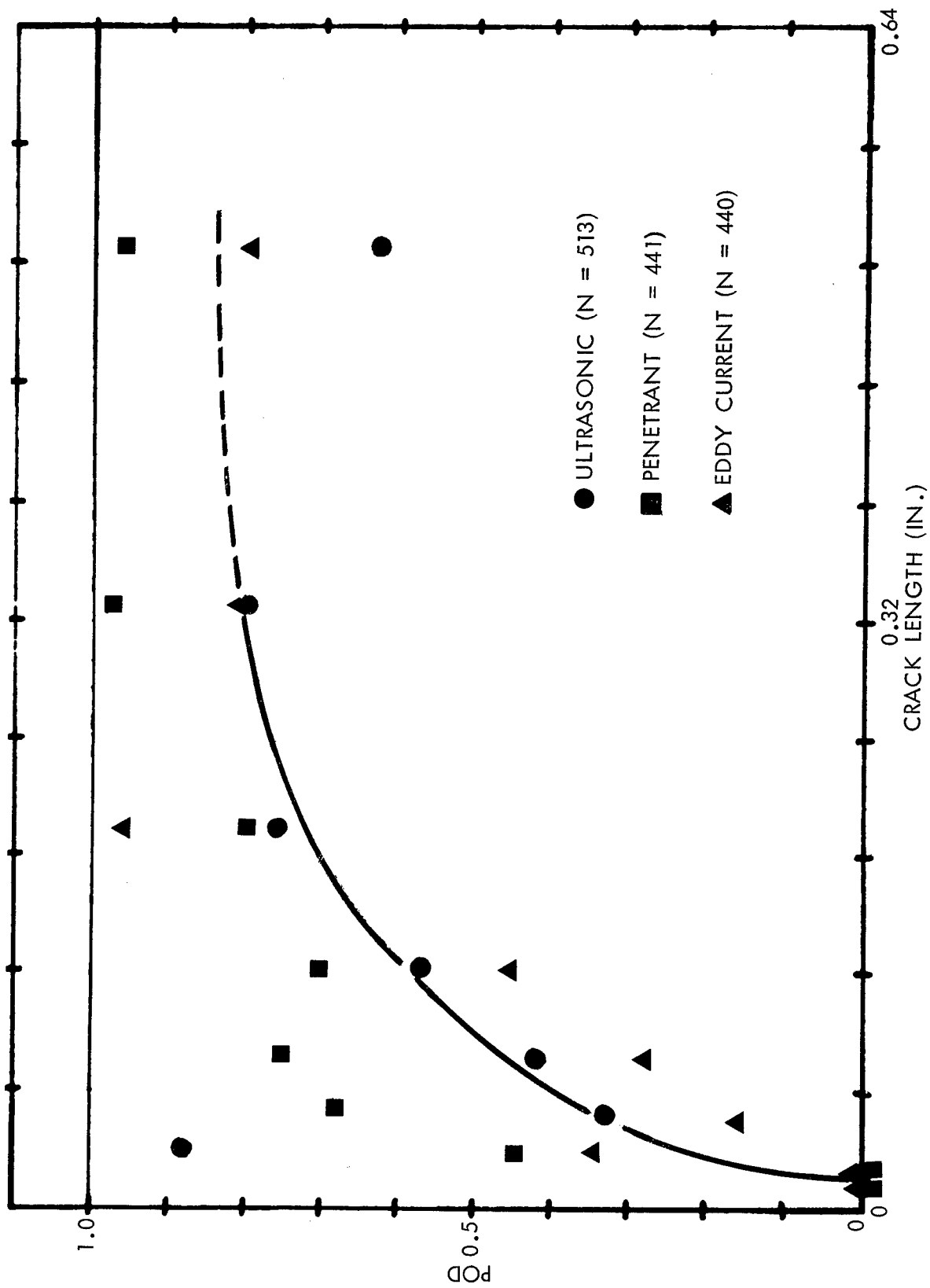


Figure 38 NDE Methods Sensitivity for Transverse Weld w/Crown by Point Estimate Method

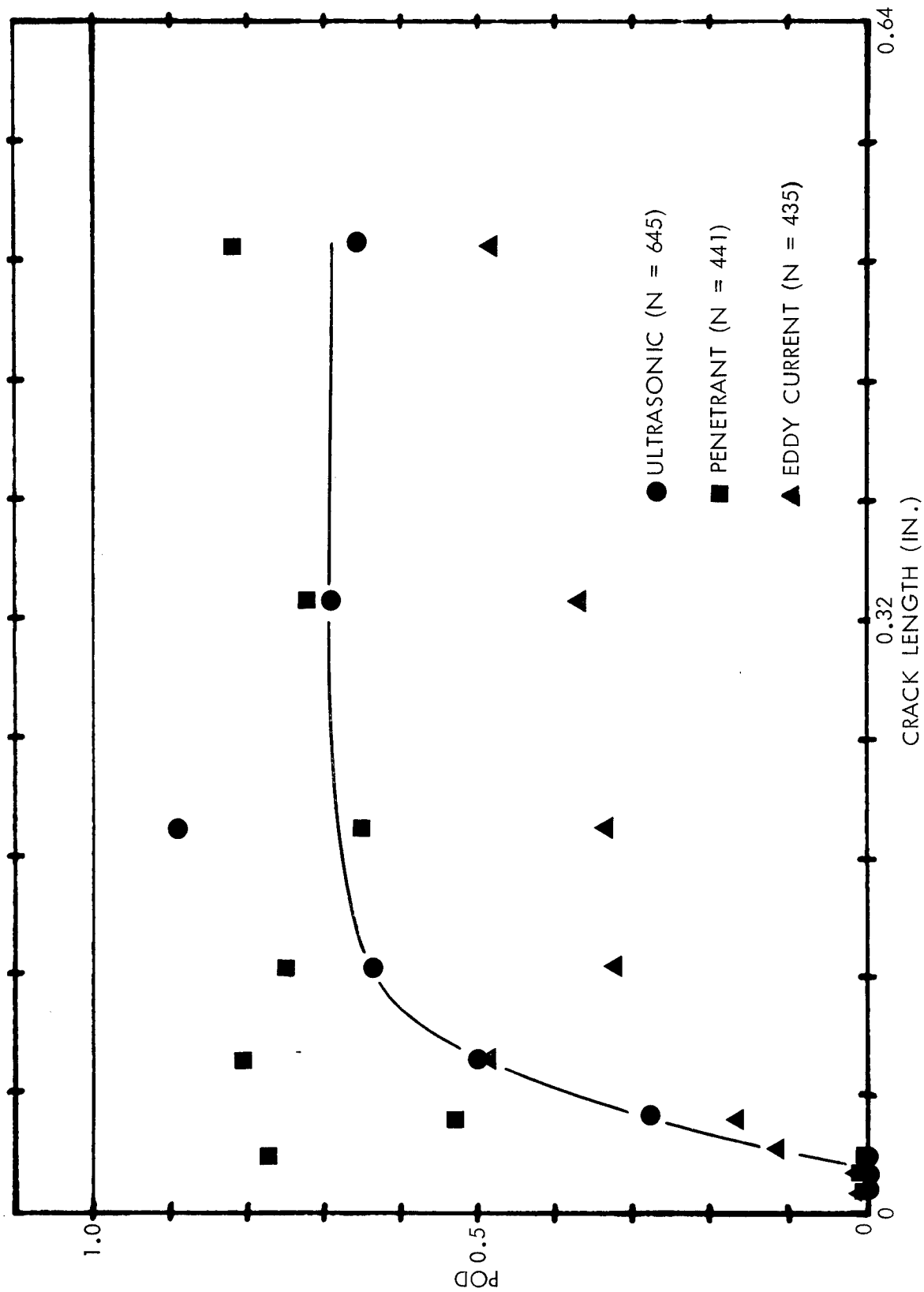


Figure 39 NDE Methods Sensitivity for Longitudinal Weld with Crown by Point Estimate Method

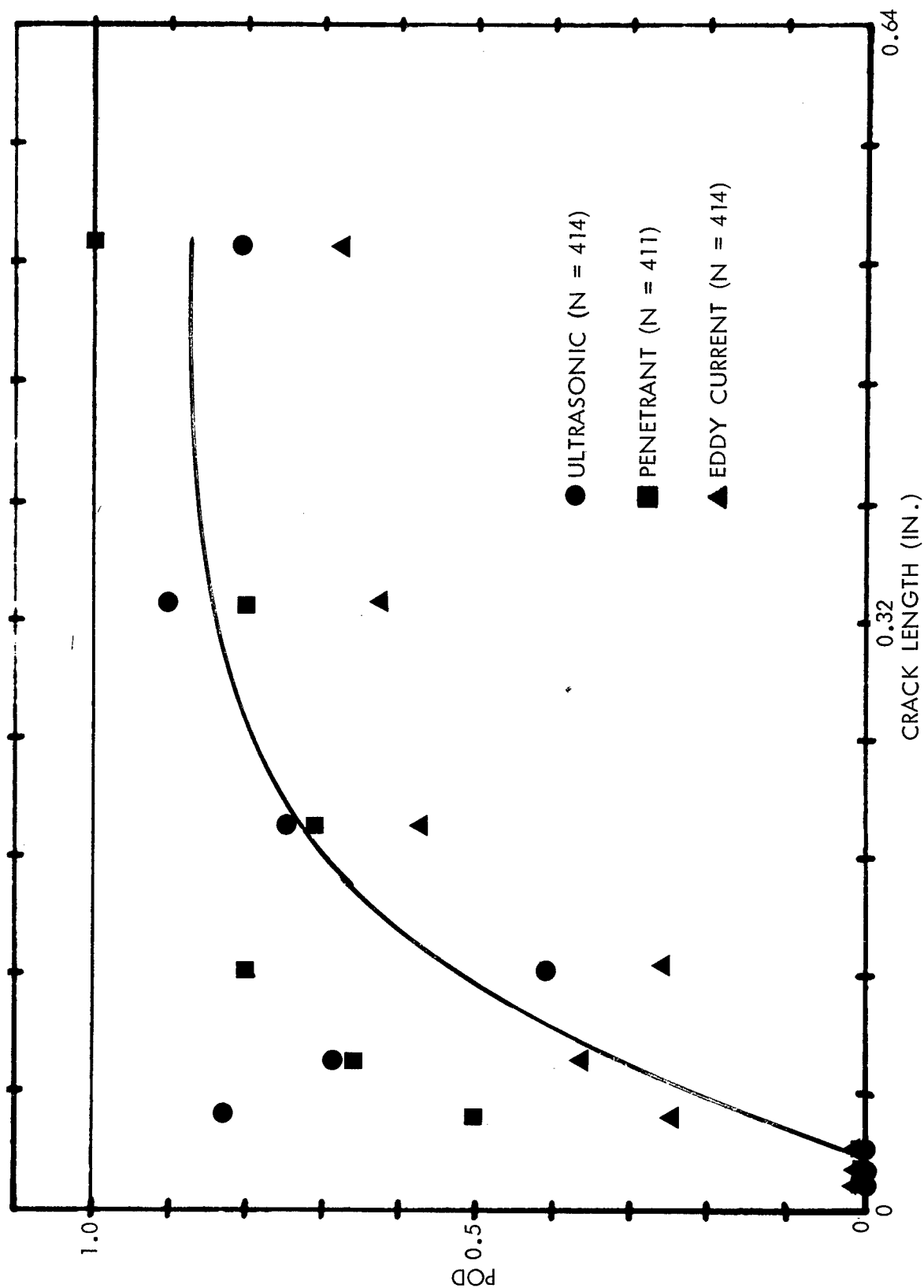


Figure 40 NDE Methods Sensitivity for Riveted Plate to Integrally Stiffened Panel by Point Estimate Method

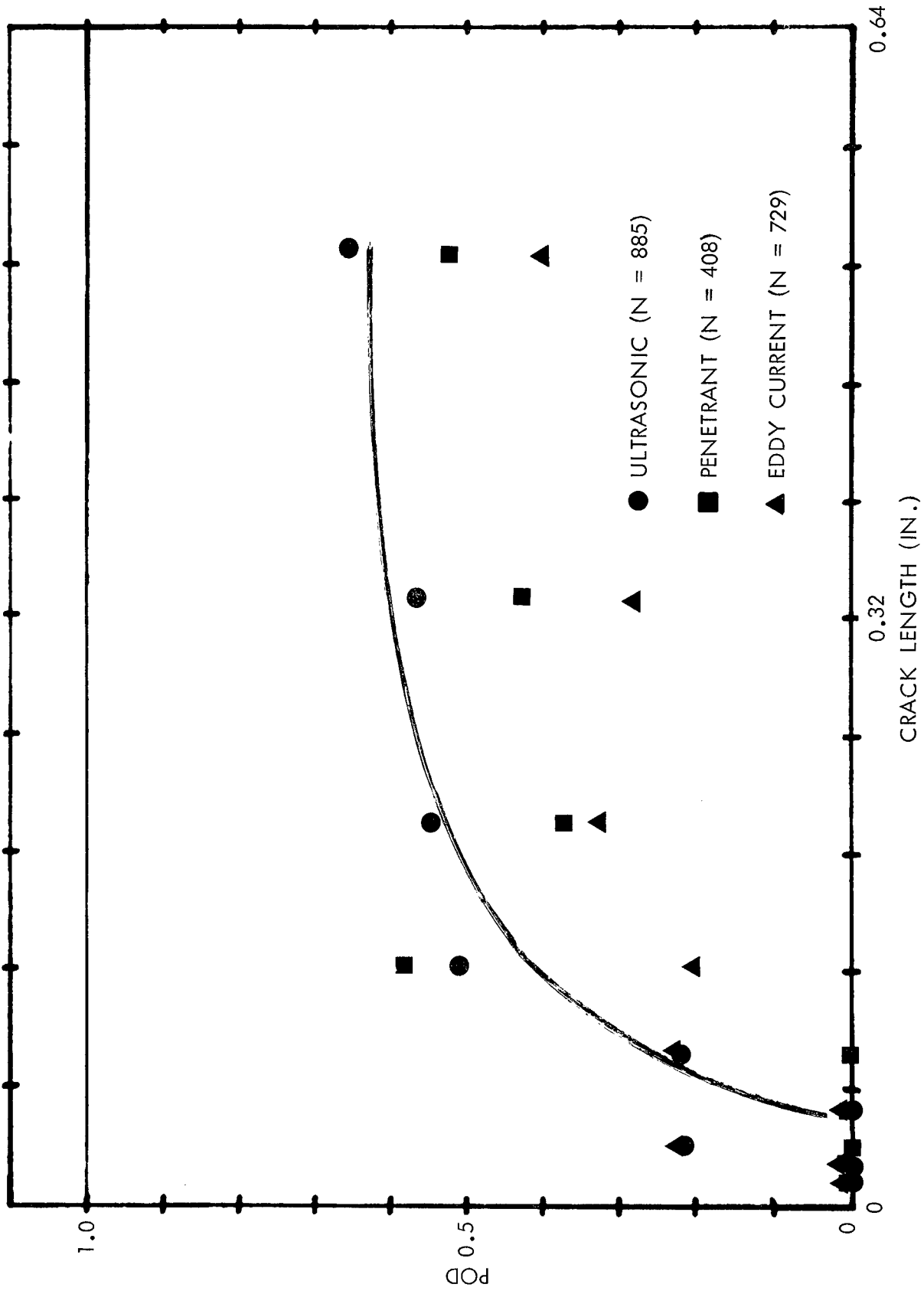


Figure 41 NDE Methods Sensitivity for Weld Panels with IOP by Point Estimate Method

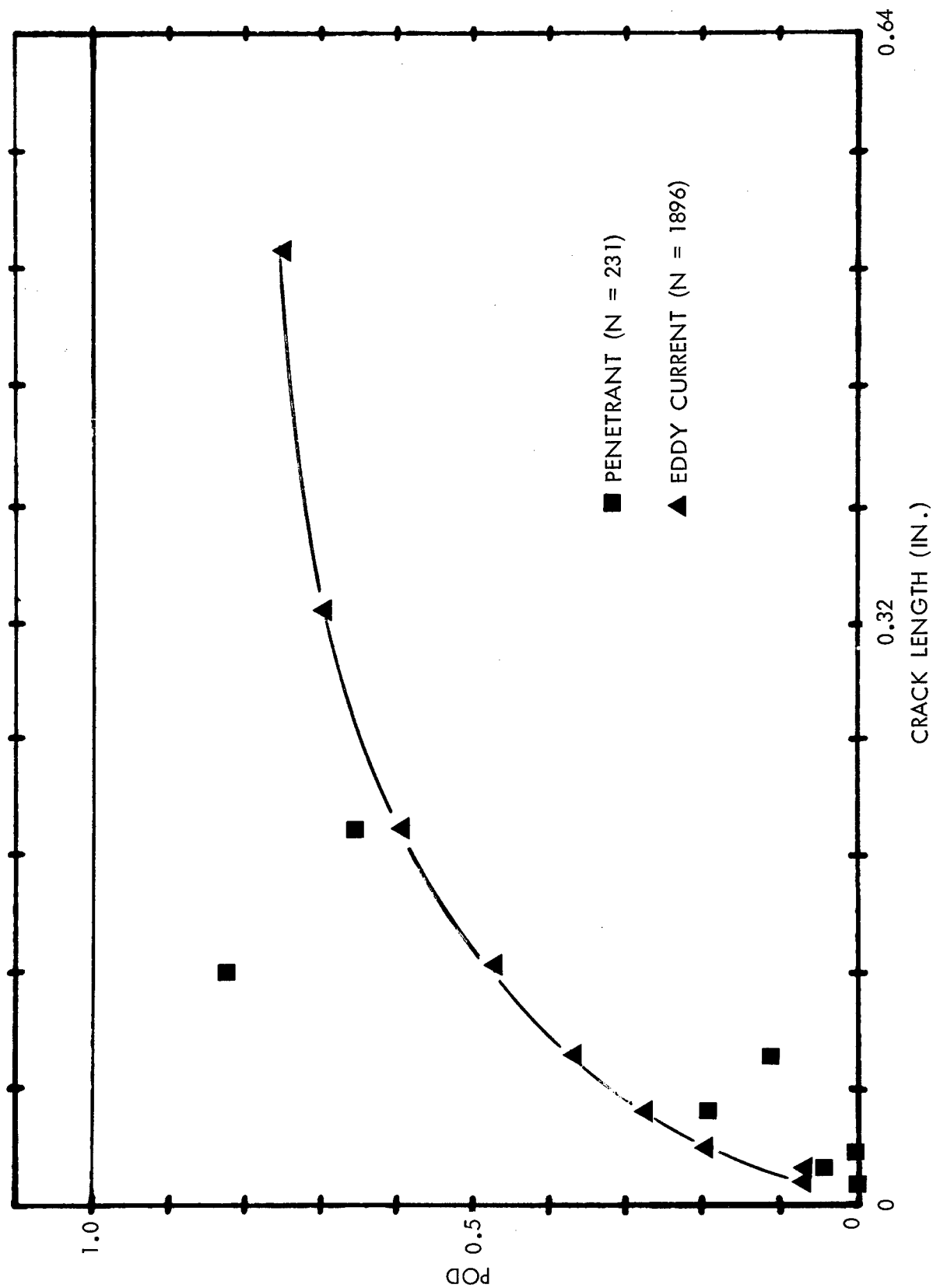


Figure 42 NDE Methods Sensitivity for Bolt Holes by Point Estimate Method

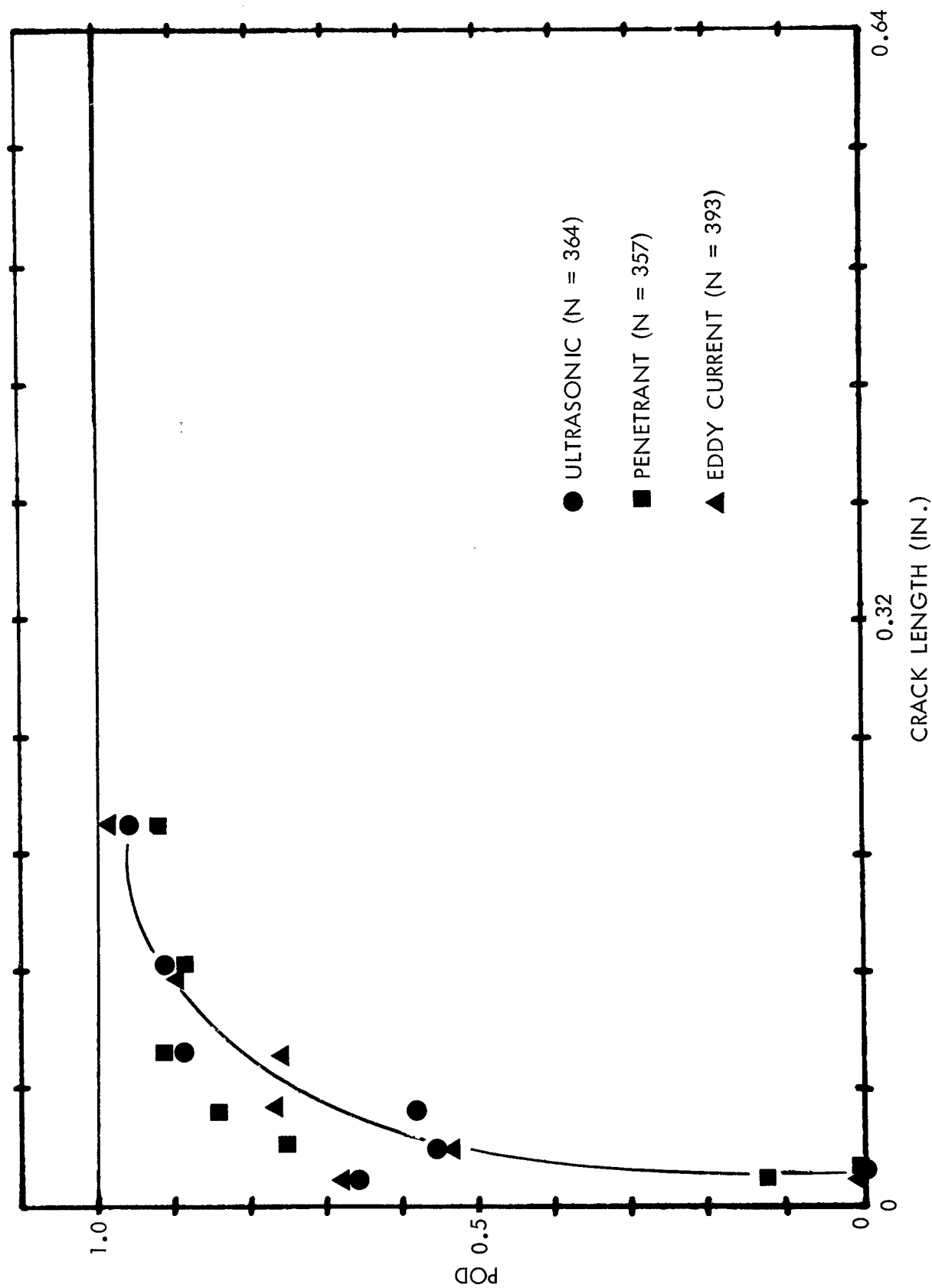


Figure 43 NDE Methods Sensitivity for Tandem T by Point Estimate Method

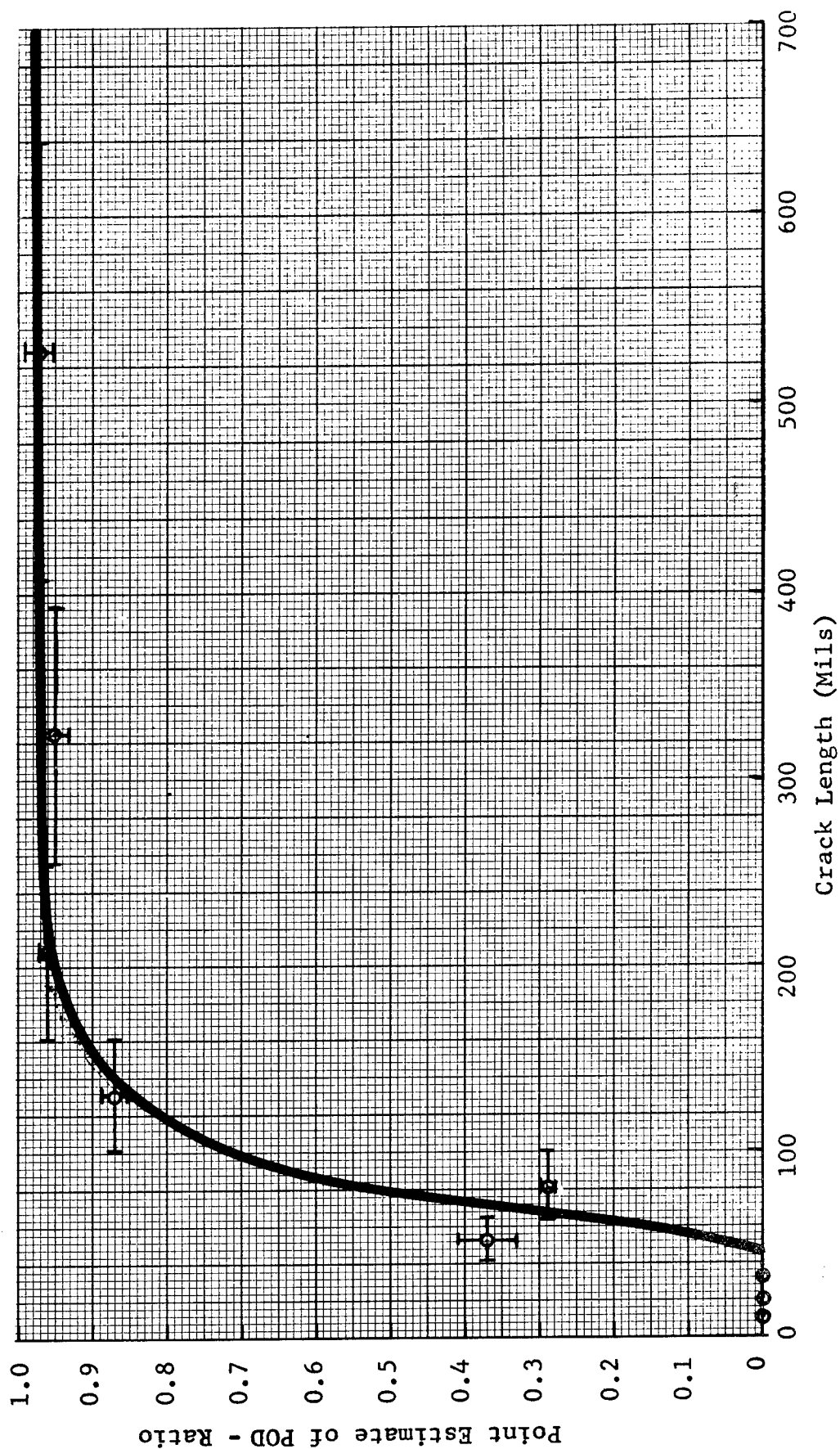


Figure 44 Transfer Function for Flat Plate/Integrally Stiffened Panel
for Ultrasonics

geometries. The main purpose of the composite POD curves, however, is to serve as a check for the adaptive learning and linear regression translation models discussed earlier. The comparison of the point estimate results with the adaptive learning and linear regression results can be easily done by transposing POD curves in Figures 36 through 43 to the flat plate curve in Figure 35. The comparison substantiated the results obtained by using the adaptive learning and linear regression.

6.2.5 Summary of Translation Model Development

A summary of the translation model development results using the adaptive learning, linear regression and point estimate methods is presented in Table 8. The PODs for the flat plate specimens were used as a common reference basis. PODs for specimens with other geometries were compared with the reference basis. The magnitude of the differences was expressed in a semi-quantitative term for comparison purpose. The results of the comparison indicated that a good agreement existed for the translation models from flat plate to integrally stiffened panel specimens for the three analytical techniques. Except for a degree of difference in the case of the ultrasonic technique using the adaptive learning technique, the models for the three techniques were in good agreement.

The successful development of a model to translate NDE sensitivity from flat plate to integrally stiffened panel specimens for the ultrasonic, penetrant, and eddy current inspections is rather useful. The integrally stiffened panel specimens represented specimens with fillet areas where the fatigue cracks were located. It has been estimated that fillet areas are the second most fatigue critical areas in advanced fighter and bomber components. The translation model for this geometry can be useful in the interpretation of NDE capability determination in demonstration programs.

TABLE 8 SUMMARY - TRANSLATION MODEL

ANALYTIC METHOD	NDT METHODS	ISP	TRANS. WLD (W/CROWN)	LONG FLUSH WLD	LONG WLD (W/CROWN)	LOP WLD	BOLT HOLES	TANDEM T	RIVETED PLATE
ADAPTIVE LEARNING	Ultrasonics	Large	Large	Large	—	—	—	Small	—
	Penetrant	Medium	No	No	—	—	—	—	—
	Eddy Current	Large	Large	Small	—	—	Medium	—	—
LINEAR REPRESSIONS	Ultrasonics	Medium	Range *	Range *	—	—	—	—	—
	Penetrant	Medium	No	No	—	—	—	—	—
	Eddy Current	Large	No	No	—	—	—	—	—
POINT ESTIMATE	Ultrasonic	Medium	Large	Medium	Large	Large	—	No	Large
	Penetrant	Medium	No	No	Large	Large	Range	No	Medium
	Eddy Current	Large	Large	No	Large	Large	Large	No	Large

* For certain crack length ranges only.

6.3 DATA DEFICIENCIES

The reliability data in the computer data bank contains primarily well documented data on aluminum flat plates, integrally stiffened panels, and weld joints. From the available data, realistic translation models were developed to translate NDE inspection results obtained from flat plate specimens to specimens with fillet areas. NDE data on bolt hole specimens are much needed. The fatigue fracture and durability critical part geometries for F-16 and B-1 are summarized in Table 9. It can be seen that fillets and curved surfaces are the second most numerous geometries accounting for 22.2 and 13.2 percent of the total critical part geometries for F-16 and B-1, respectively. The fastener holes and cutouts for F-16 and B-1 account for 72.2 and 78 percent of the total critical part geometries. The importance of a translation model for fastener hole inspections is evident from this analysis. The methodology of the translation model from flat plate specimens to integrally stiffened panels can be applied to cover the flat plate/fastener hole geometries. Presently, only a limited amount of fastener hole inspection results have been entered into the computer data bank.

A search for possible remedies to overcome the fastener hole inspection data deficiency revealed that a potentially useful data source exists. Under a previous Air Force contract for the F-111 tear down inspection at General Dynamics, 74 components of F-111 fatigue tested were inspected by eddy current, magnetic particle, and penetrant techniques^(8,9). Approximately 16,000 fastener holes were inspected by using these three techniques. The results and inspection procedures were well documented. However, the approximately 400 positive indications of fatigue cracks in these components had not been verified. If a portion of these positive indications can be selectively verified by destructive testing, the inspection results from the tear-down inspections can be a large block of useful reliability data.

Few NDE reliability data suitable for translation model development exists in the data bank for steel components and for the inspection techniques of magnetic particle and X-ray. The numbers of x-ray inspections for the aluminum flat plate specimens containing fatigue cracks in the data bank were found to be insufficient for statistical calculation. The PODs for the inspections were quite low which is understandable since it is generally

TABLE 9

ESTIMATE OF FATIGUE FRACTURE
AND DURABILITY CRITICAL PARTS FOR F-16 AND B-1

<u>Critical Part Geometry</u>	<u>F-16</u>	<u>B-1</u>
Fastener Holes	3	65
Cutouts	10	6
Filletts	4	4
Weld	-	2
Curved Surfaces	-	8
Internal Threads	-	1
Surface Edges	<u>1</u>	<u>5</u>
TOTAL	18	91

recognized that fatigue cracks are difficult to detect by using X-ray technique. In aircraft inspections, X-ray is more often used for the inspection of forgings and welds. The steel specimens used in the AFML program on Practical Sensitivity Limits (7) could be used to generate more data on X-ray and magnetic particle inspection methods. In addition, the numbers of inspections in the program (Reference 7) for cylindrically shaped specimens containing EDM compressed notch flaws were not sufficient to allow a statistically valid analysis. It is recommended that specimens used in that program be selectively used in a future validation program to augment the number of inspections.

From the standpoint of NDE parameters in the parametric studies, certain deficiencies were discovered in the existing reliability data. Inspection data on specimens with surface finishes in the range from 65 to 128 RMS were inadequate. Unfortunately, this range happened to be the finish of the as-machined surfaces of most aircraft components. For some NDE techniques such as eddy current and liquid penetrant, it was shown that the surface finish could affect the inspection sensitivity. Thus, it is important to supplement the data inadequacy in this range of commonly occurring surface finishes in order to extend the validity of the translation models. For the NDE parameter of specimen thickness, the majority of the data were obtained on specimens with thicknesses below 0.3 in. In cases where the specimen thickness does affect the inspection sensitivity, especially for the NDE techniques of X-ray, magnetic particle, and ultrasonic, it is desirable to obtain more data on specimens thicker than 0.3 in. The full extent of how the specimen thickness affects the inspection results will not be known until this data deficiency is overcome.

A serious deficiency in the reliability data bank is connected with the ultrasonic inspection. It is the second most used technique in production inspection. The majority of the data on ultrasonic inspection in the data bank related to shear wave inspection. Data on the commonly used modes in ultrasonic technique, immersion mode by compression waves and contact mode by shear wave, were grossly inadequate. In a demonstration program designed to determine the NDE capability of a production facility, it is important to assess the inspection efficiency of the equipment and the personnel in the area of ultrasonic immersion inspection. It will be noted that the ultrasonic technique in the immersion mode of operation is still one of the most widely used techniques in the field of NDE when the entire spectrum of materials and finished products in the aircraft industry is considered. The deficiency in the reliability data in this area must be remedied.

SECTION VII

OPTIMUM DEMONSTRATION

PROGRAM DESIGN

7.1 INTRODUCTION

An optimum demonstration program is required in order to establish a baseline procedural method to ensure that the requirements regarding the capabilities of the nondestructive inspection process to meet the MIL Specification requirements be firmly established. In most, if not all, of the earlier programs designed to evaluate the probability of detection of a particular inspection process, there were overwhelming external influences that dominated the various decisions made during the conduct of the demonstration program. For example, the Rockwell B-1 demonstration program was in fact a go-no-go program in which the requirement was to prove that the minimum flaw size used for the fracture design analysis of the specified fracture critical components could be detected to the predetermined degree of confidence and probability of detection. On the other hand, subsequent subcontractor demonstration programs were limited as to the ranges of flaws, numbers of observations within each flaw size range, type of flaws used, significance of the reuse of specimens and substitutability of inspection parameters, etc. Hence, one must be extremely careful in stating the initial objective and statistical hypothesis that is to be tested and to carefully evaluate the demonstration program to ensure that it does indeed test this hypothesis. For the optimum demonstration program discussed here, the hypothesis to be tested may be stated as follows:

"Can a flaw size $2c$ (inches) be detected by the nondestructive process under investigation to a minimum level of 90 percent probability of detection at a 95 percent confidence level."

This hypothesis immediately eliminates a great deal of extra testing, since no judgments are to be made regarding the POD of flaw sizes in immediately adjacent ranges. Implied in the process is the fact that flaws whose sizes are larger than the required $2c$ will be detected to at least that degree (90/95) and probably higher. The required POD is a lower bound value, and the true value of detection probability is assumed to be higher (at the 95% confidence level). No estimate is to be made of the true value of the detection probability, i.e., the statement impresses the fact that the lower bound detection probability level is 90%, but does not make any statements as to the value of the upper bound. To make a statement that the probability of detection is between 90 and 95% probability of detection at a 95% confidence level would take a great deal more specimens than that required by this optimum demonstration program.

It should be noted that this hypothesis differs from the recommended practice of ASNT "Demonstration of Nondestructive Evaluation Reliability on Aircraft Production Parts" Draft 2.(10) The purpose of the ASNT recommended practice is to develop repeatable data for fracture mechanics applications. It does not include apriori requirements as to the required degree of detection and confidence, but allows for several combinations of probability of detection and confidence levels.

The choice of the flaw size $2c$ to be demonstrated in the optimum demonstration program can be evaluated by use of the transfer function model approach. The transfer function gives the ratio of the POD for the complex specimen to the POD for the simple configuration, as a function of flaw size. Thus, if the requirement would be to detect a 0.10 inch defect in a complex structure, this would be the equivalent of a $(POD_c / POD_{fp} \times 0.010)$ size defect in a flat plate. If the transfer function were 0.80 at a 0.10 inch defects for ultrasonics, this would mean that a $2c$ value of 0.080 inches in length on the flat plate would demonstrate the equivalent POD for the complex specimen. Thus the target flaw sizes would be 0.08 inches in length in the flat plate. It should also be determined that the POD curve for the NDI method of inspection does not peak in that crack range.

7.2 SPECIMEN CONFIGURATION

In the choice of a suitable specimen geometry, two conflicting factors must be considered: (1) simplicity of specimen configuration and (2) similarity of the specimen to the fracture critical component the demonstration program is to represent.

The demonstration specimens should simulate the fracture critical components with respect to alloy, heat treat condition, metallurgical microstructure, primary and secondary processing variables. It should furthermore be representative of the surface finish, texture, surface condition (i.e. stress state of surface) and manufacturing parameters of the fracture critical component. It is immediately obvious that the validity of a demonstration program to determine the POD of penetrants obtained on castings to be used on forgings is doubtful. This would be true even if all other metallurgical and processing variables were identical.

Within these limitations as to the metallurgical similarity of the specimen type, the geometry of the specimen should be kept as simple as possible so that a controlled flaw can be produced.

The validity of the hypothesis depends upon the degree to which the specimen-defect configuration can be controlled and predetermined. For this reason, flat plate specimens would be suitable for most demonstration purposes. These plates may contain welds or bolt holes if the demonstration program is concerned with this type of fracture critical component.

The effects of specimen geometry of the POD for four NDE techniques revealed that the detection probabilities are higher in the simpler geometry than with the integrally stiffened panels. Both specimens contained fatigue cracks and were inspected by penetrant, eddy current and ultrasonics. However, the differences in POD were only found to be significant for the smallest crack length in the case of the ultrasonic technique. (c.f. Figure D-11).

Specimen Size:

The size of the plate should be consistent with the test equipment available to produce suitable defects within an optimum time frame. Specimen configuration should be such that a minimum of 4" by 8" of finished specimen size is obtained. To produce a finished specimen size with the defect randomly located within the specimen, an initial specimen size and configuration consistent with the method of producing the flaw should be developed. For example, if the defects are to be fatigue cracks, suitable three or four point bending equipment will determine the initial size of the specimen, with the added dimensional requirements dominated by the choice of loading fixture.

For most demonstration programs, the location of the defect within the 4x8 area is not critical, except that it should not be too close to any of the edges. Thus, location of the defect within the central 3x6 inches would be preferable. However, if edge cracks would be expected to be the dominant failure mode, i.e. turbine blades, the specimen defect location should consider this factor in selection of the locations.

Flaw Type:

Although prudence would recommend that the flaw type be consistent with the defect type expected to be found in the preproduction inspection program, experience has shown that small tightly closed cracks are the most difficult to detect (except perhaps for forging laps in diffusion bonds), and most closely represent the type of defect for which the fracture mechanics analysis is valid. Thus tight fatigue type cracks, while rarely encountered in preproduction components would impose the most severe, and hence the most conservative, estimate of the POD of the particular NDT procedure.

Fatigue cracks are recommended as the most convenient defect type because of the ease with which their size may be controlled, and the large body of metallurgical and fracture mechanics literature available to fully evaluate their characteristics. Fatigue cracks should be initiated in the pre-selected (randomized) location within the specimen. The location of the initiation site can be induced by a suitable choice of stress riser on the surface of the specimen.

Suitable stress risers are: electrodischarge machining (EDM), weld solidification spots, microhardness indentations, weld beads, and conventional machined slots. The size, shape and depth of the initiation procedure will influence the shape and extent of the fatigue crack in a manner that must be determined for each testing machine. It is important that the starter site be as shallow as possible so that it may be completely removed by subsequent surface machining procedures. In this respect, it should be recognized that EDM and welding initiation sites would be marginally suitable for magnetic particle inspection procedures due to the magnetic field perturbation introduced by the solidification spot which extends considerably beyond the geometric initiation size.

In the case of ultrasonic inspection techniques, elox slots that had been closed by forging showed approximately the same POD as did defects produced by fatigue. However, elox slots are not identical in nature to fatigue cracks when examined by eddy current and penetrant processes. Hence, in certain instances the compressed EDM slot may be substituted for the fatigue crack, only if unambiguous information is available regarding the degree of severity of the different types of defects.

Defect Characterization

In all instances the defect used in the demonstration program should be characterized as fully as possible, and a record of these characteristics included in the documentation of the demonstration program. These should include the stress ratios used to fatigue the specimens, the presence of or absence of subsequent corrosive conditions, subsequent tensile or compressive loadings, number of times the specimen was reused, and the history of all prior NDT procedures that have been examined using this particular specimen. It can be seen that if a specimen had been examined first by contact shear wave ultrasonics using oil at the contact medium, and then by penetrant inspection, the POD for the penetrant procedure may be decreased due to the presence of oil from the initial inspection.

Fatigue Crack Growth

The conditions for the fatigue crack growth should also be standardized. It is recommended that tension-tension fatigue with R values of -0.3 or greater be used in producing the fatigue cracks. This has been found to produce cracks whose crack opening displacements are smaller, i.e., more tightly closed than cracks produced by reversed bending or zero-max fatigue.

Defect Orientation

Defect orientation should be consistent with the procedure used to produce the defects. In the case of fatigue cracks, they will most often have to be oriented perpendicular to the longitudinal axis of the specimen. However, in most fracture critical components, the anticipated crack orientation would be known, and this factor is not considered to have a significant influence on the POD for the inspection procedure. The crack orientation would have a major effect in the case of the magnetic particle inspection technique, where combinations of crack orientation and inspection coil configurations could result in abnormally low POD results.

Defect Geometry

Defect geometry should be given serious consideration in choosing the type of loading procedure used to grow the fatigue cracks. The defect depth to surface length ratio $a/2c$ is determined by the shape of the starter notch, the loading fixture, and the defect depth to specimen thickness ratio. For eddy current procedures the depth would be an important factor controlling the POD, but for ultrasonics there is an effect of the $a/2c$ ratio on the POD, c.f. Figures 8 and 9. As would be expected, given a value of surface crack length, the POD increases as the depth of the defect increases, i.e. the reflected defect area increases. Thus, the POD may be adversely affected in the optimum demonstration program if too much of the surface is machined off to produce the required $2c$ length leaving a defect of the desired length, but with a shallow depth. The expected final $a/2c$ ratio for the specimens should be held as close to constant as possible. This may be

accomplished by considering the $a/2c$ ratio of the defect as fatigued, and calculating the $a/2c$ ratio of the defect after a surface depth containing the starter notch has been machined off. If the resulting $a/2c$ value is too small, i.e., less than 0.2, consideration should be given to further fatigue cycling.

Surface Condition

Surface finish has been demonstrated to have an effect on the POD for ultrasonics, eddy current and penetrants (Tables 5, 6, 7). It is therefore recommended that the surface finish be consistent with the finish to be used on the fracture critical components, typically 125 RMS or better. However, consideration should also be given to reproduce the type of machining procedures actually used on the fracture critical components. For example, the depth of the final cut may influence the residual stress state on the component and hence the POD. The direction of the cutting marks relative to the orientation of the defect may also be significant. The surface finish determines the amount of surface material to be removed by etching prior to inspection by penetrant procedures.

An equal number of control specimens shall be prepared in a manner identical to that used in preparing the samples containing defects. These shall be numbered in a manner as to intersperse them within the specimens containing defects. These should be verified as being "defect free" and used in the inspection program to lower the expectation value of the inspectors to at least 50%.

Specimen Identification

The markings on each specimen should be firmly attached or imprinted on the specimen in a manner so as to orient the location of the flaw in the flawed specimens, as well as identify the unflawed specimens. The markings on each flawed and/or control specimen should be changed for each inspection batch distribution so that inspectors will not be biased by the recognition of an individual specimen identification.

7.3 MANAGEMENT AND DOCUMENTATION

Since the results of the demonstration program are to be used in management decisions regarding the acceptance or rejection of the NDI processes, procedures must be carefully monitored and documented. The management determines which type of inspection is to be evaluated, i.e., production line (in-plant inspection), production line (subcontractor inspection), field service inspection, etc., and also what constitutes a failure of the inspection process.

It is important that the person or persons who conduct the NDE demonstration be identifiable in some manner. This is to ensure that subsequent components will be inspected by those persons who had contributed to the passing of the demonstration program, and that unqualified, or marginally qualified personnel will not be lumped into the inspection group. The purpose of the demonstration program is not to grade or establish pass-fail capabilities, but to ensure that the required flaw size detection capabilities as established be directly related to actual component inspections. The inspectors should be thoroughly briefed on the inspection procedures, and periodically reexamined in normal operation.

Surveillance of the NDT procedures, and compliance by both the Air Force SPO and company management is necessary.

A complete, extremely detailed and unambiguous inspection procedure document should be prepared and be available for the inspector to follow. Clearly written instructions are necessary to the success and repeatability of the inspection program. In some cases it may be important to separate out individual inspectors to determine the capabilities of different levels of training and experience, in other cases, it may be necessary to evaluate the capability of the company, grouping all inspectors together.

Process control personnel should prepare the inspection procedure documents for use in the production inspection. These procedures should be developed using identical specimens to those used in the actual demonstration program, and should not be used for any other purpose than to prepare the required document. The evaluation of these specimens for use in the production environment must include cleaning procedures, as well as determination if the specimens can be reused.

Specimens containing flaws such as fatigue cracks can be reused for eddy current, x-ray and magnetic particle and ultrasonic inspection after proper cleaning. For evaluation of reuseability of penetrant specimens, a controlled experimental investigation is necessary to determine the number of times that the specimen may be reused.

A list of the equipment used in the demonstration program will be prepared, as well as sufficient information as to important dial settings and interpretive accept-reject instructions. The inspection procedure should be prepared using specified equipment, and this equipment or a demonstrated equivalent component, should be explicitly spelled out in the inspection instructions. Calibration procedures for verification of dial settings, etc., should be included in the documentation.

The format for the reporting and identification of all flawed specimens shall be prepared by the process control personnel. These reports should be in the routine format for the inspection group so that undue attention is not drawn to the nature of the demonstration specimens.

If at the completion of the inspection program, destructive testing is necessary to verify the form, size and location of defects in the sample group used in the production inspection, these specimens should first be re-examined nondestructively by the process control personnel in the laboratory. All specimens should be examined at the completion of the program to verify the actual size, shape and location of defects for analysis in the demonstration program. Selected specimens, agreed upon by all management and technical persons involved should be destructively tested to assure the control and flaw production procedures are consistent with the intended flaw size and shape.

7.4 INSPECTION AND ANALYSIS

To evaluate the POD of 90% at a 95% confidence factor, a minimum of 29 successes in 29 trials is necessary. This means that 29 specimens containing defects must be identified as having defects by the inspector to guarantee a minimum of 90/95.

Random mixtures of control and flawed specimens should be presented to the inspection group for evaluation. Approxi-

mately 25 specimens, per inspector, per day for 3 days would be appropriate. This would result in a total of 75 inspections of both flawed and unflawed specimens, in any combination necessary to evaluate at least 29 flawed specimens.

The specimens should be cleaned and reinspected the following day if necessary until sufficient data on flawed specimens is obtained. Although a ratio of flawed to control of 1:1 is recommended, this should be considered as an absolute minimum, since normal inspection would not reveal the presence of so many defective components in each batch. It will become obvious to the inspector that these demonstration specimens are not of the usual sort when he finds a large number of defects, but at no time should the emphasis be made that "he" is being tested, instead, the NDT evaluation should be emphasized. Although few human factor data sets exist in completed form, examination of individual data sets indicated that human factor is an important component influencing the POD. Although a minimum of 29 observations of flawed specimens is necessary for the 90/95 accept criterion, it is strongly suggested that additional specimens be fabricated and inspected in the event that some of the specimens later verified as to crack length have actual lengths that fall outside of the 2c value selected for verification.

If the initial inspection program does not result in verification of the inspection capability due to a miss of a flawed specimen, decisions must be made to continue the test program or to consider the NDT process as less sensitive than anticipated⁽¹¹⁾. As outlined in the ASM article in Reference 11, the following combinations of successes and trials can be used to verify the 90/95 POD:

29 successes out of 29 trials	
45	46
59	61
72	75
85	89 .

An inspection sequence in which no misses are found is the simplest and the least costly. However, other factors may influence the decision to terminate or continue the inspection program beyond the first 29 observations.

When the total number of observation of flawed specimens is small, i.e., 30 or less, the exact binominal distribution should be used to determine the lower bound probability of detection. For large numbers of observations, the binominal distribution may be approximated by a Poisson distribution. Procedures for calculating the exact value of the lower bound POD are given in reference 11. If an assessment of the detection threshold to a finer degree is needed, the optimized probability method should be used.

The evaluation of false or error calls should be noted but not necessarily calculated or included in the analysis. At the present time, the objective of the inspection demonstration is to determine the ability to detect a defect given the fact that the defect is present, and the hypothesis does not include at present judgments about the error call values. One suggested procedure for evaluation of false calls is the conditional probability method (12), but more attention must be given to the magnitude of the weighting factors before this can be incorporated into the demonstration program. Since the false call data is recorded, at subsequent times this evaluation can be made.

7.5 VALIDATION OF TRANSLATION MODEL

The design of an optimum demonstration program can be used to conduct an experimental program to validate the translation model developed for translating NDE results obtained on flat plate specimens to specimens with complex geometries. The general philosophy and guidelines of such an experimental validation program are defined in this section. As discussed in the previous section on specimens to be used in an optimum demonstration program, flat 4 x 8 in. specimens containing fatigue cracks with controlled $a/2c$ ratio and an appropriate distribution of flaw sizes will be used as representative of specimens with simple geometries. Realistic aircraft components will be used to represent specimens with complex geometries. Fatigue cracks with flaw sizes and distributions equivalent to those on the flat plate specimens will be introduced in the fillet areas of the components. Inspections on both types of specimens with simple and complex geometries will be conducted using the same NDE parameters. The inspection results will be analyzed by using the adaptive learning, linear regression or point estimate techniques. The comparison of results for the two types of specimens will provide a basis for the validation of the translation model.

The results obtained from the on-going program "Quantitative Evaluation of Penetrant Inspection Materials and Procedures" could also be used as baseline data. The purpose of using these data is two-fold: (1) they can be used to check the validity of the parametric relationship pertained to penetrant inspection, and (2) they can be used as flat plate data to develop a translation model under the prescribed conditions. The translation model generated by these additional data can be compared with the corresponding one developed under this program.

The validity of the translation model can be further tested by using existing aircraft components under damage tolerance tests and full scale fatigue tests. Several advanced aircrafts have components under these types of tests. Realistic fatigue cracks are expected to develop in the critical areas in these components after several lives of the fatigue tests. Using these specimens and the optimum demonstration program procedures, production inspection can be conducted with the five NDE techniques. The NDE capability will be evaluated on these specimens with complex geometries and compared with that predicted by the translation model. The outcome of the validation program will be a set of military standards such as MIL-I-83444 which outlines the details to qualify NDE facilities to meet the structural integrity requirements in advanced aircraft.

S E C T I O N V I I I

C O N C L U S I O N S

The objectives of this program were to establish NDE parametric relationships, to develop a translation model, and to design an optimum demonstration program based on the parametric relationship and translation model.

The existing NDE reliability data base was enlarged, updated, and modified to serve as a basis for the parametric study and translation model development. Additional data were entered into the data bank for specimens with complex geometries.

Analytical methodologies in point estimate, linear regression techniques, and adaptive learning techniques were developed to analyze the reliability data. Computer programs were coded to establish probability of detection curves with the best statistical fit according to the three schemes.

Qualitative parametric relationships between the probability of detection and the NDE parameters was established for aluminum specimens and the NDE techniques of ultrasonic, penetrant and eddy current. The NDE parameters studied were limited to those included in the existing data.

Translation models were developed to translate the probability of detection on fatigue cracks obtained on flat plate specimens to corresponding values for specimens with more complex geometries. The scope and accuracy of the models were somewhat limited by the data base. Overall, the translation model from aluminum flat plate to fillet specimens was most successful.

Based on the parametric relationships and the translation model developed in the program, an optimum demonstration program was designed to be used as a guideline for future validation and NDE facility qualification programs.

A P P E N D I X A

SAMPLES OF COVER SHEETS FOR
EDDY CURRENT, RADIOGRAPHIC,
MAGNETIC PARTICLE, AND
PENETRANT TECHNIQUES

TABLE A-1 RELEVANT NDE PARAMETERS FOR EDDY CURRENT METHOD

DSN :	3	INSP. DATE : 1973	01-MAR-77
1)	1	NDE METHOD	EDDY CURRENT
2)	4	COMPANY NAME	MARTIN MARIETTA
3)	2	PROGRAM ID	DETECTION OF FATIGUE CRACKS
4)	1	MATERIAL	ALUMINUM 2219-T87
5)	1	DEFECT TYPE	FATIGUE CRK./NO CYCLE/REMOVE EDM
6)	0	OPERATOR ID	NA
7)	9	QUALIFICATION	PRODUCTION INSPECTOR
8)	1	INSP. ENVIRONMENT	PRODUCTION
9)	2	INSP. PROCEDURE	STD. INSP. / MULTIPLE FLAW SPEC.
10)	4	DATA RECORD TYPE	RECORD OF METER OR SCOPE DISPLAY
11)	5	MODE OF SCAN	MANUAL SCAN, INDEX AID
12)	2	REFERENCE STANDARD	FATIGUE CRACK
13)	1	DEFECT MATERIAL	AIR
14)	1	PART GEOMETRY	FLAT PLATE
15)	1	DEFECT LOCATION	FLAT PLATE SURFACE FLAW
16)	1	DEFECT VERIFICATION	SPECIMEN CUT OPEN
17)	1	SAMPLE HISTORY	AS MACHINED OR WELDED
26)	1	EQUIPMENT TYPE	NORTER NDT-3
27)	0	DIAMETER OF COIL	NA
28)	3	CONF./SHAPE OF COIL	SURFACE PROBE
29)	1	FREQUENCY	100 KHZ
30)	1	TYPE OF EC RESPONSE	AMPLITUDE
31)	0	LIFT-OFF COMP.	NA
32)	1	SIGNAL PROCESSING	STRAIGHT AMPLIFICATION
33)	1	INDEX INTERVAL	.3048 CM (.125 IN)
34)	0		NA
MCL :		CD: Y MCD:NO	SF: Y TK: Y

TABLE A-2 RELEVANT NDE PARAMETERS FOR RADIOGRAPHIC METHOD

DSN :	223	INSP. DATE :	0	01-MAR-77
1)	4	NDE METHOD	:	RADIOGRAPHY
2)	4	AIR FORCE BASE	:	MARTIN MARIETTA
3)	6	SET UP LOCATION	:	DETECTION OF TIGHTLY CLOSED FLAWS
4)	1	INSP PROC IDENT	:	ALUMINUM 2219-T87
5)	14	TECHNICIAN EVALUATIO	:	FATIGUE CRACKED WELDS
6)	3	SAMPLE IDENT	:	C
7)	7	DAY OF INSP START	:	QUALIFIED ACCORDING TO MIL-STD-453
8)	2	START/ELAPSE TIME	:	LABORATORY
9)	10	TECH. IDENT NO	:	MIL-STD-453 / MULTIPLE FLAW
10)	1	SPECIAL ENVIRONMENT	:	MANUAL RECORD OF VISUAL DISPLAY
11)	0	NCO IN CHARGE	:	NA
12)	13	SPECIAL EVALUATION	:	REF. PANEL USED / DESCRIP NOT KNOWN
13)	1	PERSONAL DATA	:	AIR
14)	12	JOB TITLE	:	TANDEM 'T'
15)	0	NDI TRAINING	:	NA
16)	0	NDI EXPERIENCE	:	NA
17)	0	SAMPLE HISTORY	:	NA
26)	0	RADIOGRAPHY	:	NA
27)	5	EQUIPMENT TYPE	:	NORELCO X-RAY 150 KU 24MA
28)	3	SOURCE ENERGY	:	45 KU FOR .3300 CM , 70 KU FOR 1.27 CM
29)	1	SOURCE STRENGTH	:	20 MILLI-AMPS
30)	1	FILM TYPE & MFG	:	BERYLLIUM
31)	1	EXPOSURE TIME	:	KODAK , TYPE M
32)	4	SOURCE TO FILM DIST	:	1.5-2.25 MIN. (THICK-ENERGY DEPEND.)
33)	2	DENSITOMETER READING	:	122 CM. (48 IN)
34)	0	DEVELOPER TIME/TEMP	:	NA
35)	1	STOP BATH TIME/TEMP	:	2.5-3.5
36)	0	FIXER TIME/TEMP	:	NA
MCL:NO		CD: Y	MCD:NO	SF: Y TK: Y

TABLE A-3 RELEVANT NDE PARAMETERS FOR MAGNETIC PARTICLE METHOD

DSN :	131	INSP. DATE :	1974	
1>	3	NDE METHOD	:	MAGNETIC PARTICLE
2>	3	COMPANY NAME	:	BOEING COMMERCIAL AIRPLANE
3>	1	PROGRAM ID	:	SENSI. LIMITS OF PROD. NDE METHODS
4>	3	MATERIAL	:	4340M STEEL 270-300 KSI
5>	9	DEFECT TYPE	:	HYDROGEN INDUCED GRINDING CRACK
6>	0	OPERATOR ID	:	NA
7>	10	QUALIFICATION	:	CERTIFIED UNDER BOEING A.C. 5953
8>	1	INSP. ENVIRONMENT	:	PRODUCTION
9>	11	INSP. PROCEDURE	:	MIL-I-6868C , MAG. PAR.
10>	0	DATA RECORD TYPE	:	NA
11>	0	MODE OF SCAN	:	NA
12>	14	REFERENCE STANDARD	:	SPEC TYP OF TYPE BEING INSPECTED
13>	1	DEFECT MATERIAL	:	AIR
14>	15	PART GEOMETRY	:	FLAT BAR
15>	21	DEFECT LOCATION	:	SURFACE FLAW
16>	1	DEFECT VERIFICATION	:	SPECIMEN CUT OPEN
17>	1	SAMPLE HISTORY	:	AS MACHINED OR WELDED
26>	2	EQUIPMENT	:	PARKER RESEARCH CO. (MOD DA-200)
27>	1	PROCEDURE	:	WET CONTINUOUS FLUORESCENT PRCE.
28>	1	MAG. PARTICAL TYPE	:	MAGNAFLUX 14A
29>	1	SUSPENSION TYPE	:	OIL & WATER BASE
MCL:NO		CD:NO	MCD:NO	SF:NO TK:NO

01-MAR-77

TABLE A-4 RELEVANT NDE PARAMETERS FOR PENETRANT METHOD

DSN :	1	INSP. DATE :	1974	
1)	2	NDE METHOD	:	PENETRANT
2)	4	COMPANY NAME	:	MARTIN MARIETTA
3)	2	PROGRAM ID	:	DETECTION OF FATIGUE CRACKS
4)	1	MATERIAL	:	ALUMINUM 2219-T87
5)	1	DEFECT TYPE	:	FATIGUE CRK./NO CYCLE/REMOVE EDM
6)	0	OPERATOR ID	:	NA
7)	8	QUALIFICATION	:	TECHNICALLY QUALIFIED
8)	1	INSP. ENVIRONMENT	:	PRODUCTION
9)	2	INSP. PROCEDURE	:	STD. INSP. / MULTIPLE FLAW SPEC.
10)	1	DATA RECORD TYPE	:	MANUAL RECORD OF VISUAL DISPLAY
11)	0	MODE OF SCAN	:	NA
12)	0	REFERENCE STANDARD	:	NA
13)	1	DEFECT MATERIAL	:	AIR
14)	1	PART GEOMETRY	:	FLAT PLATE
15)	1	DEFECT LOCATION	:	FLAT PLATE SURFACE FLAW
16)	1	DEFECT VERIFICATION	:	SPECIMEN CUT OPEN
17)	1	SAMPLE HISTORY	:	AS MACHINED OR WELDED
26)	1	PENETRANT TYPE	:	URESCO P-151
27)	1	DEVELOPER TYPE	:	URESCO D499C
28)	6	CLASS OF PENETRANT	:	GROUP 6
29)	1	REMOVER/EMULSIFIER	:	URESCO K410
30)	1	APPLICATION METHOD	:	HAND BRUSH
31)	1	DWELL TIME	:	30. MINUTES
32)	1	DEVELOPING TIME	:	30 MINUTES
33)	1	WASH TIME	:	60 MINUTES
34)	2	LIGHT INTENSITY	:	125 FT-CANDLES , 15 IN FROM FILTER
35)	2	REMOVAL/PRE-CLEANING	:	CLEANED BY ALCOHOL IN ULTRASONIC CLEANER
MCL:	Y	CD: Y	MCD:NO	SF: Y TK: Y

01-MAR-77

A P P E N D I X B

OVERALL LOGIC AND CODES OF COMPUTER PROGRAMS
FOR THE ADAPTIVE LEARNING ANALYSIS

OVERALL LOGIC OF COMPUTER PROGRAMS FOR THE ADAPTIVE LEARNING ANALYSIS

The adaptive analysis of the General Dynamics data base requires three programs:

1. Training and Testing Set Formation Program. This program performs three functions:
 - a) It selects out of the total data base those data sets that are to be analyzed.
 - b) It splits the selected data base items into two sets, a training set and a test set.
 - c) It normalizes all variables in the training and testing sets to the range -3 to $+3$ (approximately).
2. Hypersurface Fitting Program. The function of this program is to fit the training set with a (nonlinear) multinomial. The fitting procedure uses a guided, accelerated, random search with reversal and avoids overfitting through the use of the training-testing paradigm.
3. Analysis Program. This program is used with the fitted multinomials to determine the relative contribution of each independent variable to the output variable (e.g., the probability of detection).

Flowcharts, mathematical equations, and other data for these programs are presented in this appendix.

1. Definitions

Variables and Arrays

- ADELTA (m,n,6): the difference, Δa_i , between the current value of a given network coefficient, a_i , and $a_{i,btd}$, the best-to-date value of a_i . The array size variables refer to the number of rows in the network, m, the number of columns in the network, n, and the number of constants used in each element, 6.
- ACURR (m,n,6): the current trial values of the net coefficients.
- BTDDR (m,n,6): the best-to-date coefficients found for the net using the training set.
- BTDTT (m,n,6): the best-to-date coefficients found for the net using the test set.
- XTR (m,2,n₁): the training set. m=NROWS and n₁=NTR.
- XTE (m,2,n₂): the test set. m=NROWS and n₂=NTE.
- XIN (m,2): a temporary storage that holds the net input and subsequent column outputs; used in calculating net output; in general, the net input will be the k-th subarray of XTR or XTE.

YNETR(n_1): the net outputs computed using each of the n_1 subarrays of XTR.
 YNETE(n_2): the net outputs computed using each of the n_2 subarrays of XTE.
 YTR(n_1): the dependent variable subarray of the training set.
 YTE(n_2): the dependent variable subarray of the test set.

Array Size Parameters

NTR: the number of (mx2) subarrays in XTR
 NTE: the number of (mx2) subarrays in XTE
 NVAR: the number of independent variables in either XTR or XTE
 NNET: the number of elements (modules) in the network
 NROWS: the number of rows of elements in the network
 NCOLS: the number of columns of elements in the network
 NCOEF: the number of coefficients in the network

Options and Input Constants

PRINT = 0 if intermediate printout not desired, 1 if desired
 IRANN = number used to initialize the random number routine (allows exact duplication of a run if desired)
 NVAR = input from training/testing set formation program
 NTE = input from training/testing set formation program
 NTR = input from training/testing set formation program
 NNET = NROWS*NCOLS
 NROWS = NVAR/2 for a rectangular or square net
 NCOLS = NROWS in a square net
 NCOEF = 6*NNET if a six-term net element is used
 C1 = smoothing constant; set to 1.0
 C2 = smoothing constant; set to 10.0
 C3 = smoothing constant; set to $\frac{1}{2}$
 C4 = smoothing constant; set to 20
 NSTOP = trial number for unconditional search halt; set to 1000
 AMAX = parameter size constant; set to 10.0

Miscellaneous Constants

SZERO = smoothing constant computed during initialization

Indexes and Pointers

I = trial number
 J = number of times step size doubles during hill-climbing

KTR = k-th training set member
 KTE = k-th test set member
 KVAR = k-th variable in a training or testing set vector
 KNET = k-th module (element) in the network
 KROW = k-th row of the network
 KCOL = k-th column of the network
 KCOEF = k-th coefficient out of the 6*NNET total

Subroutines

RAN1: generates a random number, α , from a flat distribution; $0 \leq \alpha \leq 1$
 RAN2: generates a number from a zero-mean, unit-variance distribution; β
 AMEND(m,n,6): checks each random number produced by RAN2 to see if any have gone outside the preset boundary, $+a_{\max}$. If any have gone outside, AMEND computes a new value of ACURR which is within limits and also corrects ADELTA
 YELT: computes the output of a network element, given the input and coefficient vectors
 YNETR(NTR): computes the net output for each subarray of the training set, given a coefficient array
 YNETE(NTE): computes the net output for each subarray of the test set, given a coefficient array
 SCORR: computes the sum of the squares of the two (1xNTR) arrays YTR and the current YNETR and divides by NTR
 SCORE: computes the sum of the squares of the two (1xNTE) arrays YTE and the current YNETE and divides by NTE

Print Messages Used in Fitting Program

Header Block:

Print program name, run number, and options and data by variable name and value. If PRINT = 1, set up column headings for intermediate printout:

<u>Trial No.</u>	<u>Search Mode</u>	<u>Score, Tr</u>	<u>Delta S</u>	<u>Score, Te</u>	<u>NBTD</u>
(Message #1): I	"unguided"	SBTDR	SDELTA	SBTDE	NBTDE
(Message #2): I	"guided"	SBTDR	SDELTA	SBTDE	NBTDE
(Message #3): I	"reversal"	SBTDR	SDELTA	SBTDE	NBTDE
(Message #4): I	"accel"	SBTDR	SDELTA	SBTDE	NBTDE

Final Message:

<u>"Score, Tr"</u>	<u>"Score, Te"</u>	<u>"Best Test Trial"</u>
SBTDR	SBTDE	NBTDE

"Coefficient Set"

"a ₁ "	"a ₂ "		"a ₆ "
ABTDE(1,1,1)	ABTDE(1,1,2)	. . .	ABTDE(1,1,6)
ABTDE(2,1,1)	ABTDE(2,1,2)	. . .	ABTDE(2,1,6)
ABTDE(n,n,1)	ABTDE(n,n,6)

2. Training and Testing Set Formation Program

Data must be selected from the General Dynamics data base and transferred to an intermediate stroage which is accessible by the fitting and analysis programs. Selection is required since only a portion of the total data base is to be fitted at any one time. It appears likely that the existing selection program used with the data base could be compatible with the requirements of the adaptive analysis, and the decision as to whether to use the existing program or prepare a new one is left to the project programmer.

The division of data points to either the testing or training set should be done on a random basis, although a systematic basis such as odd-numbered points to be assigned to the testing set and even-numbered points to the training set would probably not introduce systematic biases to the sets in view of the independence of the measurements in the data base. It is recommended that the odd-even assignment rule be used to divide the data points into training and testing sets.

Each training and testing set is comprised of a set of measurement/observation vectors on specimens, together with the dependent variable that corresponds to the particular vector. E.g., let X_i be the i -th vector; then

$$X_i = (x_1, x_2, \dots, x_n)_i$$

where

x_1 = crack identification
 x_2 = crack length
 x_3 = crack depth
 x_4 = surface finish
 . . .

The t-t sets will consist of some number, m , of such vectors and corresponding dependent variables, y_i :

$$T = (X_1, y_1), (X_2, y_2), \dots, (X_m, y_m)$$

The number of elements in the training and testing sets need not be equal, but they should be approximately the same. The minimum value for m probably should be about 20, but an exact value can

only be determined by trial and error. It is important to note that if any of the independent variables, x_i , is constant for all m (in both the training and testing sets), it should be deleted from these sets since it cannot affect the fit.

For technical reasons, it is desirable to rescale all members of the training and testing sets and to organize them into three-dimensional arrays instead of two-dimensional arrays. The independent variables in the original arrays should be divided into two groups, e.g., the even and odd variables. If the number of variables is odd to begin with, it can be made even by defining a new variable whose value is zero. As discussed above, adding an unchanging variable does not affect the fit of the hypersurface. After reorganization, the sets should be an $(m, 2, n_1)$ and an $(m, 2, n_2)$ array, where m is now the number of rows in the net instead of the number of variables. Also, the dependent variable, y_k , should be split off to form a $YTR(n_1)$ and a $YTE(n_2)$ array. This three-dimensional array simplifies the later network calculations.

The rescaling is done for all samples of the dependent and independent variables. The procedure is to calculate the mean and standard deviation of all variables in the testing and training sets combined, then subtract off the mean of each variable and divide by the standard deviation. This scaling brings all variables into approximately the -3 to $+3$ range, which improves the probability that acceptable solutions for the coefficients will lie in the range $-a_{\max}$ to $+a_{\max}$, where a_{\max} is about 10.

3. Fitting Program

This program accomplishes the task of finding the best set of coefficients for the multinomial. The fitting program uses a guided, accelerated, random search with reversal, terminal search smoothing and overfitting control. The basic subroutines in this program are used over and over as can be seen in the flowchart for the program (Figure B-1). Each subroutine will be described in some detail.

3.1 Random Number Generators

The two random number generators are RAN1 and RAN2.

RAN1(n): Generates n random numbers drawn from a rectangular distribution, $0 \leq \alpha \leq 1$. These numbers are then scaled to the $-a_{\max}$ to $+a_{\max}$ range using $a_{\max}(2\alpha - 1)$. When $XXXX(n) = \text{RAN1}(n)$ is written, it is to be interpreted as calling for the generation of n scaled random numbers and replacing the array $XXXX$ by this random array.

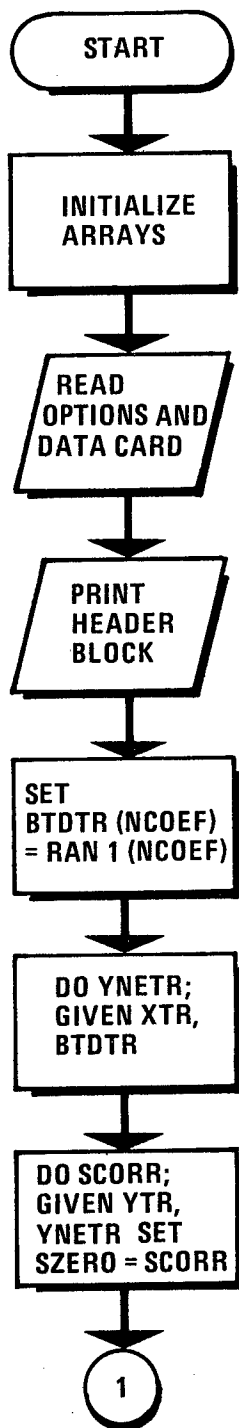


Figure B-1 Hypersurface Fitting Program Initialize and Load BTDE and SBTDE

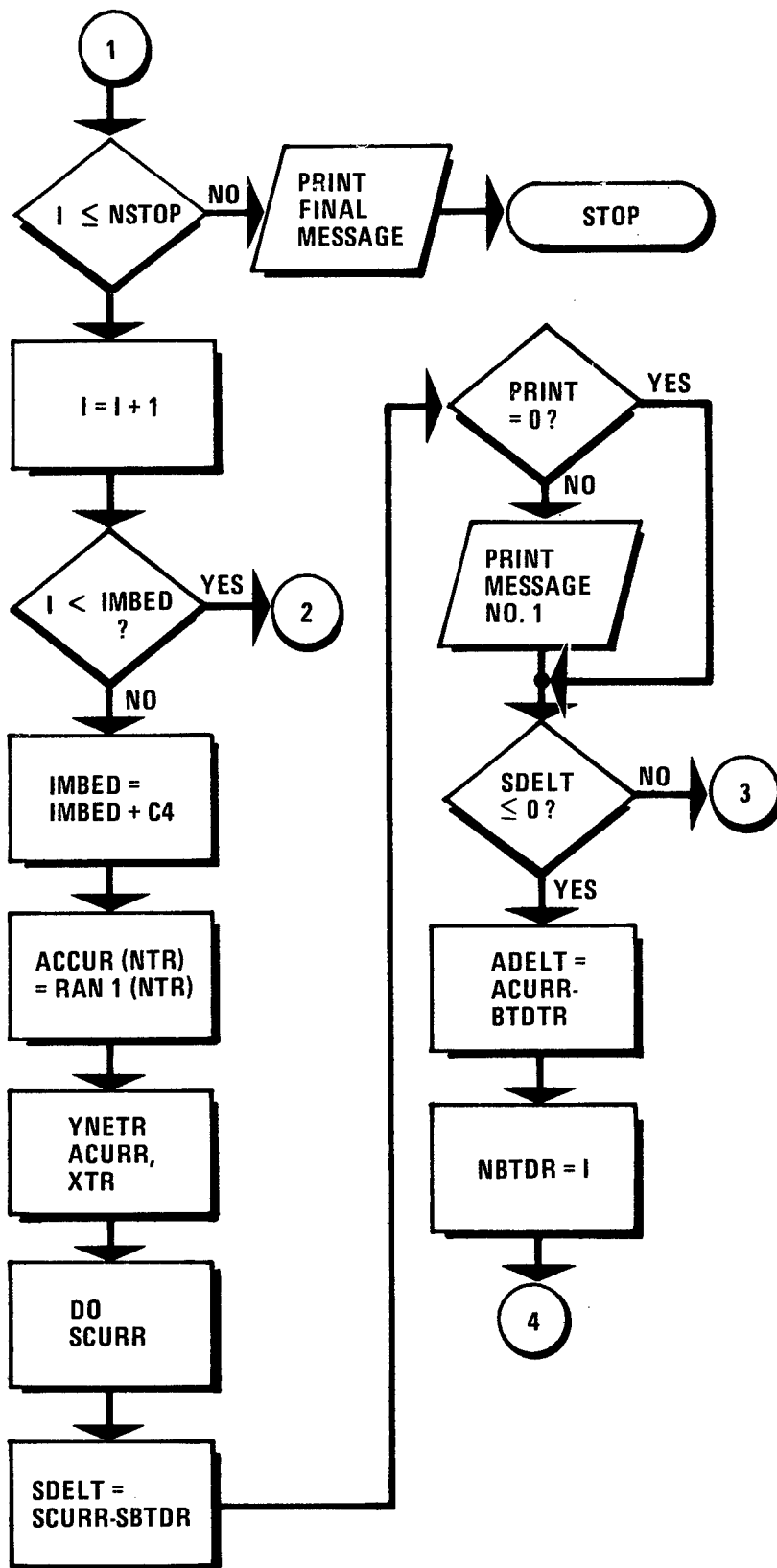


Figure B-1 Hypersurface Fitting Program (Continued) Unguided Search

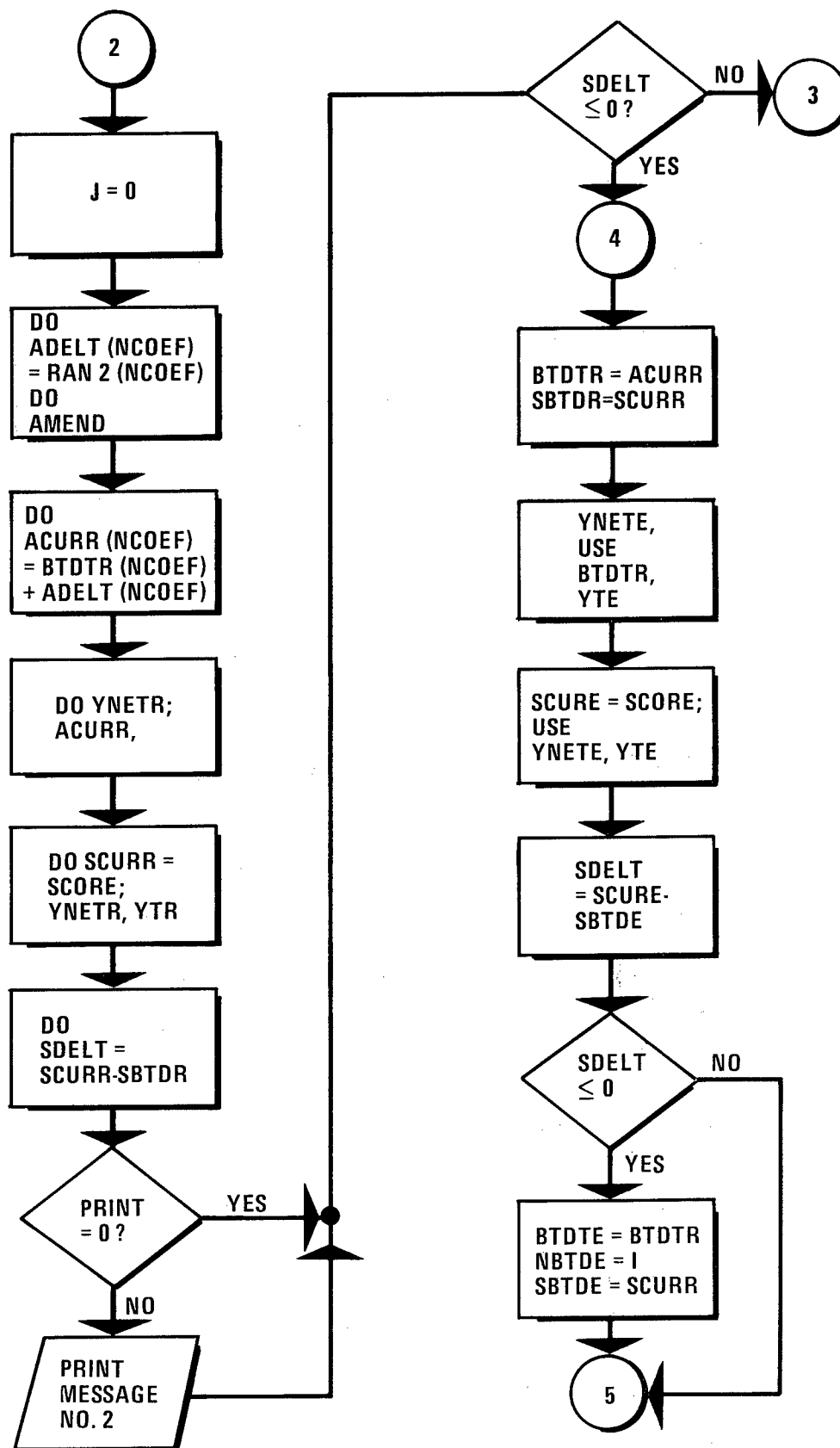


Figure B-1 Hypersurface Fitting Program (Continued) Guided Search and t-t Paradigm

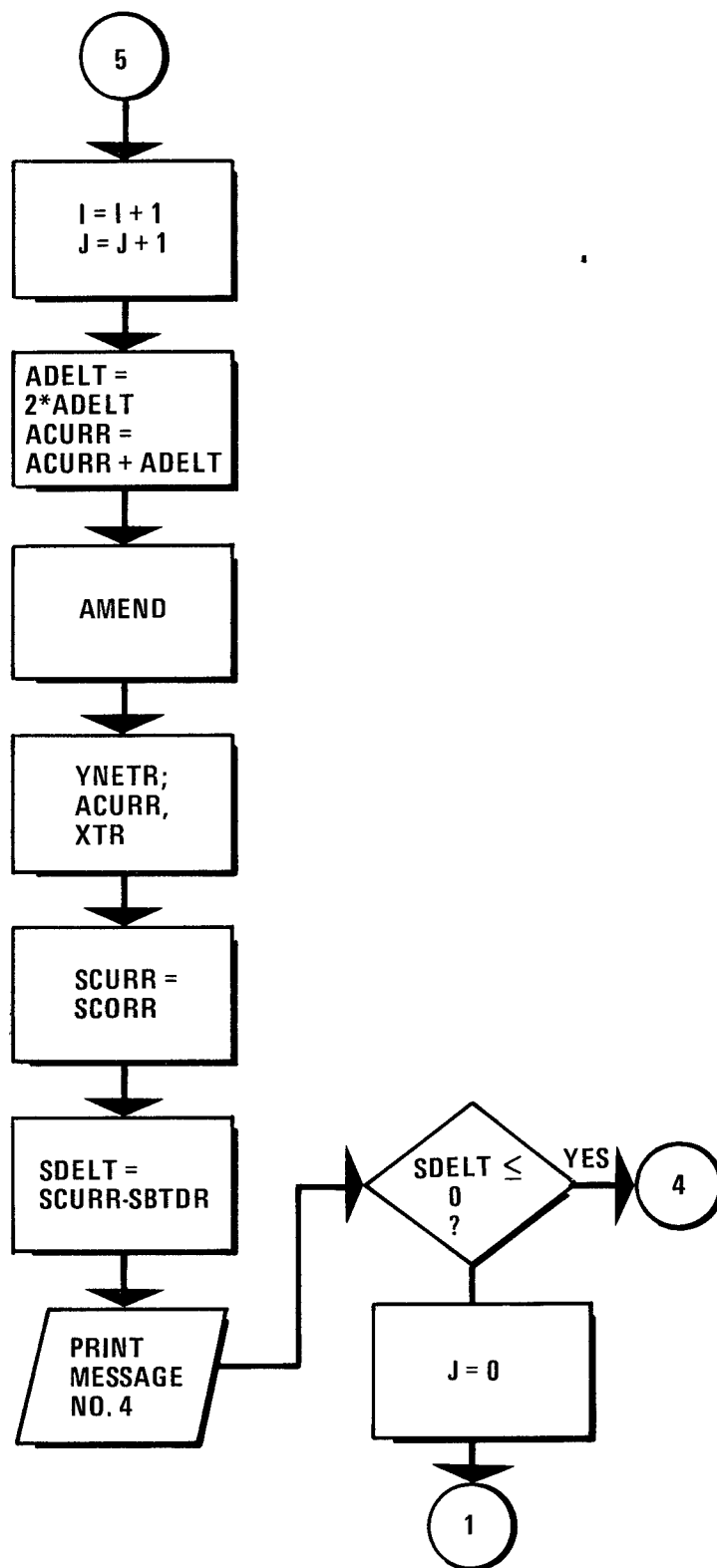


Figure B-1 Hypersurface Fitting Program (Continued) Acceleration and Hill Climbing

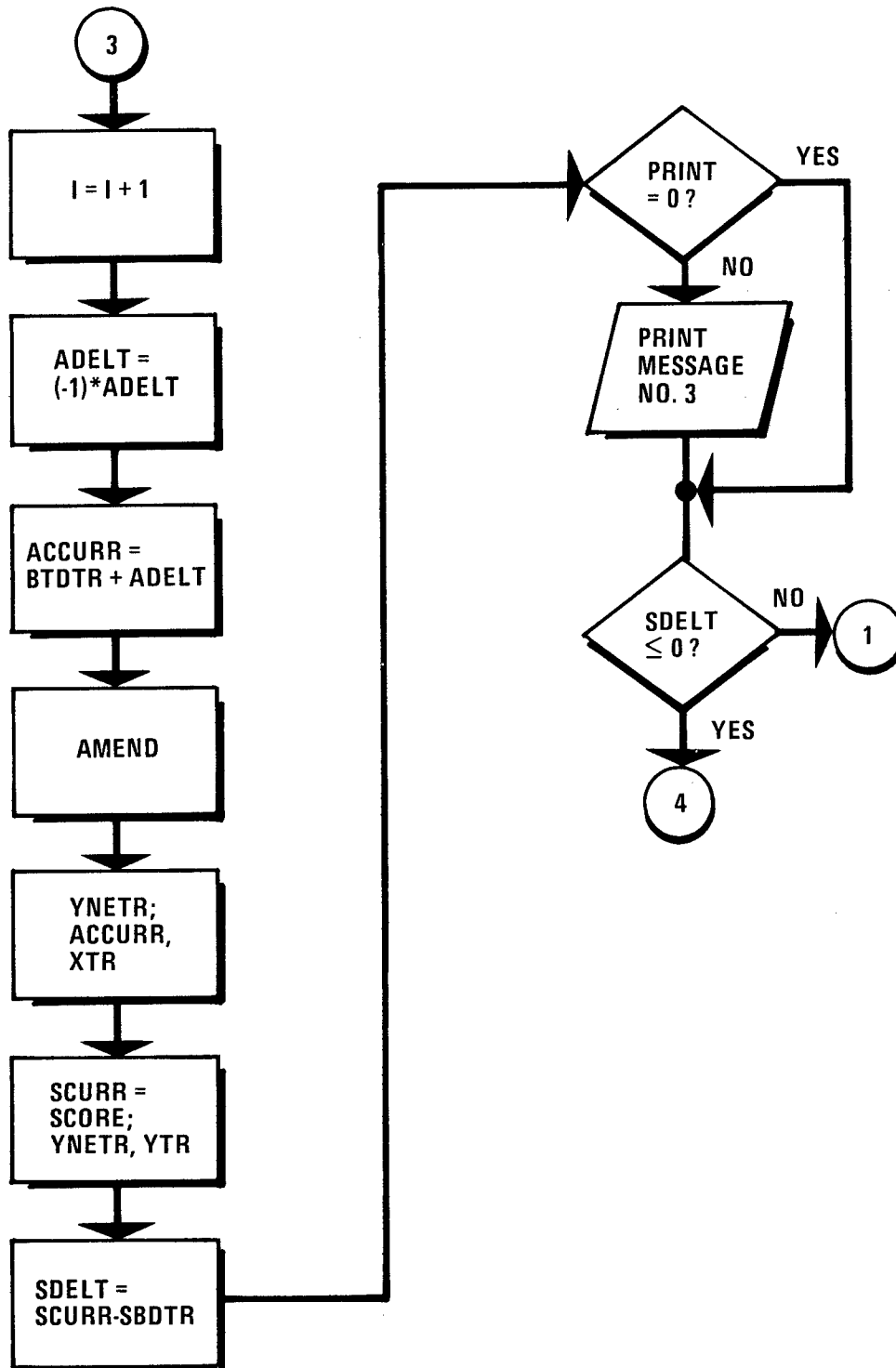


Figure B-1 Hypersurface Fitting Program (Concluded) Reversal

RAN2(n): Generates n pseudorandom numbers, β , from a zero-mean, unit-variance distribution and scales them to the proper range. If written as XXXX(n) = RAN2(n), it is interpreted to mean compute n random numbers and use them to replace XXXX. The scaling on RAN2 is:

$$\text{output} = (1/3)(C1)(\beta)(SBTDR/SZERO)^{C3}/(1 + I/C2)$$

Good starting values for C1, C2, C3 and C4, respectively, are 1, 10, 0, $\frac{1}{2}$.
The RAN2 routine must always be followed by the AMEND routine

Generally, both RAN1 and RAN2 are available in a single standard software package with most computers. If it is desired to start a run with a particular random number (which then uniquely determines all successive numbers generated) it is possible to initialize these special software packages with a fixed random number, and a test must be inserted in the program immediately after initialization of the arrays. The test would be applied to the constant IRANN: if IRANN = 0, do not initialize the random number generator; if IRANN \neq 0, initialize the random number generator with IRANN.

3.2 AMEND

This subroutine checks the coefficient vector generated by RAN2 or by reversal to see if any of the coefficients are outside the preset boundary. The basic algorithm employed can be thought of as a reflecting barrier at the boundary, and if a given Δa_i carries the i-th variable to a value $a_{\max} +$, the position of a_i is reset to $a_i -$. Since it is theoretically possible for a_i to be larger than $2a_m$, it is necessary to repeat the test after adjustment to be sure that the final a_i is in limits. This subroutine must always follow ADELTA computed from RAN2, from ADELTA = 2*ADELT, and from ADELTA = -ADELT. It is not needed for RAN1 programs, since the variables are always in limits by construction, nor is it ever used with coefficients used in computing test set values since no Δa 's are ever computed for the test set coefficients.

3.3 Scoring: SCORE and SCORR

The SCOR subroutine computes the average sum of squares of the errors in hypersurface fitting. Since scores are needed for both training sets, SCOR is always postscripted with an R or an E to distinguish between the two scores. The formula for SCORR is

$$\text{SCORR} = \left[\frac{1}{n} \right] \sum_{i=1}^{n_1} (\alpha_i - \beta_i)^2$$

where α_i and β_i are dummy variables indicating the i -th members of YTR and YNETR, respectively.

Similarly, SCORE is given by

$$\text{SCORE} = \frac{1}{n_2} \sum_{i=1}^{n_1} (\alpha_i - \beta_i)^2$$

and the dummy variables are members of YTE and YNETE.

3.4 Network Output Computation: YNETR and YNETE

Network connectivity is a pictorial representation of the order in which net inputs or intermediate column outputs must be combined using the net element algorithm to achieve computation of a multinomial. There are two connectivity patterns that have been found to have greater utility: rectangular and exponential. The algorithm for the square network is the simplest to program and has been selected for the first analyses for this program. The elements in a net should be organized into columns and the columns numbered from 1 on the input side to n at the output side. Within columns, the elements should be numbered from top to bottom. The network input vector should always be presented to the net with the variable number in ascending order from top to bottom of the net. The calculation procedure to be followed is to compute the outputs of columns from top to bottom (i.e., in order of increasing row number). This procedure guarantees that the intermediate outputs will be available when needed for any succeeding computation.

It is clear that "network connectivity" is simply an addressing scheme as far as the computer program is concerned. The reorganization of the training and testing sets into 3-dimensional arrays, discussed earlier, was designed to simplify the net addressing algorithm.

The net element computes the function

$$\eta = a_1 + a_2 \xi_1 + a_3 \xi_2 + a_4 \xi_1^2 + a_5 \xi_1 \xi_2 + a_6 \xi_2^2$$

To expand an element computation to a full net, the connectivity algorithms must specify the addresses of the coefficient vector and the input vector. The training and testing sets, which provide the inputs, were organized as $(m/2, 2, n_1)$ and $(m/2, 2, n_2)$ arrays. Let (i, j, k) be a pointer to a specific element in the array. If k is held fixed, then $x(i, j)$ is an $(m/2, 2)$ array, and this array is exactly the net input needed for that value of k . It can be noted that the index, i , in $x(i, j)$ is always the same numerical value as k_1 , the row index for the net. Recall that the number of input variables was forced to be even to allow equating i and k_1 .

The general expression for net addressing requires four indexes: (i, j, k, k_2) . The (i, k_2) pair give the row and column of the net element; the index, j , distinguishes between the 1 and 2 inputs, and k refers to the k -th member of the training set. Since the XIN array is used only for the first column calculation, it can serve as temporary storage for succeeding column outputs. To show this, let $y(i, j, k, k_2)$ be an element output. Then y can be written into $x(i, j, k)$ since there will always be twice as many x 's as y 's. Once all $m/2$ outputs for a column have been computed, then set

$$\begin{aligned} x(1, 2, k) &= x(\frac{m}{2}, 1, k), \quad i=1 \\ x(i, 2, k) &= x(i-1, 1, k), \quad i=2, \dots, m/2 \end{aligned}$$

The input array to the next column is then set up, exactly as the net inputs set up the first column inputs. It should be noticed, however, that this algorithm is equivalent to a net with a uniform pitch of 1. If another pitch pattern is desired, the above two formulas would have to be modified.

The net output can be computed once the final column calculation has been made:

$$y(k) = (2/m) \sum_{i=1}^{m/2} x(i, 1, k)$$

To distinguish between outputs computed for the training and testing sets, the notation YNETR means that the net output is computed for the training set and YNETE means that the net output has been computed for the test set. In either case, however, it is still necessary to indicate the origin of the coefficients used in the calculation.

The network element coefficients used in the calculations are the $6(m/2)^2$ elements in one of the arrays ACURR, BTDTE or BTDTR. The indexes for the a -arrays are (i, k_2, k_3) , $k=1, \dots, 6$, and the successive 1×6 arrays of coefficients are addressed directly to the proper elements.

4. Analysis Program

The analysis program approximates the first derivative of y , the net output, with respect to each variable, x_i , in the training or testing set using first difference formulas:

$$\frac{\partial y}{\partial x_i} = \frac{y(X + \Delta x \delta_{ij}) - y(X)}{\Delta x}$$

where

$$\delta_{ij} = \begin{cases} 1 & \text{if } j = i \\ 0 & \text{if } j \neq i \end{cases}$$

and

$$X = (x_1, \dots, x_i, \dots, x_{NVAR})$$

$y(X)$ is computed using the net subroutine

This calculation should be performed for each variable at each point in the training set. This procedure will produce NTR values for each partial derivative. A useful way to plot the results of this program is as a scatter plot on a $\Delta y / \Delta x_i$ vs. x_i graph, and it is very helpful to organize the $(x_i, \Delta y / \Delta x_i)$ pairs in ascending order of the x_i values. Since this procedure is used for each variable, there will be a total of $NVAR \times NTR$ points to be plotted, NTR for each variable.

Since all x_i values lie approximately in the -3 to $+3$ range after normalization, a reasonable value for Δx would be about 6×10^{-3} , which is $1/1000$ the range of the x 's. Since the mean and variance for each variable were computed in the training and testing set preparation program, the partials and the x 's could be scaled back to the original values if the means and standard deviations were preserved.

Using only a first difference analysis, it is possible to eliminate those variables which make no significant contribution to y (those for which all the points on the scatter plot lie very close to zero). A more detailed analysis can be obtained by taking only the significant or contributory variables and computing various mixed partials or by cross-plotting to obtain a family of curves with some of the other variables as parameters of the plots.

Once the significant variables have been determined, a smaller net can be fitted using only these variables. If SBTDE for the refitted, smaller net is within about 3% of its value in the larger net in which all variables were present, then the smaller net can be used for the more detailed studies and cross-plotting.

COMPUTER CODES FOR THE ADAPTIVE LEARNING ANALYSIS

The basic program consists of a main resident program and eight overlays. The main program resides in core at all times and calls in the overlays by the routine LINK as needed. Figure B-2 presents a listing of the main program.

Overlay 1

The function of Overlay 1 is to select NDE method, enter parameters to sort on, with upper and lower limits as an option, select data base and select the net input variables.

Figures B-3 through B-7 show the teletype printout from the overlays. The first response, "TITLE IS:", is a request for title. The second line prints out the title along with the date and time. Next the NDE method is specified. The next teletype response is requesting the selection of NDE parameters to sort on. These parameters must be indicated as numeric coded numbers. For operator convenience the available parameters for a given NDE method along with their numeric codes are displayed on the Tektronix 4010 scope. The teletype next responds with "IS THIS OK?", giving the operator an opportunity to change the parameters. The next teletype response asks for limits on parameters and then responds with "IS THIS OK?", giving the operator a chance to change the limits. The teletype then responds with "ENTER DATA SET # FROM KEY BOARD?". This is an option to either enter the data sets from the key board or let the computer search through the disc and locate the data sets which match the given control lines. After the data base has been specified, the teletype responds with "MORE CONTROL LINES?". This is an option which permits the operator to select a different set of parameters. After the operator responds to this option the teletype responds with "NET INPUT VARIABLES". The operator must respond with the desired net input variables. The order in which the variables are specified will determine the order that the variables are fed into the network.

```

C AL.FTN , GD/FW/MFL , MAY 2,1976
C ADAPTIVE LEARNING PROGRAM
C RESIDENT OVERLAY
      COMMON / ARRAYS / ITL(30),KDL(2,8),NAME(10,12),
      1 LV(16),LDS(100),A(17),SD(17),BTE(6,36),
      2 YTR(100),YTE(100),IYTRQ(100),IYTEQ(100)
      COMMON / CONTRL / MODE,NLS,ISD,IREC1,IREC2,
      1 MTHD,NTR,NTE,NVAR,NNET,NFOW,NCOL,NCOEFF,
      2 ABIAS,C1,C2,C3,C4,AMX,SZERO,IDM(10),XDM(5)
C DEFINE DIRECT ACCESS FILES
      DEFINE FILE 1(4500,256,U,IREC1)
      DEFINE FILE 2(2,1200,U,IREC2)
C FOFCE LOADING OF CERTAIN ROUTINES IN MOS
      X=2.*X/(1.+X)-1.
      I=X
C SELECT DATA SETS
1      CALL LINK('L1')
C SELECT POINTS FROM DATA SETS
      CALL LINK('L2')
C ARRANGE DATA POINTS AND SCAN THROUGH DATA
      CALL LINK('L3')
      CALL LINK('L4')
C ENTER FITTING CONSTANTS , INITIALIZE COEFF. ARRAY
      CALL LINK('L5')
C FIT THE DATA
      CALL LINK('L6')
C DISPLAY THE DERIVATIVES AND EVALUATE THE FIT
      CALL LINK('L7')
C PERFORM A PARAMETRIC STUDY , PLOT FAMILY OF CURVES
      CALL LINK('L8')
      GO TO 1
END

```

Figure B-2 Adaptive Learning Technique Main Program Listing

TITLE IS : PENETRANT FLAT/PLATE

PENETRANT FLAT/PLATE
NDE METHOD : PENETRANT

19-NOV-76 12:02:51

ENTER PARAMS

2 : 43

3 : 45

4 : 47

5 : 48

6 : 0

IS THIS OK ? YES

LIMITS ON PARAM : 43

LOWER,UPPER : 1,640

LIMITS ON PARAM : 47

LOWER,UPPER : 1,10

LIMITS ON PARAM : 48

LOWER,UPPER : 1,300

LIMITS ON PARAM : 0

IS THIS OK ? YES

ENTER DATA SET # FROM KEY BOARD ? YES

1:1

2:2

3:0

MORE CONTROL LINES ? NO

1 2
NET INPUT VARIABLES

1: 43

2: 17

3: 43

4: 14

5: 47

6: 48

7: 0

Figure B-3 Teletype Output from Overlay 1

VECTORS : 50

MIN POP. : 2

MAX JUMP SIZE=MJS , MAX POINTS PER SET=MPPS
SET MJS,MPPS FOR EACH DATA SET ? NO

OVERLAY 2

MJS,MPPS:2,60

IS THIS OK ? YES

USE LINEAR INPUTS ? NO

OVERLAY 3

SKIP CELL-POP. ? NO

MIN POP TO INITIATE CF=1 ? 9

OVERLAY 4

INPUT ICF(1),IPOP = 1 10

INPUT ICF(1),IPOP = 2 10

INPUT ICF(1),IPOP = 3 10

INPUT ICF(1),IPOP = 4 50

INPUT ICF(1),IPOP = 5 50

INPUT ICF(1),IPOP = 6 50

INPUT ICF(1),IPOP = 7 100

INPUT ICF(1),IPOP = 8 100

INPUT ICF(1),IPOP = 9 100

IS THIS OK ? YES

Figure B-4 Teletype Output from Overlays 2, 3, and 4

NORMALIZE ? YES

USE MEAN&STND. DEV. ? NO

CRACK LENGTH	M: 0.078	B: 0.178	S: 0.059
SAMPLE HISTORY	M: 0.197	B: 0.408	S: 0.109
CRACK LENGTH	M: 0.078	B: 0.178	S: 0.059
PART GEOMETRY	M: 0.000	B: 0.000	S: 0.585
SURFACE FINISH	M: -0.017	B: 0.729	S: 0.117
THICKNESS	M: -0.078	B: 0.797	S: 0.116

NORMALIZE Y ? NO

ZERO NON-LINEAR COEFFICIENTS ? NO

ZERO CONSTANT TERMS ? YES

ZERO BTE ARRAY ? YES

C1 : .1

C2 : 10.

C3 : .5

C4 : 20.

NCOL : 3

SET CONSTANTS FOR (A2,A3) ? NO

AMX : 1.

PRINT INTERVAL : 150

USE RANDOM NO. GENERATOR? NO

WHICH NET? 0,0

Figure B-5 Teletype Output from Overlay 5

MODE	#	BTD-TRAIN	BTD-TEST	NBTD	
UNGU	1	0.399E 00	0.349E 02	0.355E 00	0
T-T	4	0.340E 00	0.340E 00	0.302E 00	4
T-T	5	0.256E 00	0.256E 00	0.227E 00	5
T-T	6	0.681E-01	0.681E-01	0.515E-01	6
T-T	8	0.675E-01	0.675E-01	0.506E-01	8
T-T	9	0.669E-01	0.669E-01	0.495E-01	9
T-T	11	0.650E-01	0.650E-01	0.459E-01	11
T-T	16	0.635E-01	0.635E-01	0.441E-01	16
UNGU	162	0.635E-01	0.799E 01	0.441E-01	16
UNGU	302	0.635E-01	0.245E 01	0.441E-01	16
UNGU	462	0.635E-01	0.707E 00	0.441E-01	16
UNGU	602	0.635E-01	0.640E 01	0.441E-01	16
UNGU	762	0.635E-01	0.573E 03	0.441E-01	16
UNGU	902	0.635E-01	0.488E 00	0.441E-01	16
UNGU	1062	0.635E-01	0.829E-01	0.441E-01	16
UNGU	1202	0.635E-01	0.277E 01	0.441E-01	16
UNGU	1362	0.635E-01	0.243E 01	0.441E-01	16
UNGU	1502	0.635E-01	0.274E 00	0.441E-01	16
UNGU	1662	0.635E-01	0.182E 01	0.441E-01	16
UNGU	1802	0.635E-01	0.173E 04	0.441E-01	16
UNGU	1962	0.635E-01	0.344E 01	0.441E-01	16
UNGU	2102	0.635E-01	0.676E 00	0.441E-01	16
UNGU	2262	0.635E-01	0.421E 01	0.441E-01	16
UNGU	2402	0.635E-01	0.382E 02	0.441E-01	16
UNGU	2562	0.635E-01	0.405E 01	0.441E-01	16
UNGU	2702	0.635E-01	0.381E 01	0.441E-01	16
UNGU	2862	0.635E-01	0.970E 00	0.441E-01	16
UNGU	3002	0.635E-01	0.138E 02	0.441E-01	16
UNGU	3162	0.635E-01	0.124E 01	0.441E-01	16
UNGU	3302	0.635E-01	0.611E 01	0.441E-01	16
UNGU	3462	0.635E-01	0.103E 01	0.441E-01	16
UNGU	3602	0.635E-01	0.975E 00	0.441E-01	16
UNGU	3762	0.635E-01	0.366E 02	0.441E-01	16
UNGU	3902	0.635E-01	0.365E 00	0.441E-01	16
UNGU	4062	0.635E-01	0.343E 01	0.441E-01	16
UNGU	4202	0.635E-01	0.122E 02	0.441E-01	16
UNGU	4362	0.635E-01	0.215E 04	0.441E-01	16
UNGU	4502	0.635E-01	0.257E 02	0.441E-01	16
UNGU	4662	0.635E-01	0.705E 01	0.441E-01	16
UNGU	4802	0.635E-01	0.339E 01	0.441E-01	16
UNGU	4962	0.635E-01	0.246E 01	0.441E-01	16
UNGU	5102	0.635E-01	0.239E 02	0.441E-01	16
UNGU	5262	0.635E-01	0.516E 01	0.441E-01	16
UNGU	5402	0.635E-01	0.161E 02	0.441E-01	16
UNGU	5562	0.635E-01	0.182E 01	0.441E-01	16
UNGU	5702	0.635E-01	0.178E 02	0.441E-01	16
UNGU	5862	0.635E-01	0.170E 01	0.441E-01	16
UNGU	6002	0.635E-01	0.313E 02	0.441E-01	16
UNGU	6162	0.635E-01	0.131E 02	0.441E-01	16
UNGU	6302	0.635E-01	0.524E 01	0.441E-01	16
UNGU	6462	0.635E-01	0.418E 00	0.441E-01	16
UNGU	6602	0.635E-01	0.131E 00	0.441E-01	16
FINI	6705	0.186E 00	0.271E 00	0.166E 00	16

FINI TIME : 16:40:25

Figure B-6 Teletype Output from Overlay 6

PLOT RAW DATA ? NO

IS THIS OK ? YES

OVERLAY 7

LOG ? YES

VARIABLE # : 1

VARIABLE # : 3

OVERLAY 8

VARIABLE # : 0

VALUES FOR OTHER VARIABLES

2: 1

4: 1

5: 1

6: 1

DUAL PLOT ? YES

ENTER TITLE : PENETRANT FLAT PLATE A=TK1, B = TK2

VARIABLE # : 1

VARIABLE # : 3

VARIABLE # : 0

VALUES FOR OTHER VARIABLES

2: 1

4: 1

5: 1

6: 2

END THIS ? YES

Figure B-7 Teletype Output from Overlays 7 and 8

The subroutines and their functions for this overlay are listed below.

OVERLAY 1 SUBROUTINES

- LOOP - Selects data sets for data base
- SELECT - Selects parameters with upper or lower limits to sort on
- NDEMTN - Selects NDE method
- PRMTR - Lists all available parameters for a given NDE method
- VRY - Lists values for each parameter
- MWWN - Matches words with numbers
- LGND - Legend for data file
- FETCH - Reads header page for a given data set
- MATCH - Match given control line with control line from disc.

Overlay 2

The primary function of this overlay is to pick the vectors from the data base, each vector having the same common net input variables as specified. The maximum number of vectors which the program can handle is specified by two dimension blocks of 600 words each. One block is reserved for the training set and one for the testing set.

The arrays for the training (XTR) and testing (XTE) sets have the form of XXX (NTR,NVAR) where NTR is the number of vectors and NVAR is the number of net input variables. The product of NTR and NVAR cannot exceed 600. The program loops in a data set and uses a random number generator to fetch a data line for the formation of a vector. The program uses a flip/flop and the vectors are alternately thrown in the training set and the testing set. No duplicate vectors in a given data set is permitted.

The first response on the teletype from overlay 2 is "%VECTORS:". The operator response indicates the number of vectors to be selected for the training and/or testing set. The

next teletype response is "MIN POP:". The operator response indicates the min number of times a given vector must be common in data set before the vector is selected. The next response on the teletype is related to maximum jump size (MJS) and maximum vectors per set (MPPS). The program provides an option to select MJS and MPPS for each individual data set or to select values for MJS and MPPS which are common to all the data sets.

MPPS is the maximum number of vectors which will be selected from a given data set and MJS is a number when added to the number obtained from the random number generator determines which data line will be fetched from a given data set. The next teletype response is "IS THIS OK?". This is a program option which permits researching the data base.

A list of the subroutines and their functions are given below.

OVERLAY 2 SUBROUTINES

- VCTR - Sorts through designated data base and forms vectors which are a function of the net input parameters
- FETCH - Previously described
- RANDU - Generates a random number
- POD - Calculates point estimate for a given vector
- SFBIN - Divides surface finish into bins
- TKBIN - Divides thickness into bins
- CLBIN - Divides crack length into bins
- A2CBIN - Divides " $A/2C$ " into bins, where A is crack depth and 2C is crack length
- MATCHL - Matches data line with given one.

Overlay 3

The function of Overlay 3 is to set up an independent test problem with given coefficients for adaptive learning. This type of approach was used many times in the initial development of the software to determine how new ideas on fitting techniques

would improve either the convergence or the fitting of the test problem. The only teletype response associated with this overlay is an option to use linear inputs.

OVERLAY 3 SUBROUTINES

- LNRRIN - Sets up a particular problem for the adaptive learning to solve
- RANX - Sets up dimension and scaling factor for random number generator
- RANDU - Previously described
- LST - Lists the input vectors.

Overlay 4

The function of Overlay 4 is to sort through both the training and testing sets and divide the data into an array of the form (CL,SF,TK). For each cell of this array, the total number of vectors, the total population and the average POD is calculated and listed on the scope. An additional function of this overlay is to provide weighing factors in percent on vectors having a population less than a preselected number.

The first teletype response from Overlay 4 is program option to skip CELPOP. CELPOP has to be skipped when the net input variables does not include surface finish and thickness. The next response is related to the assignment of weighting factors below some minimum population. The teletype then responds with "IS THIS OK?". This is a program option which permits reselecting the weighting factors.

The subroutines and their functions for this overlay are listed below.

OVERLAY 4 SUBROUTINES

- CELPOP - Sorts through input data and divides into cells (CL,SF,TH) and determines the total number of vectors, average POD and total number of samples for each cell.
- DTLST - Lists the CELPOP results
- CONFCT - Provides weighting factors for vectors having a total population equal to or less than a given minimum population.

Overlay 5

The function of Overlay 5 is to prepare the data for the fitting program. First the data is normalized by one of two methods. One method is simply to divide each of the net input variables by its corresponding maximum value. The second method calculates a mean and determines the standard deviation. The input variable is normalized by subtracting its value from the mean and dividing by N standard deviations where N is a program integer option. An additional function of this overlay is to perform a least square linear fit (LSLF) of the POD as a function of each of the net input variables. The third function of this overlay is to initialize certain constants for the fitting program.

The first teletype response from Overlay 5 is "NORMALIZE?". This is a program option, which will either work with raw data or normalized data, depending on the operator response. Assuming the data is to be normalized the next response is "USE MEAN & STD DEV?". This is an option which determines the method of normalization to be used. The next teletype responses are related to the LSLF. Slope, intercept, and standard deviation are given for each net input variable. The next teletype response is "NORMAZIZE Y?". This is an option to normalize y (point estimate).

The remaining teletype responses for this overlay are related to the initialization of the training set coefficients as well as other constants related to the fitting program. Several questions are related to options concerning the training set coefficients. However the best results were obtained by doing an iterative search on all the coefficients simultaneously starting all the coefficients initially at zero. The three different options permit (1) constant term coefficients to be zero, (2) nonlinear coefficients to be zero and (3) set in preselected coefficients for the linear terms on all except the coefficients for the first column of nets.

The constants C1, C2 and C3 are used to calculate a scale factor for controlling size of the random numbers. AMX is also used as a scale factor on random numbers in the unguided search. NCOL is the number of columns in the network connectivity. The response to "PRINT INTERVAL" indicates frequency as function of trials that information related to score of the test set and the training set be written out on the teletype. The teletype response "USE RANDOM NO. GENERATOR?" is an option to initialize

the training set coefficients with random numbers. The teletype response "WHICH NET" permits selection of coefficients for any or all of the nets. Operation response, (\emptyset, \emptyset), returns control to the main program.

The subroutines and their functions are listed below.

OVERLAY 5 SUBROUTINES

- NRMLZ - Provides options to provide different techniques of normalizing the data and calls other subroutines to prepare the data for the adaptive learning fitting program
- LSLF - Performs least square linear fit for POD vs each of the net input variables
- LNRM - Normalizes the data by dividing each net input parameter by its corresponding maximum value
- NRML - Calculates mean and standard deviation and normalizes by subtracting the mean from each net input parameter value and dividing by the standard deviation
- PREPAR - Prepares input data
- RANX - Previously described.

Overlay 6

The function of this overlay is to perform an iterative search over bounded space for the test set coefficients for a given rectangular connectivity. The procedure employs an unguided, guided, reversal and acceleration with controlled step size in conjunction with the training-testing paradigm. Basically the procedure uses training set vectors until an improvement in score has been obtained. These same coefficients are then applied to the testing set vectors to check for improvement in the testing set score. The object of the search is to reduce the test set score to a minimum. A flow diagram of this procedure is given in Figure B-8. When the search is terminated, a listing of the final results is displayed on the 4010 scope. Examples of these displays are shown in Figures B-9 and B-10. The final results indicate the coefficients of each net; the true point estimate, the difference between the true point estimate and the predicted value, and the weighting factor for each vector.

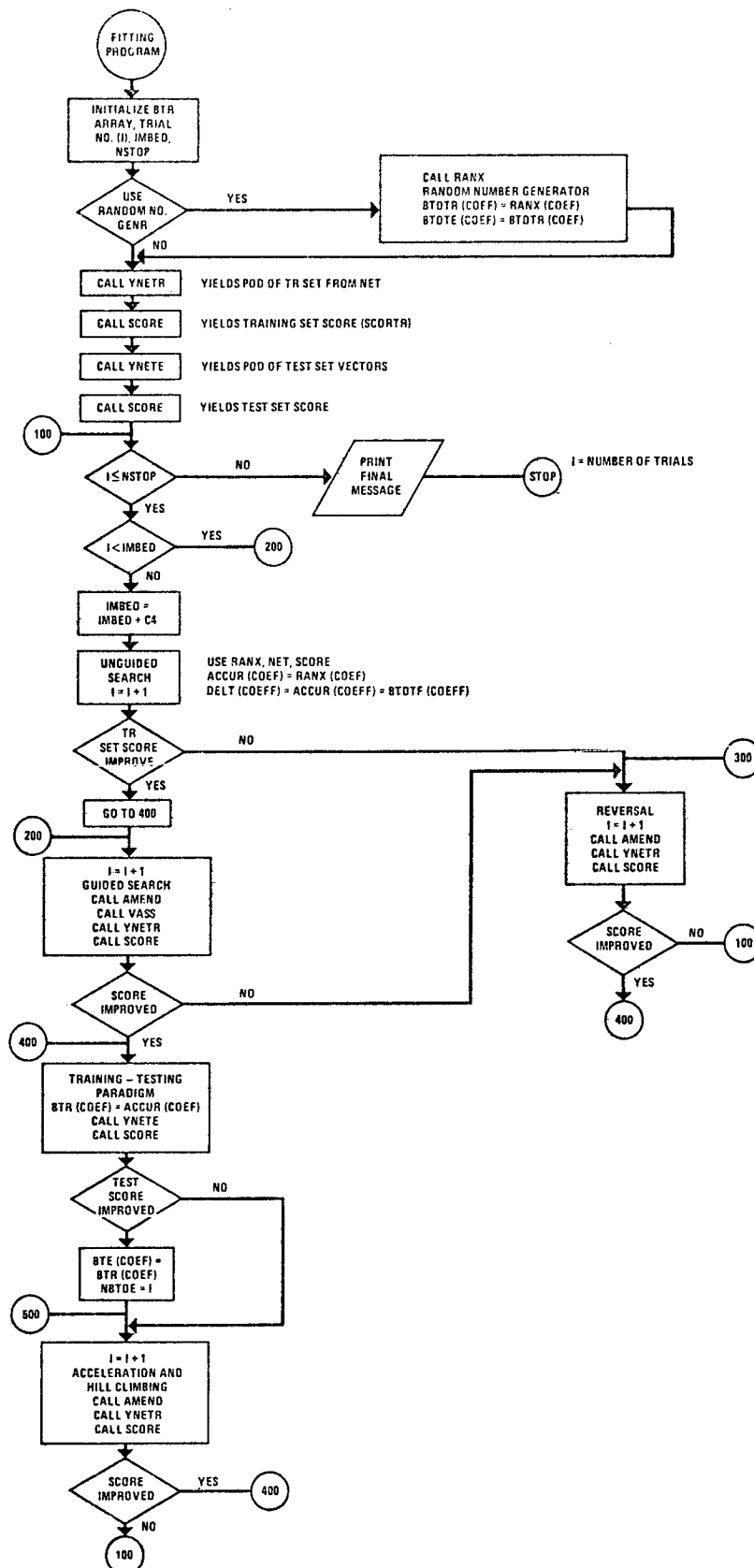


Figure B-8 Fitting Program Logic

PENETRAN FLAT/PLATE									
True Point Estimate	Dif. True & Cal.	Weighting Factor							
NETC 1, 1)	-0.01392	-0.43559	-0.56368	0.39864	0.29513	0.5027	0.5027	0.5027	0.5027
NETC 2, 1)	-0.47844	-0.58360	0.19675	-0.50660	0.41461	0.08399	0.08399	0.08399	0.08399
NETC 3, 1)	0.64957	-0.50807	-0.19351	0.27240	-0.44079	0.24029	0.24029	0.24029	0.24029
NETC 1, 2)	-0.11171	-0.83329	-0.35118	-0.99055	-0.20777	0.54009	0.54009	0.54009	0.54009
NETC 2, 2)	0.15521	0.11622	-0.80420	-0.19772	-0.51089	0.17351	0.17351	0.17351	0.17351
NETC 3, 2)	-0.13461	0.15508	-0.40804	0.07251	0.47999	-0.41751	-0.41751	-0.41751	-0.41751
NETC 1, 3)	-0.44859	-0.10582	-0.28949	-0.24296	-0.13446	0.18466	0.18466	0.18466	0.18466
NETC 2, 3)	0.40513	-0.70483	-0.13854	-0.08273	0.82630	-0.78564	-0.78564	-0.78564	-0.78564
NETC 3, 3)	0.23184	0.20443	0.21810	-0.60879	0.29417	-0.57460	-0.57460	-0.57460	-0.57460
1.000	0.218	0.810	0.394	0.833	0.338	0.167	0.093	0.093	0.093
1.000	0.237	1.000	0.123	1.000	0.553	0.333	0.036	0.036	0.036
0.296	-0.118	0.811	0.269	-0.167	-0.201	0.380	0.380	0.380	0.380
0.333	-0.021	1.000	0.440	1.000	-0.099	0.917	-0.074	-0.074	-0.074
1.000	-0.119	0.500	0.059	0.000	-0.226	0.500	-0.147	-0.147	-0.147
1.000	0.239	0.333	-0.250	0.000	-0.156	0.667	0.175	0.175	0.175
0.000	-0.119	0.500	-0.110	0.500	-0.202	0.333	-0.199	-0.199	-0.199
0.917	-0.134	0.222	-0.237	0.400	-0.214	1.000	0.121	0.121	0.121
0.167	-0.305	0.667	-0.392	0.844	0.029	0.924	0.035	0.035	0.035
0.133	-0.409	0.667	-0.000	1.000	0.040	1.000	-0.201	-0.201	-0.201
0.854	0.013	0.583	-0.050	1.000	-0.145	1.000	0.193	0.193	0.193
0.000	-0.590	1.000	0.135	1.000	-0.032	1.000	-0.099	-0.099	-0.099
0.917	-0.030	0.556	-0.150	0.889	-0.186	1.000	-0.113	-0.113	-0.113
1.000	-0.216	1.000	-0.073	0.667	0.115	0.952	-0.138	-0.138	-0.138
0.278	-0.530	1.000	-0.060	0.667	-0.224	0.333	-0.401	-0.401	-0.401

Figure B-9 Final Training Set Results

PENETRAN FLAT/PLATE		24-NOV-76		15-27-78	
NETC 1, 1)	-0.01382	-0.43559	-0.56368	0.39864	0.29513
NETC 2, 1)	-0.47844	-0.58360	0.19675	-0.50660	0.41461
NETC 3, 1)	0.64957	-0.50807	-0.19851	0.27240	-0.44079
NETC 1, 2)	-0.11171	-0.83329	-0.35118	-0.99055	-0.20777
NETC 2, 2)	0.15521	0.11622	-0.88420	-0.19772	-0.51089
NETC 3, 2)	-0.13461	0.15508	-0.40804	0.07251	0.47999
NETC 1, 3)	-0.44859	-0.10582	-0.28949	-0.24296	-0.13446
NETC 2, 3)	0.40513	-0.70483	-0.13854	-0.08273	0.32630
NETC 3, 3)	0.23184	0.20443	0.21810	-0.60879	0.29413
1.000	0.218 100	0.852 -0.031	100 0.600	0.252	100 0.000
0.389	0.093 100	0.000 -0.584	10 1.000	0.640	10 0.889
1.000	0.120 100	0.491 0.019	100 0.417	0.079	100 1.000
0.333	0.024 10	0.000 -0.269	100 1.000	0.587	50 0.806
1.000	0.134 100	0.333 0.052	50 0.556	0.202	100 0.458
0.167	-0.004 50	1.000 0.005	10 0.222	-0.459	100 0.333
0.556	0.171 100	0.000 -0.214	10 0.821	-0.241	100 0.000
0.769	-0.117 100	0.889 -0.087	100 0.000	-0.493	10 0.000
0.111	-0.286 100	0.833 0.131	100 1.000	-0.065	100 0.867
1.000	-0.050 100	0.500 -0.100	50 0.000	-0.956	10 1.000
0.909	0.145 100	0.974 0.053	100 0.778	0.084	100 1.000
1.000	0.119 10	1.000 -0.058	10 0.333	-0.445	10 0.949
0.889	0.103 100	0.926 0.058	100 0.976	-0.042	100 0.500
1.000	-0.191 10	0.667 0.035	10 1.000	-0.012	100 0.700
0.889	-0.207 100	0.917 -0.034	100 1.000	-0.013	10 1.000

Figure B-10 Final Testing Set Results

Teletype responses related to Overlay 6 indicate seven pieces of information related to the iterative search. The information indicates the type of search, trial number, the best to date training score, the present training score, the best to date test score, the latest trial number where both the training and test set scores improved, and the computed average step size.

The subroutines for this overlay and their functions are given below.

OVERLAY 6 SUBROUTINES

- FP - Fitting program which determines the coefficients of the nets
- SCORE - Sum of squares of the deviations between the computed net output and the given POD value
- NET - Computes the output of the nets for a given set of coefficients
- LSTCOF - Lists a set of coefficients for a given net configuration
- RANX - Previously described
- AMEND - Depending on an argument value, will add two sets of coefficients, subtract two sets of coefficients or multiply a set of coefficients by a factor of 2 and add to a given set
- VASS - Computes average step size.

Overlay 7

The function of this overlay is to plot either the raw data or the derivative as a function of each of the net input variables. The plot of the raw data yields a graphical representation of the hypersurface fit. Because of the type of multinominal selected and rectangular connectivity of the network the derivative remains a function of all input variables, hence the derivative plot only shows trends.

The first teletype response from Overlay 7 is "PLOT RAW DATA?". This is an option which will permit the plot of raw data or a plot of the derivatives. The next teletype response

is "IS THIS OK?". This is an option which, depending on the operator response, will loop to "PLOT RAW DATA" option or return control to the main program.

A list of Overlay 7 subroutines and their functions are listed below.

OVERLAY 7 SUBROUTINES

- DP - Computes the derivative of the POD as function of each of the input variables
- NET - Previously described
- NRML - Previously described
- RESULT - Plots the derivatives.

Overlay 8

The function of Overlay 8 is to perform a parametric study. The curves shown in the figures in Section 6.1 are results of this overlay. The plots from the parametric study will usually show net output (predicated point estimate) as a function of crack length while the remaining net input variables are fixed.

The first teletype response from this overlay is "LOG?". This is an option which, depending on the operator response, will show the results as a semi log or linear plot. The remaining responses are related to selecting the net input variable for the plot and fixing the remaining net input variables.

A list of Overlay 8 subroutines and their functions are listed below.

OVERLAY 8 SUBROUTINES

- PSP - Performs a parametric study by calculating the net output from a fixed set of input variables for each vector
- NET - Previously described
- RESULT - Plots results of the net output as a function of crack length.

A P P E N D I X C

COMPARISON OF STATISTICAL SCHEMES
FOR P.O.D. CALCULATION

THE RANGE SCHEMES

The first range scheme divides the total range of crack sizes into N approximately equal subranges. A binomial "lower 95% confidence interval" is computed from the r_i (detected cracks) and m_i (total cracks present) of the i th interval. The smallest estimated POD (Probability of Detection) in this confidence interval is then plotted over the right-hand endpoint of the crack size subrange.

The choice of N is arbitrary, but by plotting the lower estimated POD over the right-hand endpoint of the subrange, the smaller N is chosen the more conservative the procedure becomes.

If the lower estimated POD is plotted using this range scheme, there is an undesirable consequence. The sample size on which the estimate is based can be more influential in determining the estimate than the observed fraction of detections. For example, 4 detections of 4 cracks leads to a lower 95% estimate of .47, while 10 detections of 12 cracks leads to a lower 95% estimate of .56.

This scheme does not make use of relevant information from previous subranges. For example suppose that at the .04 inch subrange there are 90 cracks, all of which are detected and at the .045 inch subrange there are 6 cracks, all of which are detected.

The lower 95% estimate for the POD in the .04 inch subrange is .97, while for the .045 inch subrange the estimate is only .61. It appears reasonable to assume that the larger the crack size the more likely the crack will be detected. In the example cited, surely the estimated POD at .045 inch should be at least as large as at .040 inch. Some of the other schemes recognize and take advantage of additional relevant data by pooling to improve the precision of the estimators.

The second range scheme is to divide the total range of crack sizes in subranges of unequal length but equal numbers of cracks. This procedure does control variations in the estimates due to sample size differences, however it opens the

possibility of long intervals which lead to conservative estimates as mentioned previously. Like the first range scheme, no use is made of relevant information from the data in smaller crack length subranges.

In general both these schemes are well founded theoretically, and for cases in which large sample sizes are available for each subrange, their conservative features present little problem. However, for the present application where sample sizes are not always large, and where relevant information is available from smaller crack length subranges, these procedures are overly conservative.

"OVERLAPPING 60" SCHEME

The "overlapping 60" scheme divides the total range of crack sizes into subranges which are unequal in length and are not mutually exclusive. This scheme establishes the largest crack length subrange by grouping the largest 60 cracks together. The next largest subrange is established by dropping the largest 30 cracks from the 1st subrange and then acquiring the next largest 30 cracks from the remainder of the data. This procedure is repeated until it is no longer possible to acquire new crack sizes. After the subranges have been established, the binomial "lower 95% confidence interval" is computed, as before, from the r_i (detected cracks) and m_i (actual cracks present) in the i th subrange. Again the smallest estimate of the POD contained in the confidence interval is plotted over the right-hand endpoint of the subrange.

Since a subrange usually contains many different sizes of crack, plotting the estimated POD for the subrange over the largest crack size in the subrange produces a conservative bias (the larger the subrange the greater the bias). This scheme, like the second range scheme mentioned, controls variations in the estimates due to sample size differences, but allows the possibility of large subranges and hence conservative estimates as mentioned above. If attaining 95% confidence that the POD exceeds .90 is deemed important, then this procedure might be modified to be an "overlapping 61" or "overlapping 76" so 2 and 3 failures respectively to detect cracks would still be compatible with the 95/90 criterion, with this scheme the maximum estimated POD is about .95 with 95% confidence, regardless of how well "large" cracks are

detected. This scheme makes use of information from the previous crack size subrange to compute the estimated POD for the current subrange. This scheme does not have the option of choosing whether to use data from the previous subrange, it always uses it. The consequence is that for the portion of the crack size vs. POD curve where the POD is increasing fairly rapidly, the estimated PODs are likely to be even more conservative than the range schemes. The portion of the curve where the POD is increasing slowly is likely to be estimated less conservatively than for the range schemes.

In general the procedure is conservative, probably more conservative than the second range scheme in some portions of the POD curve and less conservative in other portions of the POD curve. This procedure is probably better in the regions of most interest (threshold detection 95/90 size ranges), but overall is still too conservative.

OPTIMUM PROBABILITY METHOD (OPM) SCHEME

The OPM procedure divides the total range into N approximately equal subranges. A lower 95% confidence interval is computed from the r_i (number of detected cracks) and the n_i (total number of cracks) of the largest subrange. Next, the second largest subrange is combined with the largest subrange and a second lower confidence interval is computed. The process of adding a new subrange and computing a new lower confidence interval is repeated until all the subranges are grouped together. The largest lower bound of these N intervals is then plotted over the right-hand endpoint of the largest subrange. The largest subrange is then eliminated from consideration and the above procedure repeated beginning with the 2nd largest subrange. The OPM procedure is terminated when a lower estimate of the probability of detection has been plotted for each subrange.

The OPM procedure estimates a lower bound on true probability of detection curve (true probability of detection is the conceptual probability of detection computed from infinite sampling information).

However, the probability that the lower estimator is less than or equal to the true POD is $.95 - \delta$ where $\delta > 0$. Therefore the confidence level is less than 95% and this aspect of the procedure is liberal. As mentioned previously, plotting the estimated POD over the right-hand endpoint of the subrange is a conservative practice.

A pair of simple examples will illustrate some of the complexities of this problem. Suppose that at crack length .04 in. there are 29 cracks and at crack length .035 in. there are 50 cracks. Further assume that the POD at crack length .04 in. is .9 and also at .035 the POD is .9. In conceptual replications of computing the lower "95% confidence" interval for crack length .040 in. using the OPM procedure, about 92.67% of the intervals computed would contain .9 (the true POD). Thus for this case, the stated "95% confidence" level is not achieved. A closer examination of the details of computing the probability that the estimated lower bound will be less than the true POD will provide some useful insights about the condition under which the OPM is most liberal. In order to compute the 92.67% of intervals containing .9 (true POD), cited previously, it is easiest to compute the probability that the interval will not contain the POD of .9 and subtract from 1. At .04 in. there are 30 possible experimental results: 0, 1, ..., 29 detected cracks. Of these results only 1 leads to a lower "95% confidence" interval which does not contain .9, namely 29 detected cracks. However, the OPM procedure does not necessarily use just data gathered at .04 in., it may incorporate data gathered at .035 in. The following is a list of mutually exclusive experimental outcomes which lead to lower "95% confidence" intervals which do not contain .9.

At .04 in.		At .035 in.
1.	29 detections <u>and</u>	0, or, 1, or 2, ... or 50 detections
2.	28 detections <u>and</u>	48 or 49 or 50 detections
3.	27 detections <u>and</u>	49 or 50 detections
4.	26 detections <u>and</u>	50 detections

The probabilities of these four mutually exclusive experimental results are computed (assuming POD = .9 at both crack lengths) and added to yield the probability of the lower bound being in error. Note that if the POD at .035 in. is less than .9, the probabilities of large numbers (46, ..., 50) of crack

detections decrease, which causes the probabilities of experimental results 1 - 4 to decrease. The result is that the probability of the lower bound being in error decreases. Since it is reasonable to assume that the POD increases with crack size, keeping the POD constant for different crack length ranges may be viewed as a worst case.

The effect of having an additional crack length range for possible incorporation is illustrated by the next example. Consider 29 cracks at .04 in., 50 cracks at .035 in. and 50 cracks at .03 in. all with a POD = .9.

As in the previous example, a list is compiled at mutually exclusive experimental outcomes which lead to lower "95% confidence" intervals which do not contain .9.

# Detections at .04 in.	# Detections at .035 in.	# Detections at .030 in.
1. 29 and	0 or 1 or ... 49 or 40	and 0 or 1 or ... 49 or 50
2. 28 and	50	and 0 or 1 or ... 49 or 50
3. 28 and	49	and 0 or 1 or ... 49 or 50
4. 28 and	48	and 0 or 1 or ... 49 or 50
5. 28 and	47	and 47 or 48 or 49 or 50
6. 28 and	46	and 48 or 49 or 50
7. 28 and	45	and 49 or 50
8. 28 and	44	and 50
9. 27 and	50	and 0 or 1 or ... 49 or 50
10. 27 and	49	and 0 or 1 or ... 49 or 50
11. 27 and	48	and 47 or 48 or 49 or 50
12. 27 and	47	and 48 or 49 or 50
13. 27 and	46	and 49 or 50
14. 27 and	45	and 50

# Detections at .04 in.	# Detections at .035 in.	# Detections at .030 in.
15. 26 and	50	and 0 or 1 or ... 49 or 50
16. 26 and	49	and 47 or 48 or 49 or 50
17. 26 and	48	and 48 or 49 or 50
18. 26 and	47	and 49 or 50
19. 26 and	46	and 50
20. 25 and	50	and 47 or 48 or 49 or 50
21. 25 and	49	and 48 or 49 or 50
22. 25 and	48	and 49 or 50
23. 25 and	47	and 50
24. 24 and	50	and 48 or 49 or 50
25. 24 and	49	and 49 or 50
26. 24 and	48	and 50
27. 23 and	50	and 49 or 50
28. 23 and	49	and 50
29. 22 and	50	and 50

As before, the probabilities of these experimental outcomes are computed (assuming $POD = .9$ for all three intervals) and added to yield the probability, .0992, and the estimated lower bound is in error. Thus there is only about 90% confidence that the lower bound will be lower than the true POD . Notice that as the number of ranges which can potentially be incorporated increases, the potential error increases. The POD for this example was kept constant over three ranges of crack length, so this example can be regarded as a "worst case" situation.

There is also a conservative aspect to this procedure, namely plotting the estimated POD over the right-hand endpoint of the crack range. This procedure is most conservative where the POD curve is increasing rapidly and least conservative when the POD curve is flat or increasing slowly.

Summary: The OPM scheme is a powerful procedure (makes the most of available data) which has a small liberal bias (the confidence is smaller than the stated 95%). The size of the bias depends on:

1. True shape of POD curve
2. Sample sizes in different ranges
3. Total number of ranges
4. Where in the interval the estimated POD is plotted

Subjective Evaluation: Overall probably the best procedure because it handles the unequal sample size problem and makes full use of available data. The price that is paid for using this procedure is the liberal bias in crack size regions where the POD curve is flat or increasing slowly.

A P P E N D I X D

EXAMPLES OF COMPUTER GENERATED
HISTOGRAMS OBTAINED BY THE POINT ESTIMATE METHOD

EXAMPLES OF COMPUTER GENERATED HISTOGRAMS OBTAINED BY THE POINT ESTIMATE METHOD

The effect of specimen thickness on the POD was shown earlier in Figure 3 in the test. Figures D-1 and D-2 present a comparison of the PODs for specimens with thicknesses of 0.214 and 0.060 in. with three ranges of surface finishes for eddy current and ultrasonic inspection techniques respectively. Figure D-3 presents similar comparison for specimens with four ranges of surface finishes for the penetrant technique. Comparisons for specimens with two ranges of surface finishes are shown in Figure D-4 for X-ray inspection. The comparisons in Figures D-1 to D-4 indicated that specimen surface finish has negligible effect on the POD for ultrasonic and X-ray methods. For eddy current and penetrant inspections the effect is noticeable only in the smallest crack length region of 0 - 0.125 in. In both cases only the smoothest range of surface finish of 0-32 RMS appeared to have different effects on the POD compared to the other surface finish ranges. For eddy current inspection the POD for the smoothest surface finish is highest in the 0-0.125 in. crack length. For penetrant inspection the POD for the smoothest surface finish range is lowest in the smallest crack length range. Comparing specimen thicknesses, the only significant difference in POD for specimens with two different thicknesses was observed for the X-ray technique.

Figures D-5, D-6, D-7 and D-8 present comparisons of POD for specimens with etched and unetched surfaces for eddy current, ultrasonic, penetrant and X-ray technique respectively. For the first three NDE techniques, results of flat plate specimens, integrally stiffened panels and a composite of these two specimen types from three different companies are presented separately. For the X-ray inspection, only the flat plate specimens have sufficient data for comparison purpose. Results presented in these figures indicated that etching of the specimen surfaces increased the POD for all NDT techniques except ultrasonics. The effect of etching in the penetrant technique appeared to be more pronounced for flat plate specimens as compared to integrally stiffened panels and composites. For eddy current technique, the effect of etching appeared to be more pronounced for the integrally stiffened panels and composite results as compared to flat specimens. No noticeable effect could be discerned from the etching for the ultrasonic technique.

A comparison of the POD for different inspectors within the same company is presented in Figure D-9 for penetrant, eddy current, and X-ray techniques. The inspection efficiency of the same class of inspectors within the same company appears to be

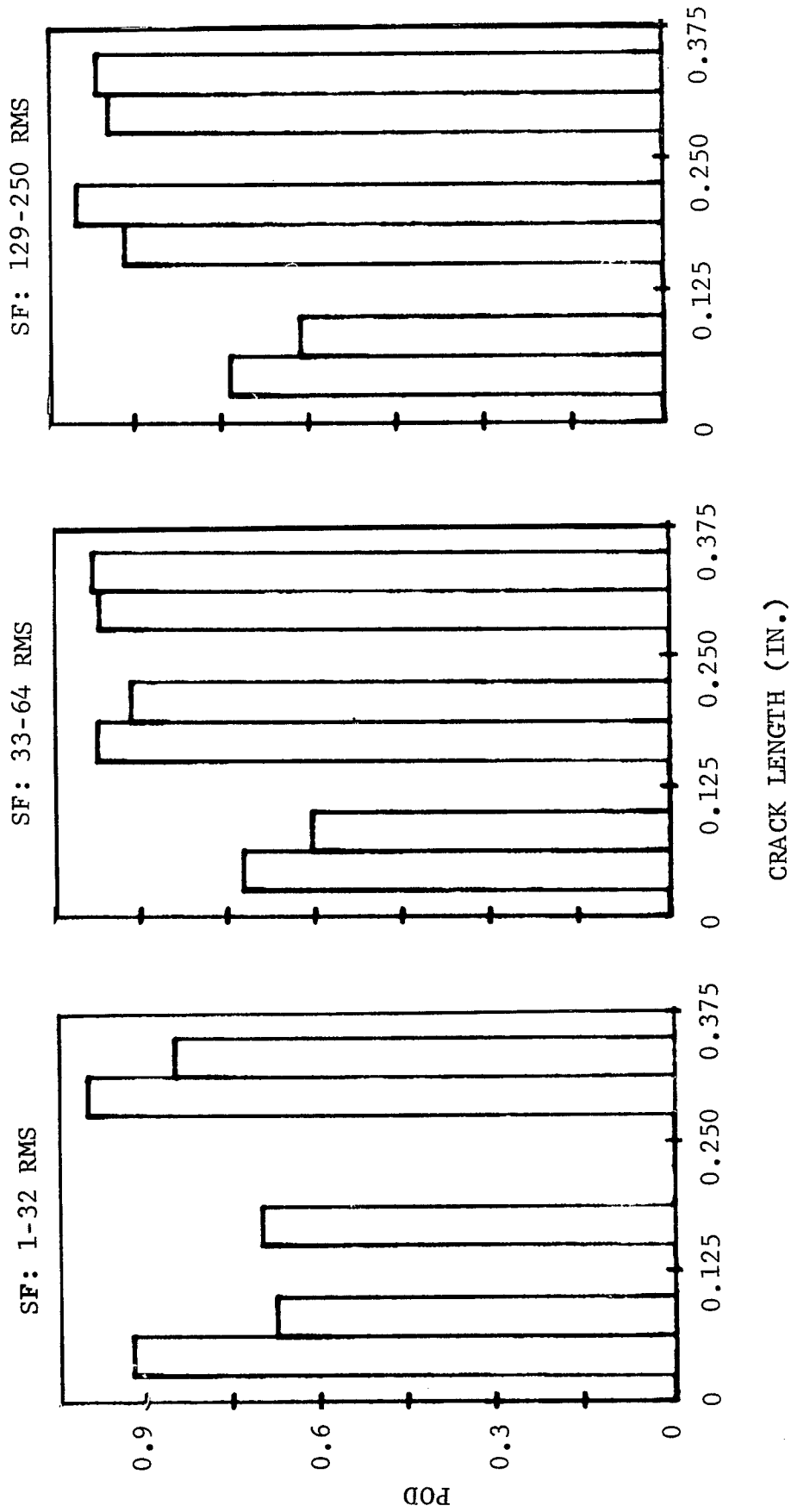


Figure D-1 Comparison of POD of Flat Plate Specimen Thickness (Eddy Current)
 (1st and 2nd Columns Represent Specimens with Thicknesses of 0.214
 and 0.060 In. Respectively. DSN = 15-18, 31)

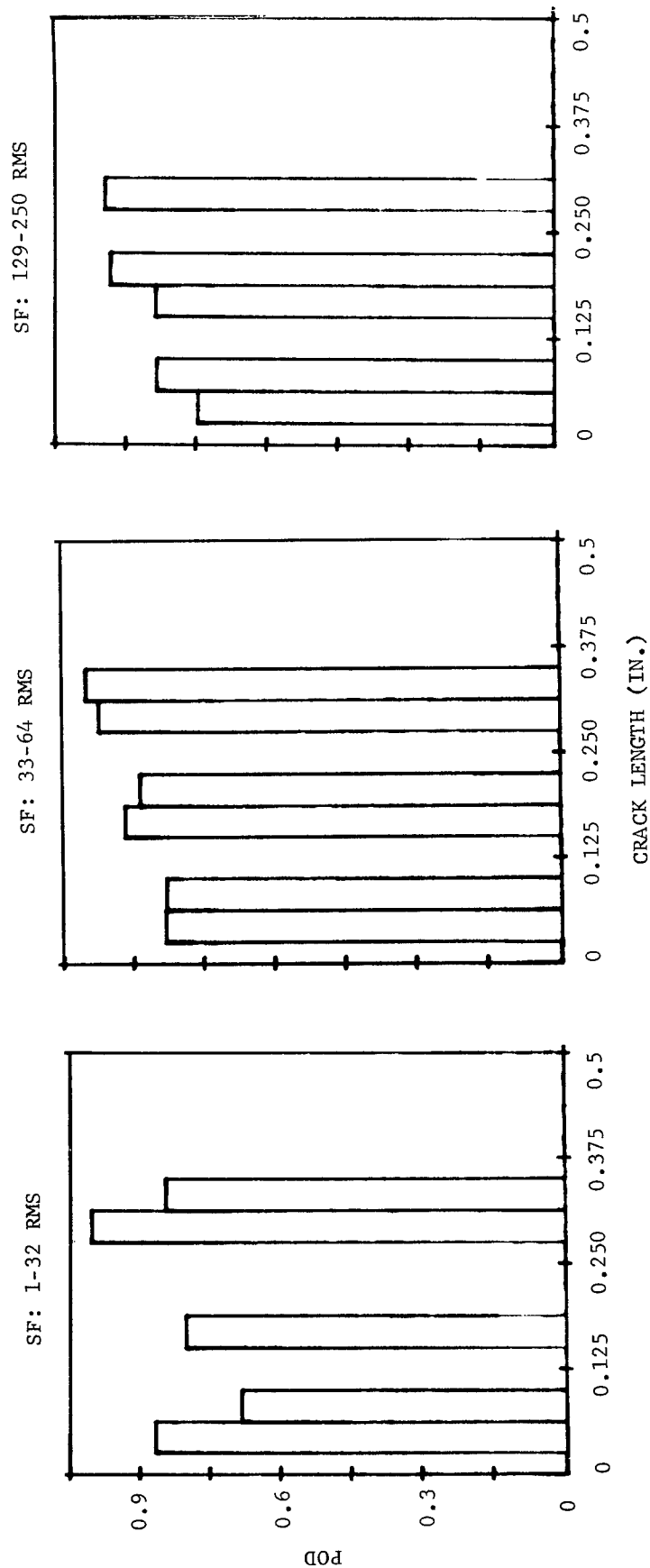


Figure D-2 Comparison of POD of Flat Plate Specimen Thickness (Ultrasonic)
 (1st and 2nd Columns Represent Specimens with Thicknesses of 0.214
 and 0.060 In. Respectively. DSN = 12,13,14,29,30)

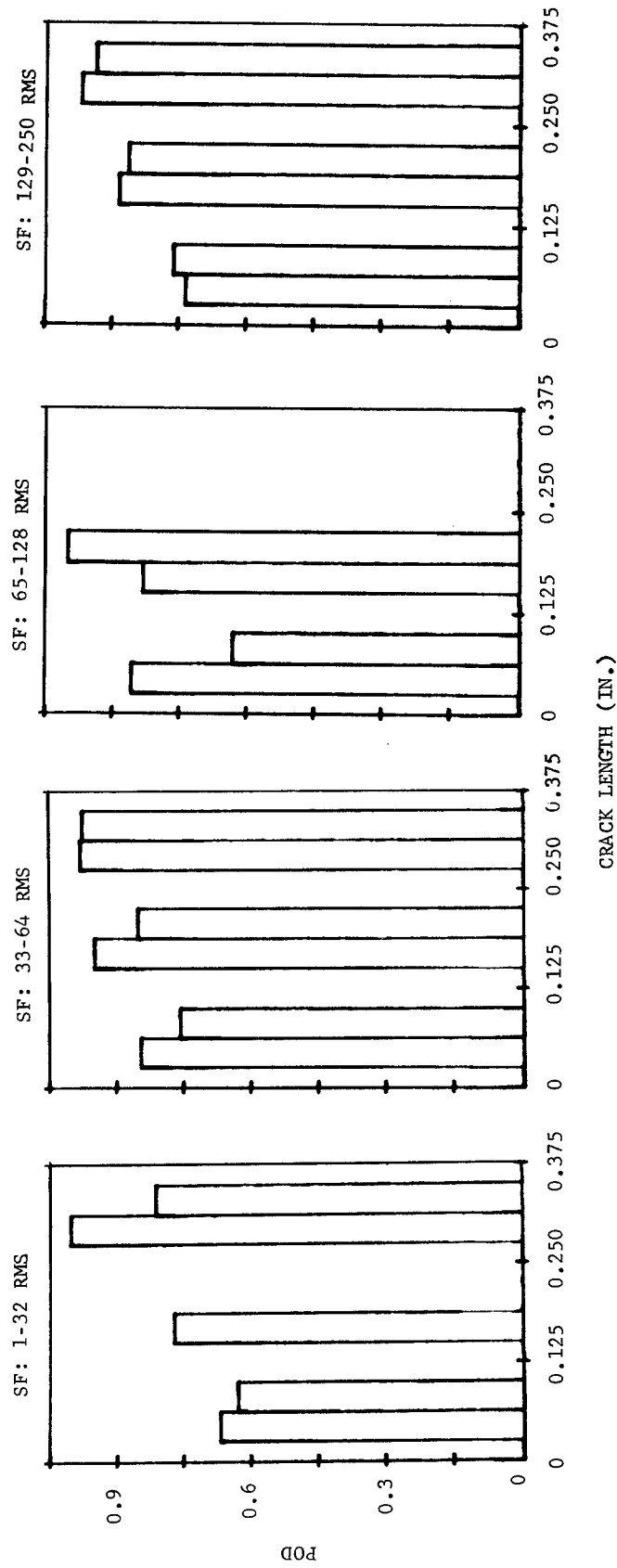


Figure D-3 Comparison of POD of Flat Plate Specimen Thickness (Penetrant)
(1st and 2nd Columns Represent Specimens with Thicknesses of
0.214 and 0.060 In. Respectively. DSN = 24-28, 60, 61)

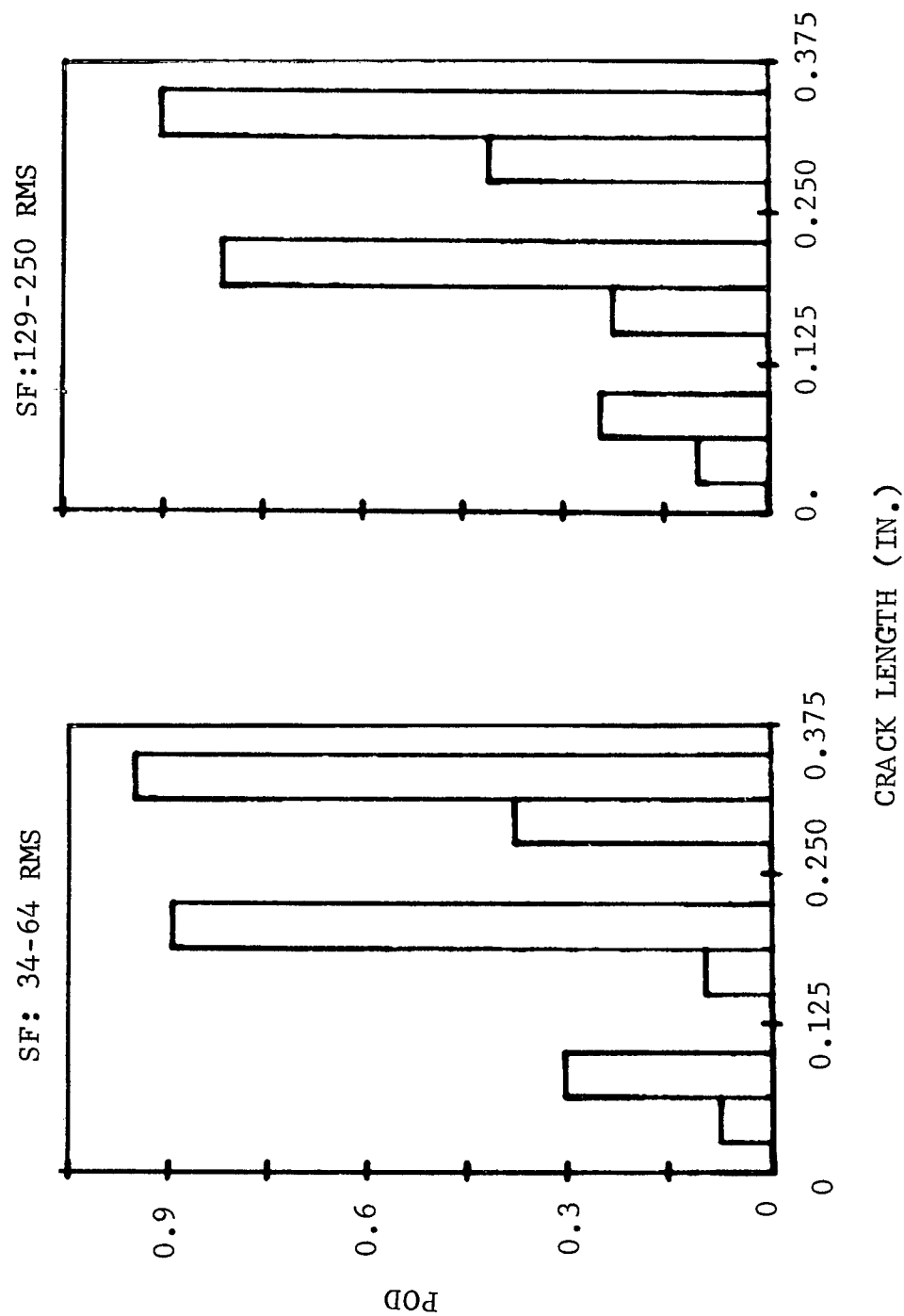


Figure D-4 Comparison of POD of Flat Plate Specimen Thickness (X-Ray)
 (1st and 2nd Columns Represent Specimens with Thicknesses
 of 0.214 and 0.060 In. Respectively. DSN = 10, 11, 20-23, 59)

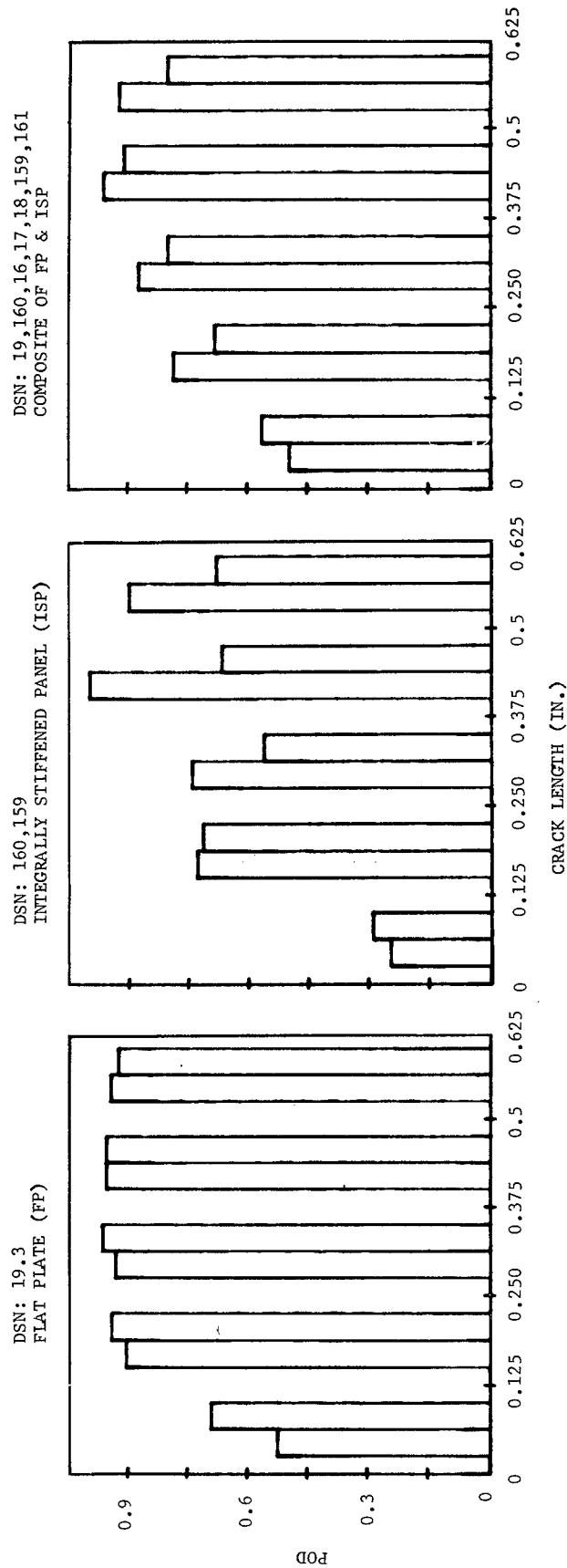


Figure D-5 Comparison of POD of Specimen History (Eddy Current) (1st and 2nd Columns Represent Specimens with Etched and Unetched Surface Treatment Respectively)

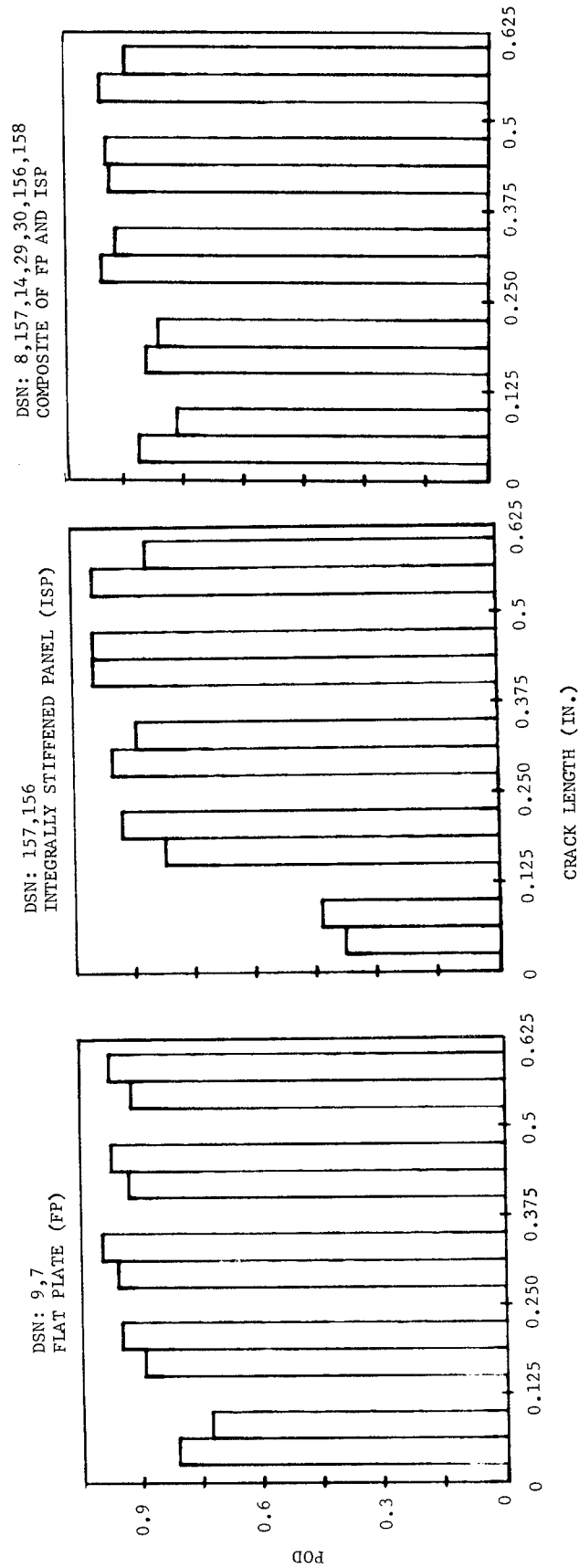


Figure D-6 Comparison of POD of Specimen History (Ultrasonic) (1st and 2nd Columns Represent Specimens with Etched and Unetched Surface Treatment Respectively)

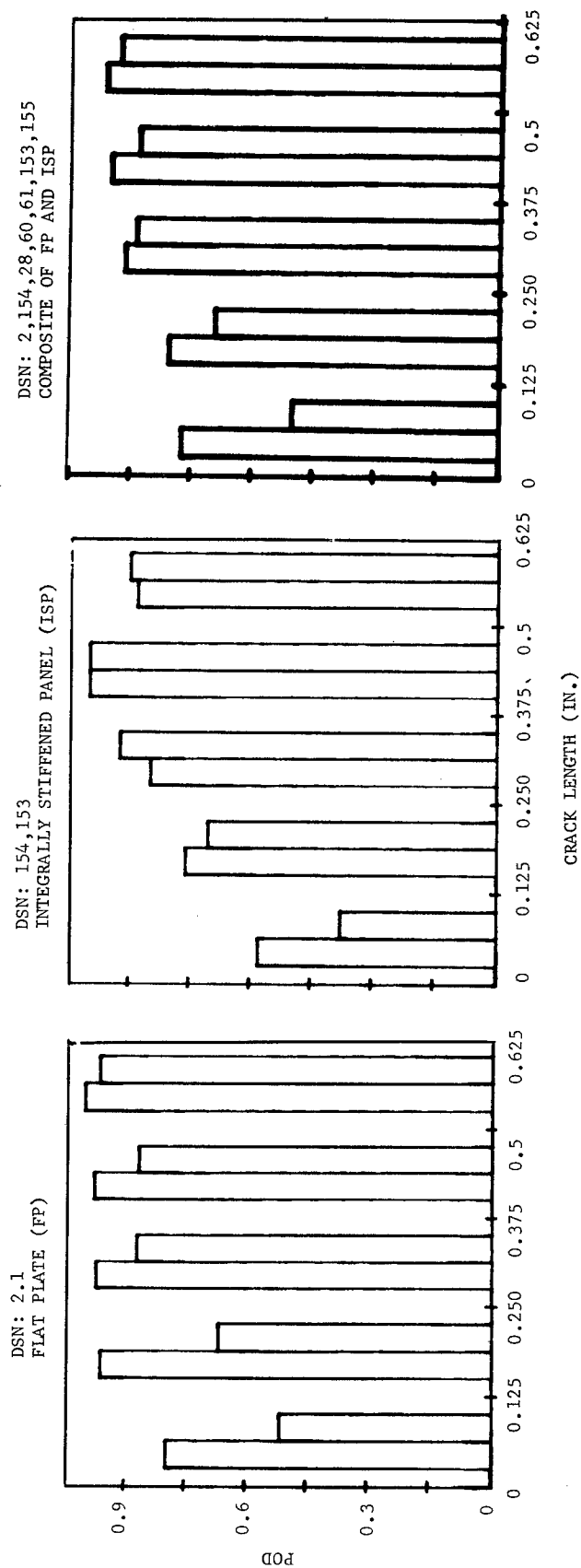


Figure D-7 Comparison of POD of Specimen History (Penetrant) (1st and 2nd Columns Represent Specimens with Etched and Unetched Surface Treatment Respectively)

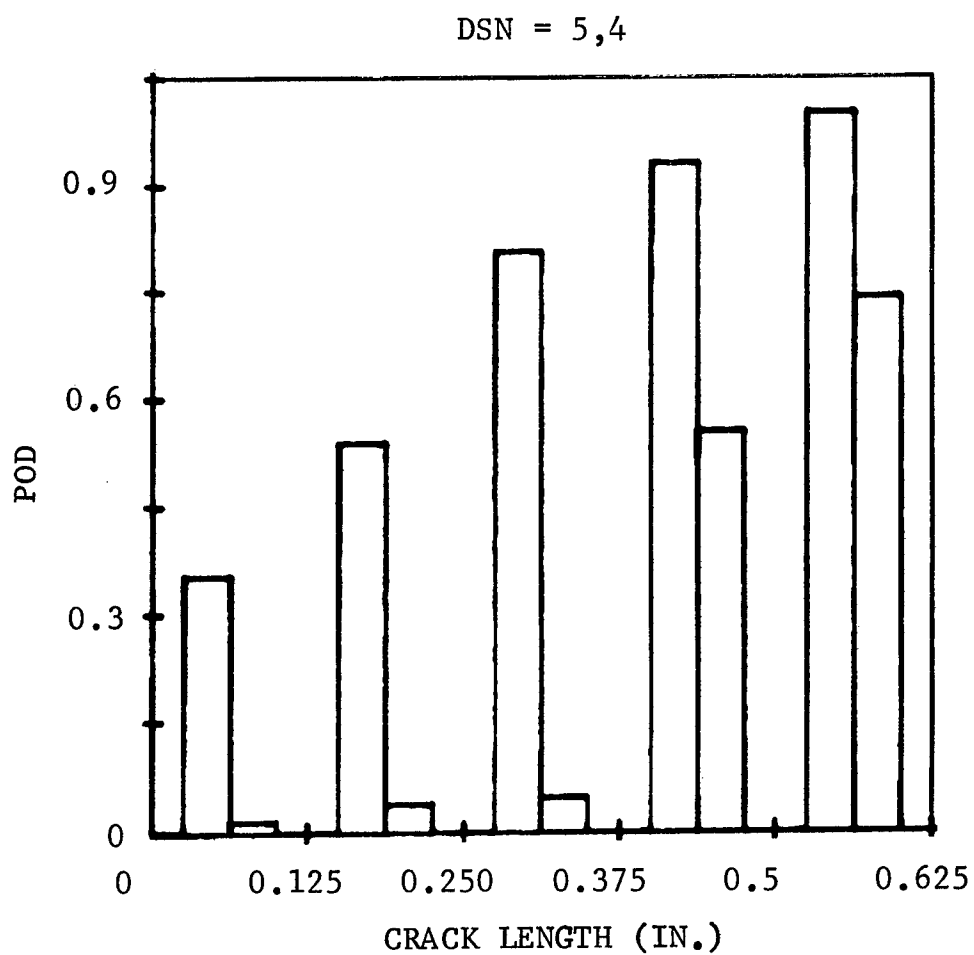


Figure D-8 Comparison of POD of Flat Plate Specimen History (X-Ray)
(1st and 2nd Columns Represent Specimens with Etched and
Unetched Surface Treatment Respectively)

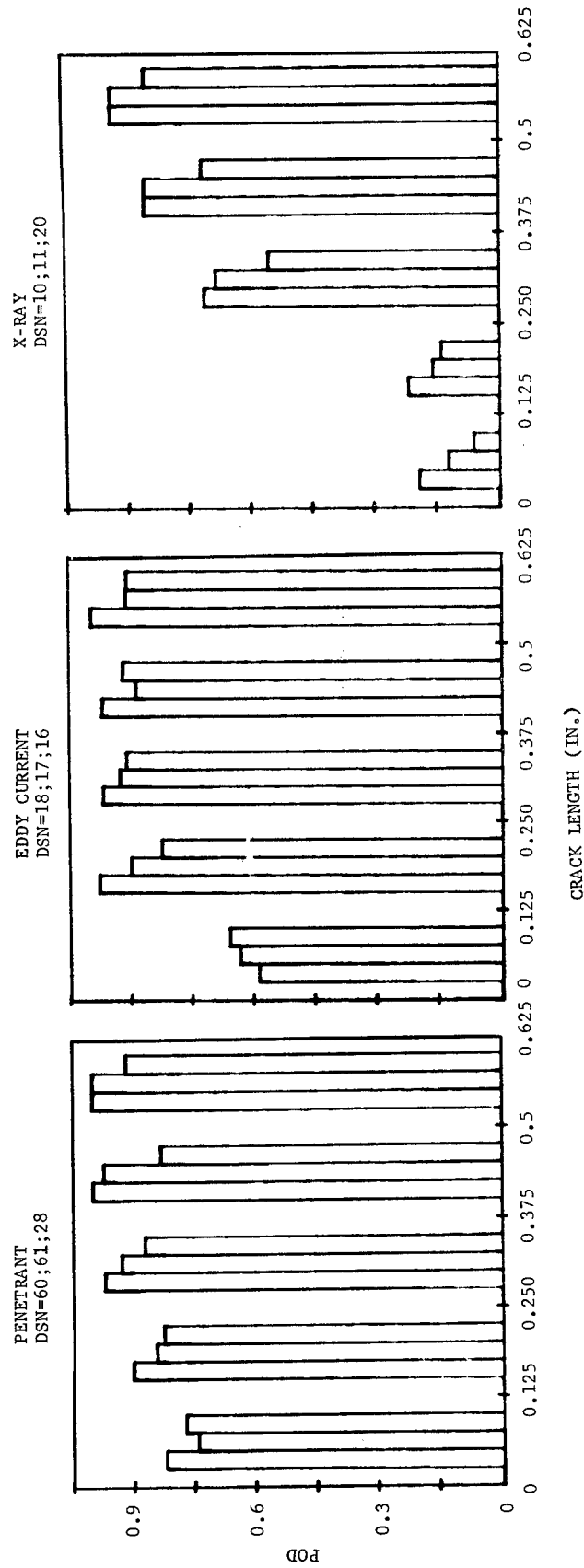


Figure D-9 Comparison of POD of Different Inspectors Using Penetrant, Eddy Current, and X-Ray Techniques on Flat Plate Specimens (1st, 2nd and 3rd Columns Represent Different Inspectors within One Company)

quite uniform. For the penetrant technique, the inspector who generated data set No. 28 is judged to be below par. The inspector who generated data set No. 18 for the eddy current technique had higher POD compared to the other two inspectors in the same company, at least in the longer crack length ranges. The inspector who generated data set No. 20 in the X-ray technique is judged to be below par. For the ultrasonic technique, different inspectors did not produce any noticeable difference in POD. Figure D-10 presents a comparison of the POD on flat plate specimens containing fatigue cracks obtained by three companies coded A, B and C using penetrant, ultrasonic, eddy current, and X-ray techniques. The POD for the first three techniques appeared to be quite similar. The largest variation in POD existed in the inspection results for the X-ray technique.

The effects of specimen geometry on POD for four NDE techniques are presented in Figures D-11, D-12 and D-13. PODs obtained on flat plate specimens and integrally stiffened panels containing fatigue cracks obtained by using penetrant, eddy current and ultrasonic inspections are shown in Figure D-11. It appears that the POD for the simpler geometry were higher than those for the more complex geometry for all three NDT techniques. However, the difference was significant only for the smallest crack length range in the case of ultrasonic inspection. Figure D-12 presents a comparison of the PODs obtained on flat plates, integrally stiffened panel (ISP) and ISP with riveted plate for the same three NDT techniques of penetrant, eddy current, and ultrasonics. For all three NDT techniques, PODs obtained on flat plates were higher than corresponding values for the other two types of specimens with more complex geometries. However, little difference could be discerned for the integrally stiffened panels with and without a riveted plate. Figure D-13 shows a comparison of the POD obtained on specimens with several part geometries by using ultrasonic, eddy current, and magnetic particle techniques. In general, no significant difference was observed for the specimen geometries represented except the tandem T versus hollow straight cylinder. However, the reason for the low POD for the latter was that the inspectors were not aware that cracks were present on the inner surfaces of the hollow cylinders.

A comparison of POD for weld specimens with as-welded and scarfed joints using penetrant, ultrasonic, and eddy current techniques is shown in Figure D-14. The PODs for the two types of specimen histories were essentially equivalent for the ultrasonic and eddy current techniques. For the penetrant technique,

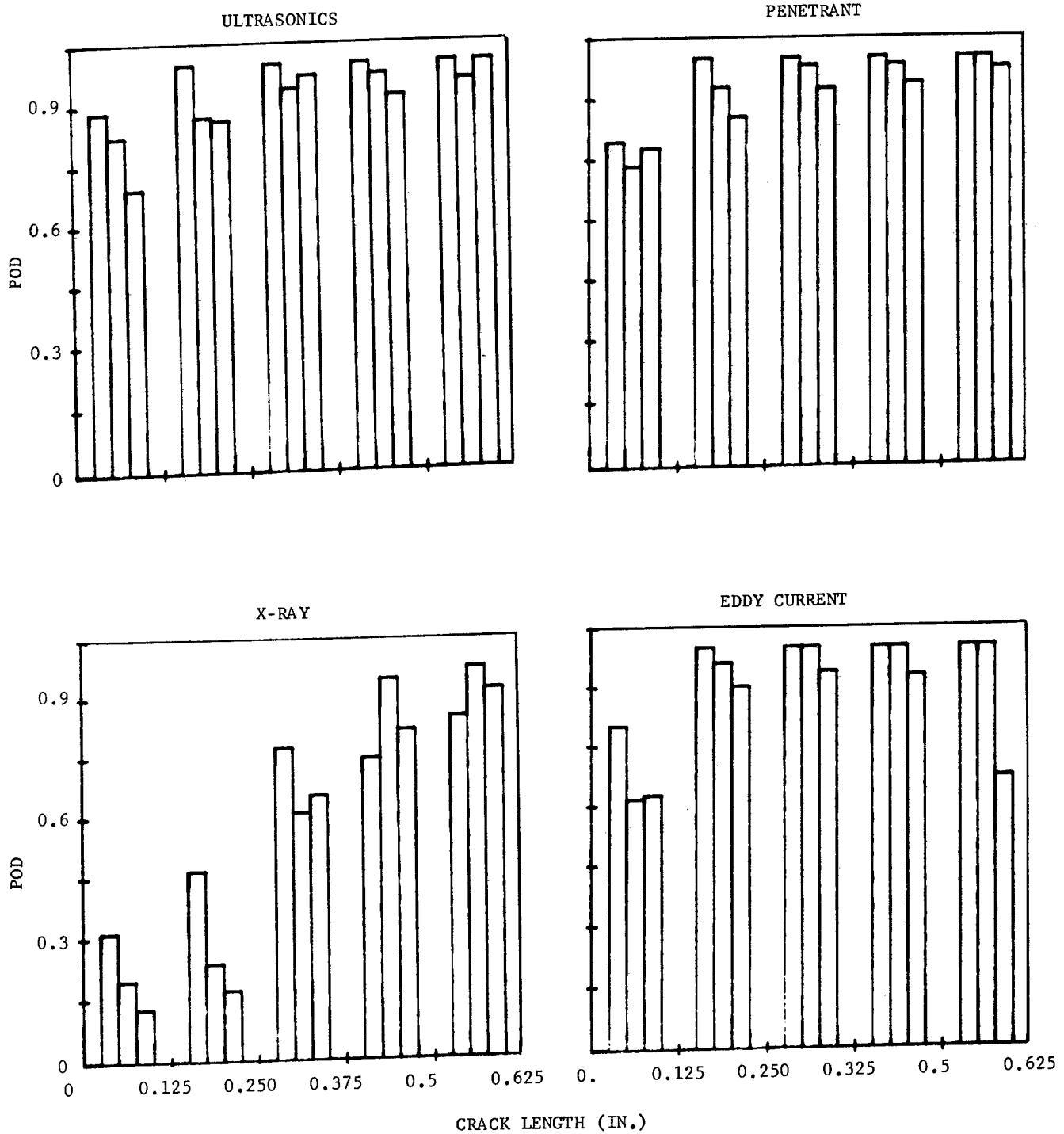


Figure D-10 Comparison of POD for Different Companies Using the Same Flat Plate Specimens (1st, 2nd, and 3rd Columns Represent Companies A, B, and C Respectively)

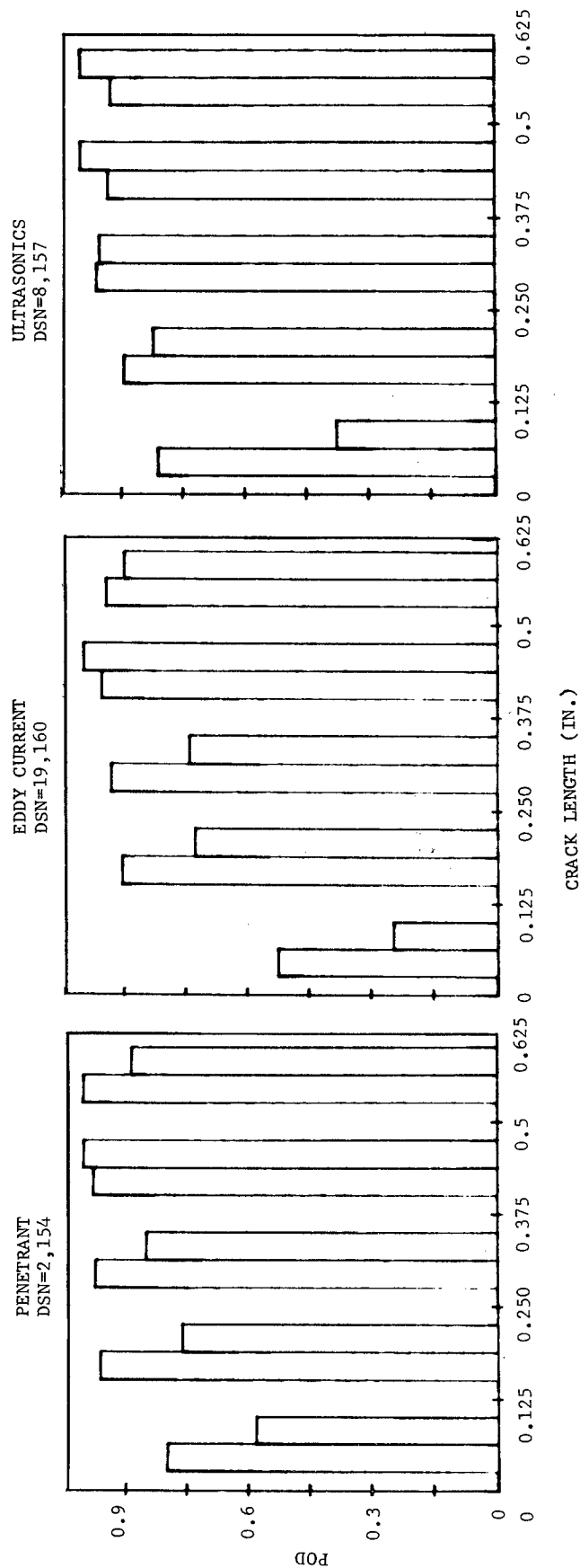


Figure D-11 Comparison of POD for Two Different Part Geometries Obtained by the Same Company (1st and 2nd Columns Represent Flat Plate and Integrally Stiffened Panel Specimen Geometries Respectively)

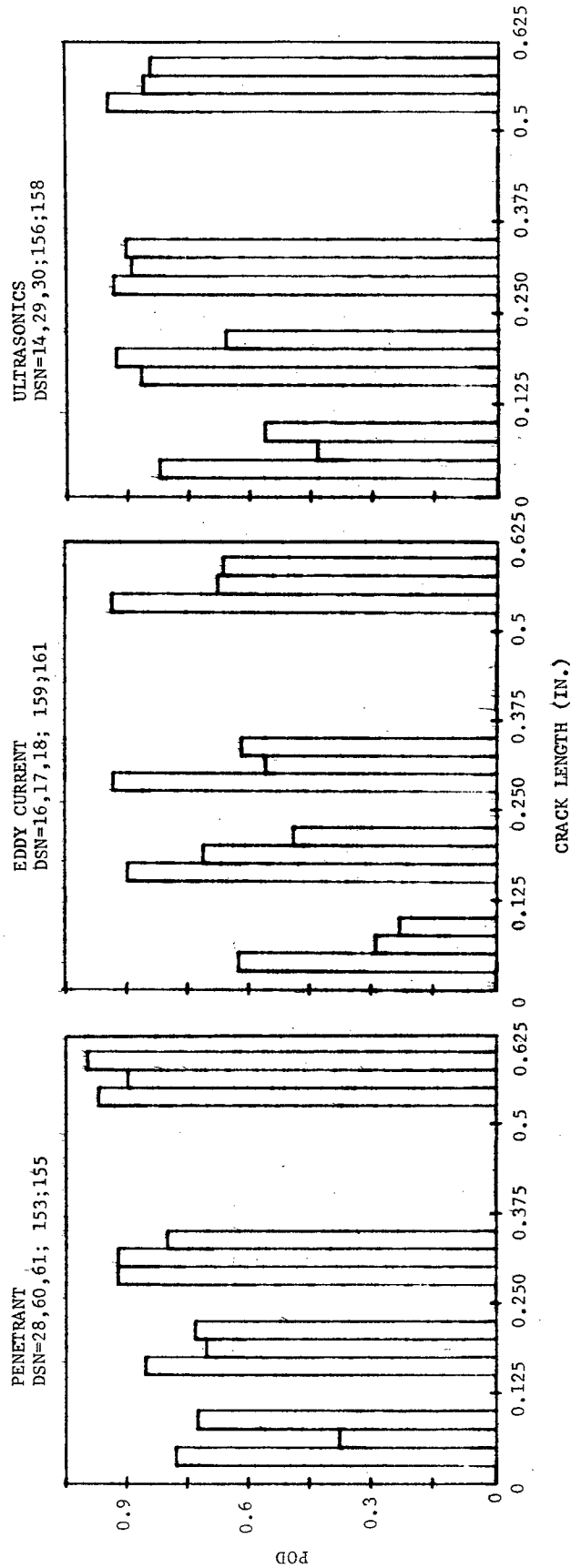


Figure D-12 Comparison of POD for Three Different Part Geometries Obtained by Three Companies (1st, 2nd and 3rd Columns Represent Specimen Geometries of Flat Plate, Integrally Stiffened Panel (ISP), and ISP with Riveted Plate Respectively)

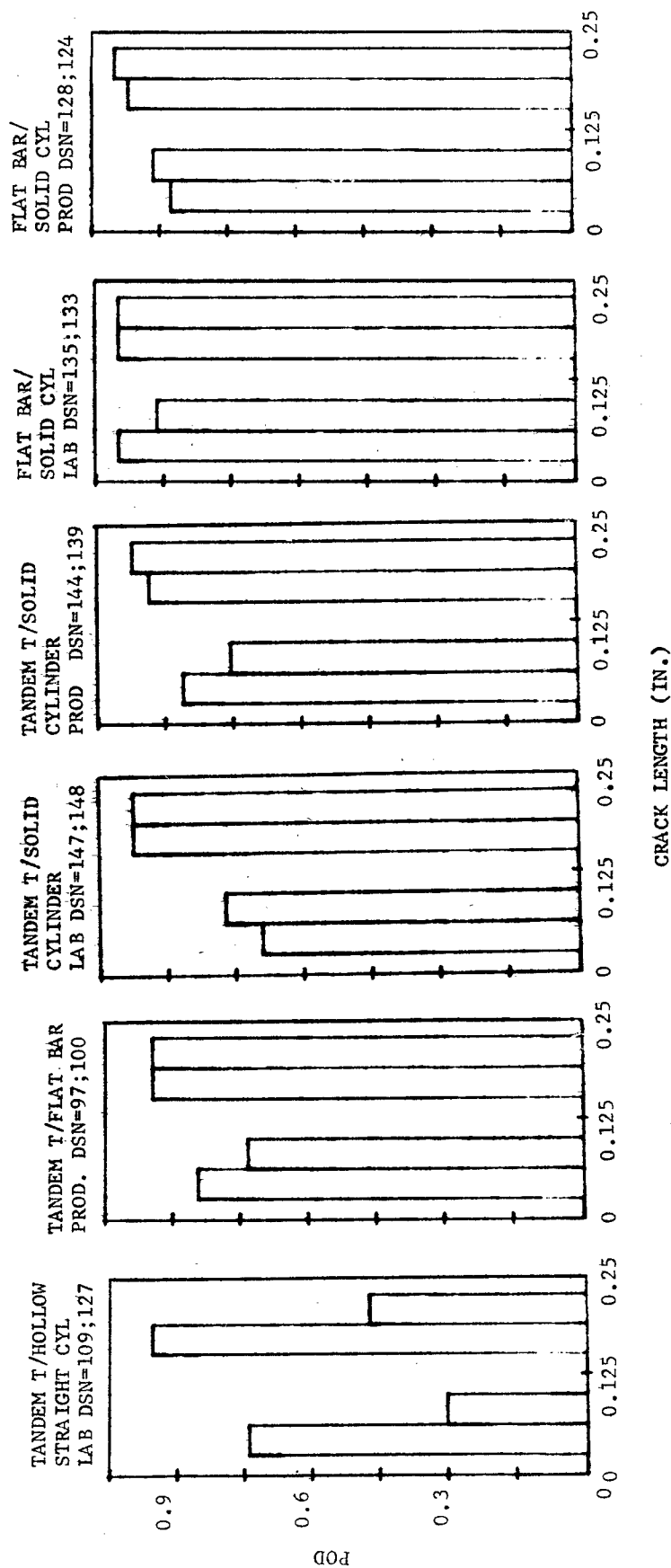


Figure D-13 Comparison of POD of Different Part Geometries Using Ultrasonic, Eddy Current and Magnetic Particle Inspections (1st and 2nd Columns Represent Specimen Geometries as Indicated Above the Histogram Bars)

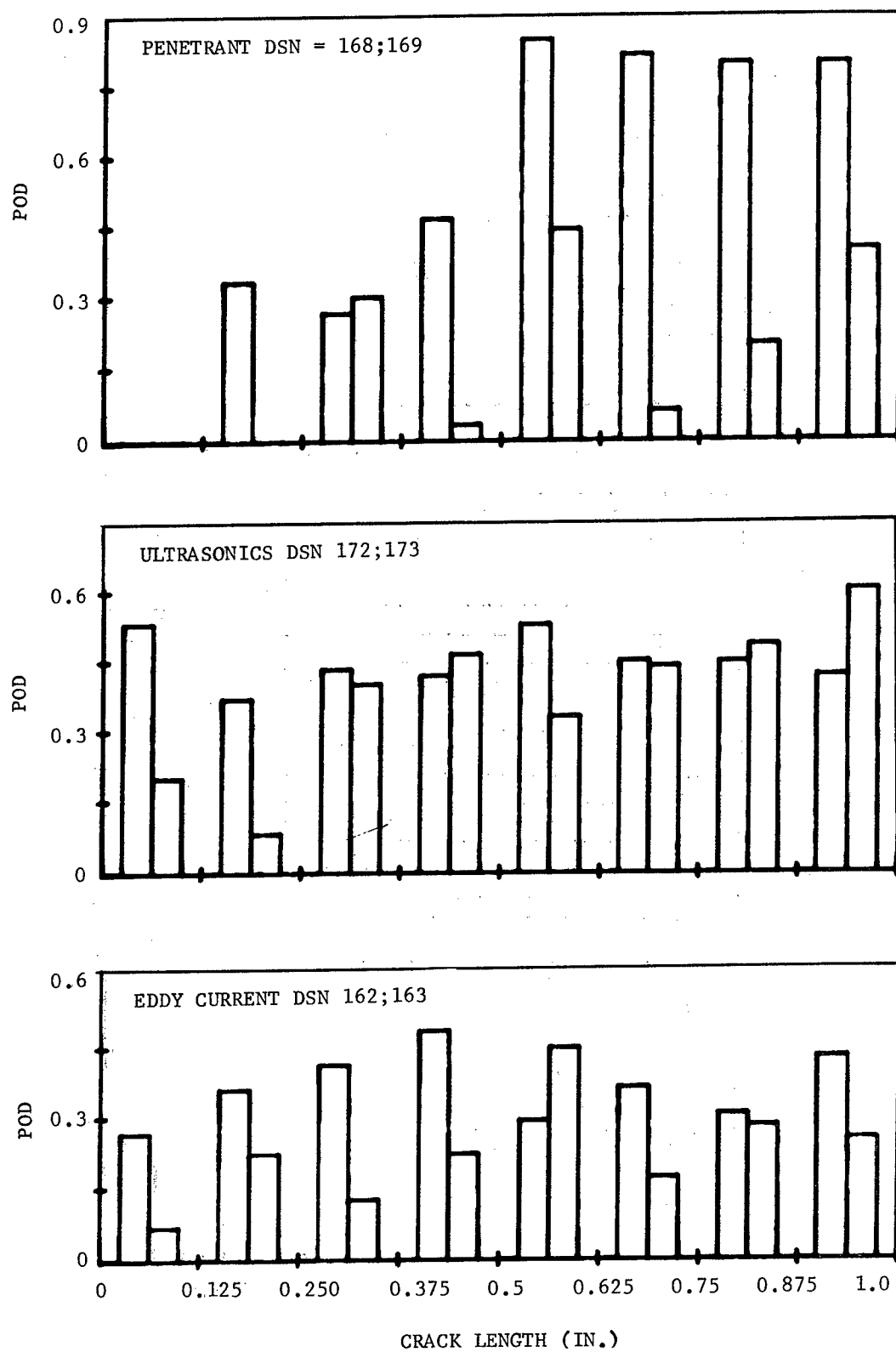


Figure D-14 Comparison of POD for Different Specimen Histories (1st and 2nd Columns Represent Specimens with As Welded and Scarfed Weld Crown Respectively)

lower PODs were evident for specimens with scarfed joints. This appeared to be contradictory to the expected trend. The reason for the anomaly could be attributed to a smearing of the scarfed surfaces of the aluminum weld specimen. The flaw openings to the specimen surface were closed by the metal chips preventing the penetration of the penetrants. Figure D-15 presents a comparison of POD for weld specimens with lack of penetration (LOP) defects inspected before and after a proof loading of 90 percent of yield stress. Except for the eddy current technique, the PODs obtained for the specimens after proof loading were much higher compared to those obtained before proof loading.

The point estimate comparison of the PODs presented in Figures D-7 to D-15 provided a good indication of the order of importance of the influencing parameters on the NDE sensitivity.

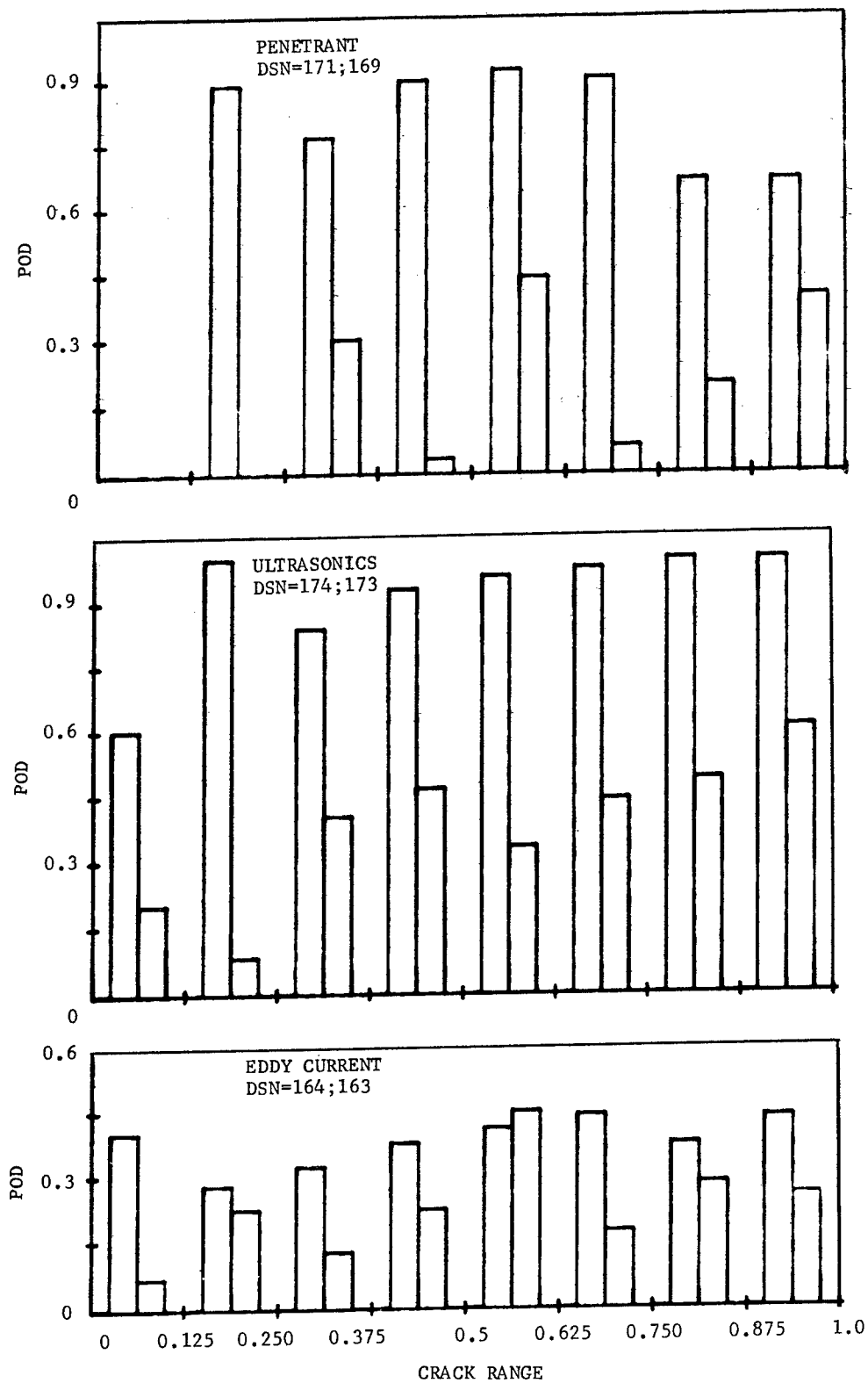


Figure D-15 Comparison of POD for Weld Specimens with Lack of Penetration Defects Before (1st Column) and After (2nd Column) Proof Loading

A P P E N D I X E

LINEAR REGRESSION TRANSLATION MODELS

LINEAR REGRESSION TRANSLATION MODEL

The following linear regression translation models were obtained by using procedures outlined in Section 5.1.2 in this report. The tables were categorized by the complex geometries to which results obtained from flat plate specimens were tabulated. Two sets of data were associated with each category of complex specimen geometry. The first set labelled "Crack Length" was obtained without entering the crack depth as a parameter. The second set labelled "Crack Depth" was obtained after the crack depth to crack length ($a/2c$) ratio was entered as a parameter. The first row of numbers in the translation model represented the coefficients accounting for the contribution to the POD from the geometry effect. The second block of numbers tabulated the contributions from nine crack length intervals. Contribution from the specimen history, surface finish, and the $a/2c$ of the specimens are shown in the third, fourth and fifth blocks of coefficients respectively in the tables.

GENERAL DYNAMICS
Fort Worth Division

TABLE E1 LINEAR REGRESSION MODEL - ULTRASONICS

TABULATION SHEET

Trans- lation Inter- action	Integrally Stiffened Panel			Riveted Plate to ISP			Weld Panel			Long. Weld w/Crown			Trans. Weld w/Crown			Long. Weld WO/Crown			Tandem T	
	Crack Length	Crack Depth	Crack Length	Crack Length	Crack Depth	Crack Length	Crack Length	Crack Depth	Crack Length	Crack Depth	Crack Length	Crack Depth	Crack Length	Crack Depth	Crack Length	Crack Depth	Crack Length	Crack Depth		
Geometry	0.106	-0.225		0.132	0.001		-0.204	0.397	-0.166	0.559	-0.119	0.097	-0.196	0.342	0.008					
Crack Length (Mils)																				
7-15	0	0		0	0		0	0	0	0	0	0	0	0	-0.386					
16-25	0	0		0	0		0	0	0.318	0	0	0	0	0	0					
26-40	0	0		0	0		-0.478	0	0.470	0.971	-0.333	-0.216	0.282	-0.720	0.011					
41-63	0.656	0.644	-0.398	-0.334	0	0	0	0	0.398	0.285	0.383	0.637	0.891	0.560	0.192					
64-100	0.019	0.164	0.388	0.402	0.501	0.103	-0.215	0	0.153	0.103	0.379	0.482	0.270	0.178	0.001					
101-160	0.019	0.051	0.420	0.501	0.372	0.002	0.103	0.269	0.207	0.006	0.200	0.495	0.097	0.062	0.039					
161-254	0.008	-0.048	0.004	0.372	0.004	0.002	0.002	0.073	-0.070	-0.156	-0.071	0.161	-0.041	-0.296	0					
255-403	-0.071	-0.032	-0.062	-0.018	-0.018	-0.130	-0.130	-0.014	0.185	0.115	-0.121	0.057	-0.042	-0.111	0					
404-640	0	0	0	0	0	0	0	0	0	0	0	0	0	0	0					
Specimen History																				
Unetched	-0.041		-0.077			0.447			0.247		-0.120		0.065		-0.077					
Etched	0		0			0			0.131		-0.066		-0.041		0					
Scarfed						0.598														
Proof-																				
Loaded						0			0		0		0							
Surface Finish (RMS)																				
Unknown	0	0	0	0	0	0	0	-0.614	0	-0.741	0	-0.531	0	-0.255	0					
1-32	0.063	0.165	-0.170	-0.209	-0.346	0.348	-0.346	0.348	-0.390	-0.527	0.041	-0.278	0.102	0.023	0					
33-64	0	0	0	0	0.006	0.326	0.006	0.326	0	-0.409	0.098	-0.246	0	0	0					
65-128	0	0	0	0	-0.088	0.349	-0.088	0.349	0	0	0	0	0	0	0					
a/2c																				
0.17		0.105		0.128		0.105		0.105		0.223		0.030		-0.130						
0.17-0.34		0.163		0.068		0		0		0.238		0.040		-0.186						
0.34		0		0		0		0		0		0		0						

TABLE E2 LINEAR REGRESSION MODEL - PENETRANT

TABLE E2 LINEAR REGRESSION MODEL - PENETRANT

TABULATION SHEET

[illegible]

GENERAL DYNAMICS
Fort Worth Division

TABLE E3 LINEAR REGRESSION MODEL - EDDY CURRENT

TABULATION SHEET

Trans- laction Inter- action	Integrally Stiffened Panel			Riveted Plate to ISP			LOP in Weld Panel			Long. Weld w/Crown			Trans. Weld w/Crown			Long. Weld wo/Crown			Tandem T		
	Crack Length	Crack Depth	Crack Length	Crack Length	Crack Depth	Crack Length	Crack Length	Crack Depth	Crack Depth	Crack Length	Crack Depth	Crack Depth	Crack Length	Crack Depth	Crack Depth	Crack Length	Crack Depth	Crack Depth	Crack Length	Crack Depth	Crack Depth
Geometry	-0.217	-0.638		0.021	-0.409	0.257	0.799	0.505	0.143	-0.187	0.125	-0.296	-0.357	-0.044							
Crack Length (Mils)																					
7-15	0	0	0	0	0	0	0	0	0	0	0	0	0	0	0	0	0	0	0	-0.698	
16-25	0	0	0	0	0	0	0	-0.689	0	0	0	0	0	0	0	0	0	0	0	0	
26-40	0	0	0	0	0	-0.744	-0.764	-0.680	-0.905	-0.373	-0.506	0.490	0.273	-0.225							
41-63	0.383	0.310	0.252	0.159	0	0	0	-0.467	-0.671	0.176	0.080	0.318	0.577	-0.180							
64-100	0.246	0.439	-0.010	0.201	0.176	0.176	-0.139	-0.350	-0.327	0.383	0.213	0.200	0.374	0.058							
101-160	0.166	0.269	0.257	0.355	0.516	0.516	0.154	-0.333	-0.430	0.040	0.215	0.237	0.022	0.094							
161-264	0.009	0.047	-0.006	-0.071	0.436	0.436	0.034	0.197	0.243	-0.132	-0.417	0.176	0.246	0							
255-403	0.298	0.322	0.028	-0.002	0.389	0.389	0.087	-0.324	-0.030	-0.038	-0.300	-0.078	0.040	0							
404-640	0	0	0	0	0	0	0	0	0	0	0	0	0	0							
Specimen History																					
Unetched	0.599			0.578			0.176		-0.072		0.140		0.201								
Etched	0.546			0.599			0		0.047		-0.083		0.020								
Scarfed	0			0			0		0		0		0								
Surface Finish (RMS)																					
Unknown	0			0			0		0		0		0								
1-32	0.097			-0.028			-0.602		0.365		0.164		0.094								
33-64	0			0			-0.244		0.691		0.178		0								
65-128	0			0			-0.516		0		0		0								

Fort Worth Division

TABLE E4 LINEAR REGRESSION MODEL - X-RAY

Trans- lation Inter- action	Crack Length (Mils)	Weld in			Long. Weld w/Crown			Trans. Weld w/Crown			Long. Weld w/Crown			Tandem T		
		Crack Length	Crack Depth	Crack Length	Crack Length	Crack Depth	Crack Length	Crack Depth	Crack Length	Crack Depth	Crack Length	Crack Depth	Crack Length	Crack Depth		
Geometry		-0.163	-0.150	0.754	1.210	0.420	0.662									
Crack Length (Mils)																
7-15		0	0	0	0	0	0	0	0	0	0	0.512				
16-25		0	0	-1.285	0	0	0	0	0	0	0	0				
26-40		-0.433	-0.037	-1.159	-0.768	-0.719	-0.541	-0.424	-0.536	-0.121						
41-63		0	0	-0.916	-0.854	-0.634	-0.479	-0.646	-0.590	-0.296						
64-100		-0.330	-0.397	-1.140	-0.903	-0.576	-0.648	-0.511	-0.807	-0.097						
101-160		-0.499	-0.639	-0.660	-0.555	-0.347	-0.373	-0.490	-0.714	-0.274						
161-254		-0.305	-0.081	-0.541	-0.405	0.059	0.080	-0.027	-0.156	0						
255-403		-0.238	-0.141	-0.527	-0.571	-0.509	-0.677	-0.456	-0.483	0						
404-640		0	0	0	0	0	0	0	0	0						
Specimen History																
Unetched		-0.108		0.187			0.072		0							
Etched		0		0.106			-0.034		0.110							
Scarfed		0		0			0		0							
Surface Finish (RMS)																
Unknown		0		0			0		0							
1-32		0.223		-0.363			0.169		0.111							
33-64		0.110		-0.302			0.168		0							
65-128		0.154		0			0		0							

REFERENCES

1. Yee, B. G. W., et. al., "Assessment of NDE Reliability Data," NASA CR-134991 (NAS3-18907), October 1976.
2. Rummel, W. D., et. al., "The Detection of Tightly Closed Flaws by Nondestructive Testing (NDT) Methods," MCR-75-212 (NAS9-13878), October 1975.
3. Rummel, W. D., et. al., "The Detection of Fatigue Cracks by Nondestructive Test Methods," NAS CR-2369 (NAS9-12276), February 1974.
4. Graybill, F. A., "Introduction to Linear Statistical Models," Vol. 1, McGraw Hill, N. Y., 1961.
5. Mucciardi, A. N., et. al., "Adaptive Nonlinear Signal Processing for Characterization of Ultrasonic NDE Waveforms - Task 1: Inference of Flat-Bottom Hole Size," AFML-TR-75-24, February 1975.
6. Shankar, R., et. al., "Adaptive Nonlinear Signal Processing for Characterization of Ultrasonic NDE Waveforms - Task 2: Measurement of Subsurface Fatigue Crack Size," April 1976.
7. Southworth, H. L., et. al., "Practical Sensitivity Limits of Production Nondestructive Testing Methods in Aluminum and Steel," AFML-TR-74-241, March 1975.
8. Halkias, J. E., "F-111A/D/E Fuselage Fatigue Test Post-Test Inspection of FW # 1-3 Fuselage Fatigue Test Component," General Dynamics Report FGT-5869, 30 June 1975.
9. Halkias, J. E., "F-111 Fuselage Fatigue Test Post-Test Inspection of FW # 1-4 Fuselage Fatigue Test Component," General Dynamics Report FGT-5870, October 1975.
10. ASNT Airframe Inspection Subcommittee Recommended Practice for a Demonstration of NDE Reliability on Aircraft Draft 2, July 1974.

11. Packman, P. F., et. al., "Reliability of Flaw Detection by Nondestructive Inspection" ASM Handbook II, ASM, Metals Park, Ohio, 1976.
12. Packman, P. F., et. al., "Reliability of Defect Detection in Welded Structures," Reliability Engineering in Pressure Vessels and Piping, ASME Booklet, June 1975.